# BRNO UNIVERSITY OF TECHNOLOGY

VYSOKÉ UČENÍ TECHNICKÉ V BRNĚ

## FACULTY OF CHEMISTRY

FAKULTA CHEMICKÁ

## INSTITUTE OF CHEMISTRY AND TECHNOLOGY OF ENVIRONMENTAL PROTECTION

ÚSTAV CHEMIE A TECHNOLOGIE OCHRANY ŽIVOTNÍHO PROSTŘEDÍ

## MODIFICATION OF ORGANIC HIGH PERFORMANCE PIGMENTS FOR APPLICATIONS IN ORGANIC ELECTRONICS

MODIFIKACE ORGANICKÝCH VYSOCE VÝKONNÝCH PIGMENTŮ PRO APLIKACE V ORGANICKÉ ELEKTRONICE

### DOCTORAL THESIS

DIZERTAČNÍ PRÁCE

**AUTHOR**          Ing. Martin Cigánek
AUTOR PRÁCE

**SUPERVISOR**          doc. Ing. Jozef Krajčovič, Ph.D.
ŠKOLITEL

**BRNO 2020**

# Specification Doctoral Thesis

| | | | |
|---|---|---|---|
| Department: | Institute of Chemistry and Technology of Environmental Protection | Academic year: | 2019/20 |
| Student: | **Ing. Martin Cigánek** | | |
| Study programme: | Chemistry, Technology and Properties of Materials | | |
| Study branch: | Chemistry, Technology and Properties of Materials | | |
| Head of thesis: | **doc. Ing. Jozef Krajčovič, Ph.D.** | | |

## Title of Doctoral Thesis:

Modification of Organic High Performance Pigments for Applications in Organic Electronics

## Doctoral Thesis:

1 Write the review on organic high–performance pigments and related molecules and their application in the fields of organic electronics.

2 Write the review on synthetic possibilities of derivatization of appropriate organic pigments and related molecules.

3 Prepare and characterize a diverse range of novel original derivatives of organic pigments and related molecules with emphasis on the incorporation of adamantyl side chains into their structures.

4 Prepare and characterize a completely novel, as yet undescribed thiophene analogue of a benzodifuranone derivative (BDF).

5 Prepare and characterize an original fluorinated polymer based on thiophene with significantly prolonged π–conjugation of the monomer.

6 Perform a comprehensive study of the influence of adamantyl side chains on the resulting properties of the selected series of alkylated DPP derivatives.

## Deadline for Doctoral Thesis delivery: 18.8.2020:

| | | |
|---|---|---|
| _ _ _ _ _ _ _ _ _ _ _ _ | _ _ _ _ _ _ _ _ _ _ _ _ | _ _ _ _ _ _ _ _ _ _ _ _ |
| Ing. Martin Cigánek<br>Student | doc. Ing. Jozef Krajčovič, Ph.D.<br>Head of thesis | doc. Ing. Jiří Kučerík, Ph.D.<br>Head of department |

| | |
|---|---|
| | _ _ _ _ _ _ _ _ _ _ _ _ |
| In Brno dated 1.9.2019 | prof. Ing. Martin Weiter, Ph.D.<br>Dean |

## ABSTRACT

The doctoral thesis deals with the study, synthesis and chemical derivatization of molecules belonging to the group of organic high-performance pigments and their potential application in the fields of organic electronics. The theoretical part of the work is focused on the latest trends in the area mentioned above, both from the application potential of specific derivatives and in terms of synthetic possibilities and their structural derivatization. The experimental part describes in detail the preparation of a wide range of intermediates and final products, including derivatives of diketopyrrolopyrroles (DPP), benzodifuranone (BDF), epindolidione (EP), naphthyridinedione (NTD) and thiophene-based polymer (PT). A total of 103 molecules were synthesized, of which 49 were final products, and 27 of them were completely novel, as yet unpublished. Herein, the main motive for the derivatization of pigment molecules is the incorporation of bulky adamantyl substituents into the resulting derivative structures. In the next part of the work, individual chemical modifications leading to the final products are discussed in more detail. In the series of *N,N′*-; *N,O′*- and *O,O′*-substituted DPP derivatives, the influence of both the alkyl chains' character and binding position in the DPP molecule on the selectivity of the reaction, the thermal and optical properties of the resulting derivatives is comprehensively described.

## ABSTRAKT

Dizertační práce pojednává o studiu, syntéze a chemické derivatizaci molekul spadajících do skupiny organických vysoce výkonných pigmentů a jejich potenciálním uplatnění v oblastech organické elektroniky. Teoretická část práce je zaměřena na nejnovější trendy v dané oblasti, a to jak z aplikačního potenciálu konkrétních derivátů, tak z pohledu syntetických možností a jejich strukturálních derivatizací. V experimentální části je pak podrobně popsána příprava pestré škály intermediátů a výsledných produktů, zahrnujících deriváty diketopyrrolopyrrolů (DPP), benzodifuranonu (BDF), epindolidionu (EP), naphthyridinedionu (NTD) a polymeru na bázi thiofenu (PT). Celkově bylo nasyntetizováno 103 molekul, přičemž 49 tvořily výsledné produkty, z nichž 27 bylo zcela nových, dosud nepublikovaných. Hlavním motivem derivatizace molekul pigmentů je zde inkorporace derivátů adamantanu do finálních struktur. V další části práce jsou blíže diskutovány jednotlivé chemické modifikace vedoucí k výsledným produktům. Na sérii *N,N′*-; *N,O′*- a *O,O′*-substituovaných derivátů DPP je popsána komplexní studie vlivu charakteru alkylových řetězců a také pozice jejich navázání v molekule DPP, a to nejen na selektivitu reakce, ale rovněž na optické i termické vlastnosti syntetizovaných produktů.

## KEYWORDS

## KLÍČOVÁ SLOVA

## DECLARATION

I declare that the doctoral thesis has been worked out by myself and that all the quotations from the used literary sources are accurate and complete. The content of the doctoral thesis is the property of the Faculty of Chemistry of Brno University of Technology and all commercial uses are allowed only if approved by both the supervisor and the dean of the Faculty of Chemistry, BUT.

## PROHLÁŠENÍ

Prohlašuji, že jsem dizertační práci vypracoval samostatně a že všechny použité literární zdroje jsem správně a úplně citoval. Dizertační práce je z hlediska obsahu majetkem Fakulty chemické VUT v Brně a může být využita ke komerčním účelům jen se souhlasem vedoucího práce a děkana FCH VUT.

.................................................

Ing. Martin Cigánek

# CONTENTS

# 1  OBJECTIVES OF THE DOCTORAL THESIS

The objectives of this doctoral thesis are:

- Write the review on organic high-performance pigments and related molecules and their application in the fields of organic electronics.

- Write the review on synthetic possibilities of derivatization of appropriate organic pigments and related molecules.

- Prepare and characterize a diverse range of novel original derivatives of organic pigments and related molecules with emphasis on the incorporation of adamantyl side chains into their structures.

- Prepare and characterize a completely novel, as yet undescribed thiophene analogue of a benzodifuranone derivative (BDF).

- Prepare and characterize an original fluorinated polymer based on thiophene with significantly prolonged π-conjugation of the monomer.

- Perform a comprehensive study of the influence of adamantyl side chains on the resulting properties of the selected series of alkylated DPP derivatives.

## 2 INTRODUCTION

Nowadays, electricity is an essential part of the daily life of most of the world's population. With the growing population of the Earth and the ever-increasing number of new technologies and their integration into the everyday life of present and future generations, the need for electricity continues to increase enormously. To meet the demand for this energy source in the future and to continue to take electricity for granted, as it is nowadays, really high demands are placed on developing new and increasingly efficient technologies that can produce electricity. Indeed, the research and development of technologies involved in generating net electricity are expanding significantly, and further growth is also expected in the coming decades, as confirmed by the graphs in *Figure 1* conducted by the independent statistical and analytical company U.S. Energy Information Administration (EIA)[1]. Significant growth in net electricity production is predicted especially for countries that are not part of the Organization of Economic Cooperation and Development (non-OECD) with an average increase of 2.3% per year from 2018 to 2050, compared with 1.0% per year in OECD countries (**1A**, *Figure 1*). This increase is necessary because of the expected growth in electricity consumption in all sectors, including industry, residential, commercial, transportation etc. (**1B**, *Figure 1*). E.g. the share of electricity used in transportation is expected to more than triple in 2050 compared to 2018, mainly because of more plug-in electric vehicles enter the fleet and electricity use for rail expands, which are today's major trends[1].
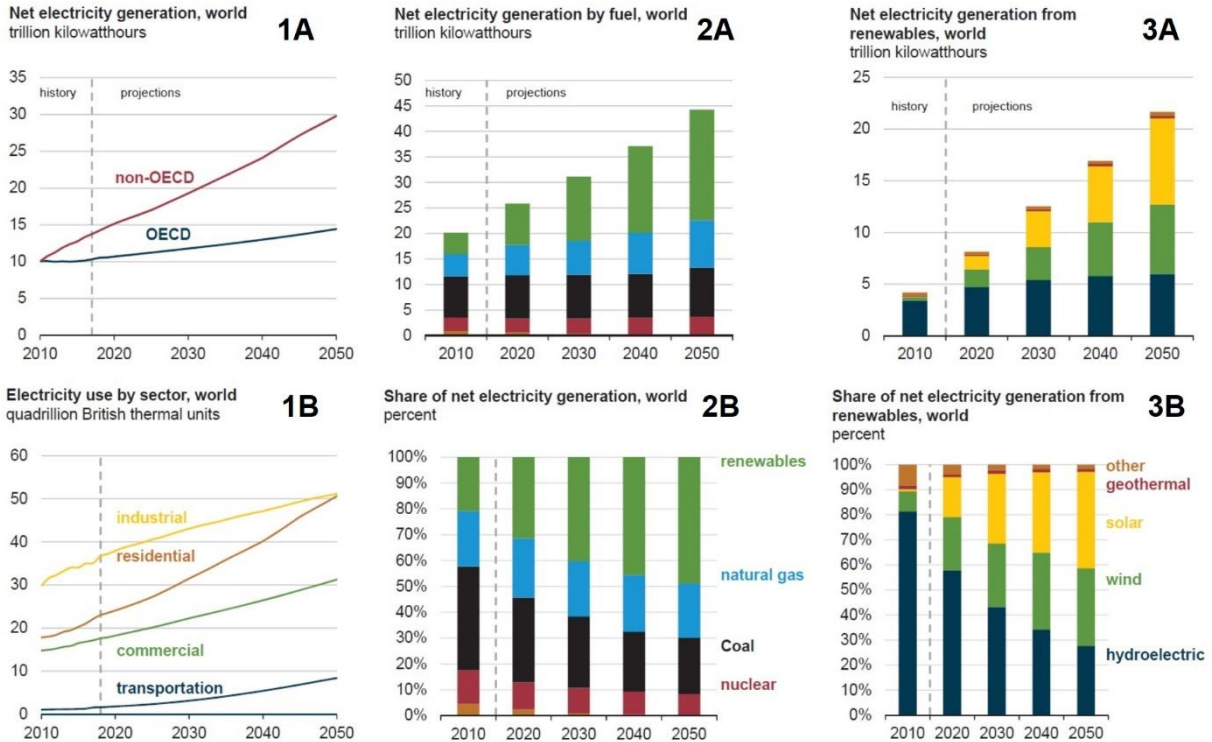


*Figure 1*: *Statistic graphs describing the development of net electricity generation and consumption by sector (1A–B), including distribution of energy sources by fuel (2A–B) and detailed analysis of renewable energy sources (3A–B) during period 2010–2050*[1].

It is clear from the **2A**–**B** graphs in *Figure 1* that the development of new technologies for net electricity generation is focused primarily on renewable sources, which are the fastest-growing source of electricity generation during the 2018 to 2050 period, rising by an average of 3.6% per year. Technological improvements and government incentives in many countries support their increased use, which is the main reason for the expected development. Based on predictions, renewable energy sources will surpass coal as the primary source of electricity generation in 2025 and by 2050 renewables will account for almost half of the world's total electricity generation (**2B**, *Figure 1*)[1].

Upon closer analysis of the share of individual areas of renewable energy sources shows that currently, the dominant hydropower source expects only modest growth, which predicts a fall in the share of electricity generation from 62% in 2018 to only 28% in 2050. On the contrary, among renewable energy sources, electricity generation from solar resources is expected to grow dramatically between 2018 and 2050, reaching 8.3 trillion kilowatt-hours (kWh), as show **3A**–**B** graphs in *Figure 1*. The main advantage of solar energy is that this technology becomes more cost-competitive and is supported by government policies in many countries. Moreover, sunlight produces about ten thousand times more energy than the current global energy consumption, which is why the sun is considered one of the best and most affordable renewable energy sources. Therefore, solar energy will account for almost 40% of total renewables generation by 2050[1].

Nowadays, still dominating crystalline silicon photovoltaic cells have been on the market for over 40 years and have probably already reached their technological and performance peaks[2]. Moreover, their production and disposal are considered uneconomical and very environmentally harmful. In the future, their use can be expected to decrease and, on the contrary, the use of organic solar cells (OSCs)[3] and related hybrid materials (perovskite-based solar cells)[4] are expected to increase, which should remove the previously mentioned disadvantages of silicon solar panels[2]. Branch of the industry dealing with these issues is called organic photovoltaics (OPV), which belongs to a huge industrial area known as printed, organic and flexible electronics.
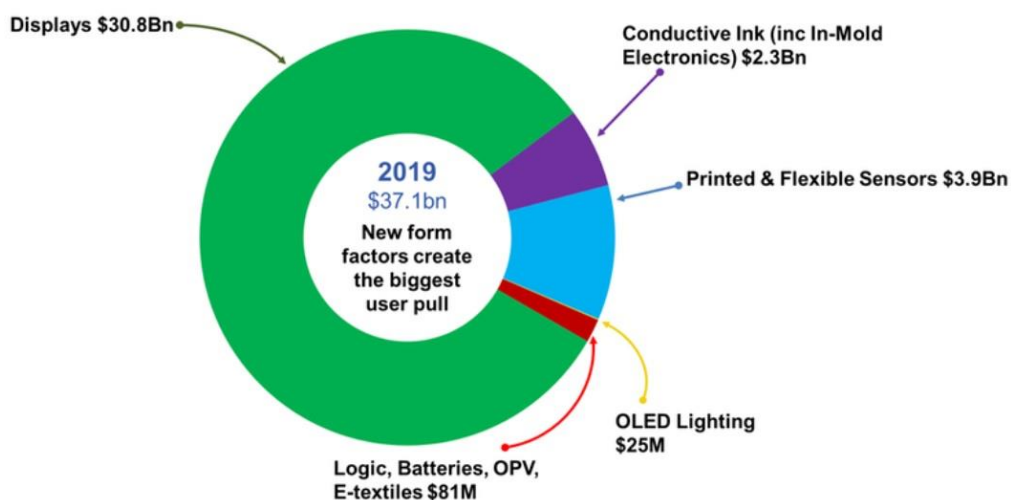


*Figure 2*: *Market snapshot for printed, organic and flexible electronics in 2019*[9]

In addition to the materials mentioned above and technologies involved in electricity generation, one of the main objectives of 21st-century research of organic electronics is the development of advanced materials that can also use this energy most effectively in modern electronic devices. There are also high demands on production costs and environmental impact of these materials, including constant miniaturization of components and meeting the growing requirements on their flexibility[5]. Thus, much effort has been put into developing narrow-band gap organic molecules, belonging to the category of semiconductors, that meet all these conditions much more easily than devices based on inorganic materials[2,6,7].

Organic electronics has been one of the most evolving disciplines of advanced material science and chemistry over the last 30 years[8]. In the past decade, a number of novel organic semiconductors have been developed and used in a wide range of organic and printed electronics fields, which are now experiencing a massive boom on the market and are currently among the most subsidized areas of science, and so it should be in the years to come. According to IDTechEx Research, the total market for printed, flexible and organic electronics will grow from $37.1 billion for 2019 to $41.2 billion in 2020 and to staggering $74 billion in 2030[9]. As shown in the graph in *Figure 2*, the majority of this market today are displays based on organic light-emitting diodes (OLED)[10], followed by printed sensors[11] and printed conductive inks[12] used predominately for photovoltaics. On the contrary, there are plenty of devices forming smaller segments, but with powerful growth potential, such as organic field-effect transistors (OFET)[13], organic solar cells (OSC)[14], biosensors[15] etc.

My present research deals with the current trends and the latest knowledge in the field of organic high-performance pigments and structurally related molecules from the perspective of their potential applications in organic electronics. My work and research are focused primarily on small organic molecules, although polymeric materials based on pigments and related molecules are also the marginally aim of interest in my research. The best electrical properties have so far been achieved with organic polymer-based semiconductors[16], which also are easily processable in the solution. Nevertheless, the undisputed and very significant advantage of small molecules compared to polymers is their monodispersity, a well-defined molecular structure and therefore more predictable properties, easier preparation and subsequent purification or modification of their structure[17]. The chemical derivatization of the molecules allows practically unlimited possibilities to optimize the required parameters, which is the main objective of my research.

# 3 THEORETICAL PART & REVIEW

## 3.1 Organic electronics and photonics

Organic electronics is currently a dynamically developing multidisciplinary modern branch of the electronics industry, using the interconnected knowledge of electronics, photonics, organic synthesis, material engineering, biotechnology and nanotechnology and many other disciplines. A crucial breakthrough in this area occurred in 1977 when polyacetylene was first prepared as an electrically conductive organic polymer[18]. In 2000, the Nobel Prize for Chemistry was awarded to three scientists Heeger, MacDiarmid and Shirakawa for this important discovery[19].

Interest in the organic electronics industry is steadily increasing, resulting in an ever-growing number of investments in research and construction of new production lines, which are gradually becoming a priority for the world's leading companies in this field[9], such as BASF, LG Display, Novaled GmbH, Samsung Display, Sony Corporation etc.[20] Therefore, it can be expected that this progressive area of electronics will affect virtually all economic sectors in the future.

Application area of photonics deals with the use of light to generate energy, transmit or detect information. From a different perspective, photonics is a technology for generating and utilizing light and many other forms of radiant energy whose quantum unit is a photon[21]. The related modern area called organic photonics deals with the above-mentioned light processes exhibiting in optical organic materials[22]. Currently, very interesting applications of organic photonics are, e.g. space technology[23], biomedicine[24], alternate energy[25], information technology[24], laser technology[26], etc. The group of materials generally applicable in the field of organic photonics belongs to a large group of organic semiconductors[22].

## 3.2 Organic materials for electronics

The basic building block of organic materials is a carbon atom, which forms single ($\sigma$-bond), double ($\sigma$-bond + $\pi$-bond) or triple ($\sigma$-bond + 2 $\pi$-bonds) bonds with other carbon atoms. There is a total of 4 electrons in the valence band of the carbon atom, in the ground state 2 in orbital 2s and one in orbital $2p_x$ and one in $2p_y$. Due to the very small energy difference between fully occupied 2s orbital and unoccupied $2p_z$, one electron is easily transferred among them, thus creating an excited state of the carbon atom, containing 4 unpaired electrons in its valence band[27–29].

The key prerequisite for the use of materials in the field of electronics is its ability to participate in charge transfer. To be able to perform this, the presence of a conjugated system of single and double bonds between carbon atoms and the presence of free charge carriers is the necessary structural parameter[18,30].

The formation of a conjugated double bonds system results in $sp^2$ hybridization of the carbon atoms, where the 2s orbital is mixed with two of the three available 2p orbitals (denoted as $2p_x$ and $2p_y$). Thus it forms the trigonal planar molecular geometry. The carbon atom is placed in the centre, and triangle tops are formed by hybridizationed orbitals with unpaired electrons, which are participating in the creation of a total of three $\sigma$-bonds. The

remaining $2p_z$ orbitals containing the unpaired electrons involved in the π-bonds formation are placed perpendicular to the plane of the triangle[27–29]. In structures containing conjugated double bonds system, π-bonds are spread over the structure, and therefore, π-electrons are delocalized over the whole skeleton of the molecule[29]. Their free mobility then allows these molecules to participate in charge transfer[31]. The described phenomenon is shown schematically in *Figure 3*.



(a)                                         (b)
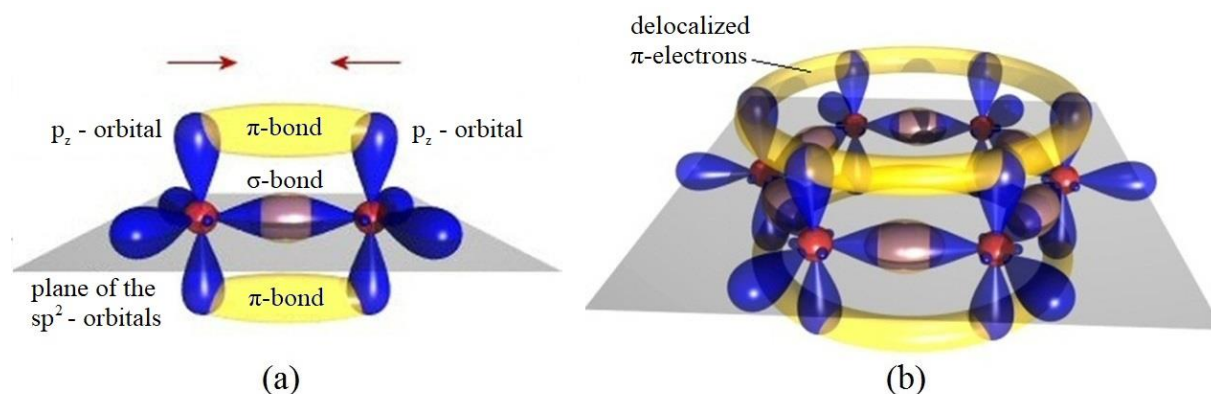
***Figure 3****: Formation of π-bonds in the ethene molecule (a) and the benzene molecule (b)*

For solid-state crystalline materials applies the band theory, which explains how the atoms in the crystal lattice overlap their orbitals, describes the states of electrons and forming of discrete energy bands[32,33]. The valence band is the last band of the electron shell containing electrons in the ground state and is therefore responsible for the formation of chemical bonds, as was discussed above. Band enabling charge transfer is called the conduction band, and it is the first unoccupied electron band in the ground state. In the case of materials known as conductors (typically metals), these two bands are in contact, respectively overlapped, and these materials are theoretically able to participate in charge transfer without any supply of energy. On the contrary, in the case of semiconductors and insulators, the valence and conduction bands are separated by a band gap, which is an energy range where no electron states can exist based on the quantisation of energy. Electrons located in the valence band can pass into the conduction band if they overcome the energy barrier, which is given by the width of the band gap. For this process, it is necessary to supply the material with energy (it can be thermal, electric or electromagnetic) of a higher value than the energy of the band gap is. Typically used units are electron volts (eV). It is generally considered that the band gap energy of semiconductors is lower than 3 eV. Materials with the band gap energy of more than 4 eV are referred to as insulators, where the flow of electrons from the valence to the conducting band becomes negligible under normal conditions[32–34].

In the case of organic semiconductors, the band gap energy denotes the energy distinction between the highest occupied molecular orbital (HOMO) and the lowest unoccupied molecular orbital (LUMO), which are the analogues to the valence and conduction bands of the above-discussed inorganic crystalline semiconductors (*Figure 4*). The HOMO and LUMO energy levels are also strongly influenced by the molecular alignment and packing of the material. Therefore, the control of HOMO–LUMO energy gap of π-conjugated systems, and hence of the band gap of the corresponding materials, is a crucial task for the organic semiconductor designing[31,35].
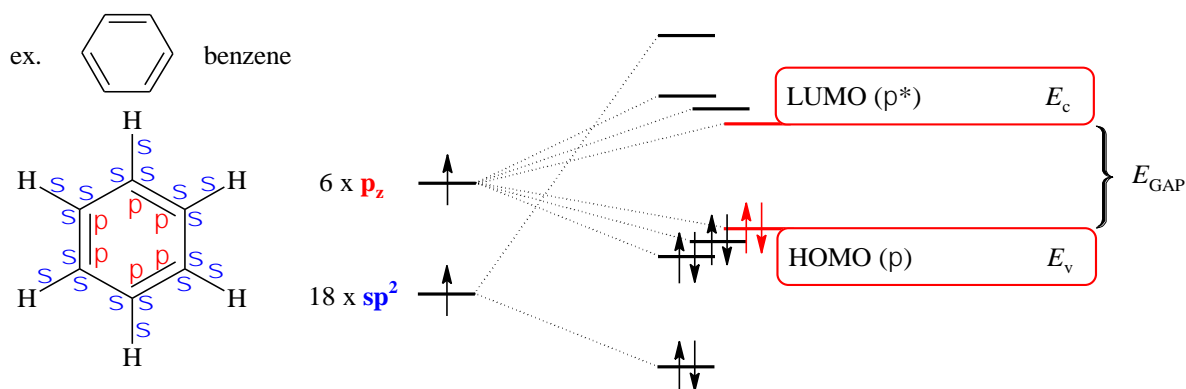
***Figure 4****: Schematic representation of the HOMO and LUMO levels for benzene*

In summary, the conducting properties of organic semiconductors are highly dependent on the band gap energy. In the case of organic π-conjugated materials, this energy is related to the electronic band structure and also depends on the pressure and temperature. Since the efficiency of charge transport across the organic thin-film layers plays a key role in the electronic devices such as OLEDs and OPVs, the knowledge of the band gap of the corresponding material is a significant factor determining the electrical conductivity of a solid. Therefore, it is clearly decisive for right choosing the organic semiconductor for the manufacturing of stable and efficient devices. Moreover, the presence of the band gap allows organic semiconductors to absorb light radiation, which extends the application potential of these materials[31,35].

Organic substances suitable for applications in organic electronics can be divided into two fundamental groups: narrow band gap low molecular weight organic compounds (usually called "small molecules")[36] and polymers[37]. The first mentioned group includes substances having a relative molecular weight in the order of tens to a maximum of hundreds of g mol$^{-1}$, while polymers are compounds possessing a relative molecular weight typically in thousands of g mol$^{-1}$ and a key parameter affecting their properties is the polydispersity. Both of these groups of substances are still an attractive subject of interest in contemporary world research[36,37], and the individual groups of derivatives that are covered by my research will be discussed in the following chapters.

### 3.2.1   Organic high-performance pigments

High-performance organic pigments are a fairly wide range of substances, with excellent intense colouring, high stability against temperature and surrounding physical phenomena. They are normally used for dyeing plastics and synthetic fibres; many of them are also included in surface coatings such as varnishes and inks[38]. A number of organic pigments are commonly found in nature, such as indigo in a plant of the same name. In most cases, however, their large-scale industrial production is also possible, which greatly contributes to the abundant expansion of pigments and the ability to find applications in other industries[38].

Over several years of research, it has been found that many molecules of organic pigments are able to participate in the transfer of charge carriers due to the presence of the delocalized π-electron system, thus rapidly incorporating them into a class of substances called semiconductors. This discovery sparked a rocket growth of interest in organic pigments in the areas of organic electronics, and these derivatives are still the focus of many research teams around the world[8,10,13–15,38].

As already mentioned, small molecules of organic pigments generally allow for a very diverse range of chemical derivatization, thereby targeting and designing the desired properties[17,39]. Organic semiconductors can be categorically divided into *n*-type, *p*-type, and ambipolar, depending on whether they mediate the transport of electrons, holes, or both types of charge carriers. The following chapters will deal with the groups of substances involved in my research, i.e. selected important organic high-performance pigments, related π-conjugated molecules and their derivatization; especially in terms of their applications in OFETs and marginally other devices, chemical modifications and structure influence on their properties.

### 3.2.1.1 Diketopyrrolopyrroles (DPPs)

The main backbone of the diketopyrrolopyrrole (DPP, **1**) molecule forms a bicyclic dilactam of aromatic character, with the systematic name 2,5-dihydropyrrolo[4,3-*c*]pyrrolo-1,4-dione (**Figure 5**). The DPP molecule was first prepared in 1974[40], and shortly thereafter it became widely used as a pigment in inks, as well as in paints for coating purposes, and its potential for applications in organic electronics has been hidden for many years. The first solution-processable DPP-based semiconductors for OPV[41] and OFET[42] devices was synthesized and reported only in 2008, and it has since been a key fragment of several thousands of scientific papers focused primarily on organic electronics[43,44]. With this discovery, the DPP molecule has indeed been recognized as a promising conjugated building unit to construct high-performance semiconducting materials for various electronic devices. Moreover, the facile synthesis of the DPP and the possibility of its easy chemical derivatization, which allows tuning the optoelectronic properties to match the requirements for the corresponding devices, are the key benefits for their widespread use[44].



R = H, alkyl, aryl, acyl

Ar = aryl, heterocycle (e.g. thiophene, furan)
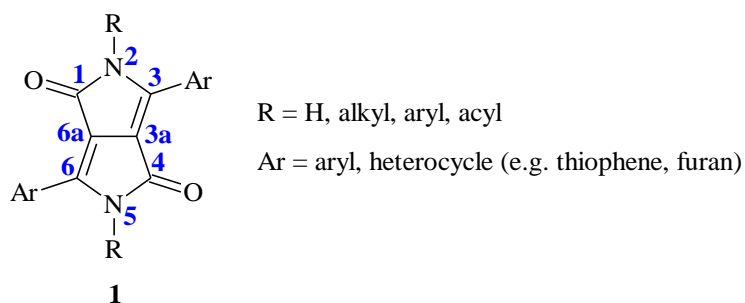
**Figure 5**: *The general skeleton of the DPP molecule (**1**) with atom numbering*

Over the last several decades, synthetic modifications of the DPPs have been able to significantly improve the performance of electronic devices based on these derivatives. Therefore, the DPP molecule has proven to be a successful building block for constructing high-performance functional materials that are suitable for a wide range of applications in the

electronic industry as already mentioned[44]. However, interest in derivatives based on the DPP molecule has so far not slackened, and even today, an average of about 150 scientific publications and more than 200 patents dealing with these organic pigments are recorded annually[45].

Concerning the transport characteristics of DPP-based small molecules in OFET devices, one of the best *n*-type material has so far been obtained as the DPP derivative **2** (***Figure 6***) prepared in 2013 by Park et al.[46] The presence of strong electron-accepting dicyanovinyl functional groups on the side thiophene rings led to the formation of a well-defined lamellar structure with highly dense-packed molecular conformation in the solid-state. Atomic force microscopy (AFM), wide-angle X-ray scattering (WAXS) and out-of-plane X-ray diffraction (XRD) measurements confirmed this quasi-planar arrangement with strong π-π interactions and *p*-orbital overlap, which greatly enhanced the electron mobility of the material. As a result, both the single-crystal OFET and vacuum deposited polycrystalline film OFET devices based on this derivative reached excellent values of electron mobility ($0.96 \ cm^2 \ V^{-1} \ s^{-1}$ and $0.64 \ cm^2 \ V^{-1} \ s^{-1}$, respectively)[46].

On the other hand, the DPP derivative **3** (***Figure 6***) with incorporated nitrile functional groups into α-positions of the thiophene rings exhibited remarkable *p*-type characteristics[47,48]. Using the AFM analysis, the topography of thin functional layers based on derivative **3** was studied at different temperatures of the deposition in the range from 20 to 90 °C. The most suitable crystalline arrangement of the layer was formed at a deposition temperature of 70 °C, where the hole mobility achieved the excellent value of $0.70 \ cm^2 \ V^{-1} \ s^{-1}$.
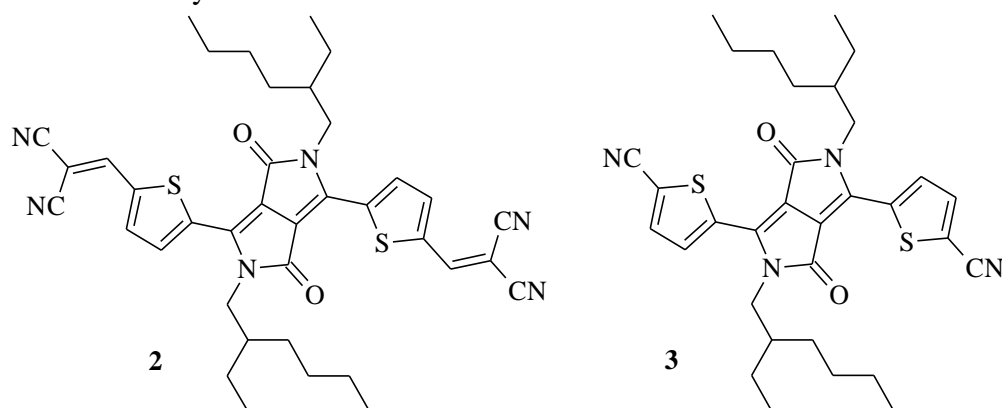


***Figure 6***: *Derivatives **2**[46] exhibiting n-type and **3**[47,48] exhibiting p-type characteristics*

When comparing these two derivatives mentioned above, it is obvious that an increase in acceptor strength can lead to a large change in the charge transport properties from *p*-type to *n*-type. Ghosh et al.[49] described the same phenomenon, where the substitution of a terminal functional group from amide (**4**) to ester (**5**, ***Figure 7***) group also changed charge carrier polarity from *p*- to *n*-type semiconductor, which was confirmed by measurements of photoconductivity and field-effect transistors. The molecule **4** exhibited moderate hole mobility $0.013 \ cm^2 \ V^{-1} \ s^{-1}$, whereas good electron mobility was observed for the derivative **5** with a value of $0.015 \ cm^2 \ V^{-1} \ s^{-1}$. Therefore, the modification of the terminal functional groups can be an efficient and simple method to alter the character of organic semiconductors.
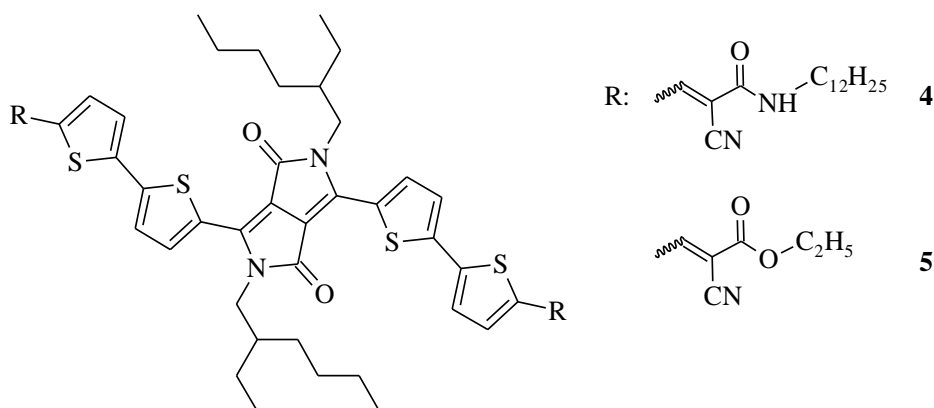
*Figure 7: Derivatives 4 exhibiting p-type and 5 exhibiting n-type characteristics*[49]

In all the above-discussed cases, DPP derivatives were substituted on the nitrogen heteroatoms by alkyl chains, specifically 2-ethylhexyl. Alkylation of the DPP derivatives is a very important and long-term most widely used modification[45], which makes the derivatives more readily applicable in many areas of organic electronics. In the case of basic *N,N'*-unsubstituted DPP derivatives, numerous intermolecular hydrogen bonds are present, causing their very low solubility in most common organic solvents. The formation of these hydrogen interactions is interrupted by introducing alkyl chains onto the nitrogen heteroatoms of the DPP derivatives, resulting in a significant increase in the solubility of *N,N'*-substituted derivatives. Thus, this modification allows for much simpler processability of the resulting materials in the solution and, therefore, their applicability in important branches of the organic electronics industry, such as printed and flexible electronics[44].
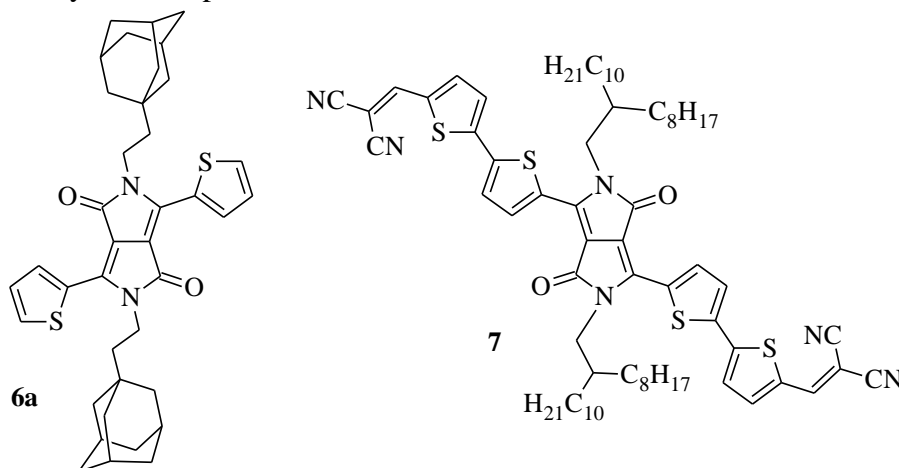


*Figure 8: Derivatives 6a[50] and 7[51] exhibiting ambipolar transport characteristics*

In 2017 Krajčovič et al.[50] prepared a very significant DPP derivative **6a** (*Figure 8*) exhibiting ambipolar characteristics by just one synthetic step, specifically by incorporating the ethyladamantyl side chains into the structure of the basic DPP core. Mobility values for holes $0.05 \ cm^2 \ V^{-1} \ s^{-1}$ and electrons $0.20 \ cm^2 \ V^{-1} \ s^{-1}$ have been achieved in the **6a**-based OFET devices, which are extremely exceptional parameters in this category of such modified DPP derivatives. For comparison, the DPP derivative **7** (*Figure 8*) purpose-designed for ambipolar properties, contains 2-octyldodecyl side chains and additionally has an extended π-conjugation through 2 thiophene rings with strong electron-accepting dicyanovinyl groups,

requires a multi-step, much more sophisticated synthetic approach[51]. In case of this derivative **7**, the values for the mobility of the holes were obtained 0.031 cm$^2$ V$^{-1}$ s$^{-1}$ and for the electrons 0.065 cm$^2$ V$^{-1}$ s$^{-1}$, therefore in both cases significantly lower than for the DPP derivative **6a**. This is due to the original and so far unexplored contribution of bulky adamantyl substituents that initiate highly organized arrangement of the DPP molecules into triads by van der Waals interactions. It leads to a more advantageous intermolecular packaging with an exceptionally low distance between conjugated DPP cores (plane-to-plane aggregations of only 3.37 Å, confirmed by X-ray diffraction analysis [XRD], *Figure 9*). This arrangement allows for the formation of very strong π-π electron stacking, responsible both for the relatively high thermostability of the material and for improving its charge carrier mobilities[50].
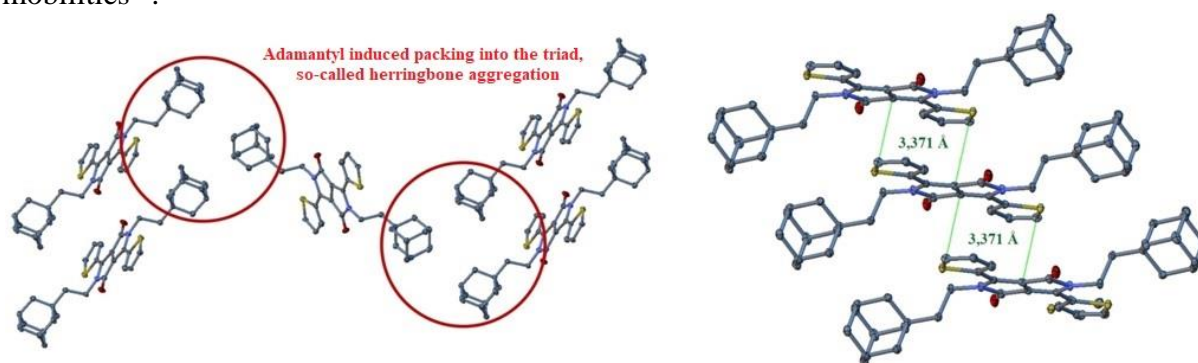


*Figure 9*: *Adamantyl-induced packing of the 6a derivative, confirmed by XRD analysis*[50]
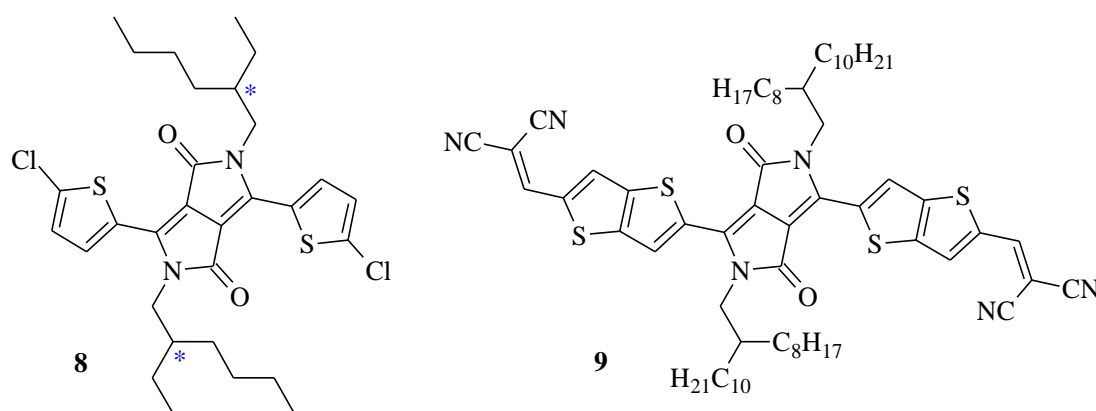


*Figure 10*: *Derivatives 8*[52] *and 9*[51] *studied OFET devices*

A very interesting study reported in 2018 by He et al.[52] deals with the importance of branched side-chain chirality for packing arrangement and thus for the mobility of the material. Stereochemically pure enantiomers (*R/R* and *S/S*) and mesomer (*R/S*) were isolated for the chlorinated DPP derivative **8** (*Figure 10*), and they were used for fabrication of both vacuum-processed thin-film transistors (TF-OFETs) and single-crystal transistors (SC-OFETs). The same trend was observed for both types of OFETs. While the enantiomers (*R/R* and *S/S*) exhibited a distinct decrease in performance and significantly faster degradation process upon storage in the ambient atmosphere; the highest so far in the literature reported *p*-type characteristic of OFET based on DPP-small molecule was reached for mesomer (*R/S*) with hole mobility of 0.74 cm$^2$ V$^{-1}$ s$^{-1}$ (for TF-OFET) and 3.40 cm$^2$ V$^{-1}$ s$^{-1}$ (for SC-OFET),

respectively. Such superior performance of (*R/S*) mesomer-based transistor was attributed to the tightly-packed coplanar structure of self-segregated DPP cores from the branched alkyl side-chains with the large π-π overlap and additional hydrogen bonds between adjacent DPP molecules. Therefore, the chirality control of branched side-chains could be very useful to achieve better charge transport properties of the materials[52].

The proof that the character of the aryl-substituents at 3,6-positions of the DPP also has a large influence on the transport properties of the resulting material was provided by the work of Lin et al.[51] They studied the effect of prolongation of π-conjugation of the derivative substituted by previously mentioned strong electron-accepting dicyanovinyl groups on charge carrier mobilities. The π-conjugation length was extended by introducing bithiophene units (**7**, ***Figure 8***) and thieno[3,2-*b*]thiophene units (**9**, ***Figure 10***). Whereas the former derivative **7** exhibited balanced electron and hole mobilities as discussed before, the DPP derivative **9** containing thieno[3,2-*b*]thiophene as the π-conjugating spacer reached a very high electron mobility of $0.80 \, \text{cm}^2 \, \text{V}^{-1} \, \text{s}^{-1}$ upon annealing at 90 °C and a hole mobility of $0.024 \, \text{cm}^2 \, \text{V}^{-1} \, \text{s}^{-1}$ at 150 °C in fabricated OFETs. It may be attributed to the different symmetries of the HOMO and LUMO energy levels of the derivatives, leading to different injection barriers for either electrons or holes[31,51]. Therefore, this type of DPP modification is another pathway to adjust the final properties of the DPP-based materials in terms of applications in organic electronics.

### 3.2.1.2 Benzodifuranones (BDFs)

The benzodifuranone (BDF, **10**) molecule contains 2 lactone groups in its structure and forms a systematic name furo[2,3-*f*][1]benzofuran-2,6-dione (***Figure 11***).



Ar = aryl, heterocycle (e.g. thiophene, furan)

**10**
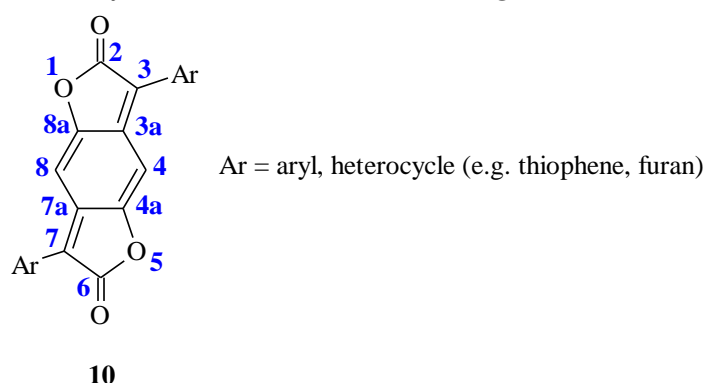
***Figure 11***: *The general skeleton of the BDF molecule (**10**) with atom numbering*

BDF derivatives rank among commercial, industrial dyes, as well as DPP derivatives. Since the 1990s, BDFs have been widely used, for example, for dyeing polyester fibres in the textile industry[53,54] and they are gradually replacing the anthraquinone and azo dyes used so far[55]. BDF derivatives excel further possibility of producing a wide spectrum of colouring, which is readily modifiable by the substituents $R_1$ and $R_2$ (**11**, ***Figure 12***), whose character significantly influences the radiation absorption of certain wavelengths[55].
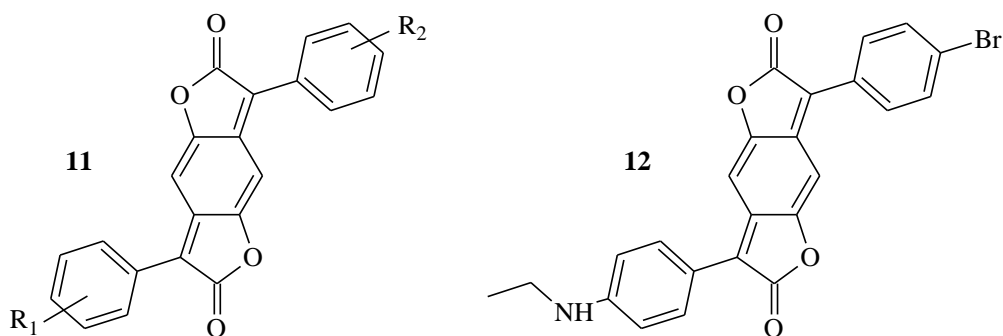
*Figure 12: Structures of the derivatives 11 and 12*[56]

In 2018 Kou et al.[56] considered the BDF derivative as a potential organic semiconductor due to the presence of the conjugated π-electron system in its structure and also due to the strong electron-acceptor character of the BDF core. In order to induce a *push-pull* effect in the molecule, which usually enhances the transport characteristics of the material, they incorporated strongly electron-donating ethylamino group into the *para*-position of the side-chain phenyl ring while the second phenyl contained the bromine atom. The resulting asymmetric BDF derivative **12** (*Figure 12*) was further used to prepare the OFET devices for the study of electrical properties.
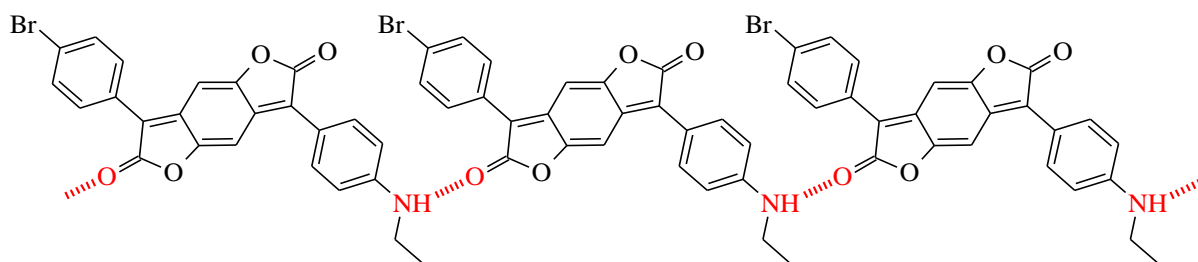


*Figure 13: Predicted mechanism of the hydrogen bonds formation in molecules of the derivative 12*[56]

The OFET devices based on the BDF derivative **12** exhibited excellent *p*-type characteristics with a maximum mobility value of the holes $0.42 \text{ cm}^2 \text{ V}^{-1} \text{ s}^{-1}$, with no significant degradation observed after two months of storage in the environment. Study of functional thin films formed by donor-acceptor material (D–A) **12** by infrared spectroscopy with Fourier transformation (FT-IR) demonstrated the presence of solid-state intermolecular hydrogen bonds (*Figure 13*) contributing to a significant increase in material crystallinity. Further, the bathochromic shift of the derivative **12** in solution by more than 100 nm was observed, indicating strong intramolecular charges of charge densities. This study[56], therefore, confirmed that also suitably modified derivatives based on BDF pigments might exhibit very promising properties of organic semiconductors, and in the future, these derivatives definitely have a great potential to find application in this field of electronics.

To the best of my knowledge, this is the only one reported utilization of the BDF material for OFET device construction.

### 3.2.1.3 Derivatives of indigo (ID) and isoindigo (IID)

Indigo is one of the world's most well known and most commonly used natural pigments. Its first confirmed use is dated to 6 000 years ago for cotton dyeing[57]. It is an intensely blue substance, originally obtained from leaves of the plant of the same name. Synthetic indigo was first prepared in 1870 and gradually replaced the natural indigo during the 19th century. Today its annual global consumption reaches several thousand tons, and it is mainly used in the textile industry[58]. The structures of the indigo (ID, **13**) molecule and its congener isoindigo (IID, **14**) are shown in the following **Figure 14**.



**13**          **14**
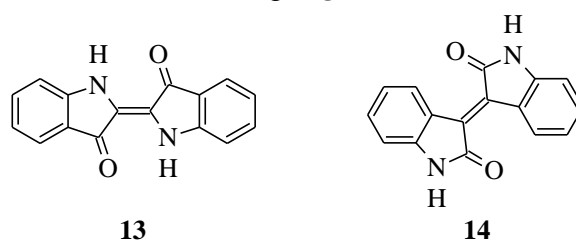
***Figure 14**: The general skeleton of the indigo (**13**) and isoindigo (**14**) molecules*

Indigo is a pigment insoluble in most common organic solvents, which has prevented its use in organic electronics for many years[59]. The first study of OFET devices based on ID derivative dated from 2012 when Sariciftci et al.[60] observed promising ambipolar transport characteristics ($\mu_{h/max} = 0.01$ cm$^2$ V$^{-1}$ s$^{-1}$ and $\mu_{e/max} = 0.01$ cm$^2$ V$^{-1}$ s$^{-1}$) in the vacuum deposited layers of derivative **13** (**Figure 15**). Sariciftci et al.[61] achieved even better properties by two years later for the derivative **15** (**Figure 15**), where the mobility values were $\mu_{h/max} = 0.11$ cm$^2$ V$^{-1}$ s$^{-1}$ and $\mu_{e/max} = 0.08$ cm$^2$ V$^{-1}$ s$^{-1}$. So far, in 2015 Mori et al.[62] published the highest obtained ambipolar characteristics for the IDs based derivatives, where the OFET devices based on the vacuum deposited layers of material **16** (**Figure 15**) exhibited mobility of the holes $0.56$ cm$^2$ V$^{-1}$ s$^{-1}$ and electrons $0.95$ cm$^2$ V$^{-1}$ s$^{-1}$. This was due to the phenyl substituents inducing the unique arrangement of the molecules of the derivative **16** in the thin layer.

Another important derivative having exceptional electrical properties is the epindolidione (EP, **17**, **Figure 15**), an analogue of indigo produced by its thermal rearrangement at 460 °C. The derivative **17** was vacuum-deposited again by Sariciftci et al.[63], and it formed a functional layer in an OFET device exhibiting an admirable *p*-type characteristic with the mobility of the holes $1.5$ cm$^2$ V$^{-1}$ s$^{-1}$.
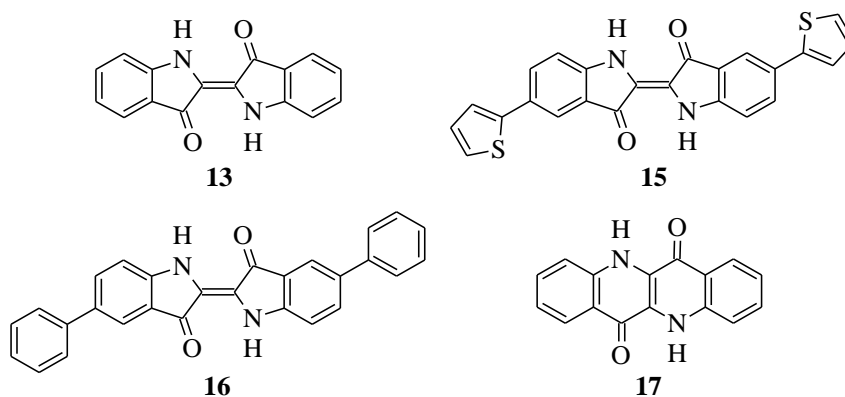
***Figure 15**: Structures of the derivatives **13**[60], **15**[61], **16**[62] and **17**[63]*

The isoindigo derivative is distinguished by its significantly higher solubility in common organic solvents compared to the indigo, which facilitates its applicability in organic electronic devices[64]. From the point of view of the structure, IID contains two lactam groups, which are part of the π-conjugated system, as well as in the case of previously discussed DPP molecule. Thus, IID derivatives may be modified by the same approach of *N,N'*-substitution reactions as well as DPPs, whereby both the solubility of the resulting derivatives and the organization of their molecules in the thin layers leading to a potential improvement in transport characteristics can be significantly influenced by incorporation of a variety of alkyl side chains. From the point of view of electrical properties, relatively small differences are between ID and IID derivatives[59].

## 3.2.2   Other structurally related substances

As already discussed, organic materials applicable in electronics must contain delocalized π-electron systems and free charge carriers in their structure and also have a narrow band gap. Obviously, organic high-performance pigments are not the only group of substances meeting these parameters. There are many structurally related molecules possessing similar properties and potential for applicability in the organic electronics area, using light absorption and emission in the ultraviolet-to-visible wavelength region, generation and transport of charge carriers, non-linear optical character and many other properties typical for these materials[65,66]. Two selected groups from these derivatives are briefly introduced and discussed in the following chapters, especially in terms of their properties and utilization.

### 3.2.2.1   Derivatives of naphthyridinedione (NTD)

The derivative referred to as naphthyridinedione (NTD, **18a**) has the systematic name 1,5-dihydro-1,5-naphthyridine-2,6-dione (***Figure 16***). Its backbone consists of the fused-ring system called naphthyridine, which is being formed by the fusion of two pyridine rings through two adjacent carbon atoms, where each ring thus contains one nitrogen heteroatom. A total of six isomers of naphthyridine can be formed (***Figure 17***). The name is dated to 1893 and is derived from the 1,8-naphthyridine derivative, which is considered as the naphthalene analogue of pyridine[67].

**18a**
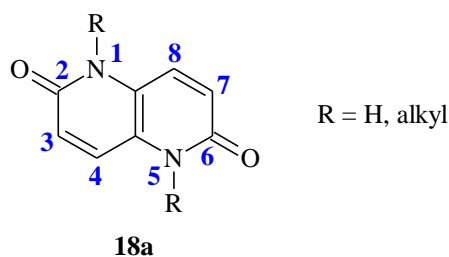
*Figure 16: The general skeleton of the NTD molecule with atom numbering*



1,5-naphthyridine    1,6-naphthyridine    1,7-naphthyridine

1,8-naphthyridine    2,6-naphthyridine    2,7-naphthyridine
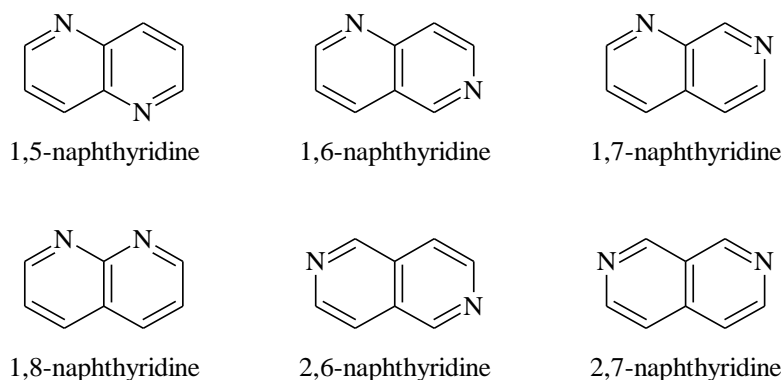
*Figure 17: All possible isomers of the naphthyridine derivative*

The NTD molecule was first synthesized in 1971 by Rapoport et al.[68], and for more than four decades, there has been no mention of the application in organic electronics of this derivative. However, the turning point came in 2013, when the NTD molecule was a key fragment of the patent related to novel polymers containing one or more units derived from the NTD and their applications as organic semiconductors especially in the areas of OPV devices and organic photodetectors (OPD)[69]. In terms of structure, the NTD is the bis-lactam unit with an electron-deficient character, thus very similar to the DPP molecule, including its potential in organic electronics applications. Although especially the difference in the ring sizes of DPP's and NTD's lactam units results in different electronic and photophysical properties, the NTD derivative again proved to be a very useful building block for organic electronics materials in 2016, when Park et al.[70] described a novel NTD based donor-acceptor type conjugated polymer (**19**, *Figure 26*) exhibiting power conversion efficiency (PCE) of up to 8.16 % in bulk heterojunction solar cells (BHJ-SCs).



**19**
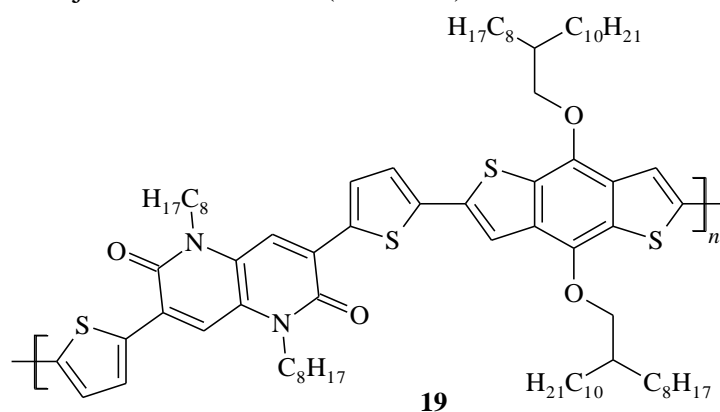
*Figure 18: The NTD polymer **19** exhibiting PCE of up to 8.16 % in BHJ-SC[70]*

In 2018 Park et al.[71] reported the interim peak of the NTDs application in organic electronics. The relationships between polymer crystallinity and photovoltaic performance were examined on a series of novel 3,7-di(thiophen-2-yl)-NTD acceptor-based conjugated polymers with 2,2'-bithiophene, thieno[3,2-b]thiophene and 3,3'-difluoro-2,2'-bithiophene donor units, respectively. The NTD-based polymer containing difluorinated bithiophene units (**20**, *Figure 19*) exhibited superior polymer crystallinity, the highest light absorptivity and the lowest HOMO energy level among the three polymers studied. Consequently, the NTD polymer **20** reached an excellent PCE of up to 9.63 % in a BHJ-SC based on this derivative. Therefore, the NTD molecule has again proven to be a versatile acceptor building block for this kind of device.
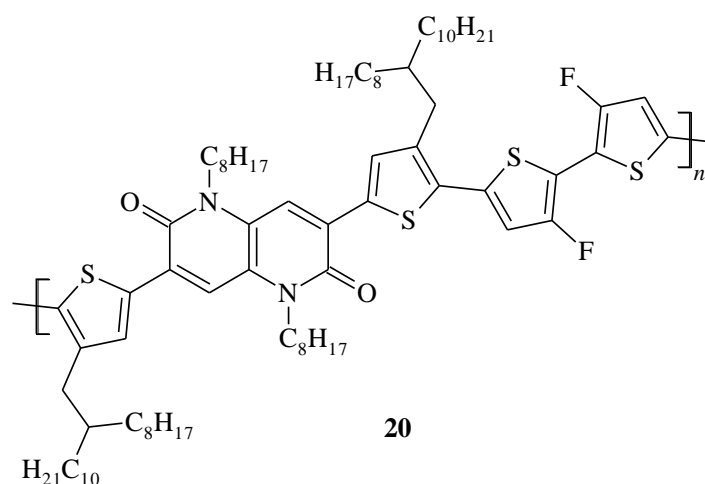


***Figure 19****: The NTD polymer **20** exhibiting an excellent crystallinity and PCE of up to 9.63 %*[71]

### 3.2.2.2 *Derivatives of polythiophene (PT)*

Thiophene is an important heteroaromatic compound consisting of a five-membered planar ring with a sulphur heteroatom (**21**, *Figure 20*). It has become one of the most studied and used heterocycles in organic chemistry and related areas due to its easy processability, high chemical stability and its synthetic applications. Thiophene is considered a very versatile unit allowing great diversity in thiophene-based chemical structures through functionalization in positions α and β or at the sulphur atom itself. Thus, indeed many regioregular oligomers and polymers with a wide range of chemical derivatization can be prepared including linear, branched, star-shaped oligomers and even thiophene dendrimers. Moreover, thiophene is a relatively cheap, easily available starting material, obtainable as a side product of petroleum distillation[72]. The industrial applicability of thiophene derivatives dates back to the late 1950s in dye chemistry[73], and over time it has spread into modern drug design[74], electronic and optoelectronic devices[75,76] and currently thiophene oligomers and polymers find particularly significant application as organic semiconductors due to their fully conjugated structures[77].

In 1986, the first solid-state OFET was fabricated utilizing a film of polythiophene (PT, **22**, *Figure 20*) as a semiconductor[78]. This device showed carrier mobility ~$10^{-5}$ cm$^2$ V$^{-1}$ s$^{-1}$. Due to very limited solubility of **22** in almost all common solvents and thus also its minimal applicability and solution processability, 3-alkylated polythiophenes (P3AT, **23**, *Figure 20*)

were most extensively investigated in terms of utilization as active layers in OFETs. In general, the introduction of alkyl chains on the π-conjugated backbone of the PT results in ameliorated solubility of the resulting polymer in most common solvents. On the contrary, it correspondingly rises the polythiophenes HOMO energy levels, which makes polymer significantly less stable in air[77].
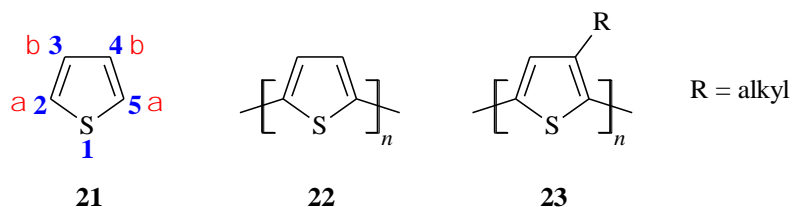


**Figure 20**: *The general skeleton of the thiophene (**21**), polythiophene (**22**) and poly-3-alkylthiophene (**23**)*

Regarding electrical properties, the **23** regioregular head-to-tail (HT) arrangement is very important as it provides larger charge carrier mobilities compared to a region-random arrangement[77]. Poly-3-hexylthiophene (**23a**, *Figure 21*) is one of the most popular and used derivatives based on P3AT, especially in photovoltaic research[79]. In the edge-on direction of adjustment on the substrate, the regioregular **23a** gives mobilities in the range of 0.05–0.20 $cm^2\ V^{-1}\ s^{-1}$. Nevertheless, devices based on this derivative showed degradation even after storing in the air for only a month, where the decrease in mobilities is amplified by increasing humidity[77]. This is primarily due to the high sensitivity of **23a** to atmospheric oxygen. Ong et al.[80] described poly-3,3‴-didodecylquaterthiophene (**24**, *Figure 21*) prepared by FeClB₃B-mediated oxidative coupling polymerization, where dodecyl chains were substituted on only half of the thiophene rings. According to transmission electron microscopic (TEM) analysis of annealed thin films of this derivative, **24** possesses a natural ability to self-organize into highly ordered lamellar π–π stacking structures, reminiscent of the self-assembly exhibited by regioregular derivatives based on **23**[81]. Therefore, organic thin-film transistor (OTFT) devices with **24** semiconductor channel layers reached the mobility of up to 0.14 $cm^2\ V^{-1}\ s^{-1}$ after annealing at 120–140 °C. In addition, **24** showed lower HOMO energy levels compared to polymer **23a**, leading to its significantly higher stability under ambient conditions in the dark[80].
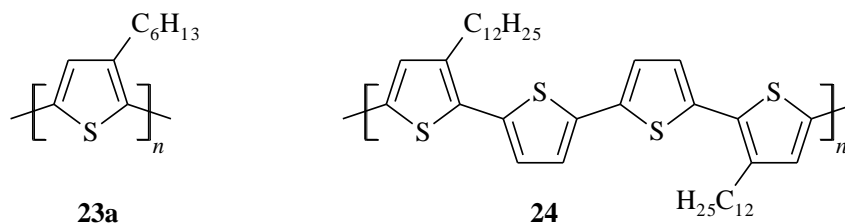


**Figure 21**: *Poly-3-hexylthiophene (**23a**) and poly-3,3‴-didodecylquaterthiophene (**24**)*

McCulloch et al.[82] described another very interesting thiophene-based polymer comprising thieno[3,2-*b*]thiophene (**25**, *Figure 22*). This fused aromatic thiophene unit has larger resonance stabilization energy than the single thiophene ring, which causes that the π-electron delocalization from thienothiophene into the backbone is less favourable. The reduced delocalization along the polymer backbone results in a lowering of the polymer HOMO

energy level, leading to good air stability of this polymer. OFET devices based on **25** reached the charge carrier mobilities of up to 0.63 cm$^2$ V$^{-1}$ s$^{-1}$ on annealed devices in a nitrogen atmosphere[82].

Müllen et al.[83] have prepared a series of four thiophene-based polymers with a central repeating unit of the benzo[2,1-*b*;3,4-*b'*]dithiophene. The optimum structure for OFET characteristics has been found for the polymer referred to herein as **26** (***Figure 22***), which was prepared with the molecular weight of 21 kg mol$^{-1}$. Linear dodecyl chains on side thiophene rings allowed its high solubility in dichlorobenzene (>20 mg mL$^{-1}$ at 50 °C), leading to its easy solution processability. The introduction of the fused benzodithiophene unit into a semiconducting polymer backbone brought key requirements for the applicability of the resulting derivative. The crucial feature is the curvature of the polymer backbone caused by the benzodithiophene, where the presence of periodic kinks leads to an efficient and modulated aggregation of the polymer to highly ordered films. However, the aggregation is not too strong, so that, unlike the other polymers described, sufficient processability of **26** is possible. Furthermore, **26** has been shown to be an ideal candidate for the application on a flexible substrate of polyethylene terephthalate (PET), where it reached high charge carrier mobilities of up to 0.5 cm$^2$ V$^{-1}$ s$^{-1}$ in top-gate OFET devices, which demonstrates the great potential of this material for industrial applications[83].
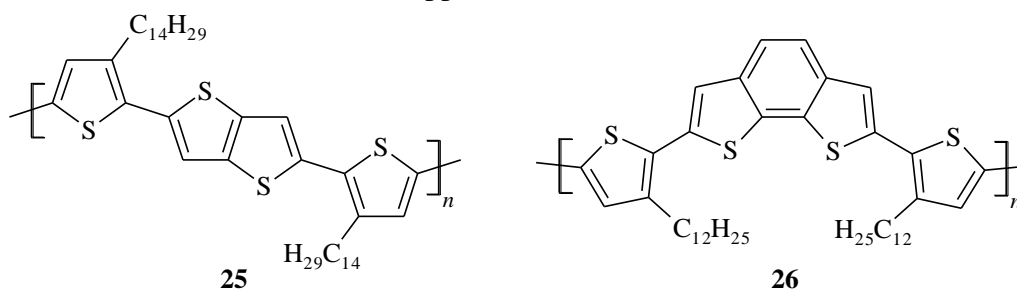


***Figure 22***: *Structures of discussed derivatives **25** and **26***

However, our team was also involved in the issue of thiophene-based derivatives, although this is only a fundamental study. In 2015 Krajčovič et al.[84] prepared a series of four phenylene-dithienyl trimmers alkylated with dodecyl chains orientated "in" or "out" (i.e. 3,3'- and 4,4'-positions) and combination with or without tetrafluorination of the phenylene unit in the centre. In the case of non-fluorinated derivative **27** (***Figure 23***), the steric hindrance in molecules caused by the "in" position of dodecyl chains prevents interaction among the conjugated cores, which results in the solid-state organization through peripheral alkyl chains. Therefore, the derivative **27** exhibited an exceptional increase in solid-state fluorescence with a quantum yield of approximately 40 %, making this material a prospective solid-state organic dye in the deep-blue region[84].
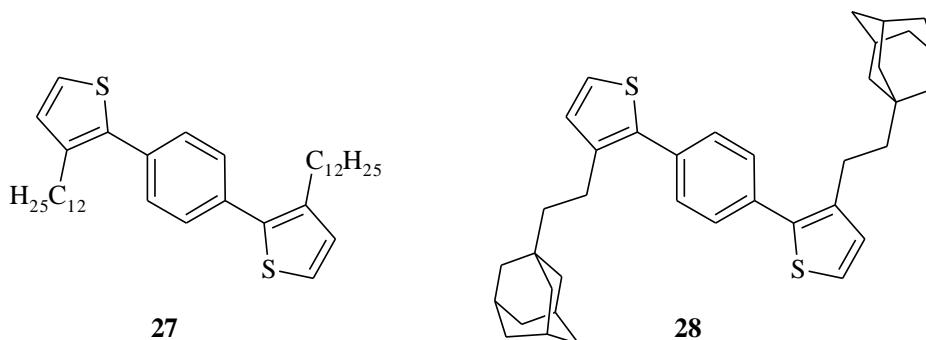
*Figure 23: Structures of discussed derivatives 27 and 28*

A year later, Krajčovič et al.[85] described a novel trimmer substituted with ethyladamantyl chains at the 3,3'-positions ("in" orientation), which is referred to herein as **28** (*Figure 23*). Due to the adamantane tendency to self-organize[86], the incorporation of these bulky alkyl chains induces the formation of highly organized crystals in the solid-state. Therefore, a high degree of self-assembly of the **28** molecules with 3D packing was observed through the hydrogen bonds between adamantyl and thienyl units and molecular pairing of the ethyladamantyl side chains. Moreover, due to the bulkiness of adamantyl groups and the interruption of π-conjugation between these alkyl units and the central phenylene-dithienyl core, the steric hindrance is provided, which prevents the intermolecular charge transfer and on the contrary, it preserves the fluorescent conditions. As a result, the derivative **28** exhibited an extraordinarily high melting point of about 250 °C (for comparison, the derivative **27** showed a melting point at approx. 50 °C) and also a significant increase in fluorescence quantum yield of up to 50 %, which is a comparable performance with some commonly used organometallic dyes. These obtained parameters, together with the relatively simple, cost-effective and environmentally-friendly potential mass production, make this material a highly attractive for use as a fluorescent dye in OLED devices[85]. In addition, the introduction of adamantyl side chains is applicable to a wide range of organic compounds, offering a great and relatively simple pathway to enhance the properties of materials for organic electronics applications[50,85].

# 4 TARGET MOLECULES AND THEIR SYNTHESIS

## 4.1 Modification of DPP derivatives

Many approaches to preparing the DPP molecule (**31**) have been developed since its discovery in the early 1970s by Farnum et al.[40], and all of them are clearly described in review from Gryko at al.[45] By far the most used method is a condensation of nitrile-derivatives (**29**) with succinic acid esters (**30**, *Scheme 1*), which are substrates derived by retrosynthetic analysis from the *Reformatsky* mechanism of the DPP molecule synthesis, developed in the early 1980s by the Ciba-Geigy AG company[87].
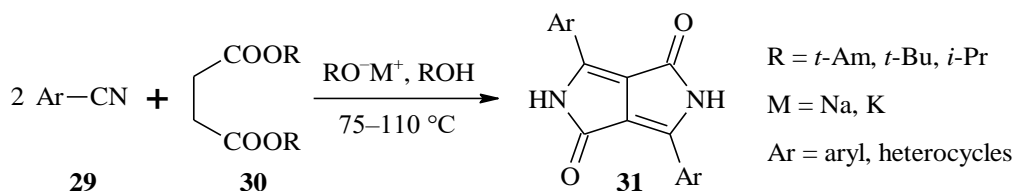


**Scheme 1**: *Succinic method to preparation the DPP molecule (31)*[87]

The DPP skeleton contains several reactive functional groups, which provides a varied range of substitution reactions, both electrophilic and nucleophilic[88], as shown in *Figure 24*.



EDG: electron-donating group / R (e.g. OH, SH, Cl)

EWG: electron-withdrawing group (e.g. CN, COOR, $NO_2$)
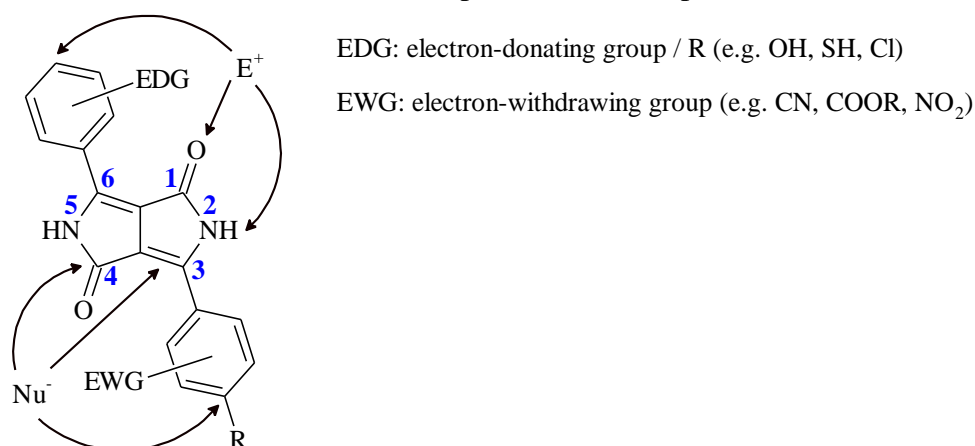
**Figure 24**: *Reactivity of the DPP skeleton with phenyl side-chains*[88]

In the following chapters, the most important modifications of DPP derivatives will be discussed from the point of view of this dissertation thesis.

### 4.1.1 *N,N′*-alkylation

Substitution of protons in lactam groups in the DPP molecule by alkyl chains is one of the most important and most used modifications[45]. Incorporation of alkyl substituents on nitrogen heteroatoms leads to significant changes in the physical and chemical properties of the resulting DPP derivatives, mainly due to interruption of intermolecular hydrogen bonds forming[89]. Therefore, alkylated DPP derivatives become much more soluble in most common organic solvents, in contrast to *N,N′*-unsubstituted derivatives which suffer from very poor solubility. Indeed, better solubility of the final DPP derivatives is usually the primary purpose of this type of modification[89].

Alkylation of the DPP molecule (**31a**) is a typical mechanism of nucleophilic substitution[90], as shown in ***Scheme 2***. In the first step, the deprotonation of nitrogen atoms occurs in the presence of a base and the subsequent formation of nucleophiles, i.e. the DPP salt. In the second step, the nucleophiles substitute halogen atoms in the appropriate haloalkanes to form alkylated-DPP (**32a**–**c**)[91].
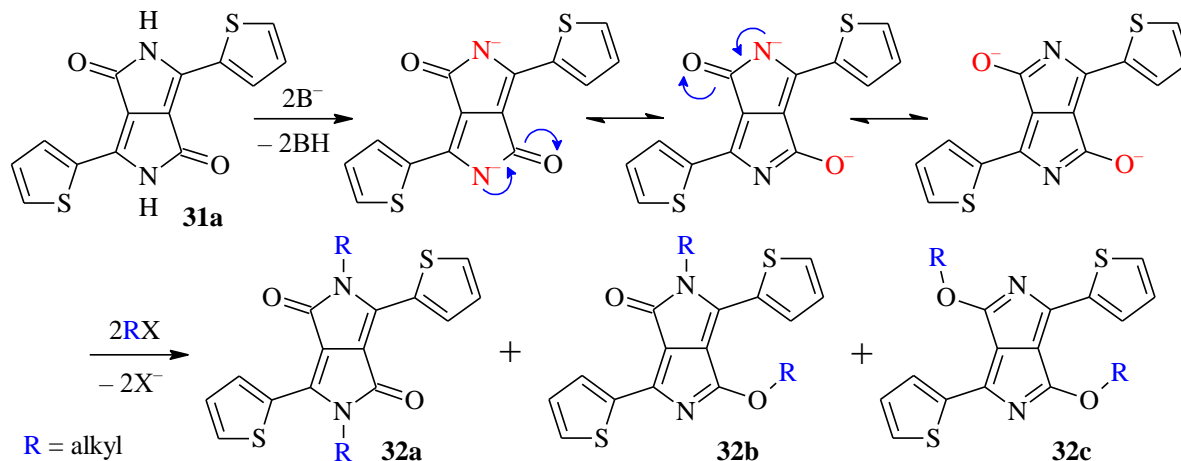


***Scheme 2****: Mechanism of nucleophilic substitution – alkylation of the DPP molecule*[91]

The limitation of this modification is the fact that the forming DPP nucleophiles have an ambiguous nature when the negative charge is divided between nitrogen and oxygen atoms of the lactam group. Because of this, the DPP-anions are effectively stabilized, and in case of DPP molecule, they provide substitution products of three types: *N,N'*-; *N,O'*- and *O,O'*-alkylated. Geerts et al.[92] firstly reported the possibility of this reaction progress and Frebort et al.[90] definitely experimentally confirmed this assumption one year later, when they alkylated asymmetrical DPP derivative and they isolated and characterized 4 from totally 8 possible products (mono-*N*-; *N,N'*-; *N,O'*- and *O,N'*-alkylated).

From the point of view of factors, which may affect the regioselectivity of the nucleophilic substitution, there are many possibilities. Wide variability is given by the use of a base in terms of its strength and a character of cation[93]. Other options are the use of solvent and reaction conditions – temperature and time[92]. The influence of factors mentioned above was studied[92], but no significant differences were observed. Typical and most widely used reagents for the alkylation of DPP derivatives are potassium or caesium carbonate ($K_2CO_3$/$Cs_2CO_3$) as bases, *N,N*-dimethylformamide (DMF) or *N*-methylpyrrolidone (NMP) as solvents and the reaction is usually carried out at a temperature higher than 100°C and for several hours (5–24)[45].

Zhao et al.[94] reported that the character of alkyl chains has a significant influence on the regioselectivity of the nucleophilic substitution of the DPP. In case of using linear alkyl chains (e.g. octyl), the major product is the *N,N'*-alkylated whereas *O,O'*-alkylated is not possible to isolate. When using branched alkyl chains (e.g. 2-ethylhexyl), a significant increase in *N,O'*- and *O,O'*-alkylated product at the expense of *N,N'*-alkylated is observed[94]. Substitution of the DPP by bulky alkyl chains was unknown until 2017[50] when the unique adamantyl-substituted DPP derivative was prepared, as was discussed in the Review part (*Chapter 3.2.1.1*). The bulky character of alkyl chains has an even more adverse effect on the

regioselectivity of the nucleophilic substitution to the *N,N'*-positions. On the other hand, a greater proportion of *N,O'*-; *O,O'*- and also mono-*N*- and mono-*O*-substituted derivatives can be expected.

Asymmetrically substituted DPP derivatives by bulky alkyl chains still remain understudied. Nonetheless, *O,O'*- and especially asymmetrical *N,O'*- substituted derivatives can be a point of interest not only from fundamental but also from a practical point of view. So the goal is to isolate and characterize these new adamantyl-substituted DPPs and then, investigate their electrical and optical properties and potential use in modern applications of organic electronics.
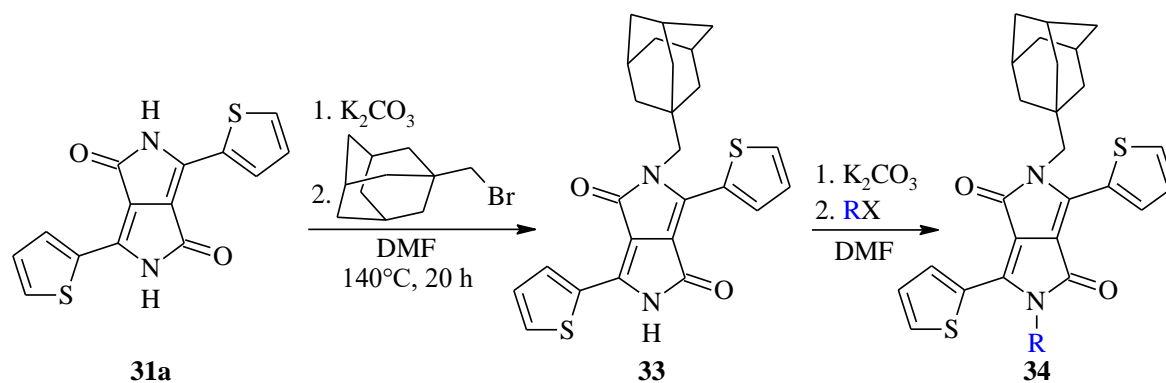


*Scheme 3*: *Preparation of the unique asymmetrical N,N'-alkylated DPP derivative (34)*

Another very important objective is to isolate and utilize the mono-alkylated DPP derivative (**33**) for the preparation of an asymmetrically substituted DPP with two different alkyl chains (**34**), as is shown in *Scheme 3*. This approach, through the incorporation of one bulky alkyl chain followed by substitution of another alkyl, is based on the already described two-step alkylation method by two different alkylating agents[95,96]. This type of material could be very interesting from the point of view of studying thin layer molecular arrangement and thus also its properties.

## 4.1.2  Variation of aromatic side chains

In most cases, the DPP derivatives contain aromatic side chains in positions 3 and 6. Their character has a crucial influence on the resulting derivatives, both in terms of reactivity and final properties[97,98]. The first known DPP molecule[40] contained phenyl aromatic rings. During the next few years, many DPP derivatives with a varied range of different aromatic substituents in these positions were described[45]. One of the most useful and most common DPP derivatives is the thiophene-containing one (**31a**)[99].

Based on the formation of the DPP molecule described in *Chapter 4.1* (*Scheme 1*), it is clear that the nearest aromatic rings in positions 3 and 6 are an integral part of the DPP molecule since its inception, without any possibility to substitute these aromatic cycles later[87]. However, the discussed succinic method of preparation the DPPs allows relatively wide variability in the use of aromatic nitrile derivatives – e.g. phenyl[100], thiophene[101], selenophene[102], furan[100], naphthalene[103], phenanthrene[104] etc. The limitation of this method is the solubility of the respective aromatic nitrile in the solvent used, most often in tertiary

alcohol (*tert*-amyl alcohol, TAA)[105]. Therefore, it is impossible to prepare a DPP derivative containing any longer polyaromatic cycle in positions 3 and 6 than previously mentioned by this approach. Based on my own experiments[106], while the 2,2'-bithiophen-5-yl containing DPP (**35**) could be prepared by the succinic method from 2,2'-bithiophene-5-carbonitrile (**36**), the [2,2':5',2''-terthiophene]-5-carbonitrile (**38**) was not suitable for the DPP derivative formation (**37**), precisely due to limited solubility in TAA (***Scheme 4***).
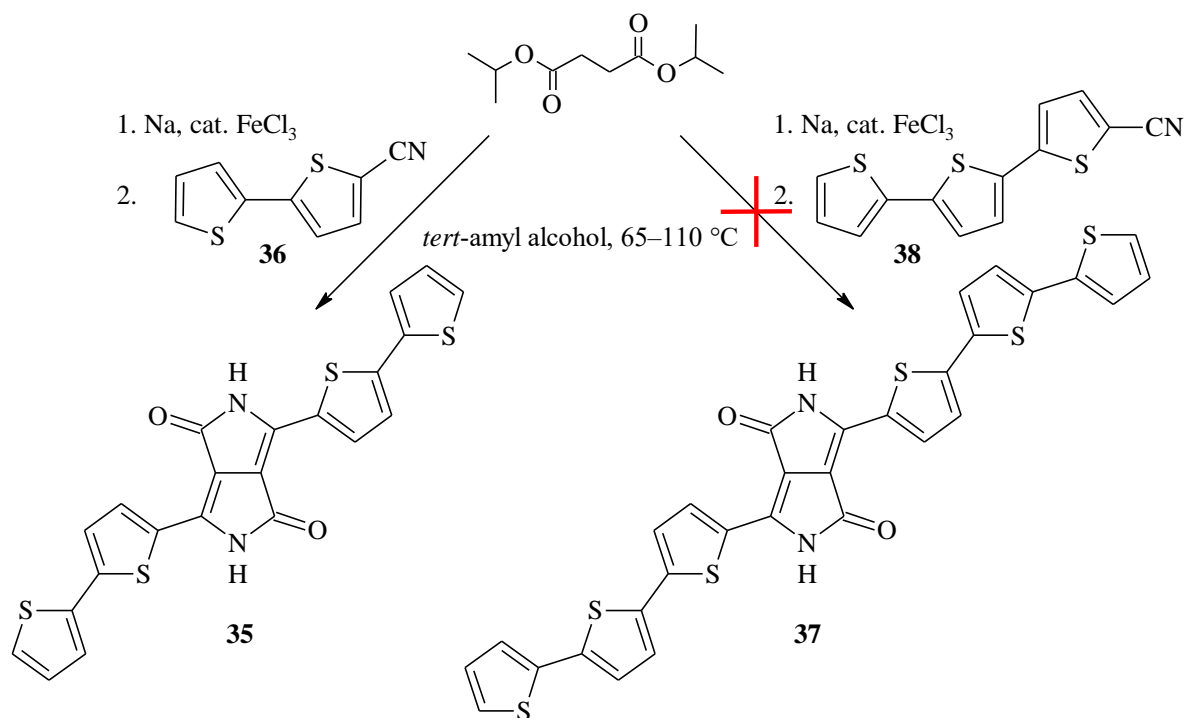


***Scheme 4***: *Preparation of polythiophene DPP derivatives by the common succinic method*

The presence of polycyclic aromatic chains in positions 3 and 6 of the DPP derivative causes the prolongation of π-electron conjugation, which is very important from the point of view of the resulting properties. This type of modification usually leads to an increase in thermostability, bathochromic shifts in absorption and emission maxima and can significantly affect thin layer arrangement of the molecules[107]. There are two main approaches to prepare DPP derivatives with prolonged π-conjugation.

### 4.1.2.1 Cross-coupling reactions

One of them is palladium-catalysed *cross-coupling* reactions, which are divided into several types. *Stille cross-coupling*[108] reaction using organotin compounds is one of the most used and explored methods for prolongation of 3,6-aryl side chains in DPP derivatives[109]. However, due to the high toxicity of organotin intermediates, the *Suzuki cross-coupling*[110,111] reaction using boronic acid derivatives is increasingly preferred to *Stille*[89]. Other options of *cross-coupling* reactions for the discussed type of DPP modification are *Heck* reaction using alkenes[112], *Sonogashira* reaction using alkynes[113] or *Buchwald-Hartwig* reaction using primary and secondary amines[114]. An overview of all above types of *cross-coupling* reactions is clearly illustrated in ***Scheme 5***, including the resulting products. All of these reactions can

be used for both prolongation of π-conjugation and chemical polymerization of the DPP derivatives.



| X = S, O, Se, –CH=CH–<br>$R_1$ = alkyl<br>$R_2$ = aryl, alkyl | Reagent | Reaction | Product |
|---|---|---|---|
| | $ArB(OAlk)_2$<br>$ArB(OH)_2$ | Suzuki | Z = –Ar |
| | $ArSnAlk_3$ | Stille | Z = –Ar |
| | $R_2$–CH=CH$_2$ | Heck | Z = −CH=CH−$R_2$ |
| | $R_2$–C≡CH | Sonogashira | Z = −C≡C−$R_2$ |
| | $R_2$–NH–$R_2$<br>$R_2$–NH$_2$ | Buchwald-Hartwig | Z = –N($R_2$)$_2$ or –NHR$_2$ |
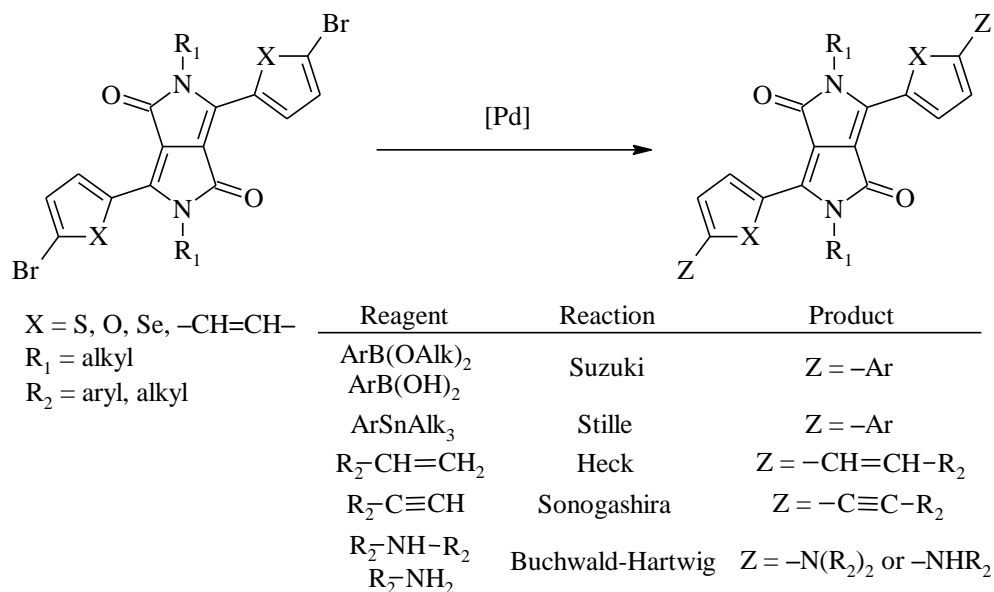
**Scheme 5**: *Possibilities of cross-coupling reactions with brominated DPP derivatives*

### 4.1.2.2 Direct arylation

A second very important approach for prolongation of π-conjugation is the direct arylation. It is a reaction of aryl halides (mostly aryl bromides) with non-activated aromatic compounds in the presence of a base and generally palladium catalyst through a concerted metalation-deprotonation (CMD) pathway[115,116]. There are two different ways: (**A**) DPP derivative may act as non-activated aryl (**32a**) and it reacts with some brominated aromatic compound to form a new C–C bond (**39**)[117]; or (**B**) brominated DPP derivative acts as arylhalide (**40**) and it reacts with a different non-activated aryl[118], as illustrated in **Scheme 6.**
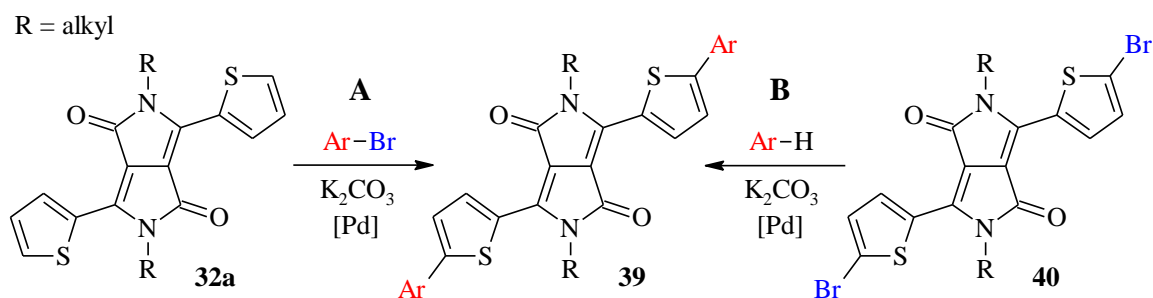


**Scheme 6**: *Two different ways of direct arylation of DPP derivatives*

Various electron-deficient aromatic compounds and thiophene rings can be used as valid arene coupling partners for direct arylation[119]. In general, thiophene has been regarded as an ideal moiety for direct arylation, where the CMD pathway results in a highly selective reaction at the 2,5-positions on the thiophene ring[119]. This makes DPP-containing thiophene derivatives as ideal candidates for this type of reaction[118]. Moreover, it was proved that both electron-deficient and electron-rich aromatics might be incorporated into the molecule of thiophene-DPP derivative (**32a**) *via* direct arylation[117].

The direct arylation method can also be used for the chemical polymerization of DPP derivatives[120]. Like thiophene, polyfluorinated aromatic compounds can also be an ideal moiety for direct arylation *via* the above-discussed CMD pathway[121]. Examples of such polyfluorinated compounds are shown in ***Scheme 7***. The relatively acidic protons on polyfluorinated compounds render them highly reactive toward aryl bromide, in this case, brominated DPP derivative (**40**), leading to the formation of DPP-based polymer (**41**) *via* direct arylation with relatively high yields without any selectivity issues[120].
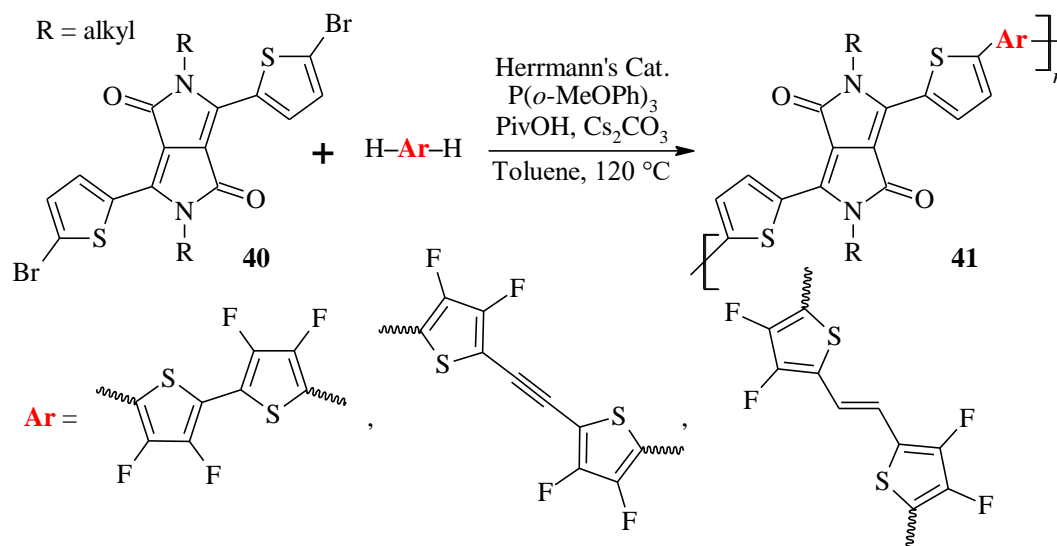


***Scheme 7****: Chemical polymerization of brominated DPP via direct arylation*

The incorporation of electron-withdrawing substituents, such as fluorine atoms, into the DPP is expected to produce a molecule with a significantly improved electron affinity and a well-ordered stacking structure due to its electron-withdrawing ability and the π-conjugation extension[118]. From this point of view, this could be a promising synthetic approach to prepare an interesting series of DPP-based fluorine polymers. In addition, reactions based on a direct arylation possess numerous advantages over common *cross-coupling* reactions, such as better compatibility with chemically sensitive functional groups, simpler catalytic systems free of phosphine ligands, fewer synthetic steps, usually higher yields and avoidance of the use of organometallic reagents in the starting materials leading to simpler by-products and higher atom economy[118].

### 4.1.3   Incorporation of functional groups

Incorporation of functional groups onto 3,6-aryl side chains of the DPP molecule is also very important and commonly used modification[45]. In terms of character, functional groups are divided into electron-accepting and electron-donating. Both types of groups can fundamentally influence the nature of the resulting DPP derivatives, both from the point of view of optical and electrical properties[122–125]. In terms of preparation such modified derivatives, there is a significant difference between both discussed types of functional groups.

### 4.1.3.1  Electron-donating groups

Typical electron-donating groups are amino substituents whose key synthons are DPP halogenated derivatives, typically chloro- (**42**) and bromoaryl DPPs (**43**). The electron-withdrawing DPP moiety facilitates classical nucleophilic aromatic substitution ($S_NAr$) in the absence of palladium catalysts, where halide DPP derivatives react with various secondary amines[124,126,127]. The reaction shown in **Scheme 8** occurs at elevated temperatures in the autoclave using highly-boiling NMP as a solvent to give the corresponding aminated DPP derivatives (**44–47**) with moderate yields[126,127].
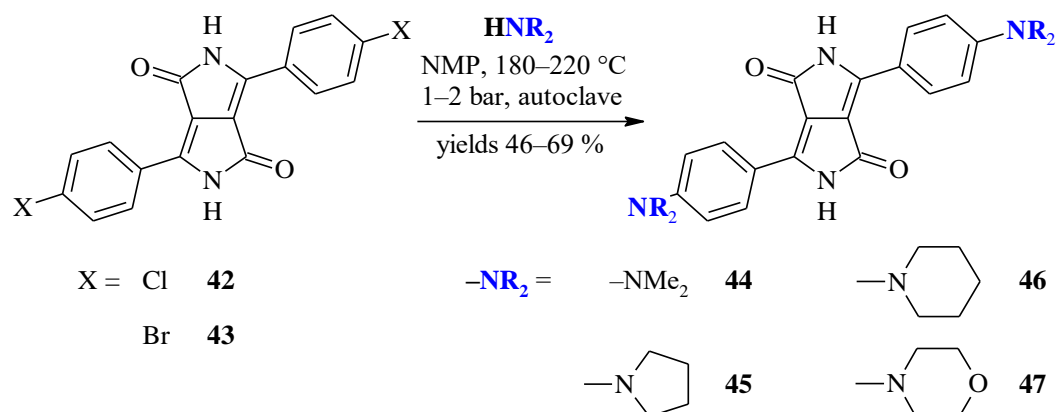


**Scheme 8**: *Nucleophilic aromatic substitution of DPP derivatives to preparation amino derivatives*

### 4.1.3.2  Electron-accepting groups

Recently, the most important and most used electron-accepting functional groups for modification the DPP derivatives are, in particular, dicyanovinyl groups[46,51] and the derivatives of rhodanine[128–130]. The key synthon for the synthesis of both of them is the formyl group. In case of basic thiophene-DPP derivative (**32a**), the *Vilsmeier-Haack* reaction cannot be performed for the introduction of the formyl groups due to a strong electron-withdrawing effect of the DPP moiety, which deactivates thiophene 5-positions for the electrophilic attack of *Vilsmeier-Haack* reagent[51].

   Formylation of the 3,6-aryl side chains in the DPP molecule is commonly carried out in two steps (**Scheme 9**). Firstly, the anion of the DPP derivative (**48**) is prepared by deprotonation of α-protons of thiophene (**32a**) with a strong base such as lithium diisopropylamide (LDA). Subsequently, the prepared anion attacks the formylating agent, usually DMF or *N*-formylpiperidine, to form the resulting formyl derivative of DPP (**49**)[131].
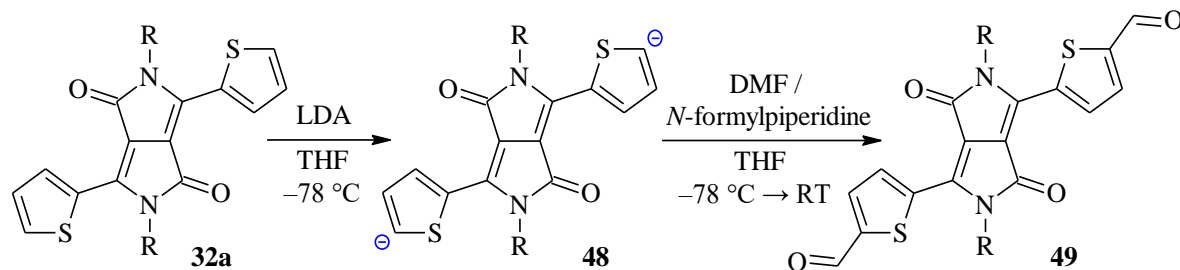


**Scheme 9**: *Lithiation of N,N'-alkylated DPP and subsequent formation of diformyl DPP derivative*

In the case of *N,N′*-ethyladamantyl substituted DPP derivative (**6a**), it is not possible to prepare its formyl-derivative by above-discussed approach with lithiation and subsequent formylation due to the very limited solubility of the material under the required conditions. According to my own experiments[106], a wide range of suitable solvents was tested (as tetrahydrofuran THF, 2-methyltetrahydrofuran, a mixture of THF and hexamethylphosphoramide HMPA) and at a relatively wide temperature range from –78 °C to 0 °C with using both DMF and *N*-formylpiperidine as formylating agents, but without any successful result.

Based on previously performed experiments[106] in the case of ethyladamantyl DPP (**6a**), it is not feasible to prepare its diformyl derivative even by other typical formylation methods such as the *Vilsmeier-Haack* reaction or the *Grignard* reaction followed by the attack of formylating reagent. The reason is most likely electron-accepting character of the DPP core, which causes the deactivation of the thiophene α-positions against the attack of the electrophilic *Vilsmeier-Hack* reagent and magnesium metalation, respectively.

The only feasible solution is the method including the incorporation of the formyl functional group to the DPP structure before its formation. A critical limitation of this method is the strongly basic conditions of sodium alcoholate during the DPP formation, which is certainly killing for the formyl functional group. The solution is to introduce a carbonyl-protecting group resisting the presence of a strong base as, e.g. dioxolane – a heterocyclic acetal[132]. The following *Scheme 10* proposes such a synthetic approach, starting with aromatic formyl (**50**), further involving the introduction of a cyano group and the protection of the formyl group (**53**)[133–135]. The formation of the DPP derivative (**54**) by the succinic method[87] is followed by its alkylation under standard conditions[91], and in the final step, protolysis is performed using hydrochloric acid (HCl) to give the desired diformyl-DPP derivative (**55**)[132].



**Scheme 10**: *The proposed synthetic approach for incorporation formyl groups to the **6a** molecule*
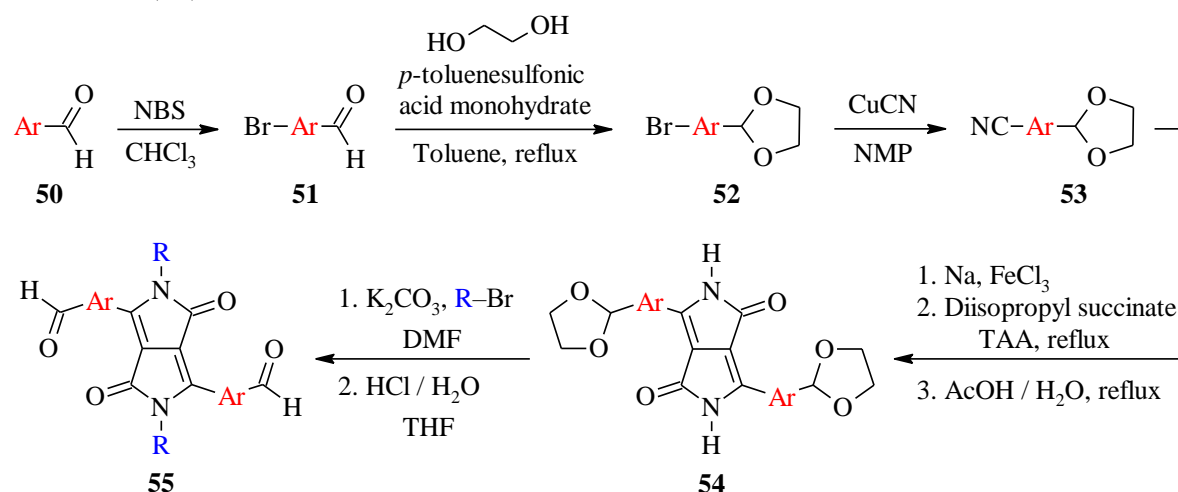
Ar = aryl, heterocycles
R = ethyladamantyl

Subsequently, the transformation of formyl groups to the strong electron-accepting functional groups, as discussed dicyanovinyl groups and the derivatives of rhodanine, is commonly used and well-described method[46,128–130]. The reaction proceeds under

*Knoevenagel condensation* conditions when the formyl derivative is reacted with the active hydrogen compound in the presence of a base and a chlorinated solvent. In the discussed case, the active hydrogen compounds are malononitrile[46,51] or *N*-alkylated derivatives of rhodanine[128–130], and the bases used are triethylamine[130], *β*-alanine[51] or aluminium oxide[46]. An overview of DPP derivatives substituted by significant strong electron-accepting groups is shown in *Figure 25*.
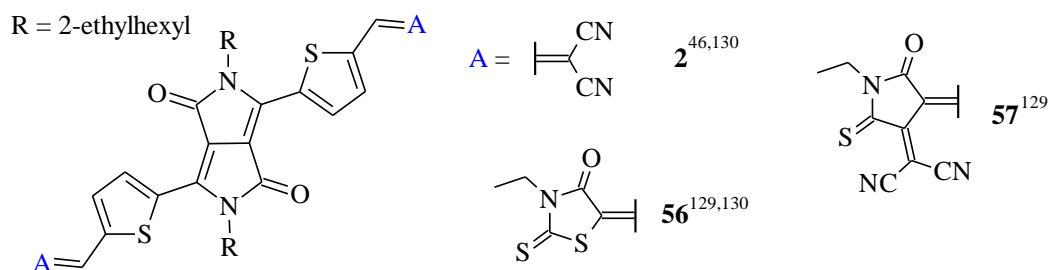


*Figure 25: DPP derivatives substituted by significant strong electron-accepting groups*

### 4.1.4 Quinoid structures of DPPs

The quinoid form is a structure based upon a quinone. In case of DPP derivatives, the quinoid structure (**58**) is formed by *Takahashi coupling* reaction of dibrominated DPP derivative (**40**) with malononitrile in the presence of a sodium hydride base and Pd(PPh$_3$)$_4$ catalyst[136]. This reaction is followed by oxidation with bromine water[137] or just by exposition on the air and subsequent mixing with dilute hydrochloric acid[138] (*Scheme 11*).
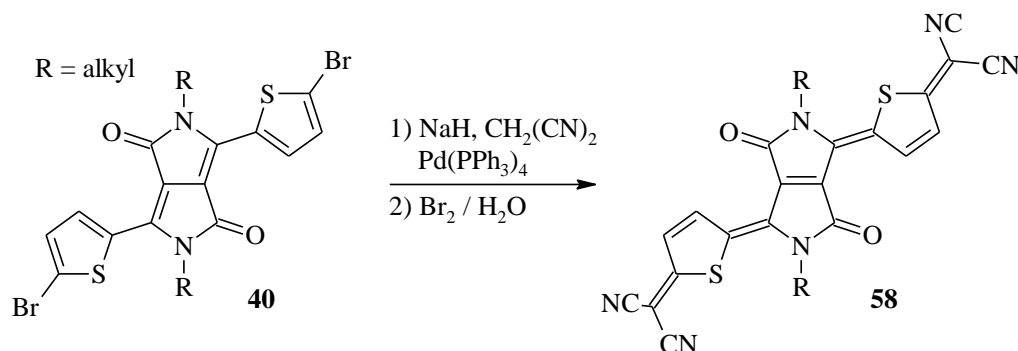


*Scheme 11: Formation of the quinoid structure of DPP (58) from the starting dibrominated DPP (40)*

Recently, Tao et al.[139] reported the optimized synthesis of quinoid DPP derivative (**31**) with new important findings. It has been found that it is necessary to use the amount of sodium hydride base only for the formation of the malononitrile anions, which subsequently react with dibrominated DPP derivative (**40**) in the presence of a large amount of palladium catalyst. It turned out that a large excess of sodium hydride (more than 4 equiv.) used by Zhu et al.[137] leads to the damaging of the DPP core. Furthermore, the reaction of malononitrile anions with dibrominated DPP requires above 50% equiv. amount of the Pd catalyst relative to the starting bromo-compound, although typical *Takahashi reaction* conditions only required the use of approx. 1% palladium catalyst[136]. Another finding is about forming of final quinoid form by oxidation when the authors in reference[138] mentioned that the intermediate reaction product could be oxidized in the air, followed by mixing with dilute

HCl. Nevertheless, Tao et al.[139] found it very unlikely and they needed to use a strong oxidant, saturated bromine aqueous solution, to convert the intermediate product to the resulting conjugated dicyanomethylene-substituted quinoid structure. However, a small amount of the product was brominated at the C4 positions of the thiophene rings by the excessive bromine during this conversion. These brominated by-products are possible to be effectively removed by column chromatography.
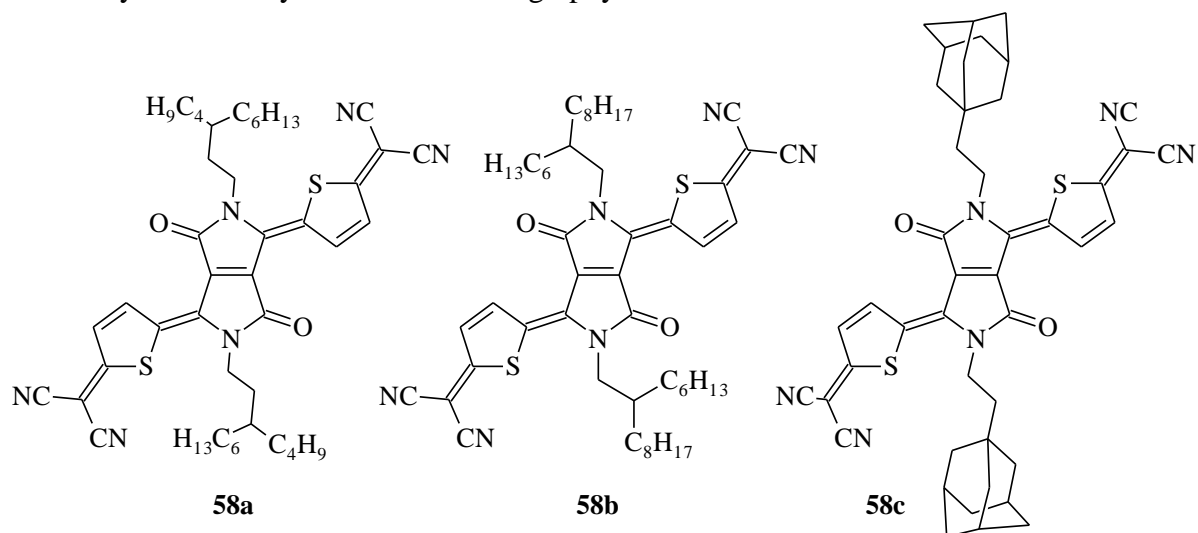


**Figure 26**: *DPP dicyanomethylene-substituted quinoid derivatives*

According to Tao et al.[139], it seems that the side alkyl chains have a significant impact on the reaction yield. While derivative **58b** was prepared in the yield of 35%, the reaction yields of derivative **58a** were not more than 13%. Unfortunately, the reason is not very clear at this moment. There is only a presumption that the position of the side chain branching point further away from the conjugated backbone causes the DPP core more susceptible to side reactions, such as the ring-opening reaction[139]. The molecule **58c** with incorporated ethyladamantyl side alkyl chains is my target derivative, and that is a great challenge to prepare it based on the latest synthetic findings.

The quinoid structure in the DPP molecule brings a very important factor of the almost planar character of its main skeleton. It allows an increase in π-π interactions that evoke a molecular arrangement improving the ability to charge carrier transport of the material. The quinoid DPP derivatives generally excel in *n*-type characteristics and air-stable properties due to their highly crystalline domains in the thin films, making them highly perspective components mainly in the field of organic field-effect transistors[137]. From this point of view, it is extremely interesting to combine modification of the DPP derivative both by incorporation of adamantyl chains and formation of the quinoid form within a single molecule, as shown by derivative **58c** (*Figure 26*).

### 4.1.5 Thioketo analogues of DPPs

Last discussed modification of the DPP derivatives relates to oxygen atoms of the dilactam moiety and their transformation to sulphur atoms *via* thionation[140]. The reaction is generally carried out using a Lawesson's reagent (LR) in chlorobenzene as a solvent and at reflux for

several hours, proceeding at high yields. The reaction structure is shown in the following *Scheme 12*, including the structure of the LR.
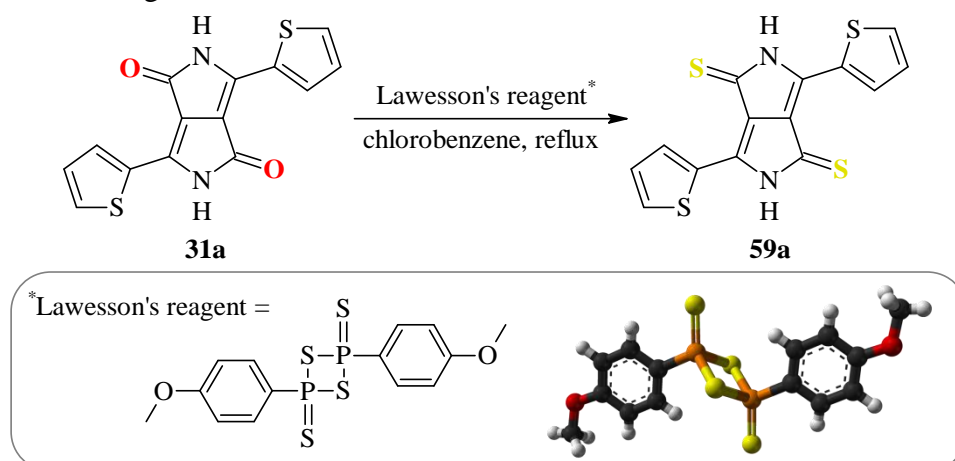


*Scheme 12*: *Preparation of dithioketopyrrolopyrrole (59a) via thionation of DPP molecule (31a)*

In the context with the previously discussed limitations of DPP alkylation, it is possible to prepare at least four DPP derivatives modified by thionation (**59–62**), as shown in *Scheme 13*. However, due to relative reactivity of nucleophilic substitution in order *S*-alkylation > *N*-alkylation > *O*-alkylation, it is possible to prepare *S*-alkylated DPP derivatives (**60**) in relatively high yields compared to other alkylated molecules[140].



Ar = aryl, heterocycles

R = alkyl chains
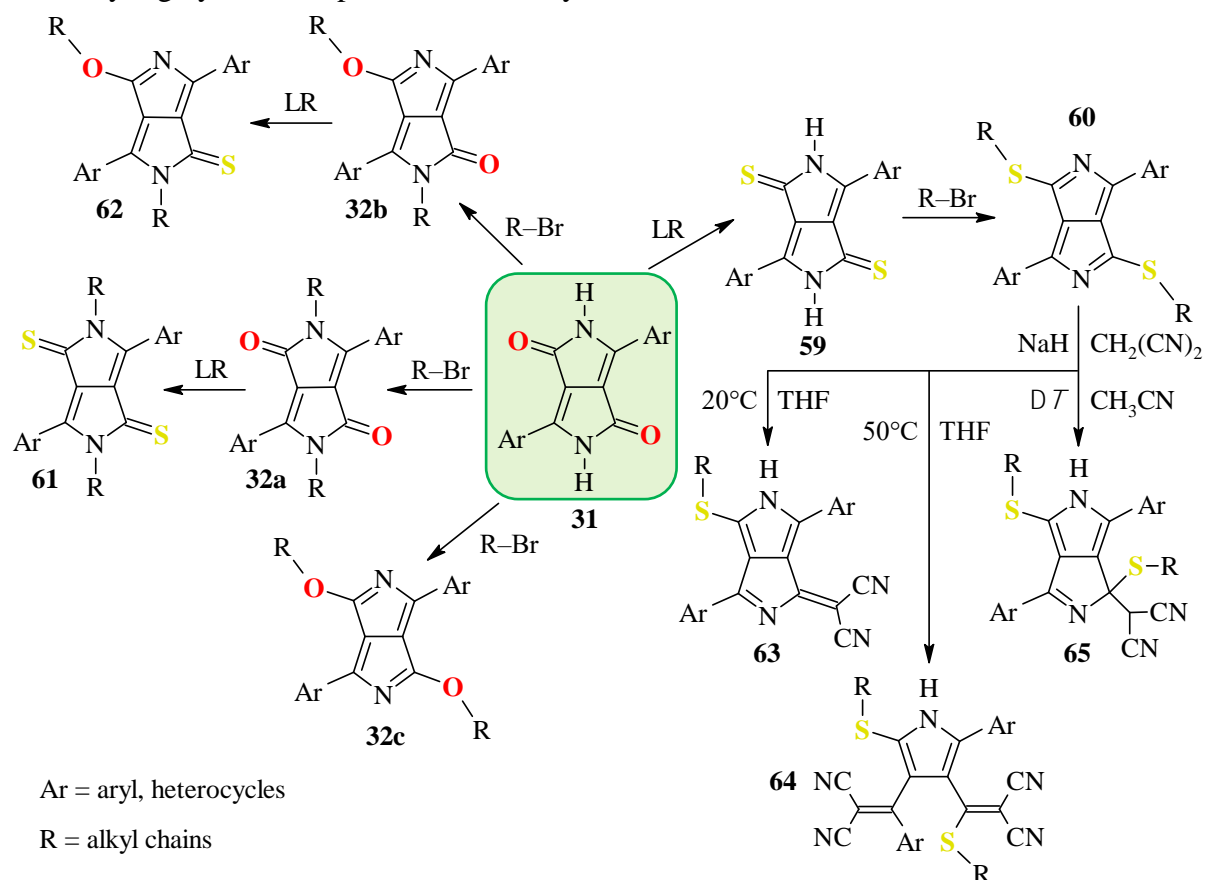
*Scheme 13*: *An overview of possible DPP modifications via thionation and subsequent*

41

Further, the structure of the *S*-alkylated dithioketopyrrolopyrrole (DTPP) molecule (**60**) undergoes nucleophilic substitution, although its reactivity is not very great[140]. For example, the reaction of the derivative **60** with sodium malononitrile at room temperature affords dicyanomethylene monosubstituted product (**63**), whereas heating of this reaction mixture to approx. 50 °C causes partial ring-opening, leading to the formation of the pyrrole derivative (**64**, *Scheme 13*). In case of heating the derivative **60** with malononitrile in acetonitrile, it only leads to formation dicyanomethylene adduct **65**[140].

Even though this is not a very commonly used modification of the DPP derivatives, several relevant articles have been published describing the interesting properties of the thioketo analogues of DPPs (DTPPs)[141–145]. Significant features of *S*-alkylated DPP derivatives (**60**) are narrower energy gaps and low-lying HOMO levels as compared to common *N*-alkylated DPPs (**32a**). In addition, **60** based chromophores exhibit unique visible and near-infrared halochromic and halofluoric properties. The reason for that behaviour is that the lactim nitrogen in derivative **60** is more basic than the lactam nitrogen in the molecule **32a** so that the acid-base reaction can occur[142]. Moreover, near-infrared thermochromic properties were described for *S*-alkylated DPPs (**60**), which means that these derivatives are able to change colour with changes in temperature reversibly[143].

Based on the above-described findings of thioketo analogues of DPPs, such modified derivatives can be used as versatile building blocks for the construction of various conjugated compounds with a low band gap in the field of organic electronics. In addition, e.g. incorporation of adamantyl side chains into thioketo modified DPP molecule may bring novel, not yet described properties.

## 4.2   Modification of BDF derivatives

The benzodifuranone (BDF, **10**) molecule was firstly prepared in the early 1980s[54]. The synthesis of BDF derivative occurs in several synthetic steps, where the key starting materials are derivatives of α-hydroxy acids (AHAs, **69**)[146]. There are two main approaches to synthesis AHAs: (**A**) The first one is *via* preparation of aryl methyl ketones (**66**) and their subsequent oxidation under *Cannizzaro reaction* conditions using selenium oxide and ytterbium triflate[147]. (**B**) The second one is *via Friedel-Crafts acylation* on a varied range of aromatic and heteroaromatic compounds to form α-keto esters (**67**), followed by their reduction to α-hydroxy esters (**68**) and finally the ester hydrolysis to AHA derivatives[148]. Both discussed approaches are shown in the following *Scheme 14*.
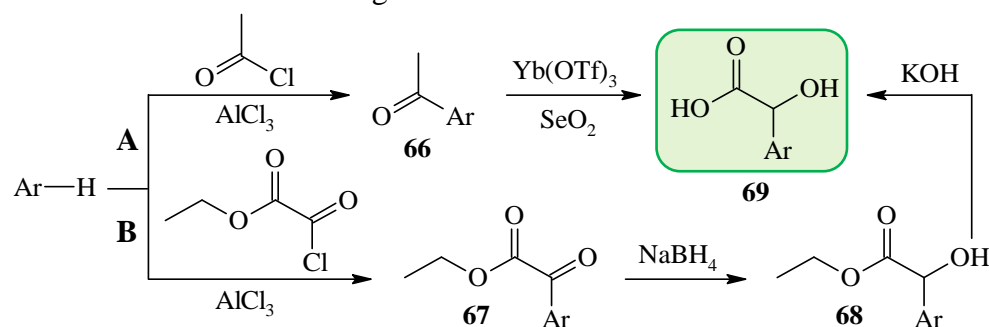


*Scheme 14*: Two main approaches to preparation α-hydroxy acids (AHA, **69**)

42

Before the formation of the resultant BDF skeleton, the mono-condensation to the benzofuranone derivative (**75**) first occurs. In the literature, two most probable mechanisms are described (**Scheme 15**). The first one (**A**) assumes acid-catalysed esterification (so-called *Fischer esterification*), where the nucleophilic oxygen atom of the hydroquinone (**70**) attacks the carboxylic carbon activated by the proton transfer from acid catalyst to the carbonyl oxygen of the AHA molecule (**71**). Then, the resulting ester (**72**) undergoes intramolecular cyclization to form the molecule **75**, containing lactone functional group. The second one (**B**) assumes the protonation of an α-hydroxy group of the AHA molecule, followed by its dehydration to form the carbocation (**73**), which reacts *via* electrophilic substitution with hydroquinone (**70**) to intermediate **74**. Subsequent intramolecular cyclization of **74** leads to the resulting molecule **75**[146,149].
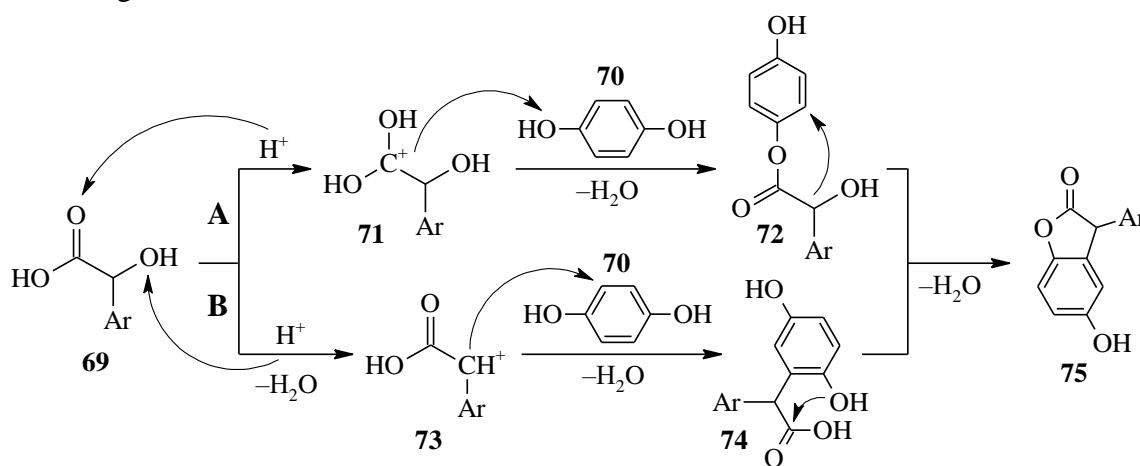


**Scheme 15**: *Formation of benzofuranone mono-condensate (75) – two possible mechanisms*[146,149]

After the mono-condensate **75** is formed, it reacts with another molecule of AHA (**69**) by one of the mechanisms described above to intermediates **76** or **77**. Their subsequent intra-molecular cyclization provides the double-condensate (**78**), containing two lactone groups (**Scheme 16**)[150].
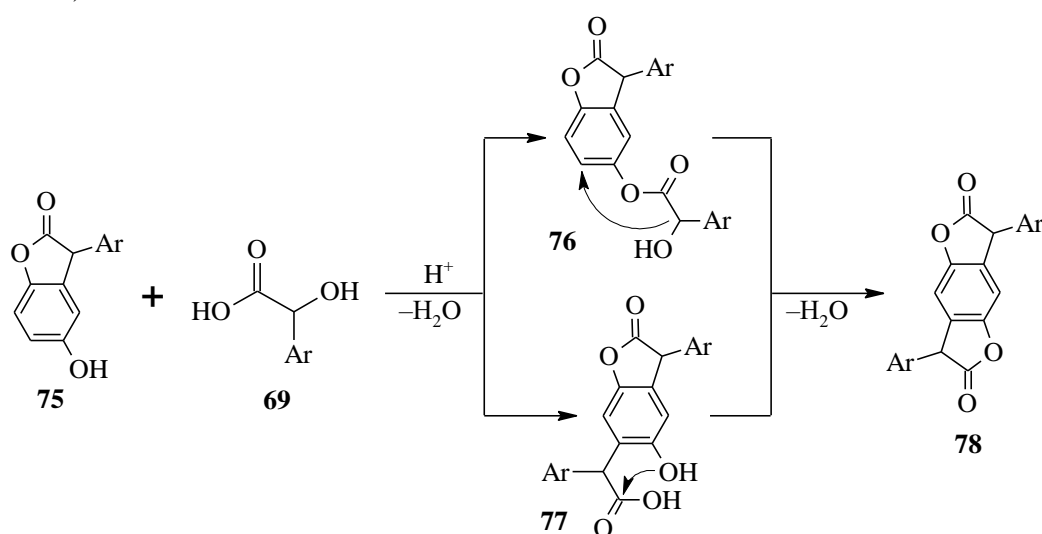


**Scheme 16**: *Formation of the final benzofuranone double-condensate (78) – two possible mechanisms*

The formation of the resulting double-condensate (**78**) has two options – (**I**) through the preparation of mono-condensate (**75**) first and subsequently the second cyclization to the final molecule **78**; (**II**) *via* direct double-condensation to the molecule **78**. The great benefit of approach (**I**) is the ability to prepare both symmetrical and asymmetrical BDF derivatives, whereas approach (**II**) provides only symmetrical BDFs[150].

The last synthetic step to the final BDF molecule is the oxidation of the derivative **78** (*Scheme 17*). For this purpose, a wide variety of solvents and oxidizing agents are used. The most commonly used solvents are 1,2-dichlorobenzene, 1,2,4-trichlorobenzene, acetic acid, sulphuric acid etc. On the other hand, typically used oxidizing agents are *m*-chloroperbenzoic acid, *p*-toluenesulfonic acid, nitrobenzene, hydrogen peroxide, potassium or ammonium persulfate, chloranil etc. The use of an oxidizing agent is derived, in particular, from its solubility in the used solvent[150].
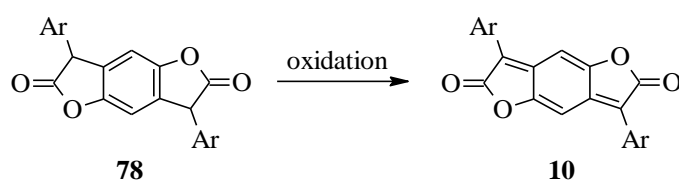


*Scheme 17: Oxidation of the di-condensate (78) to the final BDF molecule*

A wide range of BDF derivatives containing substituted phenyl rings has been described in the literature (*Figure 27*). The substitution of phenyl rings by various substituents and functional groups is the most used, well-studied method of BDF molecule derivatization. These materials find use mainly as industrial pigments[55,150], as discussed in *Chapter 3.2.1.2*.



$R_1$, $R_2$: Cl, Br, OH, CN,

$CH_3$, $CH_2CH_3$, ...

$OCH_3$, $OCH_2CH_3$, ...

CHO, $NH_2$, $NHCH_3$, ...
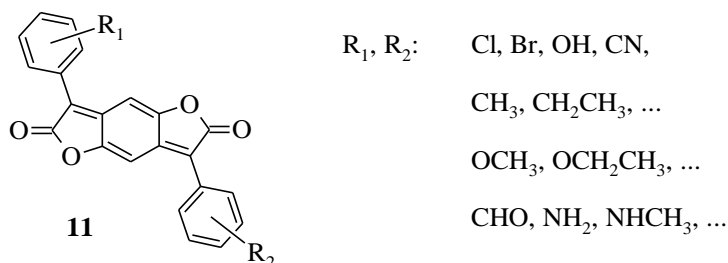
*Figure 27: Various BDF derivatives containing substituted phenyl rings (11)*

## 4.2.1   Thiophene BDF derivative

Thiophene heterocyclic compound belongs to very important molecules commonly used in organic electronics as building block[151]. To the best of my knowledge, there is no mention of thiophene substituted BDF derivatives (**79**, *Figure 28*) in the literature, so it would be a great challenge to prepare and study such a derivative.
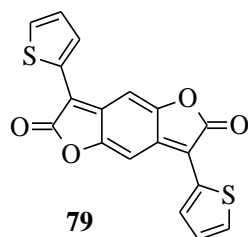
*Figure 28: Thiophene substituted BDF derivative (79)*

The synthetic pathway for thiophene substituted BDF derivative (**79**) should be the same as for the phenyl BDF derivative, as subscribed in *Scheme 14–17*. In addition, the thiophene ring has a higher electron density than benzene, which makes thiophene even more suitable for electrophilic aromatic substitution (*S*$_E$*Ar*), enabling the preparation of the key intermediate α-hydroxy acid – hydroxy(thiophen-2-yl)acetic acid (**69a**, *Scheme 18*) – by the *Friedel-Crafts acylation* to the α-position of thiophene and subsequent reduction and hydrolysis, as described above.
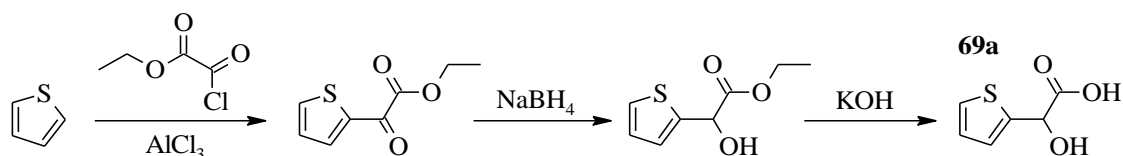


*Scheme 18: Hydroxy(thiophen-2-yl)acetic acid (69a) – the key intermediate for the BDF preparation*

### 4.2.2 Pyrrole BDF analogues

The molecule **80** is another interesting molecule similar to the BDF derivatives discussed in this chapter (*4.2*), where the oxygen heteroatoms in the five-member cycles of the main backbone are replaced by nitrogen atoms (*Figure 29*). This molecule was reported in the patent from 2013[152], where it forms the base unit in polymers potentially applicable as IR absorber, organic semiconductor in organic devices, especially in organic photovoltaic and photodiodes etc.
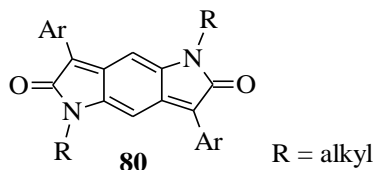


*Figure 29: Pyrrole BDF analogue (80)*

The synthetic pathway for the formation of the molecule **80** is similar as in previous cases of the BDF derivatives; however, some synthetic steps are different. The first step is the same – *Friedel-Crafts acylation* on an aromatic compound to form α-keto ester (**67**). In the next step, the molecule **67** is directly hydrolysed to α-keto acid (**81**), which is subsequently transferred to α-keto acid chloride (**82**) – more reactive than acid molecule **81** and thus more suitable for transformation to amide (**83**) *via* reaction with a primary amine, as shown in *Scheme 19*[152].
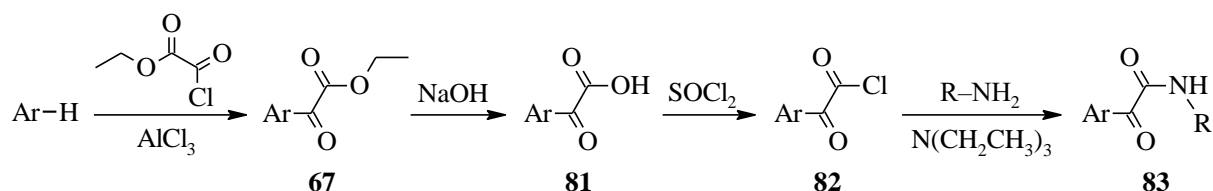
**Scheme 19**: *Synthetic pathway to α-keto amide (83) – the key intermediate to the formation of 80*

The next synthetic steps leading to the final molecule **80** by double-condensation are fundamentally different from the cyclization mechanism to the BDF derivatives, as shown in **Scheme 15–16**. The key fragment of 1,4-cyclohexanedione (**84**) is subjected to deprotonation of α-carbon using a strong base, typically sodium hydride. Subsequently, the formed anion (**85**) attacks electron-deficient carbonyl carbon in the α-keto amide (**83**) molecule to form intermediate **86**, which then undergoes double-cyclization to the resulting derivative **80**, using concentrated sulphuric acid (**Scheme 20**)[152].
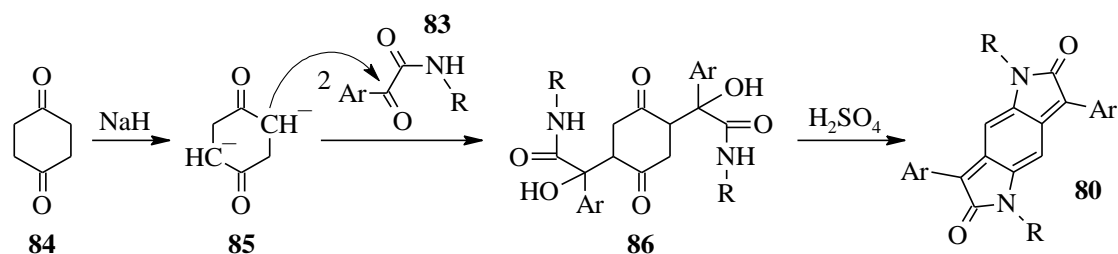


**Scheme 20**: *Reaction mechanism of double-condensation to the resulting molecule 80*

The molecule **80** contains two dilactam moieties similar to the DPP molecule. The presence of nitrogen heteroatoms in the main backbone allows the incorporation of a diverse range of alkyl chains. A great challenge would be to incorporate adamantyl chains into molecule **80**, which could bring very interesting features of the resulting derivative due to the ability of adamantyl to form highly crystalline structures. The structure of such a modified target derivative (**80a**) is shown in the following **Figure 30**.
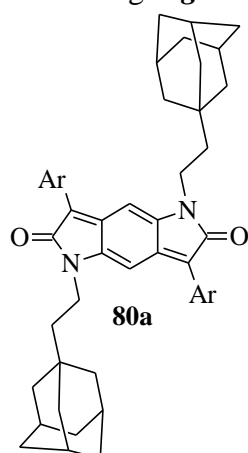


**Figure 30**: *The target derivative 80a with incorporated ethyladamantyl side chains*

## 4.3 Modification of ID/IID/EP derivatives

Structures of indigo (ID), isoindigo (IID) and epindolidone (EP) molecules were briefly discussed in the Review part (*Chapter 3.2.1.3*). The synthesis of the ID molecule has several ways[153]. The first one – *Baeyer-Drewsen synthesis* – dates back to 1882 and is based on the aldol condensation of acetone (**87**) with *o*-nitrobenzaldehyde (**88**) in the presence of sodium hydroxide solution, followed by cyclization and oxidative dimerization to the resulting molecule of ID (**13**), as shown in the following **Scheme 21**[154]. However, this synthetic pathway is still used on the laboratory scale[155].
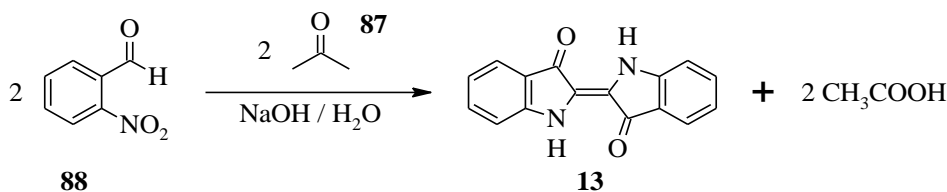


***Scheme 21***: *The Baeyer–Drewsen synthesis of the indigo molecule (**13**)*

Second synthetic pathway called *Heumann's* dating from 1897 uses *N*-(2-carboxyphenyl) glycine (**89**), which is heated to 200 °C in an inert atmosphere with sodium hydroxide as a base to form indoxyl-2-carboxylate (**90**), followed its decarboxylation to give indoxyl, which is subsequently oxidized in air to the ID molecule **13** (**A**, **Scheme 22**)[156]. Last important method is *Pfleger's synthesis* from 1901, where *N*-phenylglycine (**91**) reacts with a molten mixture of potassium and sodium hydroxide and sodium amide to form the indoxyl molecule as the stable dialkali-metal salt (**92**), which is then oxidized in air to the resulting ID molecule **13** (**B**, **Scheme 22**)[157]. Currently, these two methods for preparing the ID molecule are commonly used for industrial mass production. While the *Heumann's* pathway is simpler than the *Pfleger's*, however, the starting material **89** is more expensive than the molecule **91** for *Pfleger's synthesis*[153].
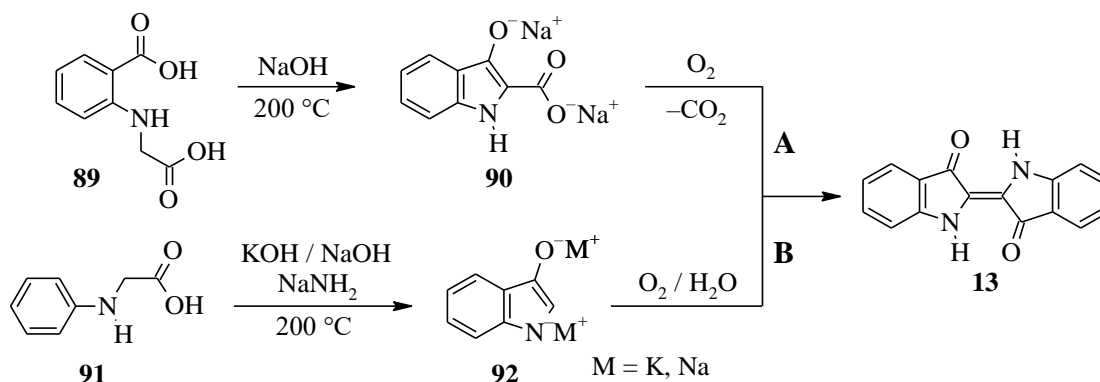


***Scheme 22***: *Heumann's (**A**)[156] and Pfleger's (**B**)[157] synthetic pathways for the indigo molecule (**13**)*

The isoindigo molecule (**14**) is another important member of the pigment group discussed in this chapter. As was mentioned in the review section (*Chapter 3.2.1.3*), the IID molecule is the congener of the ID molecule, and a general approach to the synthesis of IID derivatives is based on the acid catalysed condensation of isatin (**93**) with oxindole (**94**). The reaction is

usually performed under reflux conditions and in the presence of a mixture of hydrochloric acid and acetic acid, as is shown in *Scheme 23*[158].



**93**          **94**                                    **14**
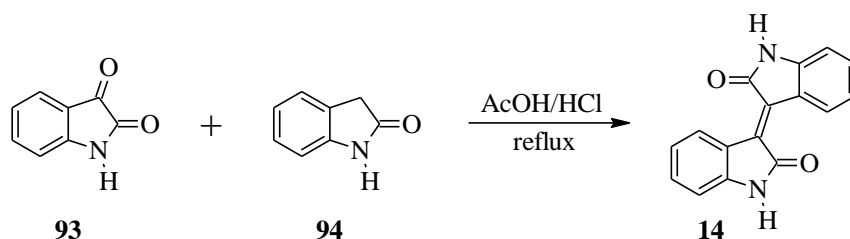
*Scheme 23: Condensation of isatin (93) with oxindole (94) to the resulting IID molecule 14*[158]

The epindolidione molecule (EP, **17**) is the third and last important molecule discussed in this chapter. The EP molecule was first synthesized in 1934 by a relatively complicated multistep reaction pathway[159]. However, in 1995, Haucke and Graness[160] reported the preparation method of the EP molecule from the ID molecule by the thermal-induced isomerisation and they explained the isomerisation mechanism. The reaction proceeds at temperature more than 450 °C and under vacuum in the vapour phase with surprisingly high yields about 80 % (*Scheme 24*)[160].



**13**                            **17**
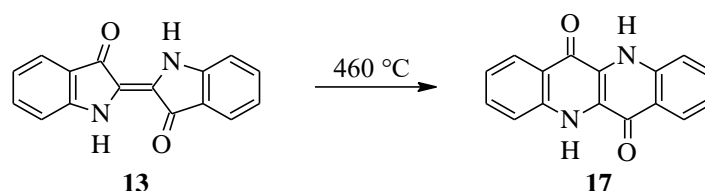
*Scheme 24: Thermal induced isomerisation of the ID molecule (13) to the EP molecule (17)*

In 2014 Głowacki et al.[161] reported convenient and versatile synthetic approach for the preparation of the EP molecule, starting with dihydroxyfumaric acid (**95**). In the first step, the acid is converted to its diester (**96**), which then reacts rapidly with aniline under the catalysis of hydrochloric acid to dimethyl bis(phenylamino)maleate (**97**) in a relatively high yield, wherein the *Z*-conformer was confirmed by ^{1}H NMR as well as by FT-IR spectroscopy. The maleate (**97**) is then isomerized in boiling Dowtherm A and under high dilution into dimethyl bis(phenylamino)fumarate (**98**), which is subsequently subjected to the *Conrad-Limpach* cyclization to give carbomethoxyquinolone (**99**) in a yield exceeding 80 %. Finally, the EP molecule is formed by the ring closure of the molecule **99** in polyphosphoric acid (PPA) under high dilution conditions and at 150 °C, followed by the hydrolysis of the PPA solution to afford EP product (**17**) as a precipitate.

The overall yield of the EP molecule with respect to the initial dihydroxyfumaric acid (**95**) was 51.1 %. However, a significant advantage of this procedure is the possibility to apply it to a wide range of variously substituted anilines as a relatively cheap and accessible building block, which thus allows the preparation of a very diverse number of EP derivatives[161].
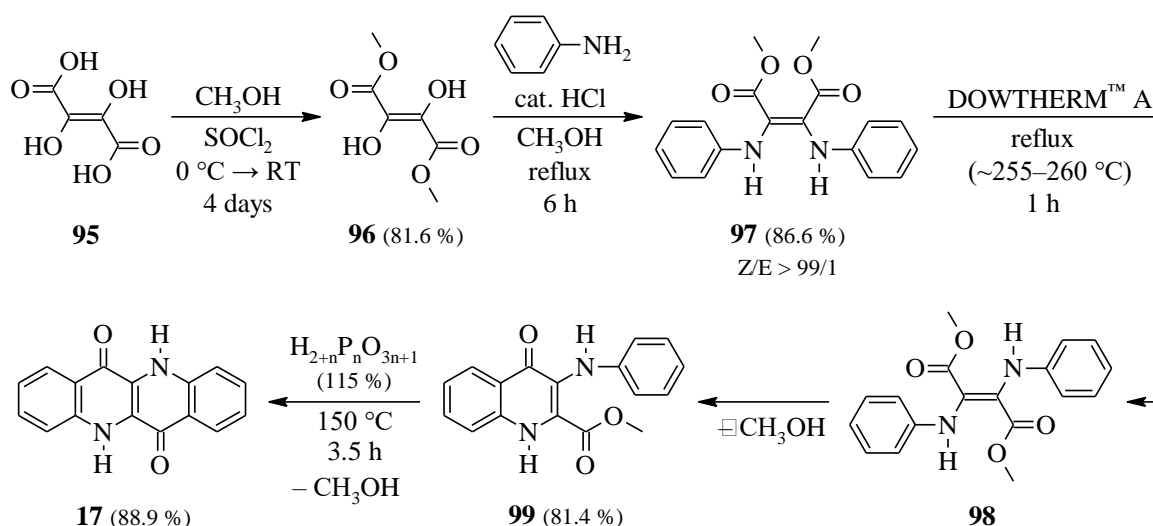
**Scheme 25**: *Synthetic approach for preparing the EP molecule from dihydroxyfumaric acid (**95**)*[161]

From the structures of derivatives ID, IID and EP discussed herein; it is obvious that these molecules can be subjected to the same modification – the nucleophilic substitution of alkyl side chains on the nitrogen heteroatoms – like the above-discussed DPP molecule. Moreover, the IID molecule is the direct analogue of the DPP molecule, containing lactam functional group. However, even in the case of the alkylation of derivatives ID, IID and EP, the limiting factor is also the substitution on the oxygen atoms, which significantly reduces the resulting yields.

### 4.3.1 Incorporation of adamantane side-chains

Based on the very positive experience with the incorporation of adamantyl side chains into the DPP molecule[50], the same approach is to be applied to this discussed group of molecules. It can be assumed that the adamantyl chains should have a significant effect on the molecule's thin layer arrangement of the resulting derivatives similarly like the adamantyl substituted DPP molecule (**6a**). The structures of the targeted derivatives are shown in *Figure 31*.
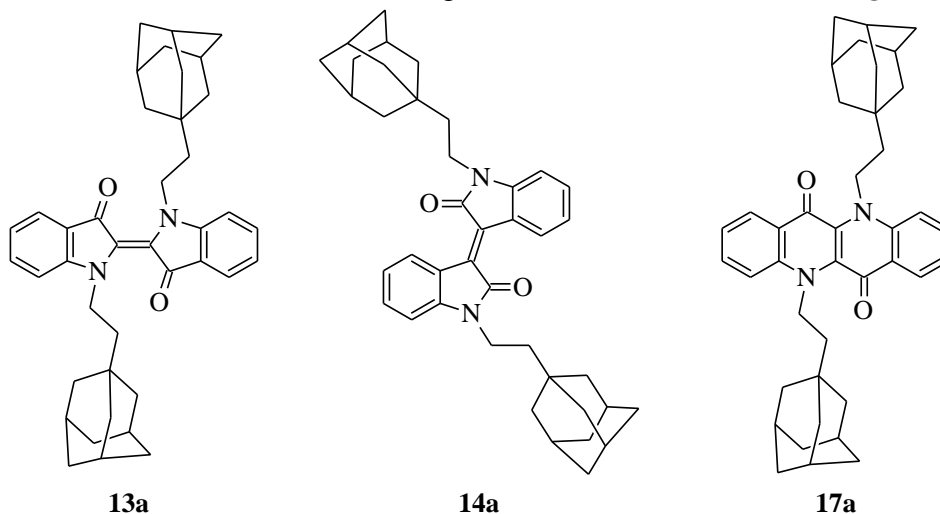


**Figure 31**: *Adamantyl substituted derivatives of ID (**13a**), IID (**14a**) and EP (**17a**)*

## 4.4 Modification of NTD derivatives

As already described, the backbone of the NTD molecule consists of naphthyridine, specifically the 1,5-naphthyridine isomer (**100**), which was first prepared in 1927 by Bobranski and Sucharda through the application of the *Skraup reaction* to 3-aminopyridine (**101**, *Scheme 26*)[67]. In 1963, Rapoport and Batcho[162] proved that the cyclization takes place exclusively through the 2-position of the **101** in the *Skraup reaction*, resulting in the molecule **100**. A ring closure through the 4-position of **101**, which would form the 1,7-naphthyridine isomer (**102**), was not obtained at all, even in the absence of a blocking group at that site[162].
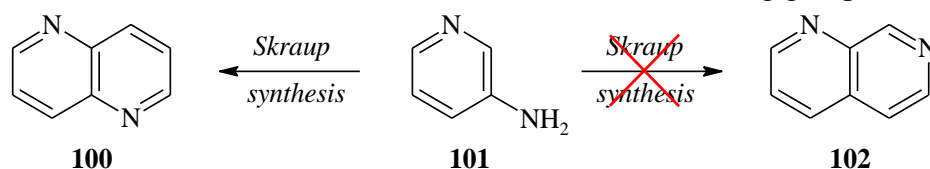


**Scheme 26**: *The Skraup synthesis of 1,5-naphthyridine (**100**) from 3-aminopyridine (**101**)*[67]

However, the above-mentioned *Skraup synthesis* is limited for the synthesis of only 1,5-naphthyridine and its alkyl derivatives[162]. The synthetic pathway for the preparation of the 1,5-dihydro-1,5-naphthyridine-2,6-dione molecule (**106**) first described in 1971 by Rapoport et al.[68] started from ethyl 6-methoxy-3-nitro-2-pyridinepyruvate (**103**), which was subjected to reductive cyclization using platinum oxide. Thus, a new six-membered ring of 1,3,4-trihydro-3-hydroxy-6-methoxy-1,5-naphthyridin-2-one (**104**) is formed and then readily dehydrated by treatment with *p*-toluenesulfonyl chloride to the derivative **105**. Its subsequent transformation to the resulting NTD molecule (**106**) is performed by 48% hydrobromic acid with a very decent yield of 83 % (*Scheme 27*)[68].
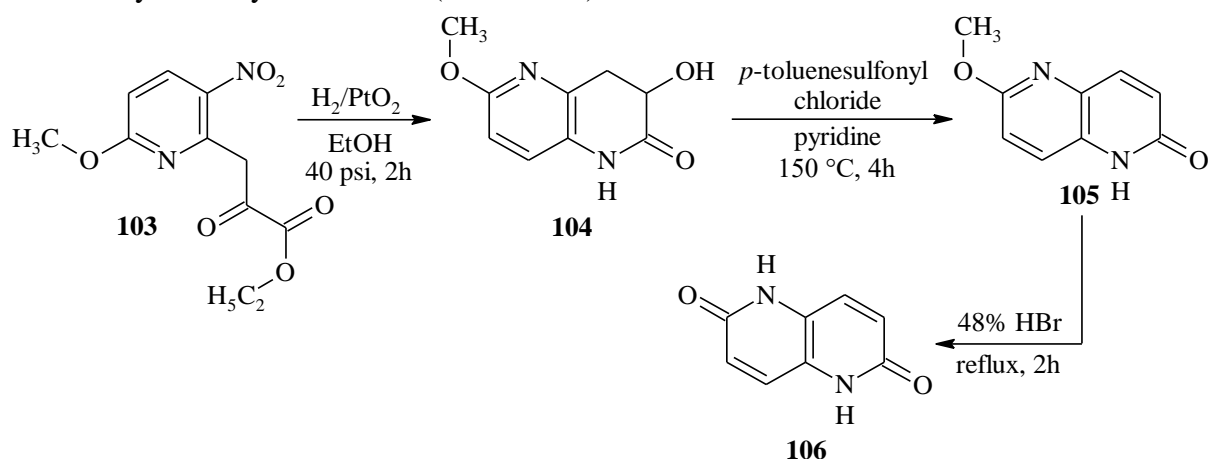


**Scheme 27**: *The original synthetic pathway of the NTD molecule preparation described in 1971*[68]

A novel and rather simpler synthetic pathway for the preparation of the NTD molecule was published in 2016 by Park et al.[70] (*Scheme 28*), when the derivative **105** is synthesized using an optimized *Heck* reaction from 2-bromo-6-methoxypyridin-3-amine (**107**)[163]. The final NTD molecule is prepared by treatment of the formed molecule **105** with hydrobromic acid, the same as in the previous case.
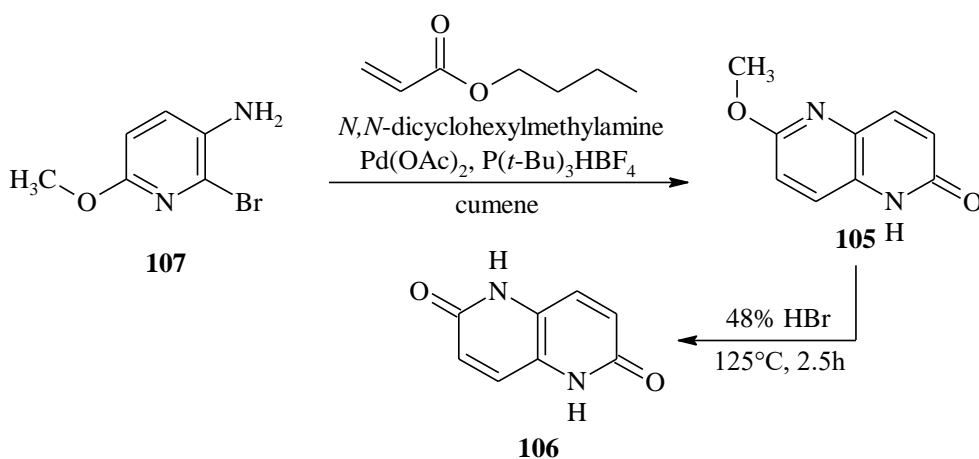
*Scheme 28: Novel and simpler synthetic pathway of the NTD molecule preparation from 2016[70]*

An alternative synthetic pathway leading to the NTD molecule was mentioned in the patent from 2017[164], where the 1,5-naphthyridine molecule (**100**) form the starting compound of the synthesis. Upon its oxidation with hydrogen peroxide, the 1,5-naphthyridine-1,5-dioxide (**108**) is formed and subsequently converted first to 2,6-dichloro-1,5-naphthyridine (**109**) using phosphoryl trichloride and then in basic conditions by reaction with methanol to 2,6-dimethoxy-1,5-naphthyridine (**110**). The final step is again the conversion of methoxy groups to keto groups by hydrobromic acid, and the resulting NTD molecule is thus prepared (*Scheme 29*).
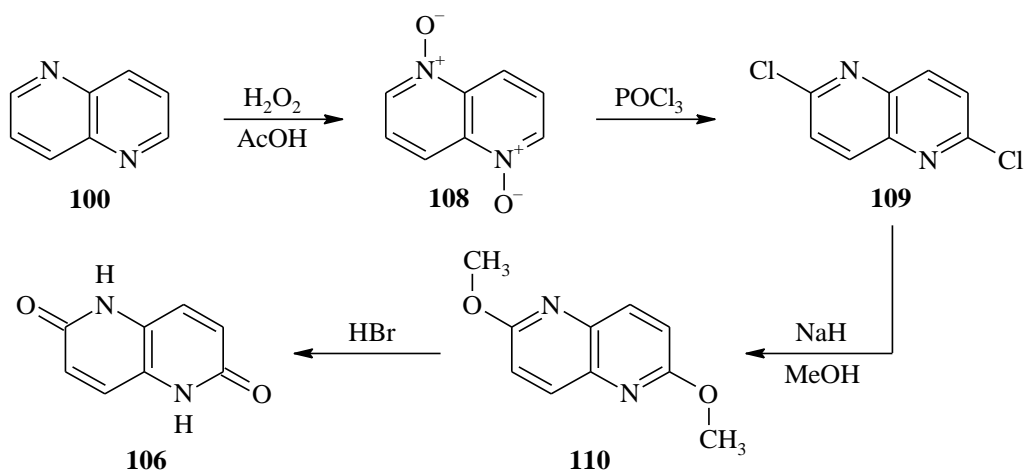


*Scheme 29: The alternative synthetic pathway of the NTD molecule preparation[164]*

### 4.4.1 *N,N'*-alkylation

Since the NTD molecule contains a bicyclic dilactam unit similar to the DPP molecule discussed above, the same phenomenon can be expected during the nucleophilic substitution of alkyl chains. In the case of alkylation with only one type of alkyl chain, the formation of a total of three derivatives can be assumed (*Scheme 30*), what is clearly described in the previously-mentioned patent[164]. However, during the NTD molecule alkylation, the *N,O'*-alkylated product (**18b**) is formed as the majority, concurrently a higher proportion of the *O,O'*-alkylated derivative (**18c**) is isolated than the *N,N'*- (**18a**) even when linear alkyl chains

51

such as dodecyl are used[164]. The same phenomenon was observed by Park et al.[70], when the target *N,N'*-dioctyl-NTD molecule was isolated in the yield of only 6.6 %. It is, therefore, a significantly different alkylation result than in the DPP molecule, wherein the *N,N'*-product is always isolated in the majority using a linear type of alkyl chain[94].
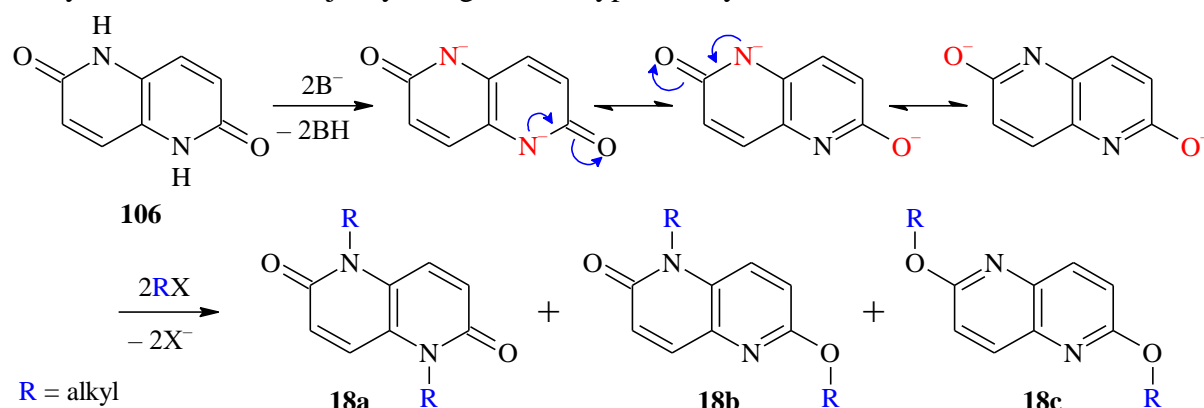


**Scheme 30**: *Mechanism of nucleophilic substitution – alkylation of the NTD molecule*

Moreover, a relatively interesting synthetic method for preparation of the NTD molecule asymmetrically alkylated with two different types of chains has been described (***Scheme 31***)[164]. The starting point is the derivative **105**, which is reacted with a haloalkane (R–X) under basic conditions to form monoalkylated methoxy-ketone derivative **111**, subsequently converted to monoalkylated-NTD molecule **112** by reaction with hydrobromic acid. In the final step, molecule **112** reacts with a different haloalkane (R'–X) to form a mixture of *N*- and *O*-alkylated derivatives (**18a'** and **18b'**) according to previously mentioned ambiguous nature of lactam anion.
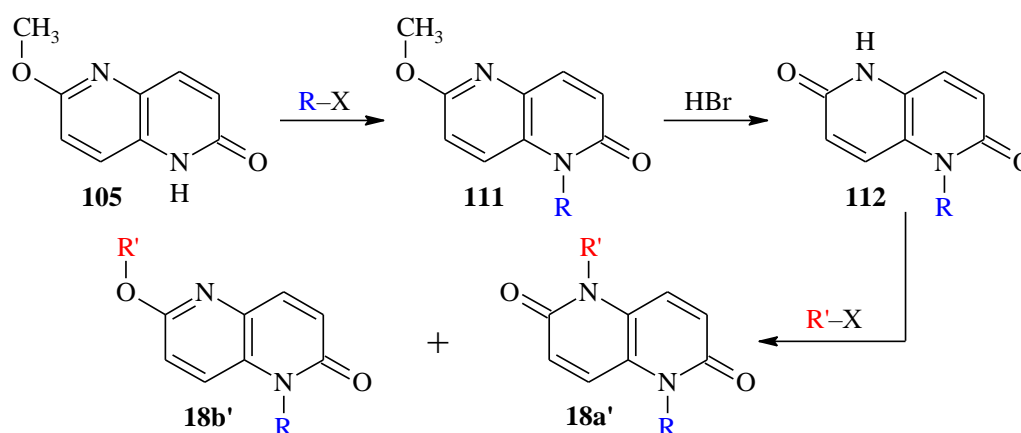


**Scheme 31**: *The synthetic method for preparation of the asymmetrically alkylated NTD molecule*[164]

Nevertheless, to the best of my knowledge, there is no mention in the literature about a comprehensive study of the influence of various factors on the alkylation progress of the NTD molecule, unlike the DPPs.

## 4.4.2 Prolongation of π-conjugation

Because the basic NTD molecule is relatively small, the extension of its structure is suitable, particularly in terms of application potential[69]. Modification of the NTD molecule is willing

exclusively in α-positions of the lactam groups (i.e. 3,7-positions of the NTD), where bromination using both liquid bromine[70] and *N*-bromosuccinimide[71] takes place with good yields (of 57 % and 70 %, respectively). However, the bromination is generally feasible only for alkylated NTD derivatives due to the very limited solubility of the basic NTD molecule in the required solvents.

The dibromo derivative (**113**) is a very versatile unit for a wide range of palladium catalysed *cross-coupling* reactions or direct arylations, as discussed for DPPs in *Chapter 4.1.2*. For further facile and unambiguous derivatization of the NTD structure, the thiophene ring is an important fragment, which can be attached to 3,7-positions of the NTD molecule instead of bromine atoms *via* various types of carbon-carbon bond forming reactions mentioned above. Indeed, a variety of NTD-based polymers is also possible to synthesize by this type of reactions. For example, Park et al.[70,71] described the synthesis of an advanced NTD-based polymer (*Scheme 32*) by a common reaction of dibromo NTD derivative (**113**) with thienyl stannane [Ar–Sn(Bu)₃] under typical *Stille cross-coupling* conditions, leading to the thiophene-NTD-monomer (**114**). After further bromination of the monomer **114**, the resulting NTD-based polymers were prepared through *Stille cross-coupling polymerization* using stannane intermediate of an electron-rich counterpart (**D**). Due to the progressive development of the field of organic synthesis and the optimization of this type of derivatization, it is now possible to achieve yields of between 60 and 90 % in the preparation of these kinds of polymers[70,71].
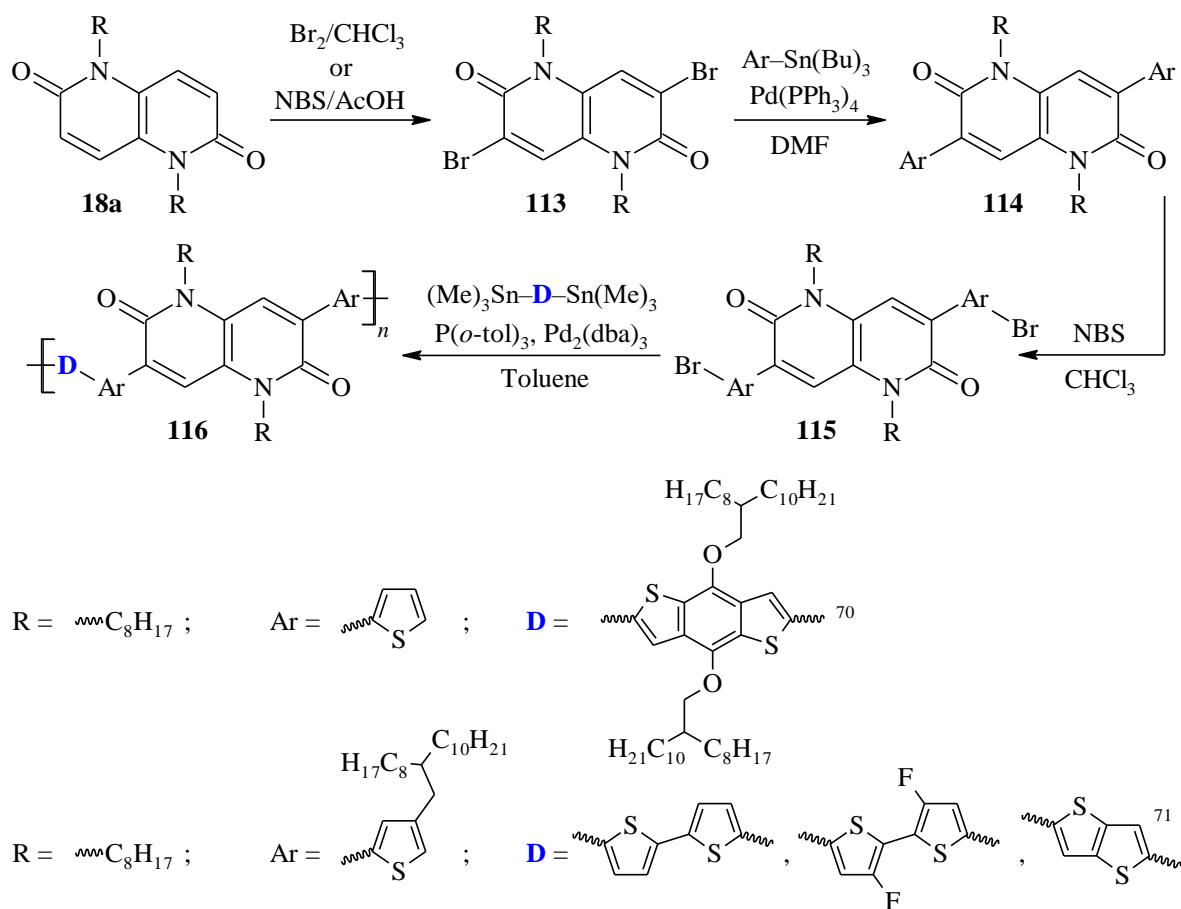


**Scheme 32**: *Preparation of the advanced NTD-based polymers Park et al.*[70,71]

53

## 5 EXPERIMENTAL PART

### 5.1 Used chemicals

*Fisher Scientific, spol. s r.o.*:

bromine (p.p.a., 99%), *N,N*-dimethylformamide (anhydrous, 99.8%), *tert*-butyl-methyl ether (p.a., 99.5%)

*Johannes Kepler Universität Linz*:

epindolidione (95%)

*Lach-Ner, spol. s r.o.*:

acetic acid (p.a, glacial 99.8%), ammonium chloride (p.a., 98%), calcium chloride (anhydrous, 96%), hydroxylamine hydrochloride (p.a.), potassium hydroxide (p.a.), sodium acetate (p.a., anhydrous), sodium hydrogen carbonate (p.a.), sodium hydroxide (p.a.), sodium chloride (p.a.), sulphuric acid (p.a., 96%)

*Linde Gas a.s.*:

argon

*MANEKO, spol. s r.o.*:

*tert*-amyl alcohol (p.a., 98%)

*PENTA, spol. s r.o.*:

acetone (p.a., 99%), dichloromethane (p.a., 99.8%), ethanol (p.a., 96%), ethyl acetate (p.a., 99%), hydrobromic acid (p.a., 48%), hydrochloric acid (p.a., 35%), chloroform (p.a., 99.8%), methanol (p.a., 99.8%), *n*-heptane (p.a., 99%), *n*-hexane (p.a., 99%), petroleum ether (p.a., 40–65 °C), potassium iodide (p.a.), sodium sulfate (p.a., anhydrous), sodium thiosulfate (purum), toluene (p.a., 99%)

*PROVISCO CS s.r.o.*:

(adamantan-1-yl)methanol (98%), 2-(adamantan-1-yl)ethan-1-ol (98%), triflic acid (98%)

*Sigma-Aldrich, Inc.*:

1,2,4-trichlorobenzene (anhydrous, ≥99%), 1,2-dichlorobenzene (anhydrous, 99%), 1,2-dichloroethane (anhydrous, 99.8%), 1,4-dibromobenzene (98%), 1,4-dibromotetrafluoro-benzene (≥99%), 1-bromododecane (97%), 1-formylpiperidine (99%), 1-methyl-2-pyrrolidinone (anhydrous, 99.5%), 2,2′-bithiophene (99%), 2-ethylhexyl bromide (95%), 2-methyltetrahydrofuran (anhydrous, ≥99%), 2-thiophenecarbonitrile (99%), 3-bromo-thiophene (97%), 4-formylbenzonitrile (95%), aluminium chloride (anhydrous, powder, 99.99%), aluminium oxide (activated, neutral), ammonium hydroxide (28%), benzonitrile (anhydrous, ≥99%), caesium carbonate (99%), copper cyanide (99%), copper(I) iodide (purum, ≥99.5%), deuterated dimethyl sulfoxide (99.96 atom.% D), deuterated chloroform (99.96 atom.% D), diethyl ether (99.5%), ethyl bromoacetate (98%), ethyl chlorooxo-acetate (98%), ethyl thioglycolate (97%), ethylene glycol (anhydrous, 99.8%), filter aid Celite® (R566, Supelco, pH > 8.5), hydroquinone (≥99%), chloranil (99%), chlorobenzene (anhydrous, 99.8%), iodine (≥99.8%), *i*PrMgCl (2.0M in THF), iron(III) chloride

(anhydrous, >97%), Lawesson's reagent (97%), lithium diisopropylamide solution (2.0M in THF/heptane), magnesium (≥99.5%), malononitrile (≥99%), mandelic acid (99%), *N*-bromosuccinimide (99%), *n*-butyllithium solution (1.6M in hexanes), *n*-butyllithium solution (2.5M in hexanes), Ni(dppp)Cl$_2$, nitrobenzene (99%), Pd(dppf)Cl$_2$, Pd(OAc)$_2$ (98%), Pd(PPh$_3$)$_4$ (99%), PdCl$_2$(PPh$_3$)$_2$ (98%), phosphoryl trichloride (99.99%), potassium carbonate (anhydrous, 99.99%), *p*-toluenesulfonic acid monohydrate (≥98.5%), silica gel (60 Å, 220–440 mesh), sodium, sodium tetrahydridoborate (99%), tetrahydrofuran (anhydrous, ≥99.9%), tetra-*n*-butylammonium bromide (for synthesis), thionyl chloride (≥99%), thiophene (≥99%), tributyltin chloride (96%), trimethyltin chloride, triphenylphosphine (99%), tris(*o*-methoxyphenyl)phosphine (96%)

*Seoul National University*:

1,5-dihydro-1,5-naphthyridine-2,6-dione (95%)

*Synthesia, a.s.*:

benzofuranyl-thienyl-DPP (95%), di-(*p*-cyanophenyl)-DPP (95%), diisopropyl succinate (p.a., 95%), naphthyl-DPP (95%)


## 5.2   Used instruments and equipment

FT-NMR spectrometer Bruker AVANCE™ III 300 MHz

FT-NMR spectrometer Bruker AVANCE™ III 500 MHz

Elemental analyser Thermo Scientific™ FLASH 2000 CHNS

Thermo Scientific TRACE™ 1300 Gas Chromatograph/ITQ 700™ Ion Trap GC/MS analyser

Kofler apparatus type KB T300 equipped with an optical system (with a 40x magnification)

TA Instruments Q5000IR (New Castle, Delaware, USA) – thermogravimetric analyser

TA Instruments Q2500 (New Castle, Delaware, USA) – differential scanning calorimetry analyser

Varian Cary Probe 50 UV-VIS spectrometer (Agilent Technologies Inc.)

Horiba Jobin Yvon Fluorolog®

Horiba Jobin Yvon FluoroCube

Refractometer ABBE AR

Analytical balance RADWAG AS 220.R2 PLUS

Precision Balance RADWAG WTC 2000

Heat gun Steinel® HL 2010 E

Julabo® immersion cooler with probe FT 902 (temp. range –90 °C)

Anton Paar Monowave 300 (Microwave synthesis reactor)

Magnetic stirrer with heating IKA® RCT basic *safety control* with temperature sensor ETS D5

Magnetic stirrer with heating Heidolph Hei-Tec with temperature sensor Pt1000

Heidolph Hei-VAP HL rotary evaporator with integrated vacuum control

Diaphragm vacuum pumps (Vacuubrand MV 2, Heidolph Rotavac Valve Tec, KNF N 810)

Oil pump Siemens D-91056

Heated Ultrasonic Cleaner Bandelin Sonorex RK 100 SH

Vacuum heated desiccator J.P Selecta "Vacuo-Temp" 4000474

Ice maker ITV Q 40 C Aire Inox

Hot air oven Memmert 100-800

Automatic pipettes 1–10 ml, 100–1000 µl (Orange Scientific), 20–200 µl (Biohit Proline)

Digital thermometer Greisinger GTH 1170 (temperature range –65 to 1150 °C)

UV hand lamp, 254/365 nm – detector for TLC analysis

Column chromatography – stationary phase Silica gel 60 Å, 220–440 mesh

Thin-layer chromatography (TLC) – Al-plates 20x20 cm with Silica gel 60 $F_{254}$, Supelco


## 5.3   Characterization techniques

### 5.3.1   Nuclear magnetic resonance spectroscopy (NMR)

$^{1}$H NMR spectra were recorded on an FT-NMR spectrometer Bruker AVANCE™ III 300 MHz or 500 MHz. $^{13}$C and $^{19}$F NMR spectra were recorded on an FT-NMR spectrometer Bruker AVANCE™ III 500 MHz. The solvents used were $CDCl_3$ and DMSO-$d_6$. Chemical shifts ($\delta$) are given in parts per million (ppm) relative to tetramethylsilane (TMS) as an internal reference. 1D and 2D NMR records were evaluated using MestReNova NMR 14 software.


### 5.3.2   Elemental analysis (EA)

Elemental analysis was measured with an elemental analyser Thermo Scientific™ FLASH 2000 CHNS using sulphanilamide as a standard.


### 5.3.3   Gas chromatography-mass spectrometry (GC-MS)

The chromatograms and mass spectra were recorded on a Thermo Scientific TRACE™ 1300 Gas Chromatograph/ITQ 700™ Ion Trap GC/MS analyser and evaluated using Thermo Scientific Xcalibur™ software.


### 5.3.4   Melting point analysis

The melting points were determined on a Kofler apparatus type KB T300 with an operating temperature range from 20 to 320 °C with an accuracy of ±1% to 200 °C and ±2% above 200 °C (temperature was not calibrated). The device is equipped with an optical system with 4x magnification of the objective lens and 10x magnification of the ocular lens.

### 5.3.5 Thermogravimetric analysis (TGA)

Thermogravimetry (TG) was conducted on a TA Instruments Q5000IR (New Castle, Delaware, USA) to analyse the thermal stability of the derivatives and changes in mass before degradation. Samples were placed on the Pt crucible sample holder and heated at 10 °C/min from room temperature to 600 °C under a stream of nitrogen (ultra-high purity) flow rate 40 mL/min. The TG records (dependence of mass on temperature) were evaluated using TRIOS and Universal analysis software provided by TA Instruments. The TG records were derived, and onsets of the derivatives were determined.

### 5.3.6 Differential scanning calorimetry (DSC)

Differential scanning calorimetry (DSC) was conducted on a TA Instruments Q2500 (New Castle, Delaware, USA) equipped with an RCS cooler to analyse the physicochemical properties of derivatives. The samples, typically 3–7 mg, were weighed to Al pans (Tzero®), hermetically sealed and measured under a stream of nitrogen (ultra-high purity) flow rate 50 mL/min. The loading temperature was 30 °C. The following temperature program was applied: heating 10 °C/min to temperature 50 °C below the degradation temperature determined using TG to delete the thermal history of the sample. The sample was quickly (15 °C/min) cooled to –90 °C and heated again at 10 °C/min. This cycle was used to estimate the physicochemical structure of the sample upon fast cooling. Then, the sample was cooled slowly (3 °C/min) to –90 °C and heated again at 10 °C/min. This cycle was used to estimate the physicochemical structure of the sample upon slow cooling. The DSC records were evaluated using TRIOS and Universal analysis software provided by TA Instruments.

### 5.3.7 Ultraviolet-visible spectroscopy (UV-VIS)

Absorption spectra of samples in both solution and thin films were measured with a Varian Cary Probe 50 UV-VIS spectrometer (Agilent Technologies Inc.). Solutions were prepared by diluting materials in organic solvents (chloroform, toluene, THF) with the concentration of materials $10^{-5}$ to $10^{-6}$ mol dm$^{-3}$. Solutions were characterized in a quartz cuvette (Herasil®, Heraeus Quarzglas Co.). Optical measurements of thin films were performed on quartz glass slides (Herasil® 102, Heraeus Quarzglas Co.) which were pre-treated by ultrasonic cleaning in the following baths: 1) Detergent Neodisher (Miele, Inc., NJ, USA) 10 min; 2) deionized (Milli-Q) water 20 min; 3) isopropyl alcohol (a.p.) 10 min. Films were deposited by spin-coating. The spin rate was 2000 rpm, and the deposed material was dissolved in chloroform. The final thickness of layers was in the range of 50–100 nm.

### 5.3.8 Fluorescence spectroscopy

The fluorescence spectra were recorded with a Horiba Jobin Yvon Fluorolog®. This apparatus, equipped with an integrating sphere, was also used to determine the fluorescence quantum yield by an absolute method. The fluorescence lifetime was measured with a Horiba Jobin Yvon Fluorocube. Samples were measured in both solution and thin films and were prepared as for the UV-VIS measurement.

## 5.4   DPP derivatives

### 5.4.1   Synthesis of basic DPPs and with extended π-conjugation

Target DPP molecules were synthesized according to the known general procedure through condensation of nitrile-derivatives with succinic acid esters, the so-called *Succinic Method*[87].

#### 5.4.1.1   Synthesis of 3,6-dithienyl-DPP (31a)



**29a**
MW = 109.15

**30a**
MW = 202.25

**31a**
MW = 300.36
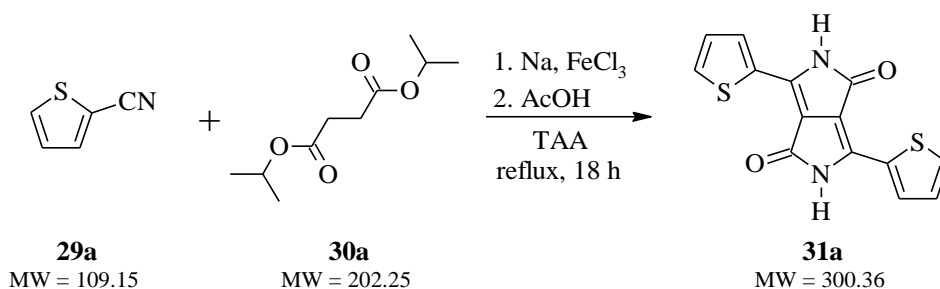
*Scheme 33*: *Synthesis of 3,6-dithienyl-DPP (31a)*

Sodium (~1.3 equiv., 7.2 g, 313.2 mmol) was dissolved in *tert*-amyl alcohol (TAA, 400 mL) with the addition of a catalytic amount of iron$^{(III)}$ chloride and heated to reflux under argon atmosphere. After the dissolution of all sodium, there was added in one portion 1.0 equiv. of **29a** (26.2 g, 240.0 mmol) and the reaction mixture was stirred at reflux for 30 min. Then, 0.65 equiv. of **30a** (31.6 g, 156.2 mmol) dissolved in TAA (80 mL) was gradually added dropwise for 4 h and the mixture was stirred at reflux for 18 h. After that, protolysis was performed by addition of diluted acetic acid to the reaction mixture cooled to 20 °C. The mixture was refluxed for 6 h, and then the heterogenic mixture was filtered while hot and the filter cake was washed with hot water and isopropyl alcohol. The crude product was refluxed in methanol for 1 h and, after that, it was filtered while hot to get pure product **31a**.

**31a**: Dark purple powder (27.5 g, yield 59%). Melting point >380 °C (lit. >360 °C)[165].

$^1$H NMR (300 MHz, DMSO-d$_6$, ppm): $\delta$ = 11.21 (s, 2H), 8.20 (d, $J$ = 3.0 Hz, 2H), 7.93 (d, $J$ = 3.1 Hz, 2H), 7.31–7.27 (m, 2H).

Anal. calcd. for $C_{14}H_8N_2O_2S_2$: C 55.98%, H 2.68%, N 9.33%; Found: C 55.42%, H 2.37%, N 9.71%.

#### 5.4.1.2   Synthesis of 3,6-diphenyl-DPP (31b)



**29b**
MW = 103.12

**30a**
MW = 202.25

**31b**
MW = 288.30
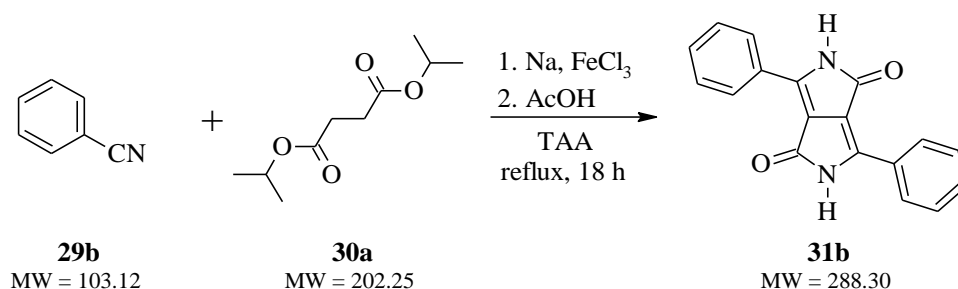
*Scheme 34*: *Synthesis of 3,6-diphenyl-DPP (31b)*

The same procedure as in the previous case (*Chapter 5.4.1.1*) was used to prepare the **31b**, starting with **29b** (1.0 equiv., 25.0 g, 242.4 mmol).

**31b**: Intense red powder (23.5 g, yield 52%). Melting point 371 °C (lit. 372 °C)[166].

$^1$H NMR (300 MHz, DMSO-d$_6$, ppm): $\delta$ = 11.29 (s, 2H), 8.43 (m, 4H), 7.55 (m, 6H).

Anal. calcd. for $C_{18}H_{12}N_2O_2$: C 74.99%, H 4.20%, N 9.72%; Found: C 74.13%, H 3.98%, N 10.02%.

### *5.4.1.3 Synthesis of 3,6-dibithienyl-DPP (35)*

**Preparation of 2,2'-bithiophene-5-carbaldehyde (118)**
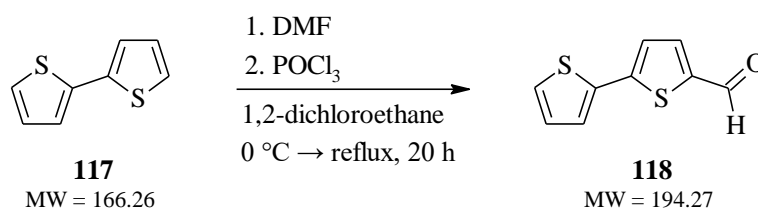


**Scheme 35**: *Preparation of 2,2'-bithiophene-5-carbaldehyde (**118**)*

**117** (10.0 g, 60.15 mmol) was dissolved in anhydrous 1,2-dichloroethane (150 mL) under argon atmosphere. After the dissolution of material, 0.98 equiv. of anhydrous DMF (4.56 mL/ 4.31 g, 58.94 mmol) was added in one portion and the reaction mixture was purged with argon for 30 min. Then, the reaction mixture was cooled to 0 °C, and at this temperature, it was added dropwise (for 20 min) 0.98 equiv. of POCl$_3$ (5.51 mL/9.04 g, 58.94 mmol) and the mixture was heated to reflux and stirred for 20 h. After that, the reaction mixture was cooled to 20 °C and poured into saturated NaHCO$_3$ solution (300 mL). Solid residues were dissolved in DCM (50 mL) and poured into the previous solution. The obtained two-phase mixture was transferred to a separating funnel, and extraction was performed (DCM/distilled water). The organic phase was finally washed with brine and dried over anhydrous Na$_2$SO$_4$ and filtered through filter aid (Celite). Concentrated obtained crude mixture was purified by silica gel chromatography eluting with toluene to get pure product **118** ($R_F$ = 0.38, eluent: toluene).

**118**: Beige solid material (10.1 g, yield 87%). Melting point 56 °C (lit. 57–58 °C)[167].

$^1$H NMR (300 MHz, CDCl$_3$, ppm): $\delta$ = 9.85 (s, 1H), 7.66 (d, $J$ = 3.9 Hz, 1H), 7.34 (m, 2H), 7.25 (d, $J$ = 3.9 Hz, 1H), 7.05 (t, $J$ = 4.3 Hz, 1H).

GC-MS (method: *2-bromo-3-dodecylthiophene*): RT = 10.25 min; m/z = 193.90.

**Preparation of 2,2'-bithiophene-5-carbonitrile (36)**
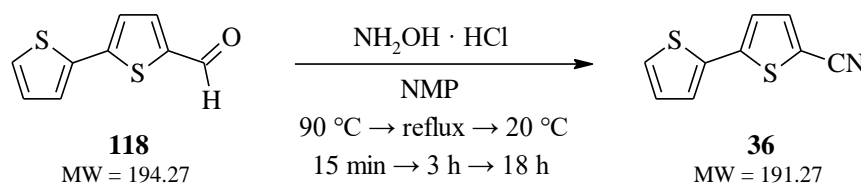


**Scheme 36**: *Preparation of 2,2'-bithiophene-5-carbonitrile (**36**)*

**118** (10.08 g, 51.89 mmol) was dissolved in anhydrous NMP (140 mL) under argon atmosphere, and the reaction mixture was heated to 90 °C and stirred for 15 min. After that, 1.50 equiv. of hydroxylamine hydrochloride (5.41 g, 77.83 mmol) was added piece by piece to the mixture and it was stirred at reflux for 3 h. Then, the reaction mixture was cooled to 20 °C and stirred overnight. After that, the reaction mixture was poured into distilled water (380 mL) and stirred for 45 min. Then, diethyl ether (150 mL) was added to the mixture and extraction was performed. The aqueous phase was washed with diethyl ether (2×90 mL), and the collected organic phases were washed with distilled water (3×250 mL), finally with brine (200 mL) and then dried over anhydrous $Na_2SO_4$ and filtered through filter aid (Celite). After removal of the solvent under vacuum, the obtained crude mixture was purified by silica gel chromatography eluting with toluene to get pure product **36** ($R_F$ = 0.78, eluent: toluene).

**36**: Beige crystal material (8.74 g, yield 88%). Melting point 73 °C (lit. 74–75 °C)[168].

$^1$H NMR (300 MHz, CDCl$_3$, ppm): $\delta$ = 7.53 (d, $J$ = 3.9 Hz, 1H), 7.36 (dd, $J$ = 5.1; 1.1 Hz, 1H), 7.29 (dd, $J$ = 3.7; 1.1 Hz, 1H), 7.15 (d, $J$ = 3.9 Hz, 1H), 7.08 (dd, $J$ = 5.1; 3.6 Hz, 1H).

GC-MS (method: *2-bromo-3-dodecylthiophene*): RT = 10.04 min; m/z = 190.91.

## Preparation of 3,6-dibithienyl-DPP (35)
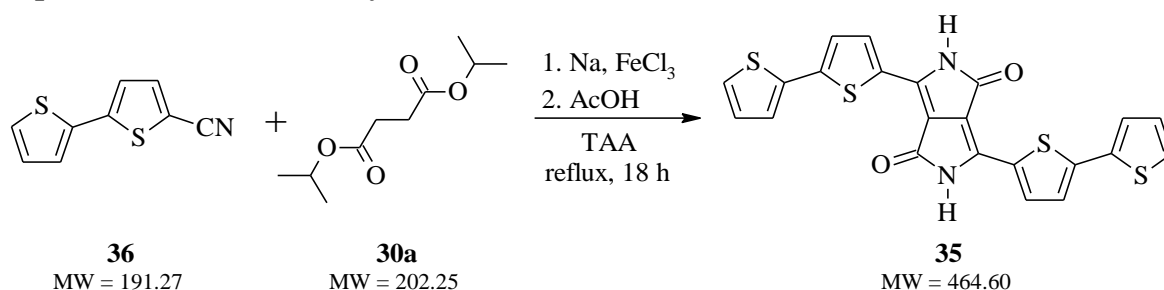


**Scheme 37**: *Synthesis of 3,6-dibithienyl-DPP (35)*

The same procedure as for the **31a** (*Chapter 5.4.1.1*) was used to prepare the **35**, starting with **36** (1.0 equiv., 3.54 g, 18.51 mmol).

**35**: Dark purple-black powder (1.94 g, yield 35%). Melting point >380 °C (lit. –).

Anal. calcd. for $C_{22}H_{12}N_2O_2S_4$: C 56.87%, H 2.60%, N 6.03%, S 27.61%; Found: C 57.00%, H 2.62%, N 6.09%, S 26.00%.

### 5.4.1.4   Synthesis of 3,6-dithieno[3,2-b]thienyl-DPP (125)

**Preparation of 3-bromothiophene-2-carbaldehyde (120)**
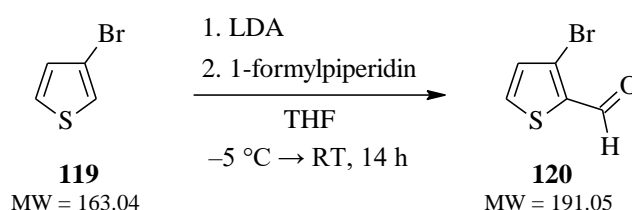


**Scheme 38**: *Preparation of 3-bromothiophene-2-carbaldehyde (120)*

**119** (9.50 g, 58.27 mmol) was dissolved in anhydrous THF (50 mL) under argon atmosphere, and the reaction mixture was cooled to –5 °C and stirred for 10 min. After that, 1.05 equiv. of LDA (2M, 30.59 mL, 61.18 mmol) was added dropwise to the mixture and it was stirred at RT for 1.5 h. Following that 1.05 equiv. of 1-formylpiperidine (7.76 mL/7.91 g, 69.92 mmol) was added and the reaction mixture was stirred at RT for 18 h. Then, the reaction was quenched with the addition of a saturated $NH_4Cl$ solution (10 mL), and extraction was performed. The reaction mixture was washed with diethyl ether (2×120 mL), and the collected organic phases were washed with distilled water (3×250 mL), finally with brine (200 mL) and then dried over anhydrous $Na_2SO_4$ and filtered through filter aid (Celite). After removal of the solvent under vacuum, the obtained crude mixture was purified by silica gel chromatography eluting with petroleum ether/toluene 4:1 (v/v) to get pure product **120** ($R_F$ = 0.18, eluent: petroleum ether/toluene 4:1).

**120**: Slightly yellowish liquid (8.46 g, yield 76%).

$^1$H NMR (300 MHz, CDCl$_3$, ppm): $\delta$ = 9.96 (s, 1H), 7.68 (dd, $J$ = 5.0; 1.2 Hz, 1H), 7.13 (dd, $J$ = 5.0; 1.3 Hz, 1H).


**Preparation of ethyl thieno[3,2-*b*]thiophene-2-carboxylate (121)**



*Scheme 39*: *Preparation of ethyl thieno[3,2-b]thiophene-2-carboxylate (**121**)*

**120** (8.05 g, 42.14 mmol) and potassium carbonate (~2.0 equiv., 11.65 g, 84.29 mmol) were stirred in anhydrous DMF (60 mL) under argon atmosphere at RT for 1 h. After that, 1.2 equiv. of ethyl thio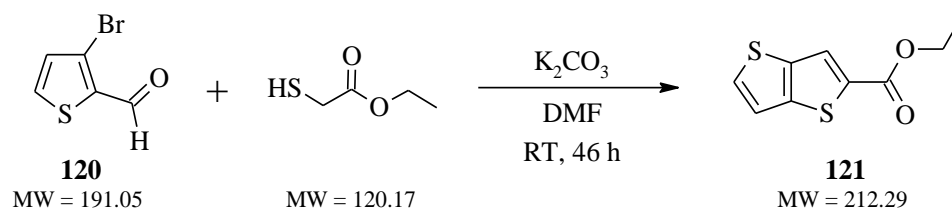glycolate (5.55 mL/6.08 g, 50.59 mmol) was added to the mixture and stirred at RT for another 45 h. Then, the reaction was quenched with the addition of distilled water (100 mL), and the reaction mixture was washed with ethyl acetate (2×80 mL). The collected organic phases were washed with distilled water (3×250 mL), finally with brine (200 mL) and then dried over anhydrous $Na_2SO_4$ and filtered through filter aid (Celite). After removal of the solvent under vacuum, the obtained crude mixture was purified by silica gel chromatography eluting with ethyl acetate to obtained pure product **121** ($R_F$ = 0.40, eluent: ethyl acetate).

**121**: Light yellow liquid (5.73 g, yield 64%).

$^1$H NMR (500 MHz, CDCl$_3$, ppm): $\delta$ = 7.98 (s, 1H), 7.56 (d, $J$ = 5.1 Hz, 1H), 7.26 (d, $J$ = 5.2 Hz, 1H), 4.35 (q, $J$ = 6.9 Hz, 2H), 1.39 (t, $J$ = 7.0 Hz, 3H).

## Preparation of thieno[3,2-*b*]thiophene-2-carboxylic acid (122)
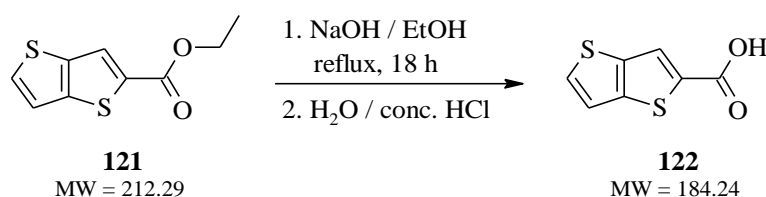


**Scheme 40**: *Preparation of thieno[3,2-b]thiophene-2-carboxylic acid (122)*

**121** (5.65 g, 26.61 mmol) was dissolved in a mixture of ethanol (120 mL) and NaOH (3 equiv., 3.20 g, 80.01 mmol). The reaction mixture was stirred at reflux for 18 h. After that, the reaction mixture was poured into distilled water (150 mL) and conc. hydrochloric acid (58 mL) was added dropwise. The formed precipitate was filtered off and washed with distilled water (3×60 mL). The crude product obtained was crystallized using *n*-heptane to afford pure product **122**.

**122**: Yellow-beige solid material (4.02 g, yield 82%). Melting point 219 °C (lit. 221–222 °C)[169].

$^1$H NMR (500 MHz, CDCl$_3$, ppm): $\delta$ = 8.11 (s, 1H), 7.65 (d, $J$ = 5.2 Hz, 1H), 7.33 (d, $J$ = 5.2 Hz, 1H).

Anal. calcd. for C$_7$H$_4$O$_2$S$_2$: C 45.63%, H 2.19%, N 0%, S 34.81%; Found: C 45.24%, H 2.31%, N 0%, S 35.12%.


## Preparation of thieno[3,2-*b*]thiophene-2-carboxamide (123)
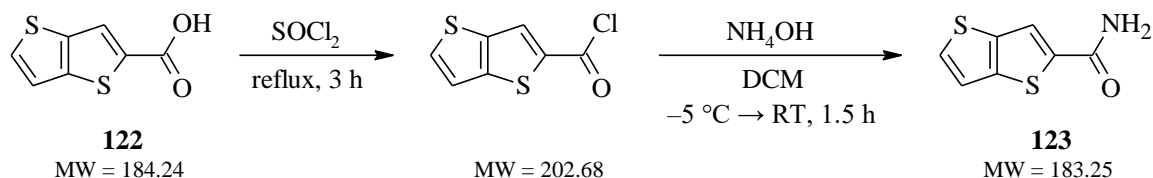


**Scheme 41**: *Preparation of thieno[3,2-b]thiophene-2-carboxamide (123)*

**122** (2.11 g, 11.45 mmol) was stirred in 60 equiv. of thionyl chloride (50 mL, 686 mmol) at reflux for 3 h. Unreacted thionyl chloride was then distilled off from the reaction mixture, and the beige-brown solid material was dissolved in DCM (25 mL). The reaction mixture was cooled to –5 °C, ammonium hydroxide (35 mL) in DCM (35 mL) was added dropwise, and the mixture was stirred at RT for 1.5 h. The obtained milky-white needles were filtered off, and the filter cake was washed with distilled water (3×90 mL), then with DCM (3×70 mL). After precise drying in a vacuum desiccator (at 80 °C for 90 min), product **123** was obtained, which was used in the next reaction step without further purification.

**123**: White-beige solid material (1.64 g, yield 78%).

$^1$H NMR (500 MHz, DMSO-d$_6$, ppm): $\delta$ = 8.08 (s, 2H), 7.82 (d, $J$ = 5.2 Hz, 1H), 7.49 (d, $J$ = 5.1 Hz, 2H).

## Preparation of thieno[3,2-*b*]thiophene-2-carbonitrile (124)



**123**
MW = 183.25

**124**
MW = 165.24
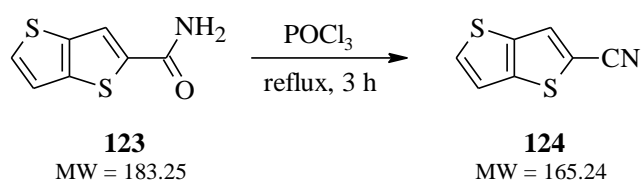
*Scheme 42*: *Preparation of thieno[3,2-b]thiophene-2-carbonitrile (124)*

**123** (1.62 g, 8.84 mmol) was stirred in 30 equiv. of phosphoryl trichloride (24.80 mL, 265 mmol) at reflux for 3 h. Unreacted phosphoryl trichloride was then distilled off from the reaction mixture, and DCM (50 mL) was added to the solid residue. After that, cold distilled water (150 mL) was added dropwise to the mixture and extraction was performed. The reaction mixture was washed with DCM (3×20 mL). The collected organic phases were then washed with saturated $NaHCO_3$ solution (150 mL), followed by distilled water (2×150 mL), finally with brine (150 mL) and then dried over anhydrous $Na_2SO_4$ and filtered through filter aid (Celite). After removal of the solvent under vacuum, the obtained crude mixture was purified by silica gel chromatography eluting with toluene/DCM 1:1 (v/v) to get pure product **124** ($R_F$ = 0.75, eluent: toluene/DCM 4:1).

**124**: Beige-yellow solid material (1.24 g, yield 85%).

^{1}H NMR (300 MHz, $CDCl_3$, ppm): $\delta$ = 7.77 (s, 1H), 7.70 (d, $J$ = 5.2 Hz, 1H), 7.29 (d, $J$ = 5.2 Hz, 1H).

## Preparation of 3,6-dithieno[3,2-*b*]thienyl-DPP (125)



**124**
MW = 165.24

**30a**
MW = 202.25

**125**
MW = 412.53
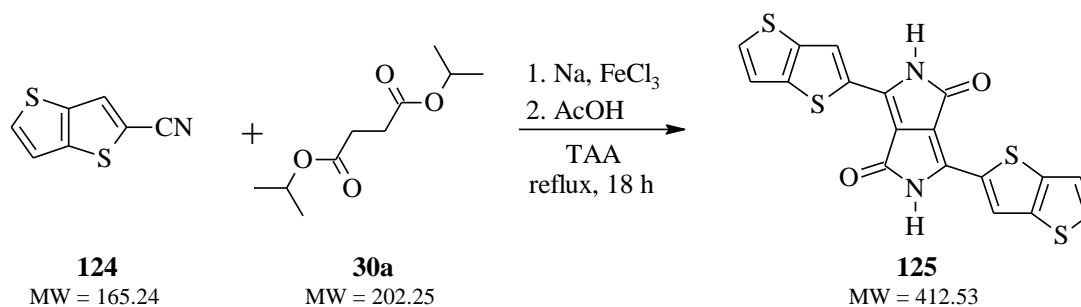
*Scheme 43*: *Synthesis of 3,6-dithieno[3,2-b]thienyl-DPP (125)*

The same procedure as for the **31a** (*Chapter 5.4.1.1*) was used to prepare the **125**, starting with **124** (1.0 equiv., 0.662 g, 4.01 mmol).

**125**: Dark blue-black powder (0.44 g, yield 41%). Melting point >380 °C (lit. –).

^{1}H NMR (500 MHz, DMSO-$d_6$, ppm): $\delta$ = 11.22 (s, 2H), 8.19 (s, 2H), 7.92 (d, $J$ = 4.2 Hz, 2H), 7.28 (d, $J$ = 3.6 Hz, 2H).

Anal. calcd. for $C_{18}H_8N_2O_2S_4$: C 52.41%, H 1.95%, N 6.79%, S 31.09%; Found: C 52.17%, H 2.02%, N 6.83%, S 30.62%.

### 5.4.2 Synthesis of basic DPPs with alkylated side 3,6-aryl units

#### 5.4.2.1 *Synthesis of 3,6-di(3-dodecylthienyl)-DPP (130)*

**Preparation of 3-dodecylthiophene (127)**



*Scheme 44: Preparation of 3-dodecylthiophene (127)*

Magnesium (~1.5 equiv., 3.0 g, 123.4 mmol) was stirred in freshly distilled diethyl ether (20 mL) with a catalytic amount of iodi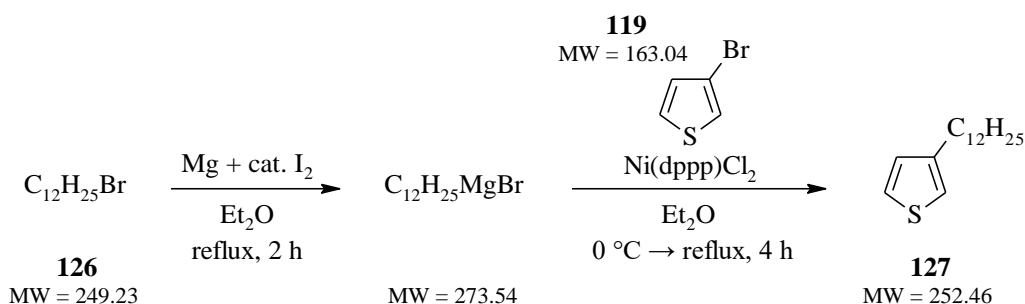ne under argon atmosphere. 1.1 equiv. of **126** (22.7 g, 91.1 mmol) diluted in freshly distilled diethyl ether (25 mL) was added dropwise to this mixture and spontaneous reflux and formation of the milky grey solution were observed. After 2 h of vigorous stirring at reflux, a Grignard reagent was prepared. 1.0 equiv. of **119** (13.5 g, 82.8 mmol) was dissolved in freshly distilled diethyl ether (20 mL), this mixture was cooled to 0 °C and Ni(dppp)Cl$_2$ (40 mg, 0.074 mmol) was added as a catalyst. The prepared Grignard reagent was then slowly added dropwise to this cooled mixture. After that, the reaction mixture was gradually heated to reflux and stirred for 4 h. During this time, additional Ni(dppp)Cl$_2$ (10 mg, 0.018 mmol) was added portion-wise to the reaction mixture. The mixture was then cooled to RT and poured into distilled water with crushed ice (100 mL) and 35% HCl (8 mL), and it was vigorously stirred for 30 min. After that, extraction was performed – the reaction mixture was washed with diethyl ether (3×40 mL). The collected organic phases were then washed with saturated NaHCO$_3$ solution (200 mL), followed by distilled water (2×180 mL), finally with brine (180 mL) and then dried over anhydrous Na$_2$SO$_4$ and filtered through filter aid (Celite). After removing the solvent under vacuum, the obtained crude mixture was dissolved in acetone (25 mL), and it was stored in the fridge for 18 h. Formed white solid (homo-coupling material) was filtered off; the filtrate was concentrated by evaporation of the solvent on a rotary evaporator to get the crude product, which was finally purified by vacuum distillation (10 mbar, oil bath 170 °C) to afford pure product **127**.

**127**: Colourless liquid (13.6 g, yield 65%).

Refractive index: $n20/D = 1.489$ (lit. 1.488)[170].

Density: $\rho25 = 0.906$ g cm$^{-3}$ (lit. 0.902 g cm$^{-3}$)[170].

$^1$H NMR (300 MHz, CDCl$_3$, ppm): $\delta$ = 7.28 (dd, $J$ = 4.8; 2.2 Hz, 1H), 6.96 (m, 2H), 2.63 (t, $J$ = 7.4 Hz, 2H), 1.62 (m, 2H), 1.38–1.27 (m, 18H), 0.87 (t, $J$ = 6.8 Hz, 3H).

GC-MS (method: *2-bromo-3-dodecylthiophene*): RT = 7.69 min; m/z = 252.23.

## Preparation of 2-bromo-3-dodecylthiophene (128)
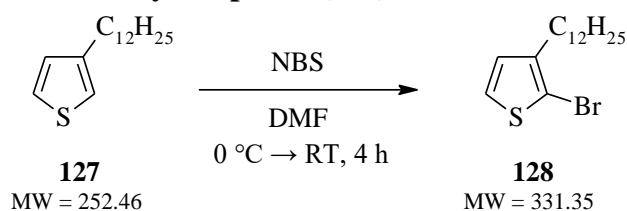


*Scheme 45: Preparation of 2-bromo-3-dodecylthiophene (128)*

**127** (11.50 g, 45.55 mmol) was dissolved in anhydrous DMF (60 mL) under argon atmosphere; then the mixture was cooled to 0 °C and protected from light by aluminium foil. 1.1 equiv. of NBS (8.92 g, 50.12 mmol) dissolved in anhydrous DMF (45 mL) was added dropwise to this mixture and after stirring at 0 °C for 2 h, the reaction mixture temperature was spontaneously heated to RT and stirred for another 2 h. The reaction mixture was then poured into distilled water with crushed ice (220 mL) and stirred for 30 min. After that, extraction was performed – the reaction mixture was washed with toluene (3×50 mL). The collected organic phases were washed with distilled water (3×200 mL), finally with brine (150 mL) and then dried over anhydrous $Na_2SO_4$ and filtered through filter aid (Celite). After removal of the solvent under vacuum, the obtained crude mixture was purified by vacuum distillation (1 mbar, oil bath 155 °C) to afford pure product **128**.

**128**: Slightly yellowish liquid (11.17 g, yield 74%).

Refractive index: $n20/D = 1.513$ (lit. 1.509)[171].

Density: $\rho_{25} = 1.108$ g cm$^{-3}$ (lit. 1.105 g cm$^{-3}$)[171].

$^1$H NMR (300 MHz, CDCl$_3$, ppm): $\delta = 7.21$ (d, $J = 5.4$ Hz, 1H), 6.78 (d, $J = 5.2$ Hz, 1H), 2.55 (t, $J = 7.2$ Hz, 2H), 1.58 (m, 2H), 1.32–1.26 (m, 18H), 0.88 (t, $J = 6.7$ Hz, 3H).

GC-MS (method: *2-bromo-3-dodecylthiophene*): RT = 12.39 min; m/z = 331.29.

## Preparation of 3-dodecylthiophene-2-carbonitrile (129)
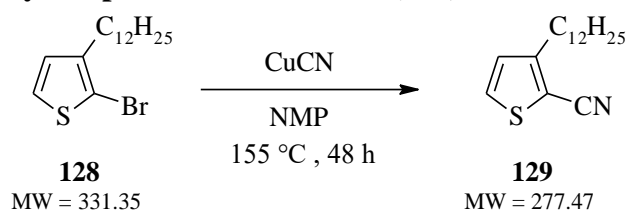


*Scheme 46: Preparation of 3-dodecylthiophene-2-carbonitrile (129)*

Copper cyanide (~2.2 equiv., 1.14 g, 12.68 mmol) was dissolved in anhydrous NMP (12 mL) under argon atmosphere, and the mixture was heated to 155 °C. **128** (1.91 g, 5.76 mmol) was added in one portion to the reaction mixture, and it was vigorously stirred at 155 °C for 48 h. The reaction mixture was then cooled to RT, and diethyl ether (20 mL) was added. This mixture was stirred for 10 min and filtered through filter paper to remove the copper salts. After that, a mixture of distilled water (65 mL) and 35% HCl (35 mL) was added to the filtrate and extraction was performed. The reaction mixture was washed with diethyl ether (3×15 mL). The collected organic phases were then washed with saturated NaHCO$_3$ solution

(100 mL), followed by distilled water (2×100 mL), finally with brine (100 mL) and then dried over anhydrous $Na_2SO_4$ and filtered through filter aid (Celite). After removal of the solvent under vacuum, the obtained crude mixture was purified by silica gel chromatography eluting with *n*-heptane/DCM 2:1 (v/v) to get pure product **129** ($R_F$ = 0.42, eluent: *n*-heptane/DCM 2:1).

**129**: Yellowish liquid (0.89 g, yield 56%).

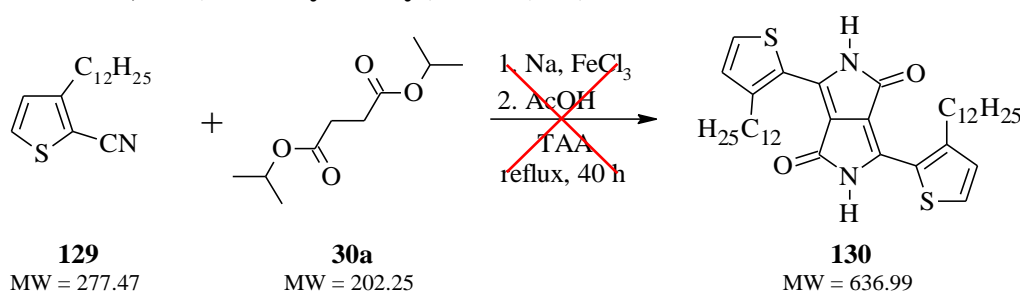$^1$H NMR (300 MHz, CDCl$_3$, ppm): $\delta$ = 7.46 (d, *J* = 5.1 Hz, 1H), 6.95 (d, *J* = 4.9 Hz, 1H), 2.78 (t, *J* = 7.1 Hz, 2H), 1.64 (m, 2H), 1.29 (m, 18H), 0.87 (t, *J* = 6.5 Hz, 3H).

GC-MS (method: *2-bromo-3-dodecylthiophene*): RT = 12.60 min; m/z = 277.15.

**Preparation of 3,6-di(3-dodecylthienyl)-DPP (130)**



**129**
MW = 277.47

**30a**
MW = 202.25

**130**
MW = 636.99

*Scheme 47: Synthesis of 3,6-di(3-dodecylthienyl)-DPP (130)*

The same procedure as for the **31a** (*Chapter 5.4.1.1*) was used to prepare the **130**, starting with **129** (1.0 equiv., 0.700 g, 2.52 mmol). However, even after stirring the reaction mixture at reflux for 40 h, no change was observed. Thus, the reaction was quenched and the starting material **129** was recovered and purified by silica gel chromatography eluting with *n*-heptane/DCM 2:1 (v/v) to get back pure **129** at 0.588 g (84%).

GC-MS (method: *2-bromo-3-dodecylthiophene*): RT = 12.59 min; m/z = 277.17.

*5.4.2.2 Synthesis of 3,6-di(5-bromo-4-dodecylthienyl)-DPP (133)*

**Preparation of 5-bromo-4-dodecylthiophene-2-carbaldehyde (131)**



**128**
MW = 331.35

**131**
MW = 359.36

*Scheme 48: Preparation of 5-bromo-4-dodecylthiophene-2-carbaldehyde (131)*

**128** (6.08 g, 18.35 mmol) was dissolved in anhydrous 1,2-dichloroethane (45 mL) under argon atmosphere. After the dissolution of all material, there was added in one portion 1.10 equiv. of anhydrous DMF (1.56 mL/1.48 g, 20.18 mmol) and the reaction mixture was purged with argon for 15 min. Then, the reaction mixture was cooled to 0 °C, and at this temperature, it was added dropwise 1.20 equiv. of POCl$_3$ (2.06 mL/3.38 g, 22.02 mmol) and

the mixture was heated to reflux and stirred for 21 h. According to GC-MS analysis, a very low reaction conversion was observed so that an additional 0.50 equiv. of DMF (0.71 mL/0.67 g, 9.18 mmol) and POCl$_3$ (0.86 mL/1.41 g, 9.18 mmol) were added and the mixture was stirred at reflux for further 4 h. The reaction mixture was then cooled to RT, poured into saturated NaHCO$_3$ solution (170 mL) and stirred for 2 h. After that, the reaction mixture was washed with DCM (3×75 mL). The collected organic phases were then washed with distilled water (3×250 mL), finally with brine (2×250 mL) and then dried over anhydrous Na$_2$SO$_4$ and filtered through filter aid (Celite). After removal of the solvent under vacuum, the obtained crude mixture was purified by silica gel chromatography eluting with petroleum ether/ toluene 4:1 (v/v) to get pure product **131** ($R_F$ = 0.15, eluent: petroleum ether/toluene 4:1).

**131**: Yellow-orange liquid (4.16 g, yield 63%).

$^1$H NMR (300 MHz, CDCl$_3$, ppm): $\delta$ = 9.77 (s, 1H), 7.53 (s, 1H), 2.57 (t, $J$ = 7.5 Hz, 2H), 1.61–1.23 (m, 20H), 0.85 (t, $J$ = 6.5 Hz, 3H).

GC-MS (method: *2-bromo-3-dodecylthiophene*): RT = 13.49 min; m/z = 359.08.


**Preparation of 5-bromo-4-dodecylthiophene-2-carbonitrile (132)**



*Scheme 49: Preparation of 5-bromo-4-dodecylthiophene-2-carbonitrile (**132**)*

**131** (3.70 g, 10.30 mmol) was dissolved in anhydrous NMP (45 mL) under argon atmosphere, and the reaction mixture was heated to 90 °C and stirred for 25 min. After that, 1.51 equiv. of hydroxylamine hydrochloride (1.08 g, 15.54 mmol) was added piece by piece to the mixture and it was stirred at reflux for 3.5 h. Then, the reaction mixture was cooled to 20 °C and poured into distilled water (150 mL) and stirred for 60 min. Then, diethyl ether (90 mL) was added to the mixture and extraction was performed. The aqueous phase was washed with diethyl ether (2×60 mL), the collected organic phases were washed with distilled water (3×250 mL), finally with brine (200 mL) and then dried over anhydrous Na$_2$SO$_4$ and filtered through filter aid (Celite). After removal of the solvent under vacuum, the obtained crude mixture was purified by silica gel chromatography eluting with petroleum ether/toluene 1:1 (v/v) to get pure product **132** ($R_F$ = 0.90, eluent: petroleum ether/toluene 1:1).

**132**: Slightly yellowish liquid (2.96 g, yield 81%).

$^1$H NMR (300 MHz, CDCl$_3$, ppm): $\delta$ = 7.31 (s, 1H), 2.54 (t, $J$ = 7.3 Hz, 2H), 1.56 (m, 2H), 1.31–1.22 (m, 18H), 0.82 (t, $J$ = 6.3 Hz, 3H).

GC-MS (method: *2-bromo-3-dodecylthiophene*): RT = 12.89 min; m/z = 356.72.

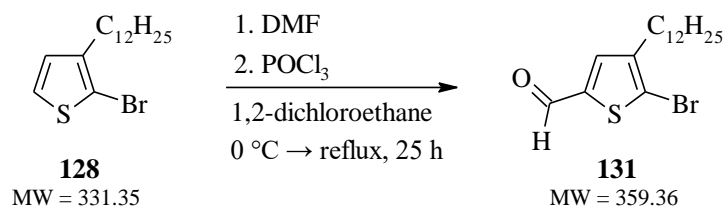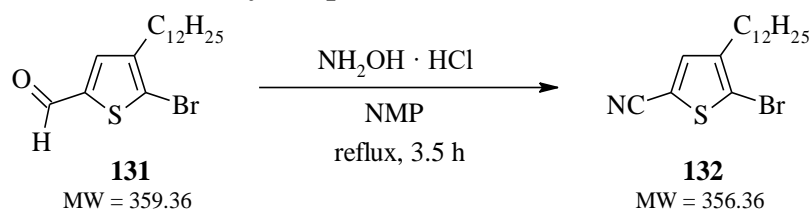**Preparation of 3,6-di(5-bromo-4-dodecylthienyl)-DPP (133)**
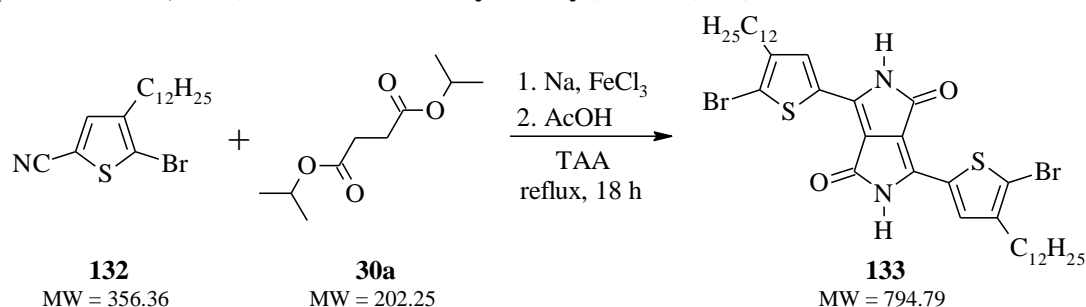


*Scheme 50: Synthesis of 3,6-di(5-bromo-4-dodecylthienyl)-DPP (133)*

The same procedure as for the **31a** (*Chapter 5.4.1.1*) was used to prepare the **133**, starting with **132** (1.0 equiv., 2.85 g, 8.00 mmol).

**133**: Dark violet waxy material (0.32 g, yield 9.4%).

Anal. calcd. for $C_{38}H_{54}Br_2N_2O_2S_2$: C 57.43%, H 6.85%, N 3.53%, S 8.07%; Found: C 57.00%, H 8.21%, N 4.28%, S 8.32%.

### 5.4.2.3 Synthesis of 3,6-di("dodecyl-(Th-Ph-Th)-trimer")-DPP (139)

**Preparation of (3-dodecyl-2-thienyl)magnesium chloride (134)**



*Scheme 51: Preparation of (3-dodecyl-2-thienyl)magnesium chloride (134)*
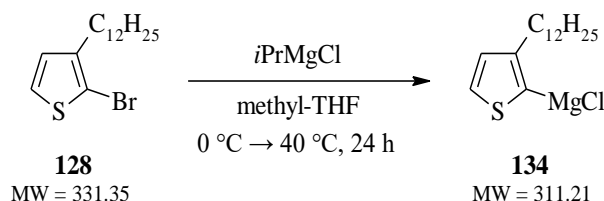
**128** (0.48 g, 1.45 mmol) was dissolved in anhydrous methyl-THF (5 mL) under argon atmosphere; then the mixture was cooled to 0 °C and 1.17 equiv. of *i*PrMgCl (2M, 0.85 mL, 1.70 mmol) was added dropwise to this mixture. After that, the reaction mixture was heated to 40 °C and stirred for 24 h. Subsequent TLC analysis confirmed the successful formation of the GR **134** (approx. 6.35 mL of the homogeneous mixture): after treating a sample of the reaction mixture with water, only a dot corresponding to the **127** molecule standard ($R_F = 0.65$) and no dot corresponding to the starting material **128** ($R_F = 0.76$) was observed in the TLC analysis (eluent: *n*-heptane). It was used directly to the next reaction step.

**Preparation of "dodecyl-(Th-Ph-Th)-trimer" (27) – approach A**
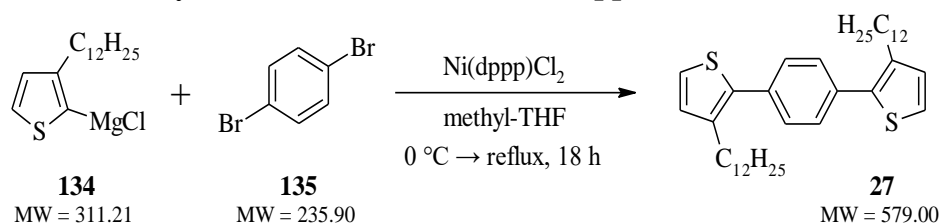


*Scheme 52: Preparation of "dodecyl-(Th-Ph-Th)-trimer" (27) by Kumada cross-coupling*

1.0 equiv. of **135** (0.166 g, 0.703 mmol) was dissolved in anhydrous methyl-THF (8 mL) under argon atmosphere, it was cooled to 0 °C and Ni(dppp)Cl$_2$ (15 mg, 0.028 mmol) was added as a catalyst. The prepared Grignard reagent **134** (a total of approx. 6.3 mL with an estimated concentration of 1.406 mmol of the GR, which corresponds to 2 equiv.) was then slowly added dropwise to this cooled mixture. After that, the reaction mixture was gradually heated to reflux and stirred for 18 h. During this time, additional Ni(dppp)Cl$_2$ (10 mg, 0.018 mmol) was added portion-wise to the reaction mixture. The mixture was then cooled to RT and poured into distilled water with crushed ice (40 mL) and 35% HCl (1 mL), and it was vigorously stirred for 10 min. After that, extraction was performed – the reaction mixture was washed with toluene (3×20 mL). The collected organic phases were then washed with saturated NaHCO$_3$ solution (100 mL), followed by distilled water (2×100 mL), finally with brine (80 mL) and then dried over anhydrous Na$_2$SO$_4$ and filtered through filter aid (Celite). After removal of the solvent under vacuum, the obtained crude mixture was purified by silica gel chromatography eluting with *n*-heptane to get pure product **27** ($R_F$ = 0.52, eluent: *n*-heptane).

**27**: Yellow-orange solid (0.078 g, yield 19%). Melting point 53 °C (lit. 54–56 °C)[85].

$^1$H NMR (500 MHz, CDCl$_3$, ppm): $\delta$ = 7.46 (s, 4H), 7.24 (d, $J$ = 5.2 Hz, 2H), 6.99 (d, $J$ = 5.2 Hz, 2H), 2.69 (t, $J$ = 7.2 Hz, 4H), 1.63 (m, 4H), 1.25 (m, 36H), 0.88 (t, $J$ = 6.2 Hz, 6H).

Anal. calcd. for C$_{38}$H$_{58}$S$_2$: C 78.83%, H 10.10%, N 0%, S 11.08%; Found: C 78.69%, H 10.31%, N 0%, S 10.98%.
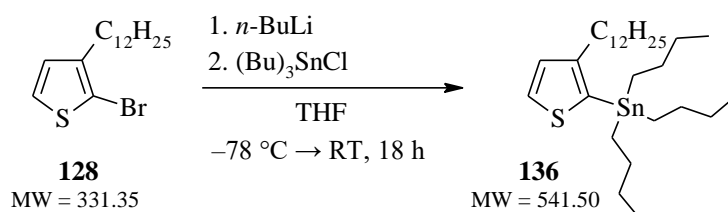

**Preparation of tributyl(3-dodecyl-2-thienyl)-stannane (136)**



*Scheme 53: Preparation of tributyl(3-dodecyl-2-thienyl)-stannane (136)*

**128** (1.00 g, 3.02 mmol) was dissolved in anhydrous THF (15 mL) under argon atmosphere, and the reaction mixture was cooled to –78 °C. After that, 1.20 equiv. of *n*-BuLi (2.5M, 1.45 mL, 3.62 mmol) was added dropwise to this mixture and it was stirred at –78 °C for 2 h. Following that 1.20 equiv. of tributyltin chloride (0.98 mL/1.18 g, 3.62 mmol) in anhydrous THF (5 mL) was added dropwise and the reaction mixture was spontaneously heated to RT and stirred for 18 h. After that, the reaction was quenched by pouring into distilled water (80 mL), and the reaction mixture was washed with diethyl ether (3×20 mL). The collected organic phases were then washed with distilled water (3×80 mL), finally with brine (80 mL) and then dried over anhydrous Na$_2$SO$_4$ and filtered through filter aid (Celite). After removal of the solvent under vacuum, Stille intermediate **136** was obtained, which was used to the next reaction step without further purification and analysis.

**136**: Yellow oily material (1.62 g, yield 99%).

## Preparation of "dodecyl-(Th-Ph-Th)-trimer" (27) – approach B
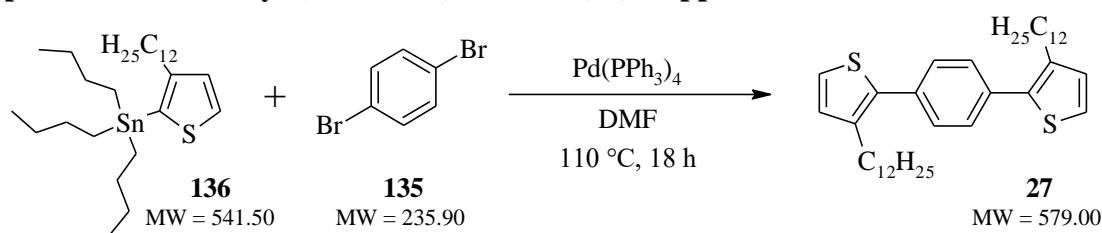


**Scheme 54**: *Preparation of "dodecyl-(Th-Ph-Th)-trimer" (27) by Stille cross-coupling*

**136** (1.490 g, 2.752 mmol), 0.40 equiv. of **135** (0.260 g, 1.102 mmol) and Pd(PPh$_3$)$_4$ (0.254 g, 0.220 mmol) as a catalyst were dissolved in anhydrous DMF (25 mL) under argon atmosphere. The reaction mixture was purged with argon for 20 min, and then it was heated to 110 °C and stirred for 18 h. After that, DMF was distilled off, toluene (25 mL) was added to the reaction mixture and extraction was performed. The organic phase was then washed with distilled water (2×60 mL), finally with brine (80 mL) and then dried over anhydrous Na$_2$SO$_4$ and filtered through filter aid (Celite). After removal of the solvent under vacuum, the obtained crude mixture was purified by silica gel chromatography eluting with *n*-heptane to get pure product **27** ($R_F$ = 0.52, eluent: *n*-heptane).

**27**: Yellow-orange solid (0.230 g, yield 36%). Melting point 52 °C (lit. 54–56 °C)[85].

$^1$H NMR (500 MHz, CDCl$_3$, ppm): $\delta$ = 7.45 (s, 4H), 7.24 (d, $J$ = 5.2 Hz, 2H), 6.98 (d, $J$ = 5.2 Hz, 2H), 2.68 (t, $J$ = 7.2 Hz, 4H), 1.63 (m, 4H), 1.25 (m, 36H), 0.87 (t, $J$ = 6.2 Hz, 6H).

## Preparation of "dodecyl-(Th-Ph-Th)-trimer-5-carbaldehyde" (137)
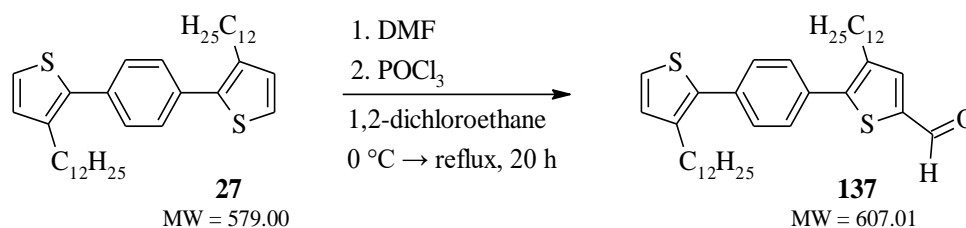


**Scheme 55**: *Preparation of "dodecyl-(Th-Ph-Th)-trimer-5-carbaldehyde" (137)*

The same procedure as for the **118** (*Chapter 5.4.1.3*) was used to prepare the **137**, starting with **27** (1.0 equiv., 0.222 g, 0.383 mmol). Concentrated obtained crude mixture was purified by silica gel chromatography eluting with petroleum ether to get pure product **137** ($R_F$ = 0.52, eluent: toluene).

**137**: Yellow semisolid material (0.084 g, yield 37%).

$^1$H NMR (500 MHz, CDCl$_3$, ppm): $\delta$ = 9.90 (s, 1H), 7.64–7.60 (m, 4H), 7.36 (s, 1H), 7.24 (d, $J$ = 5.5 Hz, 1H), 7.03 (d, $J$ = 5.3 Hz, 1H), 2.71–2.67 (m, 4H), 1.65–1.57 (m, 4H), 1.37–1.25 (m, 36), 0.90–0.87 (m, 6).

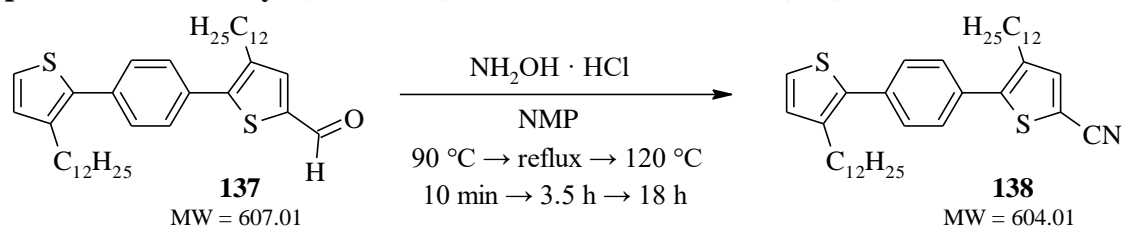**Preparation of "dodecyl-(Th-Ph-Th)-trimer-5-carbonitrile" (138)**



*Scheme 56: Preparation of "dodecyl-(Th-Ph-Th)-trimer-5-carbonitrile" (138)*

The same procedure as for the **36** (*Chapter 5.4.1.3*) was used to prepare the **138**, starting with **137** (1.0 equiv., 0.080 g, 0.132 mmol). The temperature of the reaction mixture for 18 h of stirring was increased from RT to 120 ° C. Concentrated obtained crude mixture was purified by silica gel chromatography eluting with petroleum ether/toluene 1:1 (v/v) to get pure product **138** ($R_F$ = 0.95, eluent: toluene).

**138**: Yellow semisolid material (0.073 g, yield 92%).

$^1$H NMR (500 MHz, CDCl$_3$, ppm): $\delta$ = 7.62–7.59 (m, 4H), 7.28 (d, *J* = 5.5 Hz, 1H), 7.24 (s, 1H), 7.01 (d, *J* = 5.4 Hz, 1H), 2.70–2.65 (m, 4H), 1.64–1.55 (m, 4H), 1.37–1.26 (m, 36), 0.91–0.86 (m, 6).

**Preparation of 3,6-di("dodecyl-(Th-Ph-Th)-trimer")-DPP (139)**
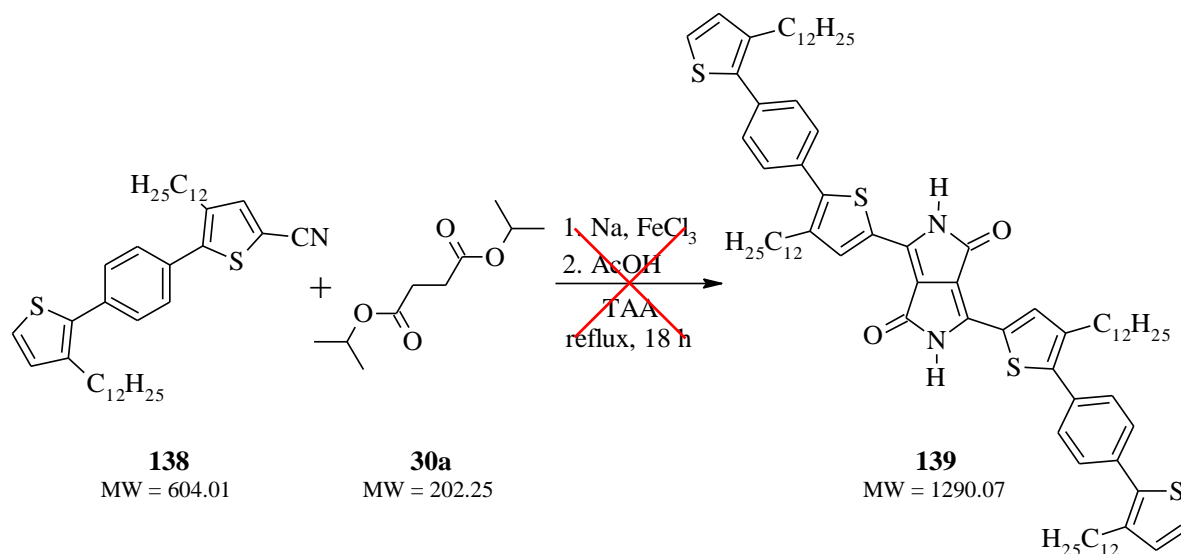


*Scheme 57: Synthesis of 3,6-di("dodecyl-(Th-Ph-Th)-trimer")-DPP (139)*

The same procedure as for the **31a** (*Chapter 5.4.1.1*) was used to prepare the **139**, starting with **138** (1.0 equiv., 0.070 g, 0.116 mmol). However, even after stirring the reaction mixture at reflux for 18 h, no formation of the DPP skeleton was observed (only a milky yellow-grey solution was observed) and thus the reaction was quenched. According to TLC analysis, starting nitrile **159** was likely to decompose so that it could not be recovered. Therefore, the reaction was unsuccessful, and product **139** was not prepared.

### 5.4.3  Synthesis of alkylating reagents

#### 5.4.3.1  *Synthesis of 1-(2-bromoethyl)adamantane (141)*



**140**
MW = 180.29

aq. HBr
reflux, 22 h

**141**
MW = 243.18
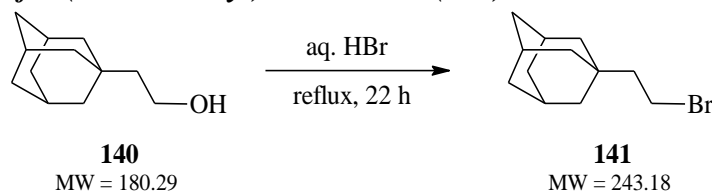
*Scheme 58: Synthesis of 1-(2-bromoethyl)adamantane (141)*

**140** (30.06 g, 166.73 mmol) was stirred in 48% hydrobromic acid (150 mL) at reflux for 22 h. The biphasic reaction mixture was then cooled to RT and washed with chloroform (3×30 mL). The collected organic phases were then washed with 96% sulphuric acid (2×30 mL), followed by saturated NaHCO$_3$ solution (2×150 mL), then with distilled water (2×200 mL), finally with brine (120 mL) and then dried over anhydrous Na$_2$SO$_4$ and filtered through filter aid (Celite). After removal of the solvent under vacuum, the obtained crude mixture was purified by crystallisation in methanol (90 mL) to get pure product **141**.

**141**: White crystals (32.4 g, yield 80%). Melting point 68 °C (lit. 68–69 °C)[172].

$^1$H NMR (500 MHz, CDCl$_3$, ppm): $\delta$ = 3.40 (m, 2H), 1.94 (m, 3H), 1.72 (m, 2H), 1.69–1.61 (m, 6H), 1.50 (m, 6H).

Anal. calcd. for C$_{12}$H$_{19}$Br: C 59.27%, H 7.88%; Found: C 59.23%, H 8.01%.

GC-MS (method: *vseobecna*): RT = 7.02 min; m/z = 242.95.

#### 5.4.3.2  *Synthesis of 1-(2-iodoethyl)adamantane (142)*



**141**
MW = 243.18

KI
acetone
reflux, 20 h

**142**
MW = 290.18

*Scheme 59: Synthesis of 1-(2-iodoethyl)adamantane (142)*

**141** (6.11 g, 25.13 mmol) and 2.50 equiv. of potassium iodide (10.43 g, 62.81 mmol) were stirred at reflux for 20 h in anhydrous acetone (100 mL) and under argon atmosphere. After that, the reaction was monitored by GC-MS analysis and 93.15% reaction conversion was observed. Acetone was then removed from the reaction mixture by a rotary evaporator, the solid residue was dissolved in *tert*-butyl-methyl ether (250 mL), and it was washed with distilled water (3×250 mL), followed by 5% solution of Na$_2$S$_2$O$_3$ (1×120 mL) and finally with brine (120 mL). The organic phase was then dried over anhydrous Na$_2$SO$_4$ and filtered through filter aid (Celite). After removal of the solvent under vacuum, the obtained crude mixture was purified by crystallisation in methanol (20 mL) to get pure product **142**.

**142**: White crystals (7.18 g, yield 98.5%). Melting point 97–99 °C (lit. –).

Anal. calcd. for C$_{12}$H$_{19}$I: C 49.67%, H 6.60%; Found: C 49.41%, H 6.84%.

GC-MS (method: *vseobecna*): RT = 7.67 min; m/z = 289.75 (purity 92%).

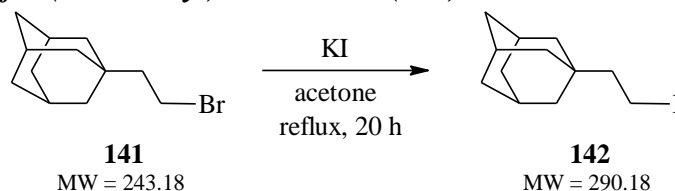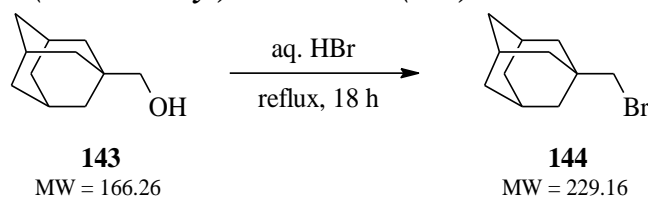### 5.4.3.3 Synthesis of 1-(bromomethyl)adamantane (144)



**143**
MW = 166.26

**144**
MW = 229.16

*Scheme 60: Synthesis of 1-(bromomethyl)adamantane (**144**)*

The same procedure as for the **141** (*Chapter 5.4.3.1*) was used to prepare the **144**, starting with **143** (1.0 equiv., 6.7 g, 40.30 mmol). The reaction time of stirring at reflux was reduced by 4 h to a total of 18 h. Concentrated obtained crude mixture was purified by crystallisation in methanol (50 mL) to get pure product **144**.

**144**: White crystals (4.42 g, yield 48%). Melting point 42 °C (lit. 42–43 °C)[173].

Anal. calcd. for $C_{11}H_{17}Br$: C 57.65%, H 7.48%; Found: C 57.47%, H 7.62%.

GC-MS (method: *vseobecna*): RT = 6.82 min; m/z = 228.94.

### 5.4.4 Synthesis of *N*- and *O*-alkylated DPPs

### 5.4.4.1 Alkylation of thienyl-DPP

**31a** (1.0 equiv., 1.0 g, 3.3 mmol) and anhydrous potassium carbonate (~5.3 equiv., 2.4 g, 17.4 mmol) were stirred at 60 °C for 1 h in anhydrous DMF (45 mL) and under argon atmosphere. Then, 3.5 equiv. (11.6 mmol) of alkyl bromide (**R–Br**) dissolved in anhydrous DMF (20 mL) was gradually added dropwise for 30 min. After 20 min of stirring, the mixture was heated to 105 °C and stirred for 2 h. DMF was then distilled off by vacuum distillation, and the solid material was further purified in order to isolate all formed products.



**31a**
MW = 300.36

**32a**     **32b**     **32c**
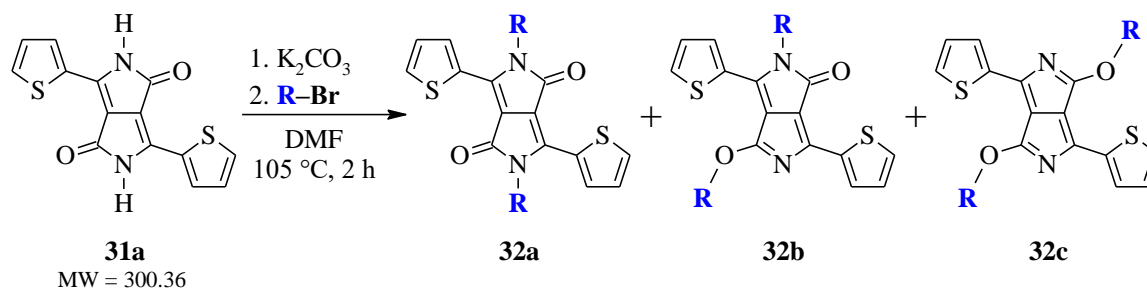
*Scheme 61: Alkylation of basic 3,6-dithienyl-DPP (**31a**)*

**Dodecyl-alkylated thienyl-DPPs**
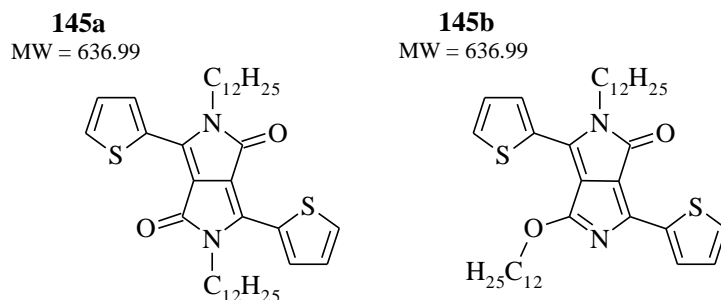


**145a**
MW = 636.99

**145b**
MW = 636.99

The solid material obtained from the reaction mixture as a distillation residue was suspended in methanol (50 mL), filtered off and washed with new methanol (2×40 mL) to give the crude product as a solid material on a filter cake. This crude product was purified by silica gel chromatography eluting with toluene to get pure product **145a** ($R_F$ = 0.38, eluent: toluene).

**145a**: Dark violet crystals (1.58 g, yield 75%). Melting point 128 °C (lit. 128 °C)[107].

$^1$H NMR (300 MHz, CDCl$_3$, ppm): $\delta$ = 8.92 (dd, $J$ = 3.9; 1.1 Hz, 2H), 7.63 (dd, $J$ = 5.0; 1.1 Hz, 2H), 7.28 (dd, $J$ = 5.0; 4.0 Hz, 2H), 4.07 (t, $J$ = 7.8 Hz, 4H), 1.74–1.41 (m, 4H), 1.35–1.20 (m, 36H), 0.87 (t, $J$ = 6.5 Hz, 6H).

Anal. calcd. for C$_{38}$H$_{56}$N$_2$O$_2$S$_2$: C 71.56%, H 8.86%, N 4.40%, S 10.07%; Found: C 71.42%, H 8.62%, N 4.61%, S 9.93%.


The solid material obtained from the reaction mixture as a distillation residue was suspended in methanol (50 mL), filtered off and washed with new methanol (2×40 mL). The crude product was obtained by evaporating methanol from the filtrate. This crude product was purified by silica gel chromatography eluting with toluene to get pure product **145b** ($R_F$ = 0.42, eluent: toluene).

**145b**: Dark violet waxy (semi-solid) material (0.13 g, yield 6%). Melting point –.

$^1$H NMR (300 MHz, CDCl$_3$, ppm): $\delta$ = 8.46 (s, 1H), 8.24 (d, $J$ = 3.5 Hz, 1H), 7.70 (d, $J$ = 4.5 Hz, 1H), 7.50 (d, $J$ = 5.0 Hz, 1H), 7.26 (dd, $J$ = 4.3; 1.8 Hz, 1H), 7.20 (t, $J$ = 4.5 Hz, 1H), 4.59 (s, 2H), 3.98 (m, 2H), 1.86 (m, 2H), 1.72 (m, 2H), 1.39–1.25 (m, 36H), 0.88 (m, 6H).

Anal. calcd. for C$_{38}$H$_{56}$N$_2$O$_2$S$_2$: C 71.56%, H 8.86%, N 4.40%, S 10.07%; Found: C 71.07%, H 8.68%, N 4.59%, S 9.91%.


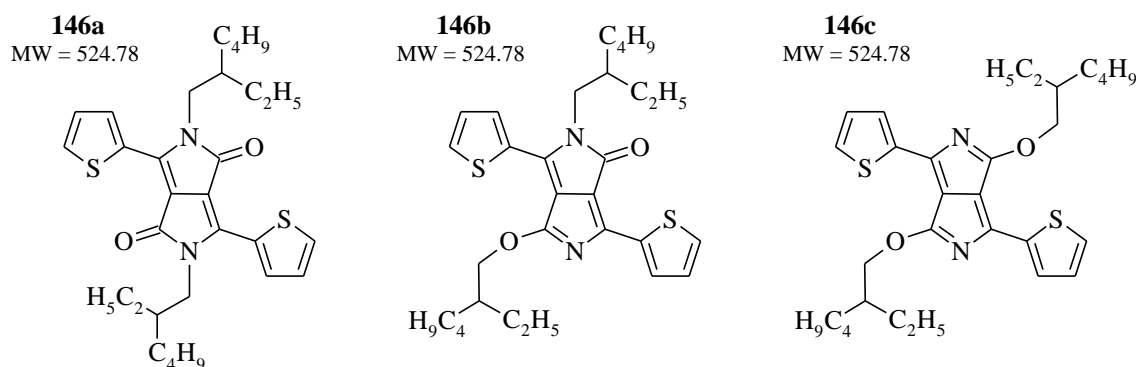**2-Ethylhexyl-alkylated thienyl-DPPs**



The solid material obtained from the reaction mixture as a distillation residue was suspended in methanol (70 mL), filtered off and washed with new methanol (2×40 mL) to give the crude product as a solid material on a filter cake. This crude product was purified by silica gel chromatography eluting with toluene to get pure product **146a** ($R_F$ = 0.26, eluent: toluene).

**146a**: Dark red crystals (0.71 g, yield 41%). Melting point 126 °C (lit. 127 °C)[107].

$^1$H NMR (300 MHz, CDCl$_3$, ppm): $\delta$ = 8.89 (dd, $J$ = 3.9; 1.2 Hz, 2H), 7.63 (dd, $J$ = 5.1; 1.2 Hz, 2H), 7.29 (dd, $J$ = 5.1; 3.9 Hz, 2H), 4.04 (m, 4H), 1.88 (m, 2H), 1.40–1.24 (m, 16H), 0.92–0.85 (m, 12H).

$^{13}$C NMR (125 MHz, CDCl$_3$, ppm): $\delta$ = 161.79, 140.44, 135.23, 130.48, 129.86, 128.41, 107.98, 45.89, 39.13, 30.25, 28.39, 23.59, 23.05, 13.99, 10.50.

Anal. calcd. for C$_{30}$H$_{40}$N$_2$O$_2$S$_2$: C 68.66%, H 7.68%, N 5.34%; Found: C 68.12%, H 7.47%, N 5.53%.

The solid material obtained from the reaction mixture as a distillation residue was suspended in methanol (70 mL), filtered off and washed with new methanol (2×40 mL). The crude product was obtained by evaporating methanol from the filtrate. This crude product was purified by silica gel chromatography eluting with toluene to get pure product **146b** ($R_F$ = 0.36, eluent: toluene). Additional pure product **146b** was obtained from the previous column chromatography of the material from the filter cake.

**146b**: Purple waxy (semi-solid) material (0.31 g, yield 18%). Melting point –.

$^1$H NMR (500 MHz, CDCl$_3$, ppm): $\delta$ = 8.48 (d, $J$ = 3.6 Hz, 1H), 8.19 (d, $J$ = 3.5 Hz, 1H), 7.68 (d, $J$ = 5.0 Hz, 1H), 7.50 (d, $J$ = 4.5 Hz, 1H), 7.22 (dd, $J$ = 5.0; 4.5 Hz, 1H), 7.19 (dd, $J$ = 4.0; 3.5 Hz, 1H), 4.52 (m, 2H), 3.94 (m, 2H), 1.79 (m, 2H), 1.38–1.23 (m, 16H), 0.91–0.85 (m, 12H).

$^{13}$C NMR (125 MHz, CDCl$_3$, ppm): $\delta$ = 166.38, 161.73, 149.62, 142.46, 138.73, 134.82, 131.63, 131.49, 130.09, 128.96, 128.23, 127.96, 114.30, 111.15, 72.45, 45.54, 39.37, 39.13, 31.26, 30.76, 30.29, 29.70, 29.09, 28.40, 24.12, 23.62, 23.03, 14.01, 11.28, 10.51.

Anal. calcd. for C$_{30}$H$_{40}$N$_2$O$_2$S$_2$: C 68.66%, H 7.68%, N 5.34%; Found: C 68.21%, H 7.54%, N 5.12%.

The solid material obtained from the reaction mixture as a distillation residue was suspended in methanol (70 mL), filtered off and washed with new methanol (2×40 mL). The crude product was obtained by evaporating methanol from the filtrate. This crude product was purified by silica gel chromatography eluting with toluene to get pure product **146c** ($R_F$ = 0.68, eluent: toluene).

**146c**: Dark purple waxy (semi-solid) material (0.06 g, yield 3%). Melting point –.

$^1$H NMR (300 MHz, CDCl$_3$, ppm): $\delta$ = 8.04 (dd, $J$ = 4.9, 2.4 Hz, 2H), 7.55 (dd, $J$ = 6.3, 3.9 Hz, 2H), 7.18 (dd, $J$ = 5.7, 3.3 Hz, 2H), 4.55 (m, 4H), 1.82 (m, 2H), 1.54–1.29 (m, 16H), 0.98–0.83 (m, 12H).

$^{13}$C NMR (125 MHz, CDCl$_3$, ppm): $\delta$ = 147.72, 147.10, 138.53, 129.01, 124.49, 123.99, 119.16, 39.51, 31.46, 30.23, 29.71, 29.08, 23.01, 14.08, 11.27.

Anal. calcd. for C$_{30}$H$_{40}$N$_2$O$_2$S$_2$: C 68.66%, H 7.68%, N 5.34%; Found: C 68.34%, H 7.93%, N 5.60%.

## Ethyladamantyl-alkylated thienyl-DPPs
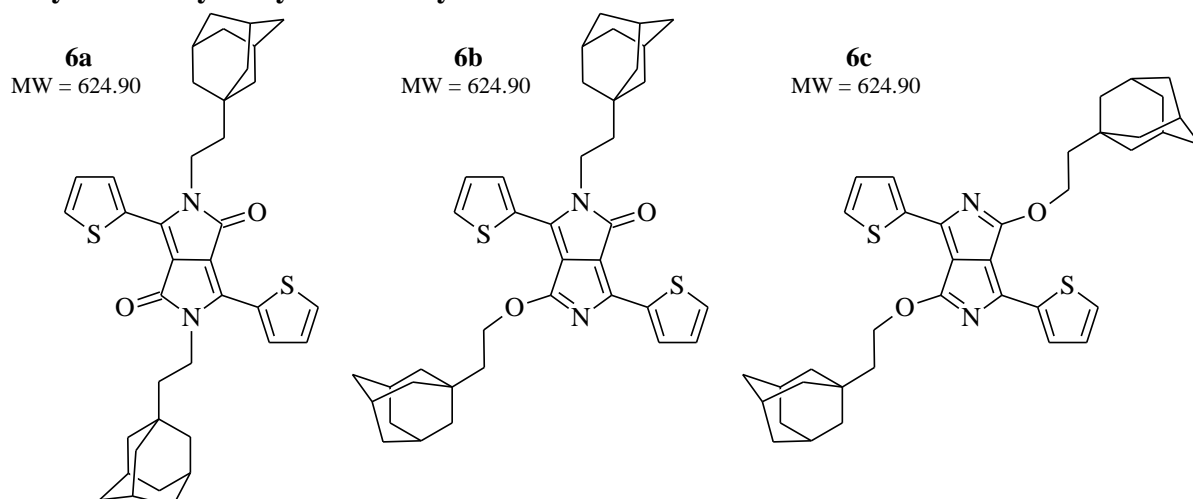
**6a**
MW = 624.90

**6b**
MW = 624.90

**6c**
MW = 624.90



The solid material obtained from the reaction mixture as a distillation residue was suspended in methanol (80 mL), filtered off and washed with new methanol (2×50 mL) to give the crude product as a solid material on a filter cake. This crude product was purified by silica gel chromatography eluting with toluene/chloroform 3:1 (v/v) followed by crystallisation in toluene with the addition of *n*-heptane to get pure product **6a** ($R_F$ = 0.60, eluent: toluene/chloroform 3:1).

**6a**: Violet crystals (0.75 g, yield 36%). Melting point 321 °C (lit. 323–324 °C)[50].

$^1$H NMR (500 MHz, CDCl$_3$, ppm): $\delta$ = 8.91 (dd, *J* = 3.9; 1.1 Hz, 2H), 7.63 (dd, *J* = 5.0; 1.1 Hz, 2H), 7.27 (dd, *J* = 5.0, 3.9 Hz, 2H), 4.14–4.11 (m, 4H), 2.02–1.97 (m, 6H), 1.75–1.68 (m, 6H), 1.68–1.63 (m, 17H), 1.57–1.49 (m, 5H).

$^{13}$C NMR (125 MHz, CDCl$_3$, ppm): $\delta$ = 161.28, 140.13, 135.23, 130.57, 129.69, 128.57, 107.87, 43.23, 42.30, 37.72, 37.11, 32.22, 28.63.

Anal. calcd. for C$_{38}$H$_{44}$N$_2$O$_2$S$_2$: C 73.04%, H 7.10%, N 4.48%, S 10.26%; Found: C 73.15%, H 7.08%, N 4.42%, S 10.38%. EI (m/z) 624.89; Found 624.97.

The solid material obtained from the reaction mixture as a distillation residue was suspended in methanol (80 mL), filtered off and washed with new methanol (2×50 mL). The crude product was obtained by evaporating methanol from the filtrate. This crude product was purified by silica gel chromatography eluting with toluene/chloroform 3:1 (v/v) to get pure product **6b** ($R_F$ = 0.65, eluent: toluene/chloroform 3:1). Additional pure product **6b** was obtained from the previous column chromatography of the material from the filter cake.

**6b**: Dark violet solid (0.41 g, yield 20%). Melting point 210 °C.

$^1$H NMR (500 MHz, CDCl$_3$, ppm): $\delta$ = 8.45 (d, *J* = 3.7 Hz, 1H), 8.25 (d, *J* = 3.8 Hz, 1H), 7.69 (d, *J* = 4.9 Hz, 1H), 7.49 (d, *J* = 4.9 Hz, 1H), 7.27 (d, *J* = 3.2 Hz, 1H), 7.21–7.15 (m, 1H), 4.67–4.63 (t, *J* = 7.1 Hz, 2H), 4.05–3.98 (m, 2H), 1.97 (dt, *J* = 7.0; 3.6 Hz, 6H), 1.72 (dd, *J* = 12.1; 3.2 Hz, 6H), 1.68–1.55 (m, 21H), 1.52–1.48 (m, 2H).

$^{13}$C NMR (125 MHz, CDCl$_3$, ppm): $\delta$ = 166.15, 161.35, 149.43, 142.41, 138.76, 135.29, 131.65, 131.48, 130.02, 129.78, 128.91, 128.23, 113.87, 111.44, 66.79, 43.34, 42.93, 42.72, 42.27, 37.43, 37.09, 37.05, 32.20, 32.01, 28.67, 28.61.

Anal. calcd. for $C_{38}H_{44}N_2O_2S_2$: C 73.04%, H 7.10%, N 4.48%; Found: C 72.81%, H 7.01%, N 4.57%.

The solid material obtained from the reaction mixture as a distillation residue was suspended in methanol (80 mL), filtered off and washed with new methanol (2×50 mL). The crude product was obtained by evaporating methanol from the filtrate. This crude product was purified by silica gel chromatography eluting with toluene/chloroform 3:1 (v/v) to get pure product **6c** ($R_F$ = 0.95, eluent: toluene/chloroform 3:1).

**6c**: Dark violet solid (0.12 g, yield 6%). Melting point 221 °C.

$^1$H NMR (300 MHz, CDCl$_3$, ppm): $\delta$ = 8.05 (dd, $J$ = 3.7; 0.8 Hz, 2H), 7.54 (dd, $J$ = 4.8; 0.7 Hz, 2H), 7.18 (dd, $J$ = 4.9, 3.9 Hz, 2H), 4.67 (t, $J$ = 7.2 Hz, 4H), 1.98 (m, 4H), 1.70–1.64 (m, 24H), 1.54 (s, 4H), 1.34–1.26 (m, 2H).

$^{13}$C NMR (125 MHz, CDCl$_3$, ppm): $\delta$ = 147.52, 146.96, 138.29, 129.09, 124.43, 123.98, 118.92, 42.50, 36.88, 31.89, 31.39, 30.05, 28.45.

Anal. calcd. for $C_{38}H_{44}N_2O_2S_2$: C 73.04%, H 7.10%, N 4.48%; Found: C 72.96%, H 6.99%, N 4.51%.

**Methyladamantyl-alkylated thienyl-DPP**



**147**
MW = 596.85
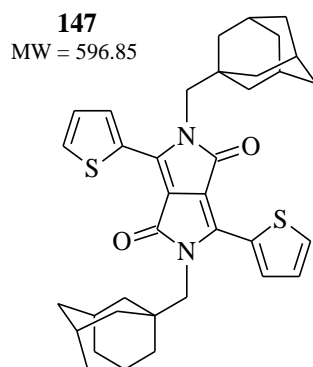
The same procedure as described in this chapter (*5.4.4.1*) as the general alkylation procedure was used to prepare the **147**; however, the reaction temperature was increased to 135 °C and the reaction time was extended to 18 h. After that, the solid material obtained from the reaction mixture as a distillation residue was suspended in methanol (70 mL), filtered off and washed with distilled water (3×50 mL) and then with methanol (2×30 mL) to give the crude product as a solid material on a filter cake. This crude product was purified by silica gel chromatography eluting with toluene/chloroform 1:1 (v/v) to get pure product **147** ($R_F$ = 0.45, eluent: toluene/chloroform 1:1).

**147**: Violet crystals (0.135 g, yield 7%). Melting point 339 °C.

$^1$H NMR (500 MHz, CDCl$_3$, ppm): $\delta$ = 8.57 (dd, $J$ = 3.9; 1.2 Hz, 2H), 7.58 (dd, $J$ = 5.0; 1.2 Hz, 2H), 7.24 (dd, $J$ = 5.0; 3.8 Hz, 2H), 3.90 (s, 4H), 1.89 (m, 6H), 1.64–1.54 (m, 13H), 1.50 (d, $J$ = 2.9 Hz, 10H), 1.26 (s, 1H).

Anal. calcd. for $C_{36}H_{40}N_2O_2S_2$: C 72.45%, H 6.76%, N 4.69%, S 10.74%; Found: C 72.62%, H 6.71%, N 4.58%, S 10.92%.

### 5.4.4.2 Synthesis of asymmetrically N,N'-alkylated-thienyl-DPP

### Preparation of mono-*N*-methyladamantyl-alkylated thienyl-DPP (148)
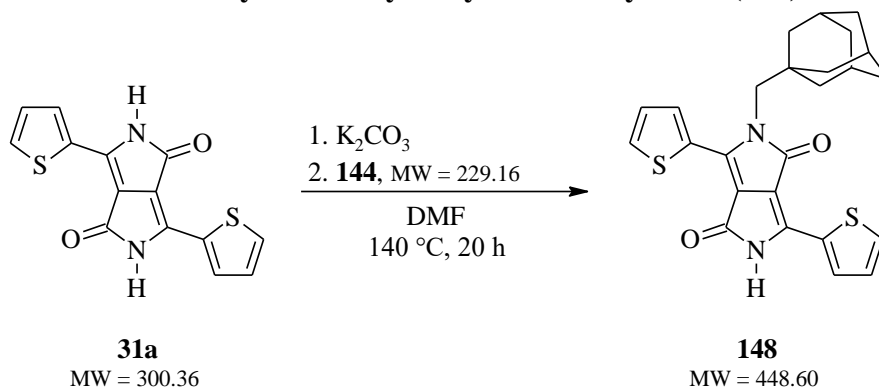


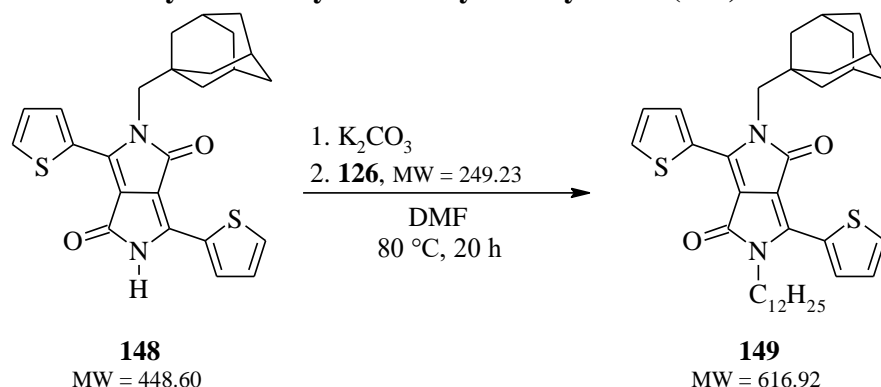*Scheme 62: Preparation of mono-N-methyladamantyl-alkylated thienyl-DPP (148)*

**31a** (1.0 equiv., 0.85 g, 2.83 mmol) and anhydrous potassium carbonate (~3.0 equiv., 1.17 g, 8.49 mmol) were stirred at 60 °C for 1 h in anhydrous DMF (60 mL) and under argon atmosphere. Then, 1-(bromomethyl)adamantane (**144**, ~1.5 equiv., 0.97 g, 4.25 mmol) was added in one portion to the reaction mixture, and it was stirred at 140 °C for 20 h. After that, the reaction mixture was poured into distilled water (350 mL), and the formed precipitate was filtered off and washed first with distilled water (3×150 mL) to remove unreacted potassium carbonate and residual DMF. The filter cake was then washed with hot chloroform (3×180 mL) to dissolve the product and separate it from the unreacted starting material **31a**. The chloroform filtrate was then concentrated to give the crude product which was further purified twice by silica gel chromatography, eluting first with DCM/*n*-heptane (4:1) followed by DCM/*n*-heptane (1:1) to get pure product **148** ($R_F$ = 0.39, eluent: DCM/*n*-heptane 4:1, eluting 3x).

**148**: Dark red solid (0.21 g, yield 15%). Melting point >340 °C.

$^1$H NMR (500 MHz, CDCl$_3$, ppm): $\delta$ = 8.54 (dt, $J$ = 3.9; 1.0 Hz, 1H), 8.37 (dt, $J$ = 3.9; 1.0 Hz, 1H), 8.25 (s, 1H), 7.61 (ddd, $J$ = 4.9; 3.9; 1.0 Hz, 2H), 7.26–7.23 (m, 2H), 3.93 (s, 2H), 1.89 (s, 2H), 1.63 (s, 1H), 1.57–1.47 (m, 10H), 1.25 (s, 4H), 0.90–0.83 (m, 1H).

Anal. calcd. for C$_{25}$H$_{24}$N$_2$O$_2$S$_2$: C 66.93%, H 5.39%, N 6.24%, S 14.30%; Found: C 67.24%, H 5.51%, N 6.13%, S 13.94%.

**Preparation of *N*-dodecyl-*N′*-methyladamantyl-thienyl-DPP (149)**



*Scheme 63: Preparation of N-dodecyl-N'-methyladamantyl-thienyl-DPP (**149**)*

**148** (1.0 equiv., 0.05 g, 0.11 mmol) and anhydrous potassium carbonate (~2.6 equiv., 0.04 g, 0.29 mmol) were stirred at 60 °C for 30 min in anhydrous DMF (5 mL) and under argon atmosphere. Then, 1-bromododecane (**126**, ~1.8 equiv., 0.05 g, 0.20 mmol) diluted in anhydrous DMF (3 mL) was added dropwise to the reaction mixture, and it was stirred at 80 °C for 20 h. After that, DMF was distilled off by vacuum distillation, the solid material was dissolved in toluene (30 mL), and extraction was performed. The organic phase was washed with distilled water (3×150 mL), finally with brine (200 mL) and then dried over anhydrous $Na_2SO_4$ and filtered through filter aid (Celite). After removal of the solvent under vacuum, the obtained crude mixture was purified by silica gel chromatography eluting with toluene to get pure product **149** ($R_F$ = 0.30, eluent: toluene).

**149**: Red-violet crystals (0.042 g, yield 61%). Melting point 128 °C.

^{1}H NMR (500 MHz, $CDCl_3$, ppm): $\delta$ = 8.93 (d, *J* = 3.9 Hz, 1H), 8.58 (d, *J* = 3.9 Hz, 1H), 7.63 (d, *J* = 5.0 Hz, 1H), 7.58 (d, *J* = 4.9 Hz, 1H), 7.28 (t, *J* = 4.4 Hz, 1H), 7.24 (t, *J* = 4.4 Hz, 1H), 4.08–4.02 (m, 2H), 3.93 (s, 2H), 1.91–1.86 (m, 3H), 1.74 (q, *J* = 7.9 Hz, 3H), 1.62 (d, *J* = 12.4 Hz, 4H), 1.54 (s, 3H), 1.49 (d, *J* = 3.0 Hz, 6H), 1.41 (d, *J* = 7.8 Hz, 2H), 1.34 (s, 3H), 1.32 (s, 4H), 1.29 (s, 8H), 1.26 (s, 30H), 0.91–0.84 (m, 10H).

Anal. calcd. for $C_{37}H_{48}N_2O_2S_2$: C 72.03%, H 7.84%, N 4.54%, S 10.34%; Found: C 73.38%, H 8.61%, N 4.03%, S 9.96%.

### 5.4.4.3 Alkylation of benzofuranyl-thienyl-DPP

The same procedure, as described in *Chapter 5.4.4.1* as the general alkylation procedure, was used for the benzofuranyl-thienyl-DPP.

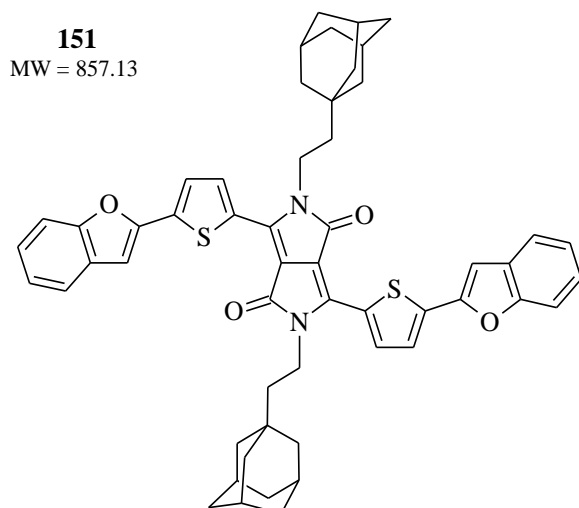**Dodecyl-alkylated benzofuranyl-thienyl -DPP**



**150**
MW = 869.23
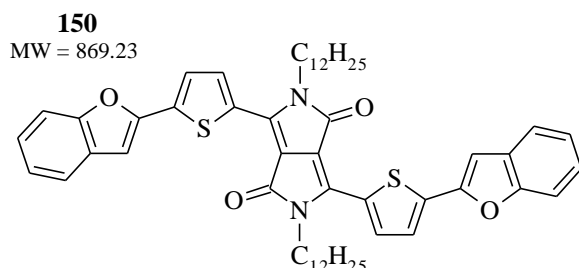
Benzofuranyl-thienyl-DPP (1.0 equiv., 0.100 g, 0.188 mmol) was used as starting material. The reaction mixture was stirred at 105 °C for 2 h, then poured into distilled water (150 mL) and the formed precipitate was filtered off and washed first with distilled water (3×60 mL) to remove unreacted potassium carbonate/residual DMF and then with methanol (2×40 mL). The solid material obtained from the filter cake was further purified twice by silica gel chromatography, both eluting with DCM/*n*-heptane (2:1) to give product **150** ($R_F$ = 0.50, eluent: DCM/*n*-heptane 2:1).

**150**: Dark blue solid (9.5 mg, yield 6%). Melting point 247 °C.

^{1}H NMR (500 MHz, CDCl$_3$, ppm): $\delta$ = 9.03 (d, $J$ = 4.0 Hz, 2H), 7.61–7.50 (m, 6H), 7.32–7.28 (m, 2H), 7.25–7.19 (m, 2H), 7.05 (s, 2H), 4.19–4.08 (m, 4H), 1.82 (m, 4H), 1.32–1.21 (m, 36H), 0.91–0.84 (m, 6H).

**Ethyladamantyl-alkylated benzofuranyl-thienyl-DPP**



**151**
MW = 857.13

Benzofuranyl-thienyl-DPP (1.0 equiv., 0.290 g, 0.545 mmol) was used as starting material. The reaction mixture was stirred at 135 °C for 17 h. Then, the solvent was distilled off, and the solid material as a distillation residue was suspended in methanol (30 mL), filtered off and washed with new methanol (2×30 mL). The filter cake was then washed with hot chloroform (2×150 mL) to dissolve the product and separate it from the unreacted starting material. The

chloroform filtrate was then concentrated to give the crude product. It was further purified first by crystallisation in toluene/*n*-heptane (20 mL/6 mL) followed by silica gel chromatography eluting with DCM/*n*-heptane 2:1 (v/v) to give product **151** ($R_F$ = 0.45, eluent: DCM/*n*-heptane 2:1).

**151**: Dark violet solid (14 mg, yield 3%). Melting point >340 °C.

^{1}H NMR (500 MHz, CDCl$_3$, ppm): $\delta$ = 9.01 (d, *J* = 4.2 Hz, 2H), 7.60–7.49 (m, 6H), 7.31–7.27 (m, 2H), 7.25–7.17 (m, 2H), 7.03 (s, 2H), 4.65–4.60 (t, *J* = 5.1 Hz, 1H), 4.07–3.99 (m, 4H), 2.01–1.95 (m, 6H), 1.74–1.65 (m, 8H), 1.67–1.58 (m, 20H), 1.52–1.45 (m, 4H).

### 5.4.4.4   Alkylation of thieno[3,2-*b*]thienyl-DPP

The same procedure, as described in *Chapter 5.4.4.1* as the general alkylation procedure, was used for the thieno[3,2-*b*]thienyl-DPP, starting with **125** (1.0 equiv., 0.152 g, 0.369 mmol) and using caesium carbonate (5.0 equiv., 0.605 g, 1.857 mmol) as the base.

**Ethyladamantyl-alkylated thieno[3,2-*b*]thienyl-DPP**
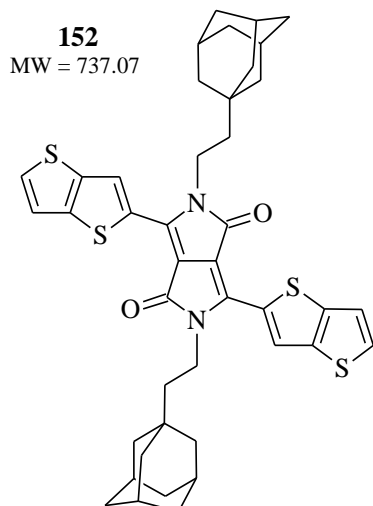


The reaction mixture was stirred at 115 °C for 18 h. Then, the solvent was distilled off, and the solid material as a distillation residue was suspended in methanol (40 mL), filtered off and washed with new methanol (2×40 mL). The filter cake was then washed with hot chloroform (2×150 mL) to dissolve the product and separate it from the unreacted starting material **125**. The chloroform filtrate was then concentrated to give the crude product which was further purified by silica gel chromatography eluting with toluene followed by precipitation in *n*-heptane (12 mL) to get product **152** ($R_F$ = 0.55, eluent: toluene).

**152**: Dark violet-blue solid (18 mg, yield 7%). Melting point 273–285 °C.

^{1}H NMR (500 MHz, CDCl$_3$, ppm): $\delta$ = 8.73 (s, 1H), 8.57 (s, 1H), 7.65 (d, *J* = 5.3 Hz, 1H), 7.52–7.47 (m, 1H), 7.38 (d, *J* = 5.2 Hz, 1H), 7.28 (d, *J* = 5.0 Hz, 1H), 4.70 (t, *J* = 6.5 Hz, 2H), 4.15–4.06 (m, 2H), 2.03–1.92 (m, 4H), 1.75–1.69 (m, 6H), 1.69–1.60 (m, 10H), 1.54 (s, 18H), 1.26 (s, 6H).

### 5.4.4.5 Alkylation of bithienyl-DPP

A procedure similar to that described in *Chapter 5.4.4.1* as the general alkylation procedure was used for the bithienyl-DPP (**35**).

**2-Ethylhexyl-alkylated bithienyl-DPP**
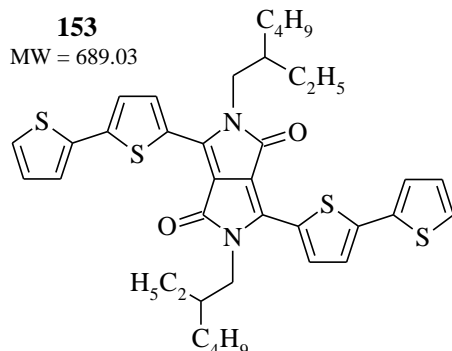


This experiment was performed a total of 5 times and each time using different reagents or reaction conditions. Their summary is given in the following ***Table 1***.

***Table 1****: Summary of performed experiments for the preparation of derivative **153***

| Experiment | #1 | #2 | #3 | #4 | #5 |
|---|---|---|---|---|---|
| bithienyl-DPP (**35**) [g/mmol] | 0.050 / 0.108 | 0.203 / 0.415 | 0.119 / 0.243 | 0.103 / 0.211 | 0.122 / 0.249 |
| Base used [g/mmol] | K$_2$CO$_3$ (7 equiv.) 0.104 / 0.753 | Cs$_2$CO$_3$ (6 equiv.) 0.812 / 2.491 | K$_2$CO$_3$ (6 equiv.) 0.202 / 1.460 | K$_2$CO$_3$ (6 equiv.) 0.175 / 1.264 | K$_2$CO$_3$ (6 equiv.) 0.207 / 1.497 |
| 2-ethylhexyl bromide [g/mmol] | (5 equiv.) 0.104 / 0.538 | (4 equiv.) 0.321 / 1.660 | (4 equiv.) 0.188 / 0.973 | (4 equiv.) 0.163 / 0.842 | (4 equiv.) 0.193 / 0.998 |
| Solvent used [mL] | DMF 15 | DMF 15 | DMF 10 | DMF 8 | DMF 10 |
| Temperature [°C] | 105 | 140 | 90 | 60 / 90 | 80 |
| Time [h] | 18 | 72 | 96 | 16 / 18 | 20 |
| Yield [mg/%] | – | – | – | **10.8 / 7.4** | **27.0 / 15.7** |

Reaction mixtures from experiments #4 and #5 were poured into distilled water (120 mL), and the formed precipitate was filtered off and washed with new methanol (3×30 mL). The filter cake was then washed with hot chloroform (2×100 mL) to dissolve the product and separate it from the unreacted starting material **35**. The chloroform filtrate was then concentrated to give

the crude product which was further purified by silica gel chromatography eluting with toluene/petroleum ether 3:2 (v/v) followed by precipitation in *n*-heptane (10 mL) to get product **153** ($R_F$ = 0.55, eluent: toluene).

**153**: Dark blue-violet crystals (best #5: 27 mg, yield 15.7%). Melting point 190 °C (lit. 191–193 °C)[122].

$^1$H NMR (500 MHz, CDCl$_3$, ppm): $\delta$ = 8.91 (d, *J* = 4.1 Hz, 2H), 7.36–7.31 (m, 6H), 7.08 (dd, *J* = 5.0; 3.7 Hz, 2H), 4.04 (m, 4H), 1.93 (m, 2H), 1.42–1.32 (m, 8H), 1.27 (dd, *J* = 11.0; 4.3 Hz, 8H), 0.92–0.87 (m, 12H).

## Methyladamantyl-alkylated thienyl-DPP



**154**
MW = 761.09

× **not confirmed**
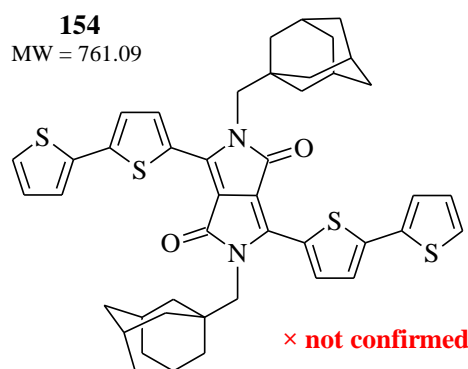
**35** (1.0 equiv., 0.50 g, 1.08 mmol) and anhydrous potassium carbonate (~5.0 equiv., 0.74 g, 5.38 mmol) were stirred at 60 °C for 1 h in anhydrous DMF (25 mL) and under argon atmosphere. Then, 1-(bromomethyl)adamantane (**144**, ~4.0 equiv., 1.00 g, 4.32 mmol) dissolved in anhydrous DMF (12 mL) was added dropwise to the reaction mixture, and it was stirred at 105 °C for 18 h. Based on TLC analysis, no reaction progress was observed, so the reaction mixture was further stirred at 130 °C for 60 h. After that, DMF was distilled off by vacuum distillation and the solid material as a distillation residue was suspended in methanol (30 mL), filtered off and washed with distilled water (2×250 mL) and methanol (2×100 mL). The filter cake was then washed with hot chloroform (2×150 mL) to dissolve the product and separate it from the unreacted starting material **35**. The chloroform filtrate was then concentrated to give the crude product, which was further purified five times by silica gel chromatography eluting with chloroform followed by precipitation in *n*-heptane (12 mL). However, only a mixture of probably *N,N'*- and *N,O'*-alkylated products was obtained (17 mg/yield 2%; TLC analysis: $R_{F,1}$ = 0.45 violet dot, $R_{F,2}$ = 0.42 dark blue dot; eluent: chloroform) and pure product **154** was not isolated (very ambiguous $^1$H NMR analysis of obtained fraction).

**Ethyladamantyl-alkylated bithienyl-DPP**

**155a**
MW = 789.15

**155b**
MW = 789.15
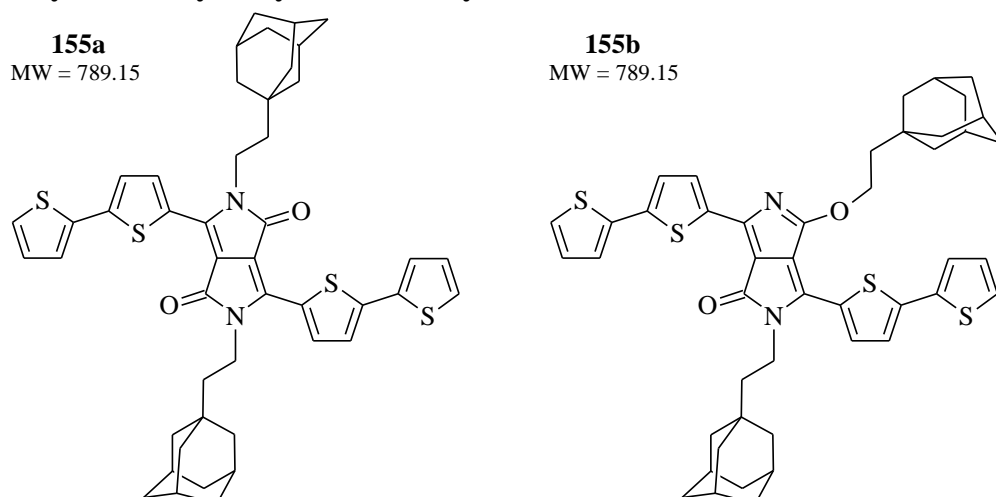


This experiment was performed a total of 4 times and each time using different reagents or reaction conditions. Their summary is given in the following *Table 2*.

*Table 2: Summary of performed experiments for the preparation of derivative **155a***

| Experiment | #1 | #2 | #3 | #4 |
|---|---|---|---|---|
| bithienyl-DPP (**35**) [g/mmol] | 0.662 / 1.425 | 0.520 / 1.119 | 0.845 / 1.819 | 1.00 / 2.152 |
| **Base used** [g/mmol] | $K_2CO_3$ (5 equiv.) 0.985 / 7.124 | $K_2CO_3$ (5 equiv.) 0.773 / 5.596 | $Cs_2CO_3$ (6 equiv.) 3.556 / 10.913 | $K_2CO_3$ (5.1 equiv.) 1.52 / 10.977 |
| **Alkylating reagent used** [g/mmol] | **141** (3.5 equiv.) 1.213 / 4.987 | **141** (3.5 equiv.) 0.953 / 3.917 | **142** (6 equiv.) 3.518 / 10.913 | **141** (4.2 equiv.) 2.18 / 8.954 |
| **Solvent used** [mL] | DMF 32 | DMF 35 | DMF/Toluene 65/10 | DMF 80 |
| **Temperature** [°C] | 100 | 105 | 80 | 105 |
| **Time** [h] | 18 | 3 | 18 | 17 |
| **Yield [mg/%]** | **14.8 / 1.3** | **78.0 / 8.8** | **194.0 / 13.5** | **57.5 / 3.4** |

The most preferred method of working up the reaction mixture is to distil off the solvent (DMF) from the reaction mixture, then suspended the distillation residue in methanol and filtered off, then wash with plenty of distilled water followed by washing with methanol and finally with hot chloroform to dissolve the product. After concentrating the filtrate, the obtained crude mixture was subjected to purification: first by crystallisation in toluene/*n*-heptane (10:1) followed by silica gel chromatography eluting with toluene (often having to be

repeated) and finally by crystallisation again in toluene/*n*-heptane (10:1, 15 μL/mg) to get pure product **155a** ($R_F$ = 0.45 violet dot/red emission under UV 365 nm, eluent: toluene).

**155a**: Deep dark blue crystals (best #3: 194 mg, yield 13.5%). Melting point 340 °C.

$^1$H NMR (500 MHz, CDCl$_3$, ppm): $\delta$ = 8.91 (d, *J* = 4.1 Hz, 2H), 7.33 (dd, *J* = 10.4; 4.6 Hz, 6H), 7.09 (dd, *J* = 5.1; 3.6 Hz, 2H), 4.18–4.11 (m, 4H), 2.01 (s, 6H), 1.77–1.69 (m, 18H), 1.59–1.52 (m, 10H).

Anal. calcd. for C$_{46}$H$_{48}$N$_2$O$_2$S$_4$: C 70.01%, H 6.13%, N 3.55%, S 16.25%; Found: C 74.29%, H 6.21%, N 3.92%, S 16.64%. EI (m/z) 789.15; Found 789.27.

In the case of experiment #1, *N,O′*-alkylated product (**155b**; $R_F$ = 0.48 intense blue dot, eluent: toluene) was also isolated and characterized in addition to *N,N′*-product.

**155b**: Dark blue solid (#1: 168 mg, yield 14.9%). Melting point 258 °C.

$^1$H NMR (300 MHz, CDCl$_3$, ppm): $\delta$ = 8.43 (s, 1H), 8.22 (d, *J* = 4.1 Hz, 1H), 7.41 – 7.29 (m, 4H), 7.21 (d, *J* = 13.5 Hz, 2H), 7.08 (ddd, *J* = 21.1; 5.1; 3.7 Hz, 2H), 4.72 (s, 2H), 4.12–4.01 (m, 2H), 2.00 (s, 6H), 1.75–1.61 (m, 20H), 1.56 (d, *J* = 8.6 Hz, 10H).

### 5.4.4.6   Synthesis of N,N′-alkylated-bithienyl-DPP

**Preparation of 2-bromothiophene (156)**



**21**
MW = 84.14

**156**
MW = 163.04
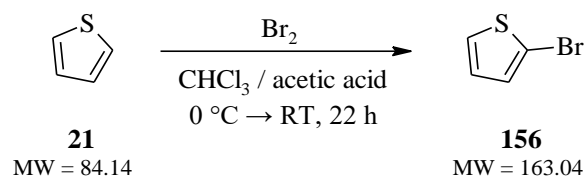
*Scheme 64: Preparation of 2-bromothiophene (**156**)*

**21** (32.0 g, 380.32 mmol) was dissolved in a mixture of chloroform and glacial acetic acid (50/50 mL), then the mixture was cooled to 0 °C and protected from light by aluminium foil. After that, 1.02 equiv. of bromine (19.98 mL/62.0 g, 387.97 mmol) was slowly (4 h) added dropwise to the reaction mixture, which was then spontaneously heated to RT and stirred for 22 h. The reaction mixture was then poured into distilled water with crushed ice (300 mL), and extraction was performed. The upper aqueous phase was washed with chloroform (3×100 mL). The collected organic phases were washed first with 20% solution of Na$_2$S$_2$O$_3$ (2×100 mL), then with 15% solution of NaOH (2×150 mL), distilled water (2×200 mL), finally with brine (150 mL) and then dried over anhydrous Na$_2$SO$_4$ and filtered through filter aid (Celite). After removal of the solvent under vacuum, the obtained crude mixture was purified by vacuum distillation (20 mbar, oil bath 75 °C) to afford pure product **156**.

**156**: Colourless liquid (19.08 g, yield 31%).

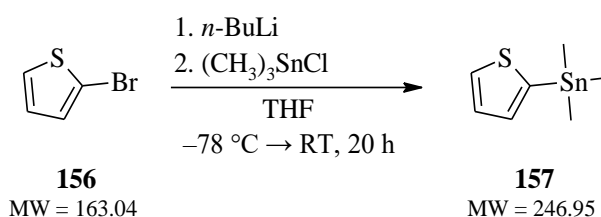Refractive index: *n*20/D = 1.584 (lit. 1.586)[174].

Density: $\rho_{25}$ = 1.684 g cm$^{-3}$ (lit. 1.684 g cm$^{-3}$)[174].

$^1$H NMR (300 MHz, CDCl$_3$, ppm): $\delta$ = 7.11 (s, 1H), 6.90 (s, 1H), 6.67 (s, 1H).

GC-MS (method: *vseobecna*): RT = 6.17 min; m/z = 162.96.

## Preparation of trimethyl-2-thienyl-stannane (157)



**Scheme 65**: *Preparation of trimethyl-2-thienyl-stannane (157)*

**156** (1.195 g, 7.183 mmol) was dissolved in anhydrous THF (40 mL) under argon atmosphere, and the reaction mixture was cooled to –78 °C. After that, 1.10 equiv. of *n*-BuLi (1.6M, 4.94 mL, 7.902 mmol) was added dropwise to this mixture and it was stirred at –78 °C for 3 h. Following that 1.20 equiv. of trimethyltin chloride (1.718 g, 8.620 mmol) dissolved in anhydrous THF (12 mL) was added quickly dropwise and the reaction mixture was then spontaneously heated to RT and stirred for 18 h. After that, the reaction was quenched by pouring into distilled water (80 mL), and the reaction mixture was washed with diethyl ether (3×50 mL). The collected organic phases were then washed with distilled water (3×280 mL), finally with brine (350 mL) and then dried over anhydrous $Na_2SO_4$ and filtered through filter aid (Celite). After removal of the solvent under vacuum, Stille intermediate **157** was obtained, which was used to the next reaction step without further purification and analysis.

   **157**: Black-brown solid (1.52 g, yield 86%).

## Preparation of *N,N'*-2-ethylhexyl-bis(5-bromo-2-thienyl)-DPP (158)
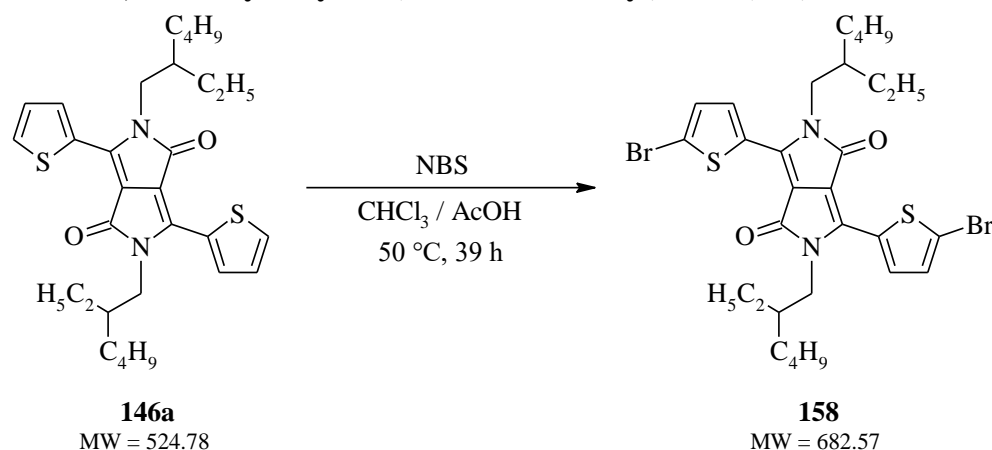


**Scheme 66**: *Preparation of N,N'-2-ethylhexyl-bis(5-bromo-2-thienyl)-DPP (158)*

**146a** (0.685 g, 1.305 mmol) was dissolved in a mixture of chloroform, and glacial acetic acid (60/6 mL) and the reaction apparatus was protected from light by aluminium foil. After that, 2.50 equiv. of NBS (0.581 g, 3.263 mmol) was added in one portion, and the reaction mixture was stirred at 50 °C for 39 h. The reaction mixture was then poured into distilled water with crushed ice (250 mL) and stirred for 2 h. After that, extraction was performed – the reaction mixture was washed with chloroform (3×60 mL). The collected organic phases were washed with distilled water (3×200 mL), saturated $NaHCO_3$ (1×150 mL), finally with brine (150 mL)

and then dried over anhydrous Na$_2$SO$_4$ and filtered through filter aid (Celite). After removal of the solvent under vacuum, the obtained crude mixture was purified by silica gel chromatography eluting with toluene to get pure product **158** ($R_F$ = 0.85, eluent: toluene).

**158**: Dark violet solid (0.37 g, yield 41%). Melting point 138 °C.

$^1$H NMR (500 MHz, CDCl$_3$, ppm): $\delta$ = 8.65 (d, $J$ = 4.2 Hz, 2H), 7.23 (d, $J$ = 4.2 Hz, 2H), 3.97–3.92 (m, 4H), 1.85–1.77 (m, 2H), 1.38–1.22 (m, 16H), 0.90–0.84 (m, 12H).

Anal. calcd. for C$_{30}$H$_{38}$Br$_2$N$_2$O$_2$S$_2$: C 52.79%, H 5.61%, N 4.10%, S 9.40%; Found: C 53.09%, H 5.99%, N 4.02%, S 9.11%.

**Preparation of *N,N′*-ethyladamantyl-bis(5-bromo-2-thienyl)-DPP (159)**



**6a**
MW = 624.90

**159**
MW = 782.69
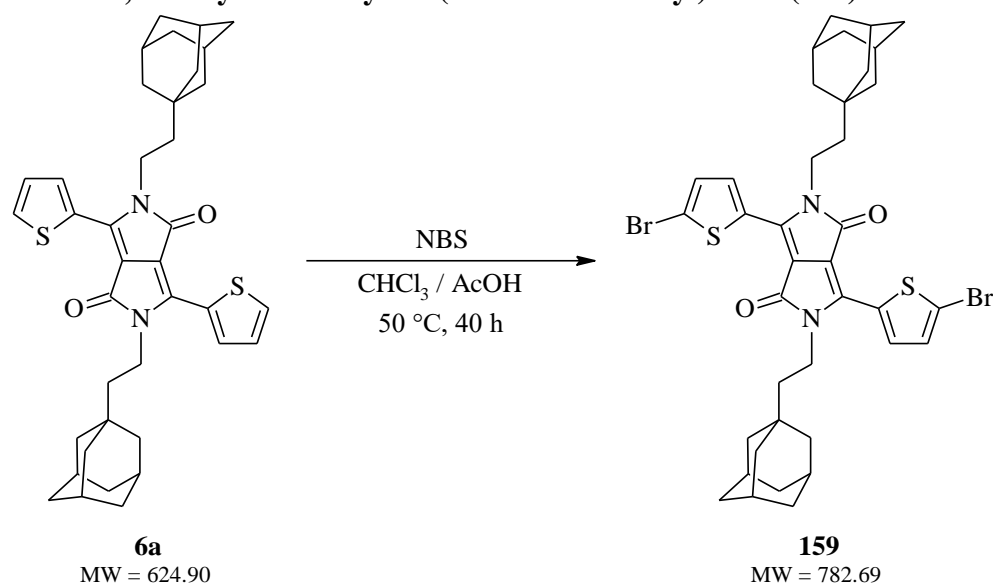
*Scheme 67: Preparation of N,N'-ethyladamantyl-bis(5-bromo-2-thienyl)-DPP (**159**)*

The same procedure as for the **158** was used to prepare the **159**, starting with **6a** (1.0 equiv., 0.85 g, 1.36 mmol). The reaction time of stirring at reflux was extended by 1 h to a total of 40 h. The obtained crude mixture was purified by silica gel chromatography eluting with toluene followed by precipitation in methanol (20 mL) to get product **159** ($R_F$ = 0.81, eluent: toluene).

**159**: Dark violet crystals (0.49 g, yield 46%). Melting point 337–340 °C.

$^1$H NMR (300 MHz, CDCl$_3$, ppm): $\delta$ = 8.64 (d, $J$ = 4.2 Hz, 2H), 7.23 (d, $J$ = 4.1 Hz, 2H), 4.07–3.99 (m, 4H), 1.96–1.87 (m, 6H), 1.71–1.60 (m, 6H), 1.54–1.45 (m, 17H), 1.42–1.29 (m, 5H).

Anal. calcd. for C$_{38}$H$_{42}$Br$_2$N$_2$O$_2$S$_2$: C 58.31%, H 5.41%, N 3.58%, S 8.19%; Found: C 59.70%, H 5.81%, N 3.63%, S 7.15%.

## Preparation of *N,N'*-2-ethylhexyl-bithienyl-DPP (153)
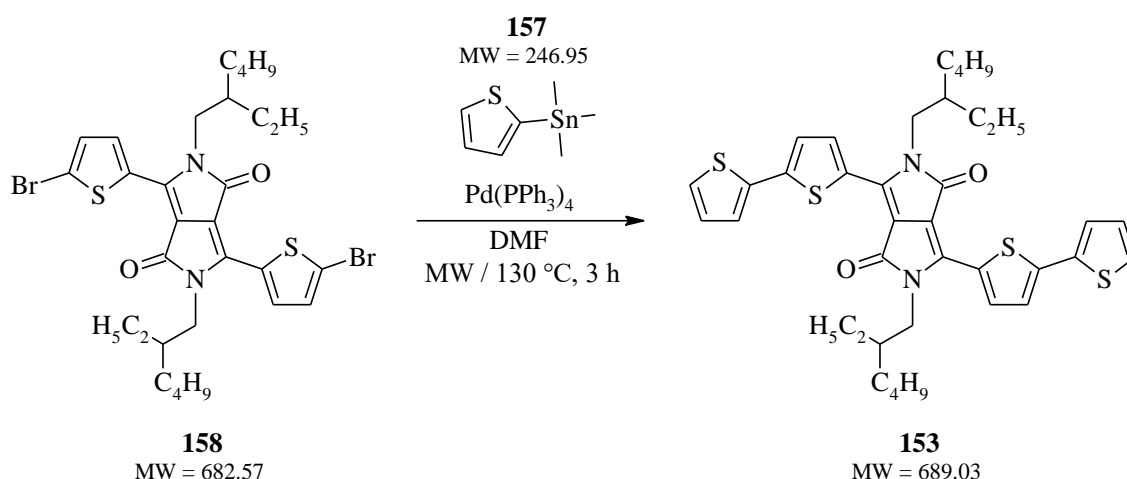


*Scheme 68*: *Preparation of N,N'-2-ethylhexyl-bithienyl-DPP (153)*

**158**, ~3 equiv. of **157** and Pd(PPh₃)₄ as a catalyst were dissolved in anhydrous DMF under argon atmosphere in a microwave reactor. The reaction mixture was purged with argon for 10 min in an ultrasonic bath, and then it was transferred to a microwave oven, and the experiment was set to "**pulzy**" method. The reaction mixture was then poured into distilled water, formed precipitate was filtered off and washed with methanol. The filter cake was then dissolved in chloroform, it was washed with distilled water and concentrated to give the crude product, which was purified by precipitation in hot methanol (~240 μL/mg) followed by silica gel chromatography eluting with petroleum ether → toluene. The final precipitation of the purified material in methanol (~240 μL/mg) affords pure product **153** ($R_F$ = 0.55, eluent: toluene). A summary of performed experiments is given in the following **Table 3**.

**Table 3**: *Summary of performed experiments for the preparation of derivative 153*

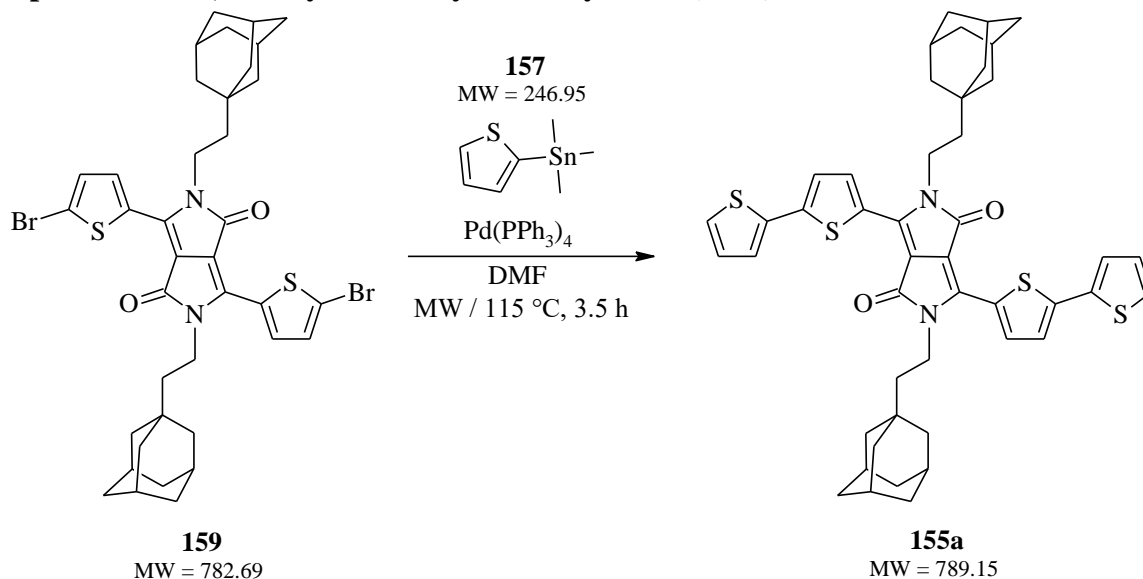| Experiment | #1 | #2 |
|---|---|---|
| **158** [g/mmol] | 0.182 / 0.253 | 0.155 / 0.216 |
| **157** [g/mmol] | (2.70 equiv.) 0.169 / 0.684 | (3.15 equiv.) 0.168 / 0.680 |
| **Pd(PPh₃)₄** [g/mmol] | (0.08 equiv.) 0.023 / 0.020 | (0.08 equiv.) 0.020 / 0.017 |
| **Solvent used** [mL] | DMF 15 | DMF 16 |
| **Temperature** [°C] | 60 → 90 → 60 (4x) / 60 → 115 → RT | 60 → 90 → 60 (4x) / 60 → 130 → RT |
| **Overall time** [h] | 3.5 | 3 |
| **Yield [mg/%]** | **49.8** / 28.5 | **85.6** / 57.6 |

**153**: Dark blue-violet crystals (best #2: 85.6 mg, yield 57.6%). Melting point 191 °C (lit. 191–193 °C)[122].

^{1}H NMR (500 MHz, CDCl₃, ppm): $\delta$ = 8.91 (d, $J$ = 4.1 Hz, 2H), 7.34–7.31 (m, 6H), 7.08 (dd, $J$ = 5.0; 3.7 Hz, 2H), 4.04 (h, $J$ = 7.1 Hz, 4H), 1.93 (m, 2H), 1.44–1.31 (m, 8H), 1.27 (dd, $J$ = 11.0; 4.2 Hz, 8H), 0.92 (d, $J$ = 6.4 Hz, 6H), 0.87 (t, $J$ = 7.1 Hz, 6H).

Anal. calcd. for $C_{38}H_{44}N_2O_2S_4$: C 66.24%, H 6.44%, N 4.07%, S 18.61%; Found: C 67.08%, H 7.11%, N 3.83%, S 18.13%.

## Preparation of *N*,*N'*-ethyladamantyl-bithienyl-DPP (155a)



**157**
MW = 246.95

**159**
MW = 782.69

**155a**
MW = 789.15

Pd(PPh₃)₄
DMF
MW / 115 °C, 3.5 h

*Scheme 69*: *Preparation of N,N'-ethyladamantyl-bithienyl-DPP (155a)*

The same procedure as for the **153** was used to prepare the **155a**, starting with **159** (1.0 equiv., 0.188 g, 0.23 mmol). The reaction conditions were the same as in experiment #1 for the preparation of derivative **153** described above. Work-up of the reaction mixture and purification of the crude product were also identical. As a result, pure product **155a** was obtained ($R_F$ = 0.45, eluent: toluene).
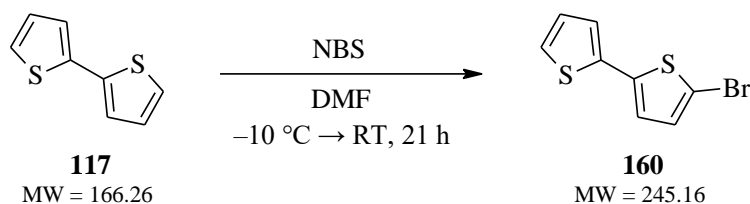
**155a**: Deep dark blue-black crystals (51 mg, yield 28.3%). Melting point 340 °C.

^{1}H NMR (500 MHz, CDCl₃, ppm): $\delta$ = 8.91 (d, $J$ = 4.1 Hz, 2H), 7.35–7.30 (m, 6H), 7.09 (dd, $J$ = 5.1; 3.6 Hz, 2H), 4.16–4.12 (m, 4H), 2.02 (s, 6H), 1.76–1.69 (m, 18H), 1.58–1.52 (m, 10H).

Anal. calcd. for $C_{46}H_{48}N_2O_2S_4$: C 70.01%, H 6.13%, N 3.55%, S 16.25%; Found: C 70.89%, H 6.19%, N 3.22%, S 15.94%.

### 5.4.4.7 Synthesis of N,N'-alkylated-terthienyl-DPP

**Preparation of 5-bromo-2,2'-bithiophene (160)**



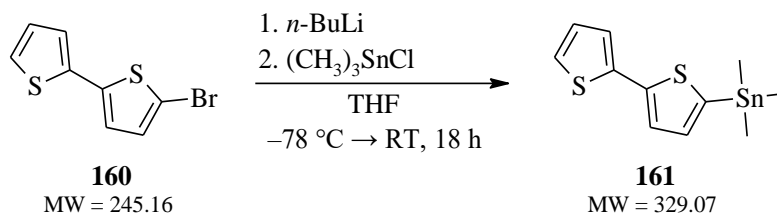*Scheme 70: Preparation of 5-bromo-2,2'-bithiophene (160)*

The same procedure as for the **128** (*Chapter 5.4.2.1*) was used to prepare the **160**, starting with **117** (1.0 equiv., 2.02 g, 12.16 mmol). The reaction time of stirring at RT was extended by 17 h to a total of 21 h. Obtained crude mixture was purified by vacuum distillation (1 mbar, oil bath 240 °C) to afford pure product **160** ($R_F$ = 0.60, eluent: *n*-heptane).

**160**: Greenish solid (2.11 g, yield 71%). Melting point 32 °C (lit. 32–33 °C)[175].

$^1$H NMR (300 MHz, CDCl$_3$, ppm): $\delta$ = 7.23 (d, $J$ = 3.6 Hz, 1H), 7.11 (d, $J$ = 3.4 Hz, 1H), 7.03 (m, 1H), 6.97 (d, $J$ = 3.4 Hz, 1H), 6.93 (d, J = 3.3 Hz, 1H).

GC-MS (method: *JJ_vseobecna met*): RT = 7.18 min; m/z = 245.96 (purity 83%).

**Preparation of [2,2'-bithiophen]-5-yltrimethyl-stannane (161)**



*Scheme 71: Preparation of [2,2'-bithiophen]-5-yltrimethyl-stannane (161)*

The same procedure as for the **157** (*Chapter 5.4.4.6*) was used to prepare the **161**, starting with **160** (1.0 equiv., 0.97 g, 3.28 mmol). The reaction time of stirring at RT was reduced by 2 h to a total of 18 h. Stille intermediate **161** ($R_F$ = 0.50, eluent: *n*-heptane) was obtained and used to the next reaction step without further purification.

**161**: Dark blue-black solid (1.17 g, yield 108%).

$^1$H NMR (300 MHz, CDCl$_3$, ppm): $\delta$ = 7.24 (d, $J$ = 3.4 Hz, 1H), 7.15 (d, $J$ = 3.5 Hz, 2H), 7.03 (d, $J$ = 3.4 Hz, 1H), 6.95 (t, $J$ = 3.4 Hz, 1H), 0.33 (s, 9H).

## Preparation of *N*,*N'*-2-ethylhexyl-terthienyl-DPP (162)
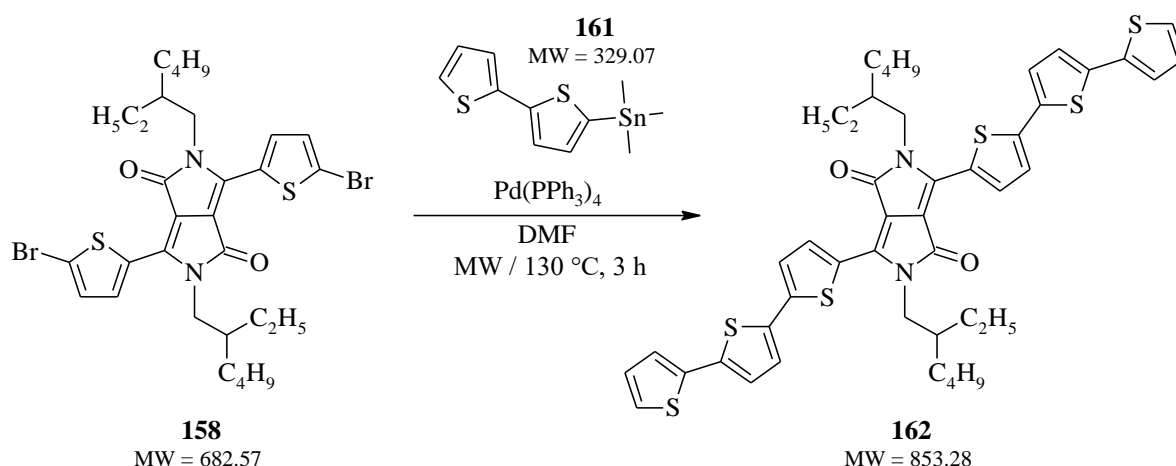


*Scheme 72: Preparation of N,N'-2-ethylhexyl-terthienyl-DPP (162)*

The same procedure as for the **153** (*Chapter 5.4.4.6*) was used to prepare the **162**, starting with **158** (1.0 equiv., 0.165 g, 0.23 mmol) and **161** (3.0 equiv., 0.224 g, 0.68 mmol) as Stille intermediate. The reaction conditions and work-up of the reaction mixture were the same as in experiment #2 for the preparation of derivative **153** described above. The obtained crude mixture was purified by double precipitation in hot methanol (~100 µL/mg) followed by double silica gel chromatography eluting with petroleum ether → DCM. The obtained material was further purified by *Soxhlet extraction* (solvent: methanol; approx. 120 cycles) and finally by precipitation in methanol (~400 µL/mg) to afford pure product **162** ($R_F$ = 0.65, eluent: toluene).

**162**: Dark greenish crystals (129 mg, yield 65.8%). Melting point 205 °C.

$^1$H NMR (500 MHz, CDCl$_3$, ppm): $\delta$ = 8.93 (d, *J* = 4.1 Hz, 2H), 7.30 (d, *J* = 4.1 Hz, 2H), 7.26 (dd, *J* = 5.0; 1.1 Hz, 2H), 7.22 (td, *J* = 2.5, 1.3 Hz, 4H), 7.13 (d, *J* = 3.8 Hz, 2H), 7.04 (dd, *J* = 5.1, 3.6 Hz, 2H), 4.10–4.00 (m, 4H), 1.93 (m, 2H), 1.43–1.35 (m, 8H), 1.31–1.25 (m, 8H), 0.91 (dt, *J* = 18.5, 7.2 Hz, 12H).

Anal. calcd. for C$_{46}$H$_{48}$N$_2$O$_2$S$_6$: C 64.75%, H 5.67%, N 3.28%, S 22.55%; Found: C 64.98%, H 5.71%, N 3.43%, S 22.67%.

## Preparation of *N*,*N'*-ethyladamantyl-terthienyl-DPP (163)

The same procedure as for the **153** (*Chapter 5.4.4.6*) was used to prepare the **163**, starting with **159** and **161** as Stille intermediate (set to "pulzy" method in a microwave oven). A summary of performed experiments is given in the following **Table 4**. Work-up of the reaction mixture was the same as in experiment #1 for the preparation of derivative **153** described above. The obtained crude mixture was purified by double precipitation in hot methanol (~450 µL/mg) followed by *Soxhlet extraction* (solvent: methanol; approx. 140 cycles) and finally by precipitation in methanol (~500 µL/mg) to afford pure product **163** ($R_F$ = 0.38, eluent: toluene/chloroform 1:1).
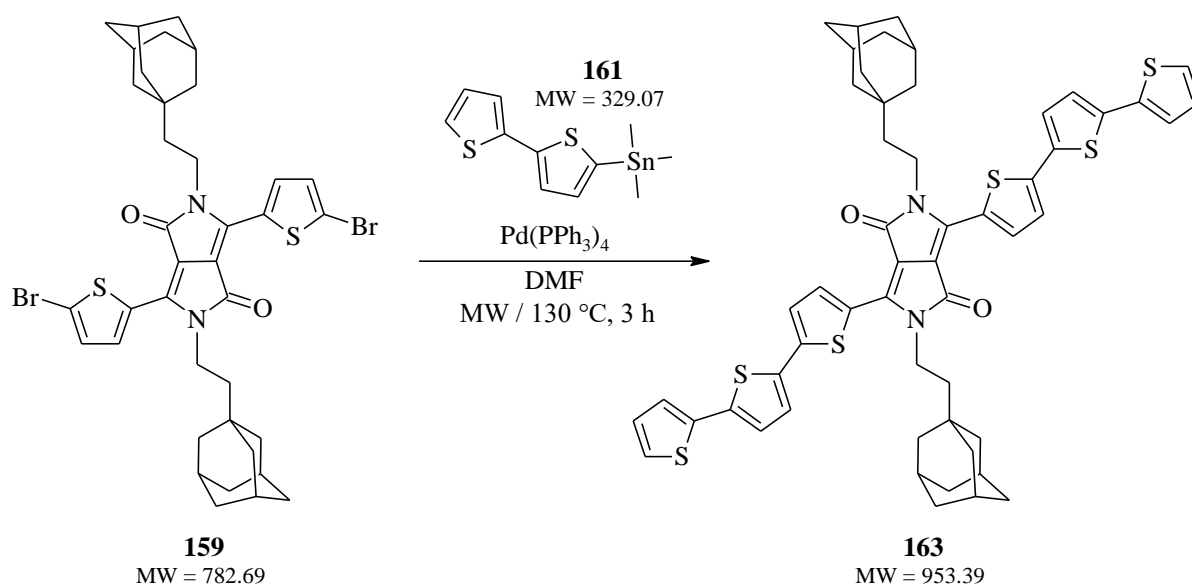
**Scheme 73**: *Preparation of N,N'-ethyladamantyl-terthienyl-DPP (**163**)*

**Table 4**: *Summary of performed experiments for the preparation of derivative **163***

| Experiment | #1 | #2 |
|---|---|---|
| **159**<br>[g/mmol] | 0.184 / 0.223 | 0.127 / 0.154 |
| **161**<br>[g/mmol] | (3.50 equiv.)<br>0.257 / 0.782 | (2.90 equiv.)<br>0.147 / 0.447 |
| **Pd(PPh₃)₄**<br>[g/mmol] | (0.10 equiv.)<br>0.026 / 0.022 | (0.09 equiv.)<br>0.016 / 0.014 |
| **Solvent used**<br>[mL] | DMF<br>16 | DMF<br>16 |
| **Temperature**<br>[°C] | 60 → 90 → 60 (4x) /<br>60 → 115 → RT | 60 → 90 → 60 (4x) /<br>60 → 130 → RT |
| **Overall time**<br>[h] | 3.5 | 3 |
| **Yield [mg/%]** | **135.1 / 63.5** | **116.8 / 79.5** |

**163**: Dark violet-black crystals (best #2: 117 mg, yield 79.5%). Melting point >340 °C.

^{1}H NMR (500 MHz, CDCl₃, ppm): $\delta$ = 8.92 (d, *J* = 4.2 Hz, 2H), 7.31 (d, *J* = 4.1 Hz, 2H), 7.28 (m, 2H), 7.23 (d, *J* = 3.8 Hz, 4H), 7.15 (d, *J* = 3.8 Hz, 2H), 7.06–7.04 (m, 2H), 4.18–4.14 (m, 4H), 2.03 (s, 6H), 1.78–1.68 (m, 18H), 1.56–1.50 (m, 10H).

Anal. calcd. for $C_{54}H_{52}N_2O_2S_6$: C 68.03%, H 5.50%, N 2.94%, S 20.18%; Found: C 68.39%, H 6.13%, N 2.72%, S 17.64%.
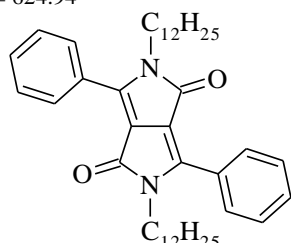
### 5.4.4.8 Alkylation of phenyl-DPP

The same procedure, as described in *Chapter 5.4.4.1* (*Scheme 61*) as the general alkylation procedure, was used for the phenyl-DPP (**31b**: 1.0 equiv., 1.00 g, 3.47 mmol).

### Dodecyl-alkylated phenyl-DPPs

**164**
MW = 624.94



The solid material obtained from the reaction mixture as a distillation residue was suspended in methanol (50 mL), filtered off and washed with new methanol (2×40 mL) to give the crude product as a solid material on a filter cake. This crude product was purified by silica gel chromatography eluting with toluene to get pure product **164** ($R_F$ = 0.56, eluent: toluene).

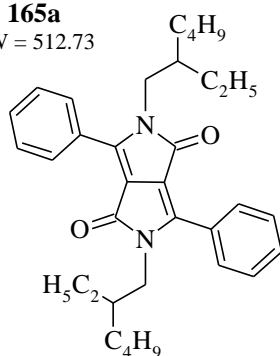**164**: Orange crystals (1.37 g, yield 63%). Melting point 114 °C (lit. 112 °C)[165].

$^1$H NMR (300 MHz, CDCl$_3$, ppm): $\delta$ = 7.82–7.79 (m, 4H), 7.53–7.51 (m, 6H), 3.74 (t, $J$ = 7.6 Hz, 4H), 1.73–1.57 (m, 4H), 1.30–1.19 (m, 36H), 0.87 (t, $J$ = 6.6 Hz, 6H).

Anal. calcd. for C$_{42}$H$_{60}$N$_2$O$_2$: C 80.72%, H 9.68%, N 4.48%; Found: C 80.84%, H 9.47%, N 4.41%.

### 2-Ethylhexyl-alkylated phenyl-DPPs

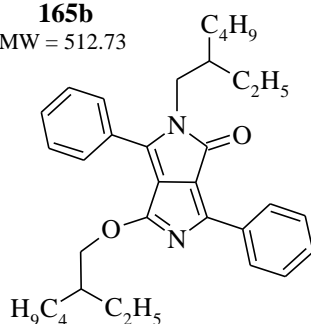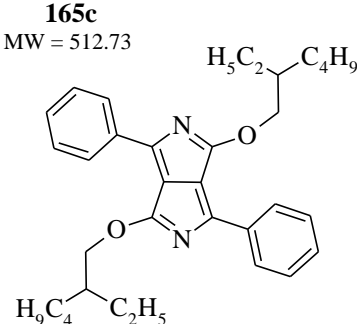**165a**
MW = 512.73

**165b**
MW = 512.73

**165c**
MW = 512.73



The solid material obtained from the reaction mixture as a distillation residue was suspended in methanol (50 mL), filtered off and washed with new methanol (2×40 mL) to give the crude product as a solid material on a filter cake. This crude product was purified by silica gel chromatography eluting with toluene to get pure product **165a** ($R_F$ = 0.38, eluent: toluene/chloroform 1:1).

**165a**: Orange-yellow crystals (0.19 g, yield 12%). Melting point 166–168 °C.

$^1$H NMR (300 MHz, CDCl$_3$, ppm): $\delta$ = 7.81 (m, 4H), 7.51 (m, 6H), 3.71 (m, 4H), 1.87–1.75 (m, 2H), 1.38–1.25 (m, 16H), 0.91–0.85 (m, 12H).

Anal. calcd. for $C_{34}H_{44}N_2O_2$: C 79.65%, H 8.65%, N 5.46%, Found: C 79.81%, H 8.74%, N 5.34%.


The solid material obtained from the reaction mixture as a distillation residue was suspended in methanol (50 mL), filtered off and washed with new methanol (2×40 mL). The crude product was obtained by evaporating methanol from the filtrate. This crude product was purified by silica gel chromatography eluting with toluene to get pure product **165b** ($R_F$ = 0.65, eluent: toluene/chloroform 1:1). Additional pure product **165b** was obtained from the previous column chromatography of the material from the filter cake.

**165b**: Brown-orange waxy (semi-solid) material (0.05 g, yield 3%). Melting point –.

^{1}H NMR (300 MHz, CDCl3, ppm): $\delta$ = 8.57 (d, $J$ = 6.8 Hz, 2H), 7.68 (d, $J$ = 7.9 Hz, 2H), 7.54–7.48 (m, 3H), 7.46–7.41 (m, 3H), 4.43 (m, 2H), 3.66 (m, 2H), 1.76 (m, 2H), 1.37–1.25 (m, 16H), 0.91–0.87 (m, 12H).

Anal. calcd. for $C_{34}H_{44}N_2O_2$: C 79.65%, H 8.65%, N 5.46%, Found: C 80.04%, H 8.91%, N 5.22%.
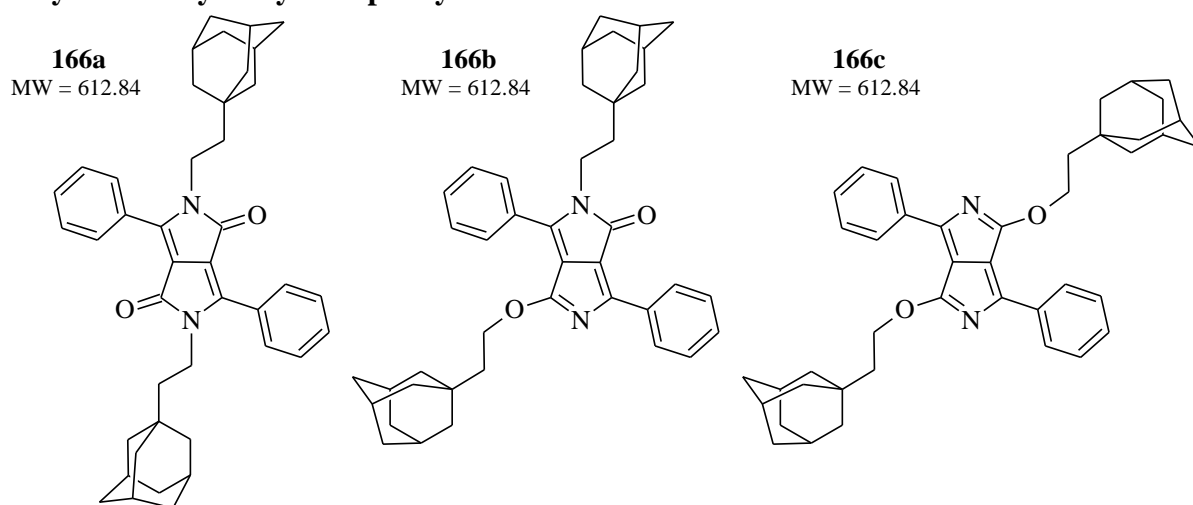

The solid material obtained from the reaction mixture as a distillation residue was suspended in methanol (50 mL), filtered off and washed with new methanol (2×40 mL). The crude product was obtained by evaporating methanol from the filtrate. This crude product was purified by silica gel chromatography eluting with toluene to get pure product **165c** ($R_F$ = 0.80, eluent: toluene/chloroform 1:1).

**165c**: Brown purple waxy (semi-solid) material (0.007 g, yield 0.4%). Melting point –.

^{1}H NMR (300 MHz, CDCl3, ppm): $\delta$ = 8.29 (m, 4H), 7.45 (m, 6H), 4.59 (m, 4H), 1.83 (m, 2H), 1.57–1.34 (m, 16H), 0.96–0.85 (m, 12H).

Anal. calcd. for $C_{34}H_{44}N_2O_2$: C 79.65%, H 8.65%, N 5.46%, Found: C 79.85%, H 8.69%, N 5.52%.


**Ethyladamantyl-alkylated phenyl-DPPs**



**166a**
MW = 612.84

**166b**
MW = 612.84

**166c**
MW = 612.84

The solid material obtained from the reaction mixture as a distillation residue was suspended in methanol (100 mL), filtered off and washed with new methanol (3×50 mL) to give the crude product as a solid material on a filter cake. This crude product was purified by silica gel chromatography eluting with toluene/chloroform 1:1 (v/v) to get pure product **166a** ($R_F$ = 0.15, eluent: toluene/chloroform 1:1).

**166a**: Intense orange crystals (0.29 g, yield 14%). Melting point 323 °C.

$^1$H NMR (500 MHz, CDCl$_3$, ppm): $\delta$ = 7.83 (m, 4H), 7.53 (m, 6H), 3.77 (m, 4H), 1.92 (s, 6H), 1.68 (d, $J$ = 12 Hz, 4H), 1.58 (d, $J$ = 12 Hz, 4H), 1.48–1.42 (m, 18H), 1.26 (s, 2H).

Anal. calcd. for C$_{42}$H$_{48}$N$_2$O$_2$: C 82.31%, H 7.90%, N 4.57%, Found: C 82.43%, H 7.71%, N 4.64%.


The solid material obtained from the reaction mixture as a distillation residue was suspended in methanol (100 mL), filtered off and washed with new methanol (3×50 mL). The crude product was obtained by evaporating methanol from the filtrate. This crude product was purified by silica gel chromatography eluting with toluene to get pure product **166b** ($R_F$ = 0.55, eluent: toluene/chloroform 1:1). Additional pure product **166b** was obtained from the previous column chromatography of the material from the filter cake.

**166b**: Orange-red solid (0.36 g, yield 18%). Melting point 223 °C.

$^1$H NMR (500 MHz, CDCl$_3$, ppm): $\delta$ = 8.55 (d, $J$ = 7.0 Hz, 2H), 7.69 (d, $J$ = 8 Hz, 2H), 7.55–7.51 (m, 3H), 7.48–7.42 (m, 3H), 4.56 (s, 2H), 3.75–3.71 (m, 2H), 1.93 (s, 6H), 1.70 (m, 4H), 1.62 (m, 4H), 1.54– 1.42 (m, 19H), 1.27 (s, 1H).

Anal. calcd. for C$_{42}$H$_{48}$N$_2$O$_2$: C 82.31%, H 7.90%, N 4.57%, Found: C 82.16%, H 7.62%, N 4.71%.


The solid material obtained from the reaction mixture as a distillation residue was suspended in methanol (100 mL), filtered off and washed with new methanol (3×50 mL). The crude product was obtained by evaporating methanol from the filtrate. This crude product was purified by silica gel chromatography eluting with toluene to get pure product **166c** ($R_F$ = 0.82, eluent: toluene/chloroform 1:1).

**166c**: Brown solid (0.09 g, yield 4%). Melting point 270 °C.

$^1$H NMR (300 MHz, CDCl$_3$, ppm): $\delta$ = 8.31 (m, 4H), 7.44 (m, 6H), 4.73 (t, $J$ = 6.5 Hz, 4H), 1.99 (s, 6H), 1.73–1.66 (m, 27H), 1.53 (m, 1H).

Anal. calcd. for C$_{42}$H$_{48}$N$_2$O$_2$: C 82.31%, H 7.90%, N 4.57%, Found: C 82.04%, H 7.82%, N 4.73%.

### 5.4.4.9 Alkylation of p-cyanophenyl-DPP
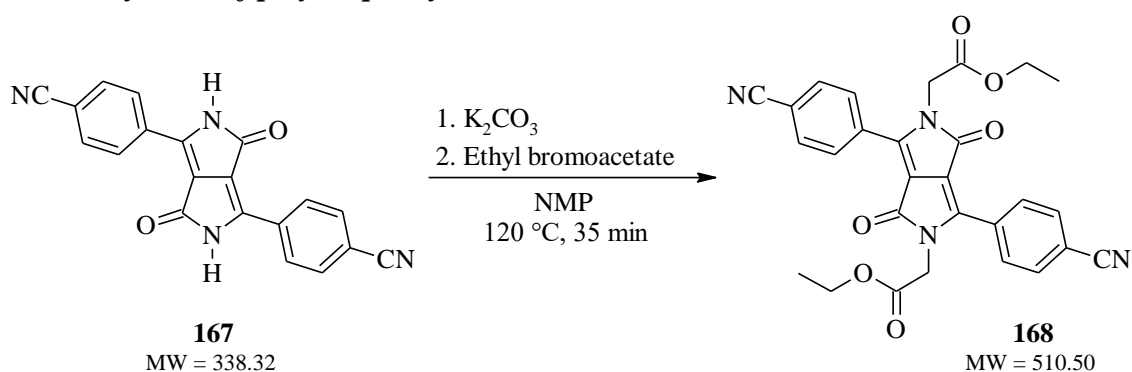


**Scheme 74**: Alkylation of di-(p-cyanophenyl)-DPP (**167**) – preparation of derivative **168**

**167** (1.0 equiv., 1.00 g, 2.96 mmol) and anhydrous potassium carbonate (~10 equiv., 4.08 g, 29.56 mmol) were stirred at 120 °C for 45 min in anhydrous NMP (80 mL) and under argon atmosphere. Then, ethyl bromoacetate (~10 equiv., 3.28 mL/4.94 g, 29.56 mmol) dissolved in anhydrous NMP (24 mL) was added dropwise (for 35 min) to the reaction mixture, and it was stirred at 120 °C for 35 min. After that, the reaction mixture was cooled to RT and poured into distilled water with crushed ice (200 mL). The formed precipitate was filtered off and washed with distilled water (2×250 mL) and methanol (4×50 mL) to give the crude product as a solid material on a filter cake. This crude product was purified by silica gel chromatography eluting with chloroform followed by crystallisation in methanol to get pure product **168** ($R_F$ = 0.15, eluent: chloroform).

**168**: Bright orange solid (0.19 g, yield 13%). Melting point 179 °C (lit. 177–179 °C)[176].

$^1$H NMR (300 MHz, CDCl$_3$, ppm): $\delta$ = 7.91–7.87 (m, 4H), 7.83–7.79 (m, 4H), 4.47 (s, 4H), 4.20 (q, $J$ = 7.1 Hz, 4H), 1.24 (t, $J$ = 7.1 Hz, 6H).

Anal. calcd. for C$_{28}$H$_{22}$N$_4$O$_6$: C 65.88%, H 4.34%, N 10.97%; Found: C 65.92%, H 4.26%, N 10.75%.

### 5.4.4.10 Alkylation of naphthyl-DPP

A procedure similar to that described in *Chapter 5.4.4.1* as the general alkylation procedure was used for the naphthyl-DPP.

**Ethyladamantyl-alkylated naphthyl-DPP**



**169**
MW = 712.96
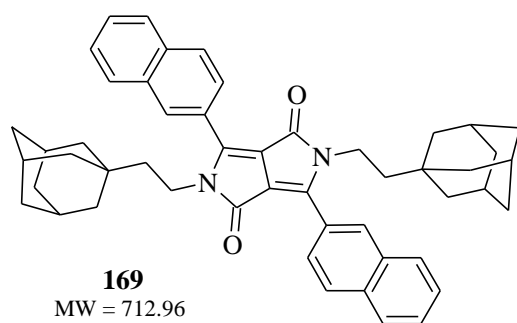
This experiment was performed a total of 3 times and each time using different reagents or reaction conditions. Their summary is given in the following **Table 5**.

**Table 5**: *Summary of performed experiments for the preparation of derivative **169***

| Experiment | #1 | #2 | #3 |
|---|---|---|---|
| naphthyl-DPP [g/mmol] | 0.051 / 0.132 | 0.053 / 0.135 | 0.153 / 0.393 |
| **Base used** [g/mmol] | $K_2CO_3$ (5 equiv.) 0.091 / 0.659 | $K_2CO_3$ (5 equiv.) 0.093 / 0.676 | $Cs_2CO_3$ (5 equiv.) 0.640 / 1.964 |
| **141** [g/mmol] | (4.5 equiv.) 0.144 / 0.593 | (3.65 equiv.) 0.120 / 0.493 | (3.85 equiv.) 0.368 / 1.513 |
| **Solvent used** [mL] | DMF 30 | DMF 30 | DMF 30 |
| **Temperature** [°C] | 90 → 135 | 90 | 115 |
| **Time** [h] | 96 / 16 | 20 | 17 |
| **Yield [mg/%]** | – | **2.3 / 2.4** | **14.0 / 5.0** |

The most preferred method of working up the reaction mixture is to distil off the solvent (DMF) from the reaction mixture, then dissolve the distillation residue in chloroform and filter it and wash with plenty of hot chloroform. The organic phase as a filtrate was then washed with distilled water (3×150 mL), dried over anhydrous $Na_2SO_4$ and filtered through filter aid (Celite). After removal of the solvent under vacuum, the obtained crude mixture was purified by silica gel chromatography eluting with toluene followed by precipitation in *n*-heptane to get pure product **169** ($R_F$ = 0.35, eluent: toluene).

**169**: Intense orange solid (best #3: 14 mg, yield 5%). Melting point >340 °C.
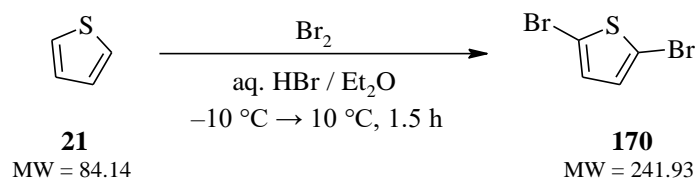
^{1}H NMR (500 MHz, $CDCl_3$, ppm): $\delta$ = 8.41–8.38 (m, 2H), 8.01–7.93 (m, 6H), 7.90 (dd, *J* = 7.6; 1.7 Hz, 2H), 7.61–7.54 (m, 4H), 3.91–3.86 (m, 4H), 1.91 (s, 6H), 1.67 (d, *J* = 12.3 Hz, 6H), 1.62–1.51 (m, 22H).

Anal. calcd. for $C_{50}H_{52}N_2O_2$: C 84.23%, H 7.35%, N 3.93%; Found: C 84.54%, H 7.26%, N 3.92%.

### 5.4.5    Synthesis of DPP-based polymers

#### *5.4.5.1    Polymerization by cross-coupling reactions*

#### Preparation of 2,5-dibromothiophene (170)



**21**
MW = 84.14

**170**
MW = 241.93

*Scheme 75*: *Preparation of 2,5-dibromothiophene (**170**)*

**21** (30.2 g, 358.93 mmol) was dissolved in diethyl ether (72 mL) and the mixture was cooled to –10 °C and protected from light by aluminium foil. After that, 48% aq. hydrobromic acid (110 mL) was slowly added, and the mixture was again cooled to –10 °C. A mixture of bromine (2 equiv., 36.8 mL/114.8 g, 718.35 mmol) and 48% aq. hydrobromic acid (112 mL) was then slowly added dropwise (for 40 min) to the reaction mixture, which increased the temperature to 10 °C and it was stirred for 50 min at this conditions. Then the organic phase was separated, and the aqueous phase was washed with DCM (4×50 mL). The collected organic phases were washed first with 20% solution of $Na_2S_2O_3$ (2×100 mL), then with distilled water (2×200 mL), finally with brine (150 mL) and then dried over anhydrous $Na_2SO_4$ and filtered through filter aid (Celite). After removal of the solvent under vacuum, the obtained crude mixture was purified by vacuum distillation (1 mbar, oil bath 60 °C) to afford pure product **170**.

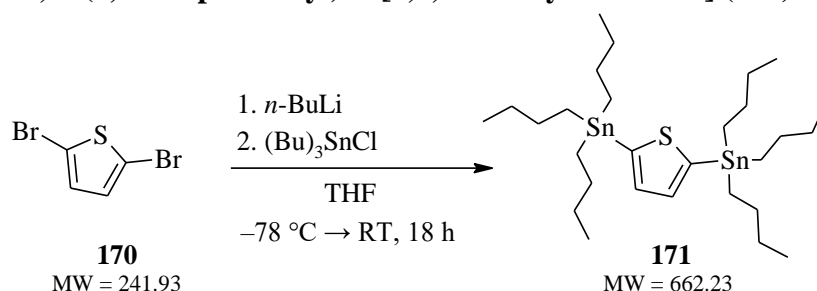   **170**: Slightly yellowish liquid (69.93 g, yield 81%).

   Refractive index: $n20/D = 1.628$ (lit. 1.629)[177].

   Density: $\rho_{25} = 2.149$ g cm$^{-3}$ (lit. 2.147 g cm$^{-3}$)[177].

   $^1$H NMR (300 MHz, CDCl$_3$, ppm): $\delta = 6.82$ (s, 2H).

   GC-MS (method: *vseobecna*): RT = 6.28 min; m/z = 241.92.


#### Preparation of 1,1'-(2,5-thiophenediyl)bis[1,1,1-tributyl-stannane] (171)



**170**
MW = 241.93

1. *n*-BuLi
2. (Bu)$_3$SnCl

THF

–78 °C → RT, 18 h

**171**
MW = 662.23

*Scheme 76*: *Preparation of 1,1'-(2,5-thiophenediyl)bis[1,1,1-tributyl-stannane] (**171**)*

The same procedure as for the **157** (*Chapter 5.4.4.6*) was used to prepare the **171**, starting with **170** (1.0 equiv., 0.97 mL/2.08 g, 8.60 mmol) and using tributyltin chloride (3.0 equiv., 6.97 mL/8.37 g, 25.70 mmol) as the reagent instead of trimethyltin chloride. The reaction time

of stirring at RT was a total of 18 h. Stille intermediate **171** was obtained and used to the next reaction step without further purification.

**171**: Brown liquid (5.80 g, yield 102%).

$^1$H NMR (300 MHz, CDCl$_3$, ppm): $\delta$ = 7.35 (s, 2H), 1.61–1.55 (m, 12H), 1.39–1.29 (m, 12H), 1.14–1.10 (m, 12H), 0.94–0.85 (m, 18H).

## Preparation of thienyl-bridged *N,N'*-ethyladamantyl-DPP polymer (172)

**159** (0.90 equiv., 0.181 g, 0.231 mmol), **171** (1.00 equiv., 0.200 g, 0.257 mmol), Pd(OAc)$_2$ (0.06 equiv., 0.0032 g, 0.014 mmol), CuI (0.20 equiv., 0.010 g, 0.051 mmol) and PPh$_3$ (0.20 equiv., 0.013 g, 0.051 mmol) were dissolved in a mixture of freshly distilled toluene (3.0 mL) and anhydrous DMF (2.0 mL) under argon atmosphere. The reaction mixture was purged with argon for 30 min in an ultrasonic bath, and then it was stirred at 110 °C for 120 h. However, even after that, only the starting material and some decomposition fragments were observed according to TLC analysis. Thus, the reaction was quenched.
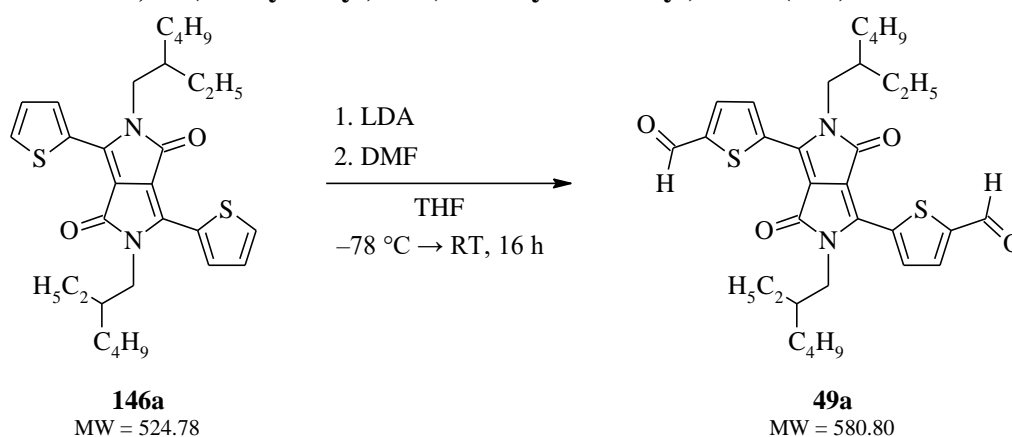
**172**: *No product was isolated.*
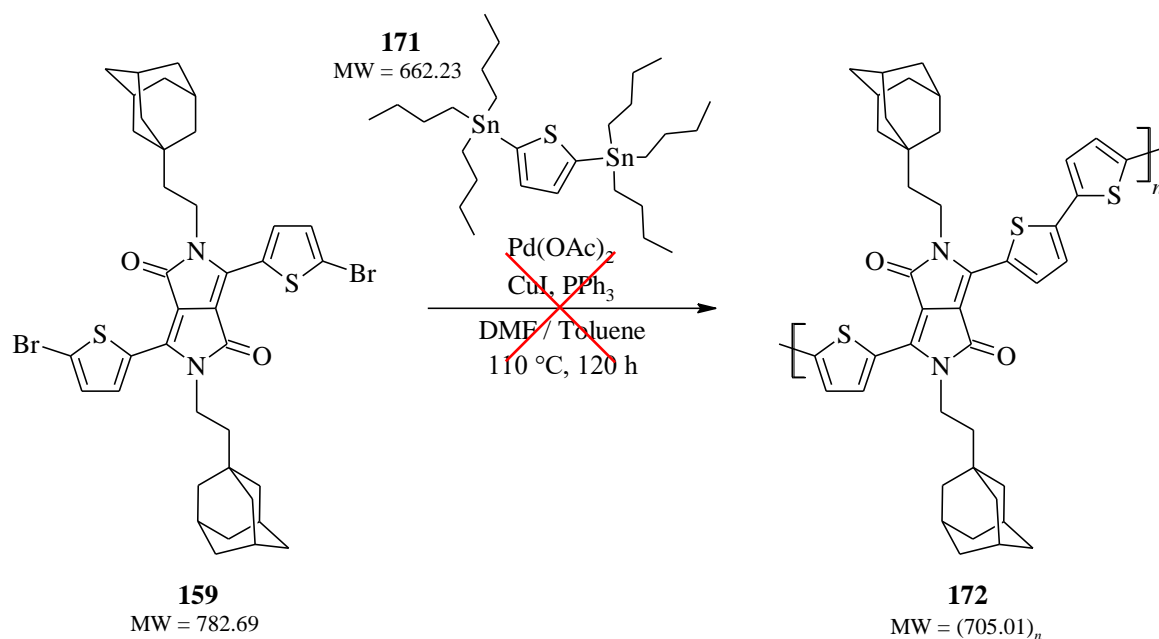


**Scheme 77**: *Preparation of thienyl-bridged N,N'-ethyladamantyl-DPP polymer (**172**)*

### 5.4.6   Incorporation of electron-accepting groups into DPPs

#### 5.4.6.1   *N,N'-(2-EtHex)-bis(5-dicyanovinyl-2-thienyl)-DPP*

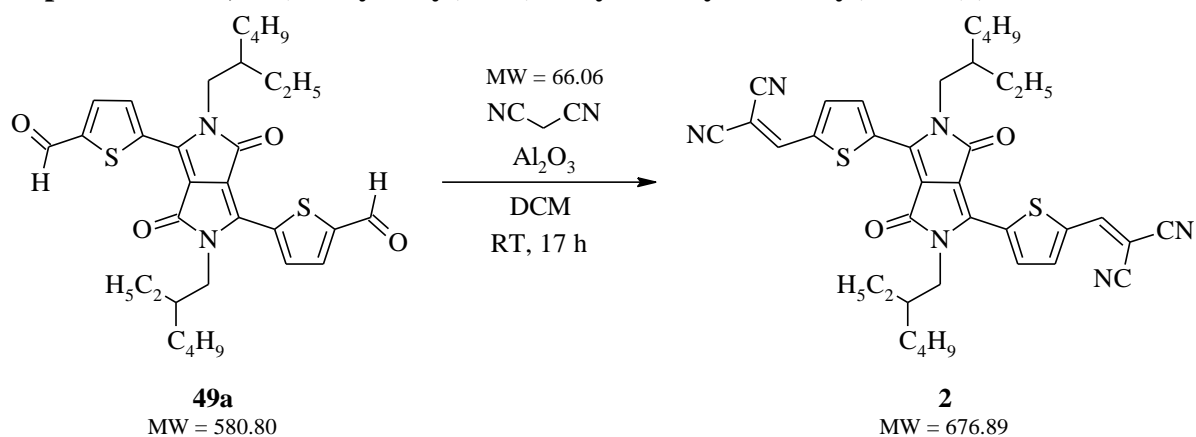**Preparation of *N,N'*-(2-ethylhexyl)-bis(5-formyl-2-thienyl)-DPP (49a)**



*Scheme 78: Preparation of N,N'-2-ethylhexyl-bis(5-formyl-2-thienyl)-DPP (**49a**)*

**146a** (0.50 g, 0.95 mmol) was dissolved in anhydrous THF (20 mL) under argon atmosphere, and the reaction mixture was cooled to –78 °C and stirred for 15 min. After that, 4.20 equiv. of LDA (2M, 2.00 mL, 4.00 mmol) was added dropwise to the mixture and it was stirred at –78 °C for 2 h. Following that 5.15 equiv. of DMF (0.38 mL/0.36 g, 4.91 mmol) was rapidly added to the solution, and the reaction mixture temperature was spontaneously heated to RT and stirred for another 16 h. Then, the reaction was quenched with the addition of DCM (80 mL), and extraction was performed. The reaction mixture was washed with DCM (2×30 mL), and the collected organic phases were washed with distilled water (2×150 mL), finally with brine (200 mL) and then dried over anhydrous $Na_2SO_4$ and filtered through filter aid (Celite). After removal of the solvent under vacuum, the obtained crude mixture was purified by silica gel chromatography eluting with DCM/*n*-hexane/ethyl acetate 6:3:1 (v/v/v) to get pure product **49a** ($R_F$ = 0.40, eluent: DCM/*n*-hexane/ethyl acetate 6:3:1).

**49a**: Dark purple solid (0.08 g, yield 15%).

$^1$H NMR (300 MHz, CDCl$_3$, ppm): $\delta$ = 10.03 (s, 2H), 9.03 (d, *J* = 4.2 Hz, 2H), 7.87 (*d*, J = 4.2 Hz, 2H), 4.12–3.97 (m, 4H), 1.86–1.78 (m, 2H), 1.40–1.18 (m, 16H), 0.94–0.81 (m, 12H).

**Preparation of *N*,*N*′-(2-ethylhexyl)-bis(5-dicyanovinyl-2-thienyl)-DPP (2)**



*Scheme 79*: *Preparation of N,N'-2-ethylhexyl-bis(5-dicyanovinyl-2-thienyl)-DPP (2)*

**49a** (0.050 g, 0.086 mmol), malononitrile (3.0 equiv., 0.017 g, 0.258 mmol) and aluminium oxide (7.0 equiv., 0.061 g, 0.603 mmol) were stirred in DCM (30 mL) at RT for 17 h. The reaction mixture was then filtered off, and the filter cake was washed with DCM (2×20 mL). After removal of the solvent under vacuum, the obtained crude mixture was purified by silica gel chromatography eluting with DCM/ethyl acetate 20:1 (v/v) to get pure product **2** ($R_F$ = 0.15, eluent: chloroform).

**2**: Dark blue solid (0.024 g, yield 41%).

$^1$H NMR (300 MHz, CDCl$_3$, ppm): $\delta$ = 9.21 (d, *J* = 4.3 Hz, 2H), 7.89 (s, 2H), 7.85 (d, *J* = 4.5 Hz, 2H), 4.09 (dd, *J* = 8.0; 3.8 Hz, 4H), 1.89–1.83 (m, 2H), 1.39–1.18 (m, 16H), 0.97–0.81 (m, 12H).

### 5.4.6.2 Preparation of diformyl-phenyl-DPP – testing approach

**Preparation of 4-(1,3-dioxolan-2-yl)benzonitrile (53a)**
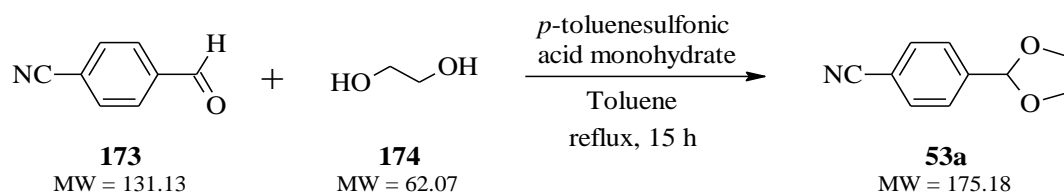


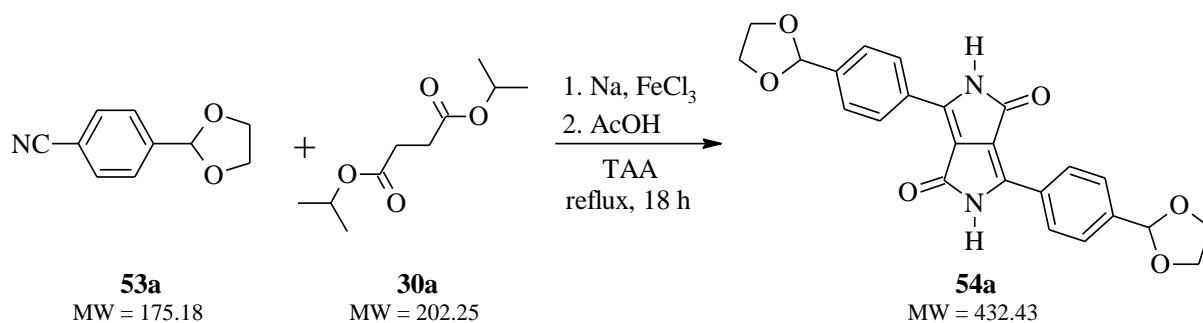*Scheme 80*: *Preparation of 4-(1,3-dioxolan-2-yl)benzonitrile (53a)*

**173** (0.25 g, 1.90 mmol) and ethylene glycol (**174**; 5 equiv., 0.52 mL/0.59 g, 9.50 mmol) were vigorously stirred in toluene (10 mL). After that, *p*-toluenesulfonic acid monohydrate (0.02 equiv., 7.3 mg, 0.038 mmol) was added, and the reaction mixture was heated to reflux and stirred for 15 h to remove water and ethylene-glycol using Dean-Stark apparatus. The reaction mixture was then cooled to RT, an aqueous solution of NaOH (2.5M, 5 mL) was added to quench the reaction, and it was extracted with toluene (3×20 mL). The collected organic phases were washed with distilled water (90 mL), then dried over anhydrous Na$_2$SO$_4$ and filtered through filter aid (Celite). After removal of the solvent under vacuum, the

obtained crude mixture was purified by silica gel chromatography eluting with DCM to get pure product **53a** ($R_F$ = 0.33, eluent: DCM).

**53a**: White solid (0.24 g, yield 72%). Melting point 42 °C (lit. 45 °C)[178].

$^1$H NMR (300 MHz, CDCl$_3$, ppm): $\delta$ = 7.67 (d, $J$ = 8.2 Hz, 2H), 7.59 (d, $J$ = 8.1 Hz, 2H), 5.85 (s, 1H), 4.15-4.03 (m, 4H).

## Preparation of bis[4-(1,3-dioxolan-2-yl)-phenyl]-DPP (54a)



Scheme 81: Preparation of bis[4-(1,3-dioxolan-2-yl)-phenyl]-DPP (**54a**)

The same procedure as for the **31a** (*Chapter 5.4.1.1*) was used to prepare the **54a**, starting with **53a** (1.0 equiv., 0.20 g, 1.14 mmol).

**54a**: Purple-red solid (0.11 g, yield 34%). Melting point >340 °C (lit. >300 °C)[179].

Anal. calcd. for C$_{24}$H$_{20}$N$_2$O$_6$: C 66.66%, H 4.66%, N 6.48%; Found: C 66.47%, H 4.72%, N 6.36%.

### *5.4.6.3 N,N'-EtAd-bis(5-dicyanovinyl-2-thienyl)-DPP – approach A*
### Preparation of thiophene-2-carbaldehyde (50b)
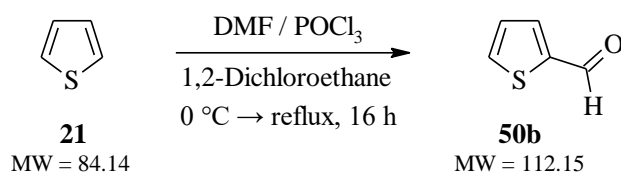


Scheme 82: Preparation of thiophene-2-carbaldehyde (**50b**)

Anhydrous DMF (1.01 equiv., 37.2 mL/35.10 g, 480.2 mmol) was added dropwise to POCl$_3$ (0.99 equiv., 44.0 mL/72.15 g, 470.6 mmol) maintained at 0 °C, and Vilsmeier-Haack reagent was prepared. After 45 min, compound **21** (1.00 equiv., 38.1 mL/ 40.00 g, 475.4 mmol) dissolved in anhydrous 1,2-dichloroethane (220 mL) was added to the above Vilsmeier-Haack reagent, and the reaction mixture was then heated to reflux and stirred for 16 h. After that, the reaction was cooled to RT and quenched by hydrolysis with saturated aqueous sodium acetate solution (400 mL) for 4 h. The reaction mixture was then extracted with DCM (4×90 mL), the collected organic phases were washed with saturated NaHCO$_3$ solution (250 mL), followed by distilled water (2×350 mL), finally with brine (300 mL), then dried over anhydrous Na$_2$SO$_4$ and filtered through filter aid (Celite). After removal of the solvent under vacuum, the

obtained crude mixture was purified by vacuum distillation (10 mbar, oil bath 85 °C) to afford pure product **50b**.
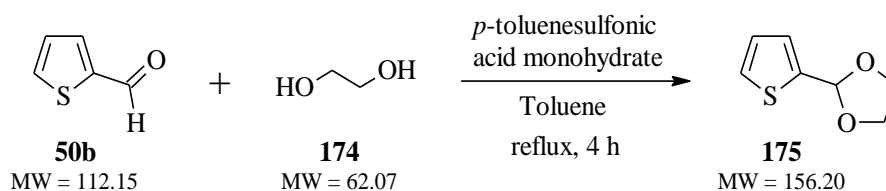
**50b**: Yellowish liquid (40.52 g, yield 76%).

Refractive index: $n20/D = 1.591$ (lit. 1.591)[180].

Density: $\rho_{25} = 1.21$ g cm$^{-3}$ (lit. 1.20 g cm$^{-3}$)[180].

$^1$H NMR (300 MHz, CDCl$_3$, ppm): $\delta = 9.91$ (s, 1H), 7.76 (d, $J = 6.3$ Hz, 1H), 7.68 (d, $J = 4.9$ Hz, 1H), 7.21 (dd, $J = 6.2$; 4.9 Hz, 1H).

GC-MS (method: *JJ_vseobecna met*): RT = 11.82 min; m/z = 111.90 (purity 98%).


## Preparation of 2-(thiophen-2-yl)-1,3-dioxolane (175)



*Scheme 83: Preparation of 2-(thiophen-2-yl)-1,3-dioxolane (**175**)*

The same procedure as for the **53a** (*Chapter 5.4.6.2*) was used to prepare the **175**, starting with **50b** (1 equiv., 2.37 mL/2.84 g, 24.81 mmol). The reaction time of stirring at fine reflux was reduced by 11 h to a total of 4 h. Work-up of the reaction mixture was identical to the above experiment. The obtained crude mixture was purified by vacuum distillation (20 mbar, oil bath 120 °C) to afford pure product **175**.

**175**: Slightly yellowish liquid (2.50 g, yield 64%).

$^1$H NMR (300 MHz, CDCl$_3$, ppm): $\delta = 7.34$ (dd, $J = 5.1$; 1.1 Hz, 1H), 7.21–7.13 (m, 1H), 7.02 (dd, $J = 5.2$; 3.5 Hz, 1H), 6.11 (s, 1H), 4.20–3.98 (m, 4H).

GC-MS (method: *JJ_vseobecna met*): RT = 14.06 min; m/z = 156.13 (purity 99%).


## Preparation of 2-(5-bromothiophen-2-yl)-1,3-dioxolane (52b)
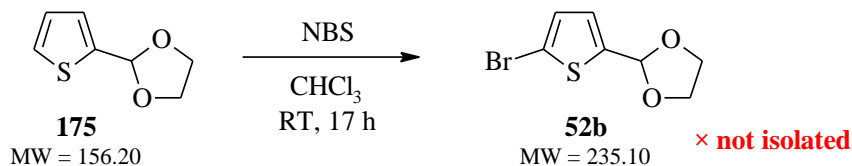


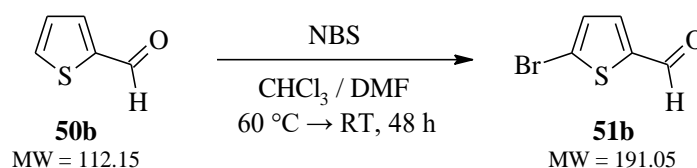*Scheme 84: Preparation of 2-(5-bromothiophen-2-yl)-1,3-dioxolane (**52b**)*

**175** (0.75 g, 4.71 mmol) was stirred in dried chloroform (15 mL) under argon atmosphere; then the mixture was protected from light by aluminium foil and 1.10 equiv. of NBS (0.92 g, 5.18 mmol) was added piecewise. The reaction mixture was stirred at RT for 17 h, and then it was poured into distilled water with crushed ice (50 mL) and stirred for 30 min. After that, extraction was performed – the reaction mixture was washed with chloroform (3×20 mL), the collected organic phases were then washed with distilled water (2×100 mL), finally with brine

(80 mL), dried over anhydrous $Na_2SO_4$ and filtered through filter aid (Celite). After removal of the solvent under vacuum, the obtained crude mixture was analysed by GC-MS analysis (method: *JJ_vseobecna met*; RT = 15.89 min; m/z = 234.90; content 19%). However, in approximately the same content, the crude mixture contained a total of 4 components, as was also confirmed TLC analysis. Thus, the purification of the crude mixture was not performed.

**52b**: *No pure product was isolated.*

### 5.4.6.4   N,N'-EtAd-bis(5-dicyanovinyl-2-thienyl)-DPP – approach B

**Preparation of 5-bromothiophene-2-carbaldehyde (51b)**



*Scheme 85: Preparation of 5-bromothiophene-2-carbaldehyde (51b)*

The same procedure as for the **52b** (*Chapter 5.4.6.3*) was used to prepare the **51b**, starting with **50b** (1.0 equiv., 4.29 mL/5.15 g, 45.00 mmol) and using a mixture of chloroform (100 mL) and DMF (10 mL) instead of pure chloroform. The reaction temperature was increased to 60 °C, and after 1 h of stirring at that temperature, the reaction mixture was stirred at RT for another 47 h. The obtained crude mixture was purified by silica gel chromatography eluting with DCM to get pure product **51b** ($R_F$ = 0.60, eluent: DCM).
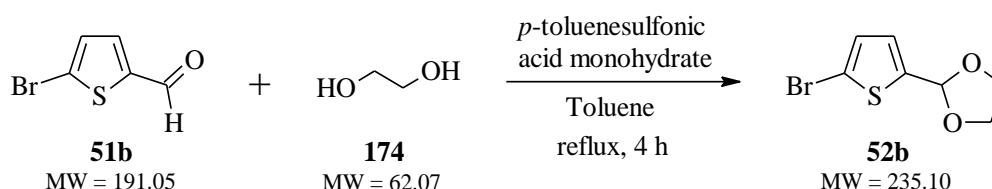
**51b**: Yellow-brownish liquid (3.58 g, yield 42%).

Refractive index: $n20/D$ = 1.636 (lit. 1.637)[181].

Density: $\rho_{25}$ = 1.606 g cm$^{-3}$ (lit. 1.607 g cm$^{-3}$)[181].

$^1$H NMR (300 MHz, CDCl$_3$, ppm): $\delta$ = 9.79 (s, 1H), 7.53 (d, *J* = 4.3 Hz, 1H), 7.19 (d, *J* = 4.1 Hz, 1H).

GC-MS (method: *JJ_vseobecna met*): RT = 13.99 min; m/z = 190.91 (purity 98%).

**Preparation of 2-(5-bromothiophen-2-yl)-1,3-dioxolane (52b)**



*Scheme 86: Preparation of 2-(5-bromothiophen-2-yl)-1,3-dioxolane (52b)*

The same procedure as for the **175** (*Chapter 5.4.6.3*) was used to prepare the **52b**, starting with **51b** (1.0 equiv., 2.10 g, 9.89 mmol). The reaction conditions and work-up of the reaction mixture were identical. The obtained crude mixture was purified by vacuum distillation (15 mbar, oil bath 180 °C) to afford pure product **52b**.
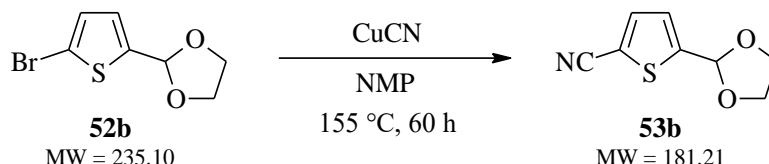
**52b**: Slightly yellow liquid (1.71 g, yield 74%).

$^1$H NMR (300 MHz, CDCl$_3$, ppm): $\delta$ = 6.98–6.89 (m, 2H), 6.02 (s, 1H), 4.05–3.95 (m, 4H).

GC-MS (method: *JJ_vseobecna met*): RT = 15.91 min; m/z = 234.90 (purity 95%).

**Preparation of 5-(1,3-dioxolan-2-yl)thiophene-2-carbonitrile (53b)**



**Scheme 87**: *Preparation of 5-(1,3-dioxolan-2-yl)thiophene-2-carbonitrile (53b)*

The same procedure as for the **129** (*Chapter 5.4.2.1*) was used to prepare the **53b**, starting with **52b** (1.0 equiv., 0.93 g, 3.76 mmol) and copper cyanide (1.2 equiv., 0.40 g, 4.51 mmol) as a reagent. The reaction time of stirring at 155 °C was extended by 12 h to a total of 60 h. The reaction mixture was then cooled to RT, poured into distilled water (250 mL), and it was extracted with *tert*-butyl-methyl ether (5×75 mL). The collected organic phases were washed with distilled water (3×350 mL), finally with brine (300 mL), then dried over anhydrous Na$_2$SO$_4$ and filtered through filter aid (Celite). After removal of the solvent under vacuum, the obtained crude mixture was purified by silica gel chromatography eluting with toluene to get pure product **53b** ($R_F$ = 0.30, eluent: toluene).
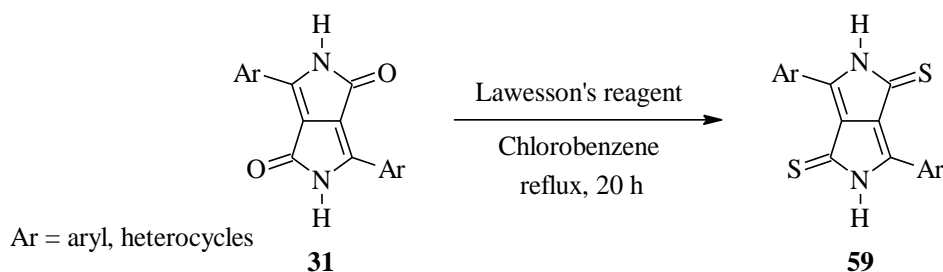
**53b**: Yellowish oily material (0.19 g, yield 27%).

$^1$H NMR (500 MHz, CDCl$_3$, ppm): $\delta$ = 7.51 (d, $J$ = 3.8 Hz, 1H), 7.13 (dd, $J$ = 3.8; 0.7 Hz, 1H), 6.10 (d, $J$ = 0.6 Hz, 1H), 4.14–3.99 (m, 4H).

GC-MS (method: *JJ_vseobecna met*): RT = 17.64 min; m/z = 181.09 (purity 95%).

## 5.4.7 Synthesis of thioketo analogues of DPPs (DTPPs)

### 5.4.7.1 Synthesis of basic DTPPs and with extended π-conjugation



**Scheme 88**: *Synthetic approach to the preparation of dithioketopyrrolopyrroles (DTPPs)*

DPP molecule **31** (1.0 equiv.) was stirred with Lawesson's reagent (2.1 equiv.) in extra dry chlorobenzene (dilution approx. 50 mL/g) under argon atmosphere. The reaction mixture was first purged with argon at RT for 30 min and then stirred at reflux for 20 h. After that, the reaction mixture was cooled to RT, filtered off, and the filter cake was washed with methanol.

The solid material from the filter cake was suspended in methanol (approx. 50 mL/g), refluxed overnight, then filtered off while hot and washed with methanol. The whole process was repeated once again and the obtained solid on the filter cake was carefully dried under vacuum at 60 °C for 20 h to get pure DTPP molecule **59**.

**Thienyl-2,5-dihydropyrrolo[3,4-*c*]pyrrole-1,4-dithione (59a)**
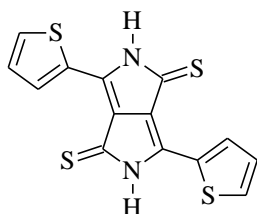


**59a**
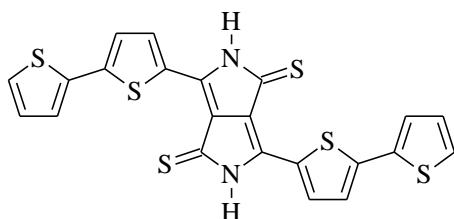MW = 332.49

**59a**: Black-green powder (3.39 g, yield 87%). Melting point >320 °C.

$^1$H NMR (300 MHz, DMSO-d$_6$, ppm): $\delta$ = 12.81 (s, 2H), 9.01 (dd, $J$ = 4.1; 1.1 Hz, 2H), 8.05 (dd, $J$ = 4.8; 1.0 Hz, 2H), 7.39 (dd, $J$ = 3.9; 4.8 Hz, 2H).

Anal. calcd. for C$_{14}$H$_8$N$_2$S$_4$: C 50.57%, H 2.43%, N 8.43%, S 38.58%; Found: C 50.95%, H 2.34%, N 8.48%, S 38.32%.

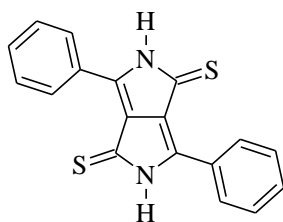**Bithienyl-2,5-dihydropyrrolo[3,4-*c*]pyrrole-1,4-dithione (176)**



**176**
MW = 496.73

**176**: Black powder (1.02 g, yield 96%). Melting point >320 °C.

Anal. calcd. for C$_{22}$H$_{12}$N$_2$S$_6$: C 53.19%, H 2.44%, N 5.64%, S 38.73%; Found: C 53.41%, H 2.08%, N 5.63%, S 38.92%.

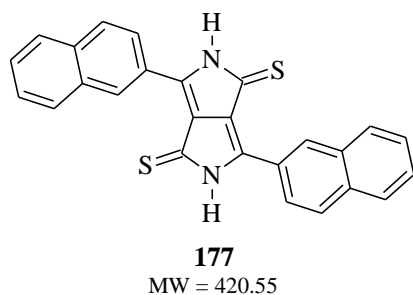**Phenyl-2,5-dihydropyrrolo[3,4-*c*]pyrrole-1,4-dithione (59b)**



**59b**
MW = 320.43

**59b**: Black-blue powder (1.01 g, yield 82%). Melting point >320 °C.

$^1$H NMR (500 MHz, DMSO-d$_6$, ppm): $\delta$ = 12.72 (s, 2H), 8.90–8.86 (m, 4H), 7.72–7.67 (m, 2H), 7.59 (t, $J$ = 7.8 Hz, 4H).

Anal. calcd. for C$_{18}$H$_{12}$N$_2$S$_2$: C 67.47%, H 3.77%, N 8.74%, S 20.01%; Found: C 67.96%, H 3.84%, N 9.10%, S 18.90%.
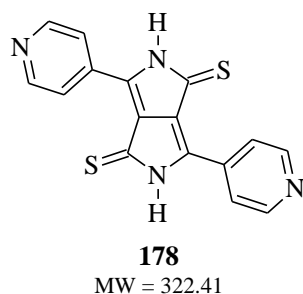
## Naphthyl-2,5-dihydropyrrolo[3,4-*c*]pyrrole-1,4-dithione (177)



**177**
MW = 420.55

**177**: Dark red-black powder (0.33 g, yield 87%). Melting point >320 °C.

Anal. calcd. for C$_{26}$H$_{16}$N$_2$S$_2$: C 74.25%, H 3.83%, N 6.66%, S 15.25%; Found: C 75.06%, H 3.87%, N 6.74%, S 14.93%.

## Pyridinyl-2,5-dihydropyrrolo[3,4-*c*]pyrrole-1,4-dithione (178)
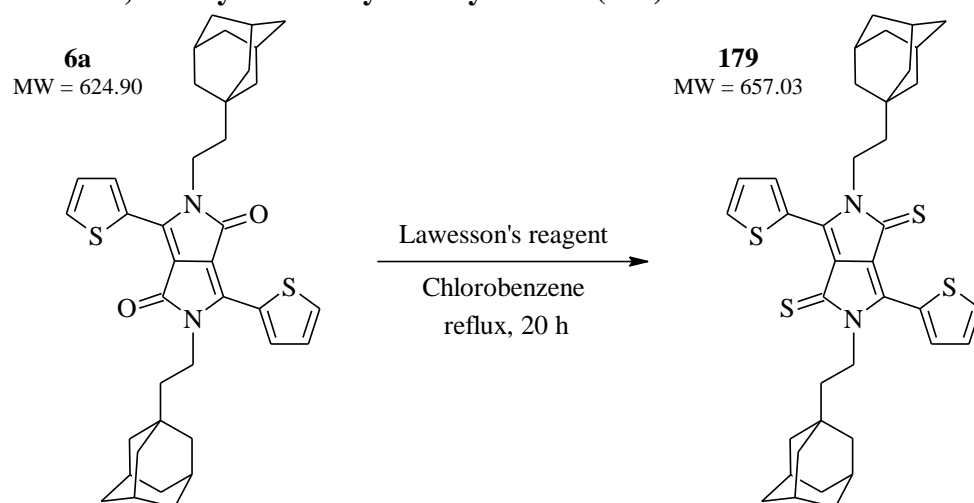


**178**
MW = 322.41

**178**: Deep violet-black powder (0.63 g, yield 52%). Melting point >320 °C.

Anal. calcd. for C$_{16}$H$_{10}$N$_4$S$_2$: C 59.61%, H 3.13%, N 17.38%, S 19.89%; Found: C 60.08%, H 3.17%, N 16.98%, S 19.41%.

## 5.4.7.2 Synthesis of N-alkylated DTPPs

## Preparation of *N,N'*-ethyladamantyl-thienyl-DTPP (179)



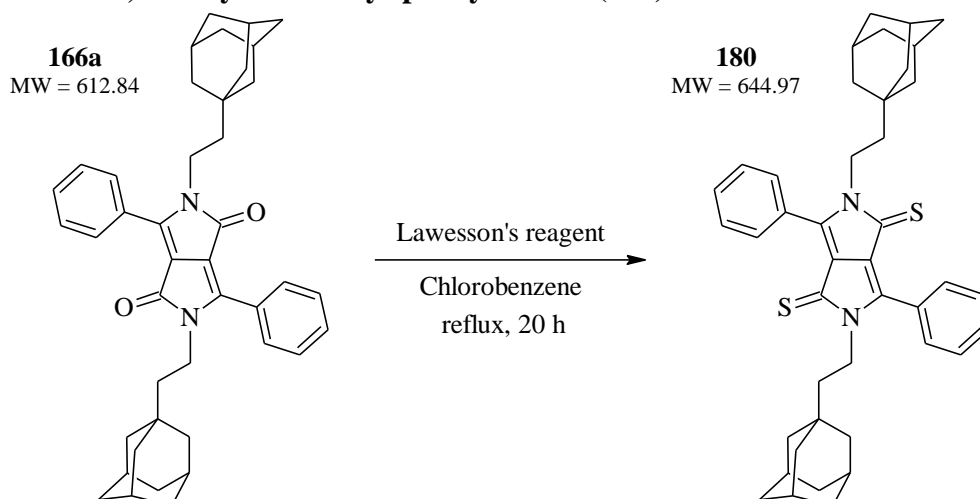**Scheme 89**: *Preparation of N,N'-ethyladamantyl-thienyl-DTPP (**179**)*

**6a** (1.0 equiv., 0.050 g, 0.076 mmol) was stirred with Lawesson's reagent (2.1 equiv., 0.065 g, 0.161 mmol) in extra dry chlorobenzene (8 mL) under argon atmosphere. The reaction mixture was first purged with argon at RT for 35 min and then stirred at reflux for 20 h. After that, the reaction mixture was cooled to RT and poured into methanol (40 mL). The formed precipitate was filtered off and washed with methanol (2×25 mL). The solid material from the filter cake was suspended in new methanol (30 mL/g), refluxed overnight, then filtered off while hot and washed with methanol (2×25 mL) again. The obtained solid on the filter cake was carefully dried under vacuum for 17 h to get pure product **179** ($R_F$ = 0.55, eluent: toluene).

**179**: Dark violet-green crystals (0.039 g, yield 79%). Melting point 196 °C.

$^1$H NMR (500 MHz, CDCl$_3$, ppm): $\delta$ = 8.98 (dd, $J$ = 3.8; 1.2 Hz, 2H), 7.74 (dd, $J$ = 5.1; 1.2 Hz, 2H), 7.30 (dd, $J$ = 5.1, 3.8 Hz, 2H), 4.53–4.47 (m, 4H), 1.94 (d, $J$ = 17.8 Hz, 6H), 1.70–1.54 (m, 24H), 1.52–1.40 (m, 6H).

Anal. calcd. for C$_{38}$H$_{44}$N$_2$S$_4$: C 69.47%, H 6.75%, N 4.26%, S 19.52%; Found: C 70.03%, H 6.77%, N 4.31%, S 18.98%.

**Preparation of *N,N'*-ethyladamantyl-phenyl-DTPP (180)**



*Scheme 90: Preparation of N,N'-ethyladamantyl-phenyl-DTPP (**180**)*

The same procedure as for the **179** was used to prepare the **180**, starting with **166a** (1.0 equiv., 0.050 g, 0.078 mmol).

**180**: Green-grey solid (0.032 g, yield 61%). Melting point 182 °C.

$^1$H NMR (500 MHz, CDCl$_3$, ppm): $\delta$ = 7.88–7.77 (m, 4H), 7.64–7.54 (m, 4H), 7.37–7.32 (m, 2H), 3.93–3.86 (m, 4H), 1.88 (s, 12H), 1.57 (d, $J$ = 14.5 Hz, 8H), 1.46 (s, 4H), 1.39–1.30 (m, 12H), 1.33–1.23 (m, 4H).

Anal. calcd. for C$_{42}$H$_{48}$N$_2$S$_2$: C 78.21%, H 7.50%, N 4.34%, S 9.94%; Found: C 78.64%, H 7.79%, N 4.21%, S 10.38%.

### 5.4.7.3 Synthesis of S-alkylated DTPPs

The DTPP molecule **59** (1.0 equiv.) was stirred with anhydrous potassium carbonate (~5 equiv.) in dried acetone (dilution approx. 100 mL/g) under argon atmosphere. The reaction mixture was purged with argon at RT for 20 min and then, 3.5 equiv. of alkyl bromide (**R–Br**) was added in one portion. After another 10 min of purging with argon, the reaction mixture was heated to reflux and stirred for 20 h. Acetone was then removed from the reaction mixture by a rotary evaporator to obtain the crude product, which was further purified to get pure *S*-alkylated DTPP derivative **60**.
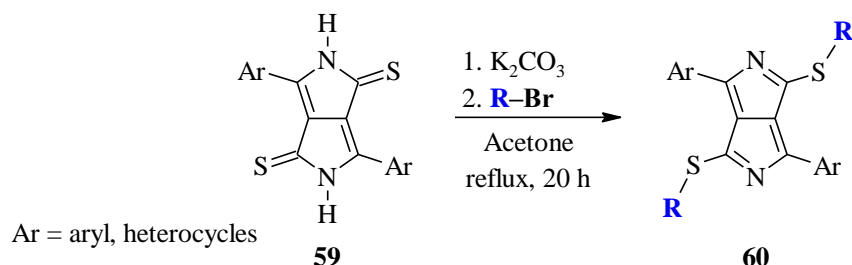


*Scheme 91: Alkylation of basic dithioketopyrrolopyrroles (DTPPs, **59**)*

## Dodecyl-alkylated thienyl-DTPP
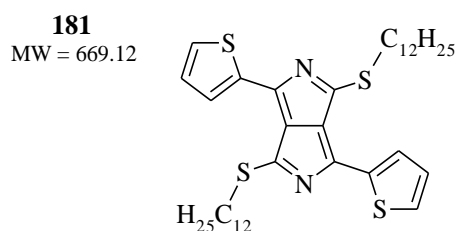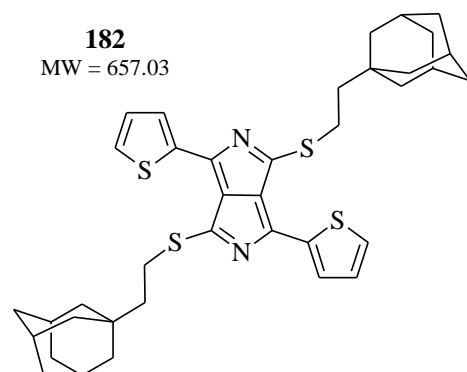
**181**
MW = 669.12



The crude product was purified by silica gel chromatography eluting with petroleum ether →
petroleum ether/toluene 1:1 (v/v) to get pure product **181** ($R_F$ = 0.90, eluent: toluene).

**181**: Dark blue crystals (0.094 g, yield 47%). Melting point 120 °C.

^{1}H NMR (300 MHz, CDCl₃, ppm): $\delta$ = 8.08 (s, 2H), 7.63 (d, $J$ = 4.9 Hz, 2H), 7.28–7.25
(m, 2H), 3.50 (s, 4H), 1.56–1.45 (m, 4H), 1.36–1.23 (m, 38H), 0.92–0.84 (m, 6H).

Anal. calcd. for $C_{38}H_{56}N_2S_4$: C 68.21%, H 8.44%, N 4.19%, S 19.17%; Found: C 69.41%,
H 7.52%, N 4.05%, S 16.46%.


## Ethyladamantyl-alkylated thienyl-DTPP

**182**
MW = 657.03



The crude product was purified by silica gel chromatography eluting with toluene followed by
dissolving the purified material in a small amount of chloroform (10 mL) and slowly adding it
dropwise to vigorously stirred petroleum ether (200 mL). The formed precipitate was filtered
off and washed with petroleum ether (20 mL) to get pure product **182** ($R_F$ = 0.85, eluent:
toluene).

**182**: Dark violet-blue crystals (0.419 g, yield 63%). Melting point 301 °C.

^{1}H NMR (300 MHz, CDCl₃, ppm): $\delta$ = 8.06 (d, $J$ = 3.8 Hz, 2H), 7.63 (d, $J$ = 5.0 Hz, 2H),
7.25 (d, $J$ = 3.8 Hz, 2H), 3.48–3.42 (m, 4H), 2.01 (s, 4H), 1.76 (s, 2H), 1.71–1.61 (m, 22H),
1.53 (s, 4H), 1.26 (s, 4H).

Anal. calcd. for $C_{38}H_{44}N_2S_4$: C 69.47%, H 6.75%, N 4.26%, S 19.52%; Found: C 70.25%,
H 6.55%, N 4.56%, S 17.35%.

## Methyladamantyl-alkylated thienyl-DTPP

**183**
MW = 628.98



× **not confirmed**
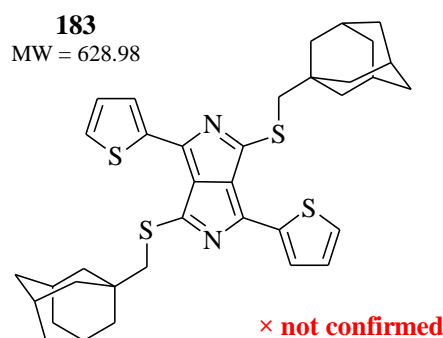
Due to poor reactivity, the reaction time of stirring at reflux was extended by 52 h to a total of 72 h. The crude product was purified by silica gel chromatography eluting with toluene. A dark green solution of probably product **183** was obtained ($R_F$ = 0.15, eluent: toluene), however, during the removal of the solvent under vacuum, the obtained material changed colour from dark green to a brown solid.

**183**: Dark brown solid (0.028 g, yield 10%).

^{1}H NMR (300 MHz, CDCl3, ppm): *Not confirmed*.
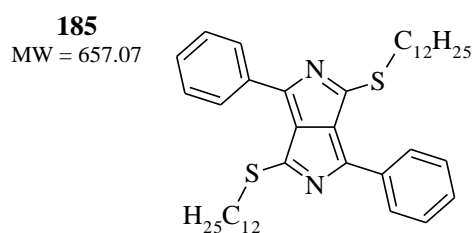

## Ethyladamantyl-alkylated bithienyl-DTPP
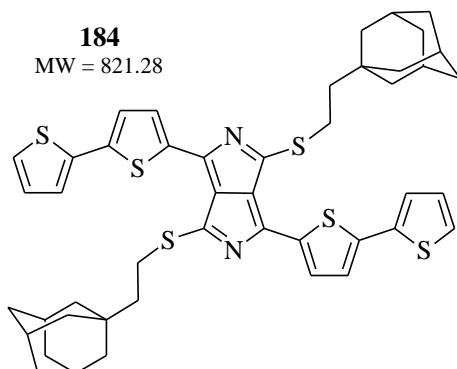
**184**
MW = 821.28



The crude product was purified by silica gel chromatography eluting with toluene → chloroform followed by dissolving the purified material in a small amount of chloroform (6 mL) and slowly adding it dropwise to vigorously stirred petroleum ether (200 mL). The formed precipitate was filtered off and washed with petroleum ether (20 mL) to get pure product **184** ($R_F$ = 0.80, eluent: toluene).

**184**: Dark violet-green crystals (0.085 g, yield 20%). Melting point 310 °C.

^{1}H NMR (300 MHz, CDCl3, ppm): $\delta$ = 7.98 (s, 2H), 7.35 (s, 6H), 7.09 (s, 2H), 3.48 (s, 4H), 2.03 (s, 6H), 1.79–1.61 (m, 20H), 1.51 (d, $J$ = 14.7 Hz, 8H).

Anal. calcd. for $C_{46}H_{48}N_2S_6$: C 67.27%, H 5.89%, N 3.41%, S 23.43%; Found: C 67.92%, H 5.76%, N 3.64%, S 22.97%.

## Dodecyl-alkylated phenyl-DTPP

**185**
MW = 657.07



× **not confirmed**

The crude product was purified by silica gel chromatography eluting with toluene. An intense purple solution of probably product **185** was obtained ($R_F$ = 0.75, eluent: toluene), however, during the removal of the solvent under vacuum, the obtained material changed colour from purple to a violet-brownish semisolid.

**185**: Violet-brownish semisolid (0.019 g, yield 6%).

^{1}H NMR (300 MHz, CDCl$_3$, ppm): *Not confirmed*.
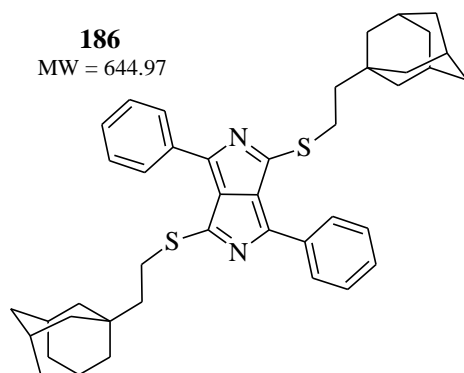

## Ethyladamantyl-alkylated phenyl-DTPP

**186**
MW = 644.97



The crude product was purified by silica gel chromatography eluting with toluene followed by dissolving the purified material in a small amount of chloroform (5 mL) and slowly adding it dropwise to vigorously stirred petroleum ether (230 mL). The formed precipitate was filtered off and washed with petroleum ether (20 mL) to get pure product **186** ($R_F$ = 0.70, eluent: toluene).

**186**: Dark purple crystals (0.126 g, yield 30%). Melting point 269 °C.

^{1}H NMR (300 MHz, CDCl$_3$, ppm): $\delta$ = 8.20 (dd, $J$ = 6.9; 3.0 Hz, 4H), 7.53–7.47 (m, 6H), 3.48–3.42 (m, 4H), 2.02–1.98 (m, 6H), 1.73 (s, 4H), 1.67 (d, $J$ = 12.4 Hz, 6H), 1.65–1.59 (m, 14H), 1.53 (s, 4H), 1.26 (s, 4H).

Anal. calcd. for C$_{42}$H$_{48}$N$_2$S$_2$: C 78.21%, H 7.51%, N 4.34%, S 9.94%; Found: C 78.38%, H 7.76%, N 4.37%, S 9.17%.
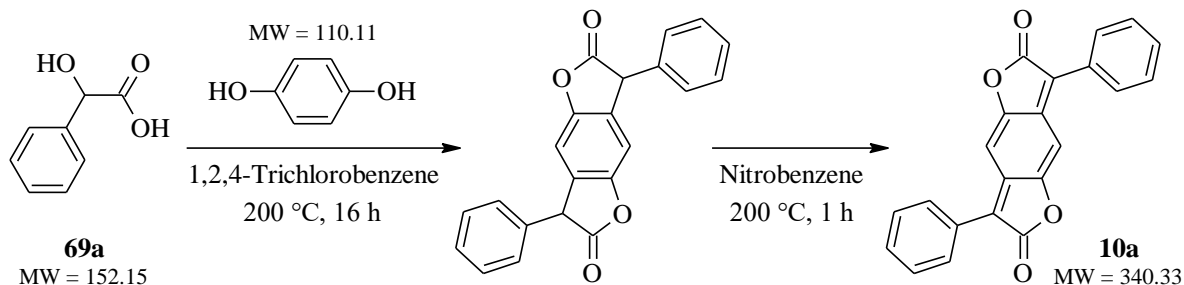
## 5.5 BDF derivatives

### 5.5.1 Synthesis of symmetrical BDF derivatives

#### 5.5.1.1 Diphenyl-BDF derivative (10a)

**Preparation of 3,7-diphenylbenzo[1,2-b:4,5-b′]difuran-2,6-dione (10a) – approach A**



*Scheme 92: Preparation of 3,7-diphenylbenzo[1,2-b:4,5-b']difuran-2,6-dione (**10a**) – approach A*
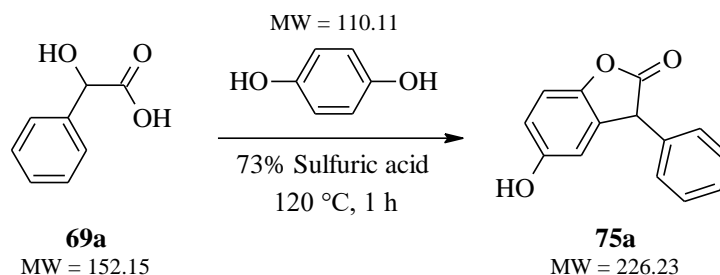
Mandelic acid **69a** (2.50 g, 16.43 mmol) and hydroquinone (0.5 equiv., 0.90 g, 8.17 mmol) were dissolved in 1,2,4-trichlorobenzene (25 mL) and stirred at 200 °C for 16 h in an apparatus equipped with a Dean-Stark trap. The reaction mixture was then cooled to 50 °C, nitrobenzene (1.3 equiv., 2.19 mL/2.63 g, 21.35 mmol) was added and the mixture was heated to 200 °C and stirred for another 1 h. After that, the reaction mixture was cooled to RT and poured into methanol (50 mL). The formed precipitate was filtered off, washed with methanol (30 mL) and dried in air. The obtained solid was then purified by crystallisation in toluene (6 mL) to get pure product **10a**.

**10a**: Yellow solid (1.06 g, yield 38%). Melting point 297 °C (lit. 298 °C)[54].

$^1$H NMR (300 MHz, CDCl$_3$, ppm): $\delta$ = 7.80 (d, $J$ = 7.1 Hz, 4H), 7.53 (q, $J$ = 6.9 Hz, 6H), 6.91 (s, 2H).

Anal. calcd. for C$_{22}$H$_{12}$O$_4$: C 77.64%, H 3.55%; Found: C 77.51%, H 3.52%.

**Preparation of 5-hydroxy-3-phenyl-1-benzofuran-2(3H)-one (75a)**



*Scheme 93: Preparation of 5-hydroxy-3-phenyl-1-benzofuran-2(3H)-one (**75a**)*

Mandelic acid **69a** (1.00 g, 6.57 mmol) and hydroquinone (2.5 equiv., 1.81 g, 16.44 mmol) were stirred in 73% sulphuric acid (5 mL) at 120 °C for 1 h. The reaction mixture was then cooled to RT and carefully poured into distilled water with crushed ice (80 mL). The formed precipitate was filtered off, washed with distilled water (until pH ~7) and methanol (20 mL).

The obtained solid was then dried in air and purified by crystallisation in toluene (3 mL) to get pure product **75a**.

**75a**: White powder (0.86 g, yield 58%). Melting point 161 °C (lit. 165 °C)[150].

Anal. calcd. for $C_{14}H_{10}O_3$: C 74.33%, H 4.46%; Found: C 73.92%, H 4.38%.

**Preparation of 3,7-diphenylbenzo[1,2-*b*:4,5-*b'*]difuran-2,6-dione (10a) – approach B**
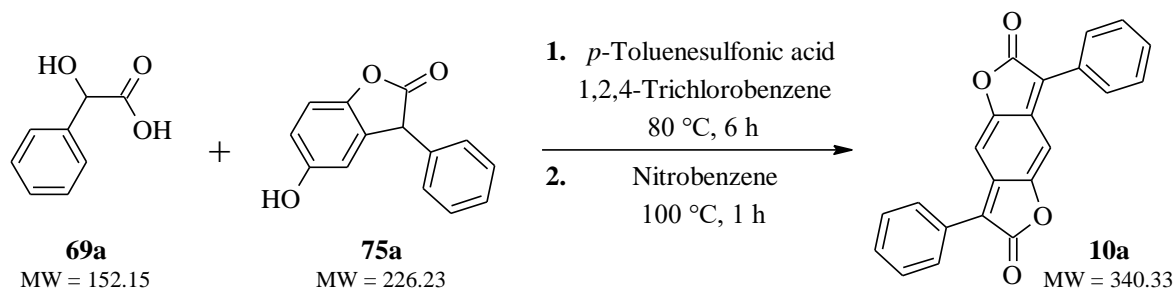


**Scheme 94**: *Preparation of 3,7-diphenylbenzo[1,2-b:4,5-b']difuran-2,6-dione (10a) – approach B*

Mandelic acid **69a** (0.19 g, 1.25 mmol), half-condensed intermediate **75a** (1.0 equiv., 0.29 g, 1.28 mmol) and *p*-toluenesulfonic acid monohydrate (1.1 equiv., 0.26 g, 1.37 mmol) were stirred in 1,2,4-trichlorobenzene (6 mL) at 80 °C for 6 h. The reaction mixture was then cooled to 50 °C, nitrobenzene (1.3 equiv., 0.17 mL/0.20 g, 1.63 mmol) was added and the mixture was heated to 100 °C and stirred for another 1 h. After that, the reaction mixture was cooled to RT and poured into methanol (20 mL). The formed precipitate was filtered off, washed with methanol (10 mL) and distilled water (15 mL) and dried in air. The obtained solid was then purified by crystallisation in toluene (2 mL) to get pure product **10a**.
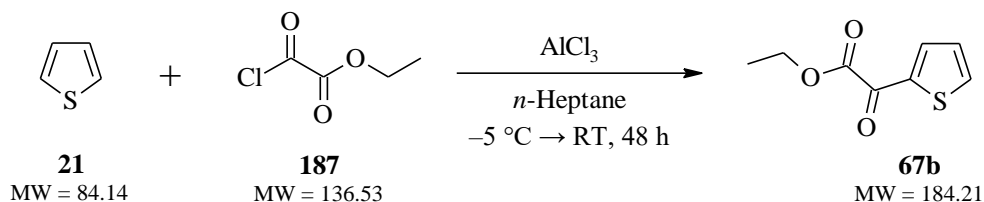
**10a**: Yellow solid (0.15 g, yield 35%). Melting point 295 °C (lit. 298 °C)[54].

$^1$H NMR (300 MHz, CDCl$_3$, ppm): $\delta$ = 7.80 (d, *J* = 7.0 Hz, 4H), 7.59–7.47 (m, 6H), 6.91 (s, 2H).

Anal. calcd. for $C_{22}H_{12}O_4$: C 77.64%, H 3.55%; Found: C 77.46%, H 3.51%.

### 5.5.1.2 Dithienyl-BDF derivative (10b)

**Preparation of ethyl oxo(thiophen-2-yl)acetate (67b)**



**Scheme 95**: *Preparation of ethyl oxo(thiophen-2-yl)acetate (67b)*

**21** (11.0 g, 130.73 mmol) was stirred in *n*-heptane (150 mL) under argon atmosphere, and the reaction mixture was cooled to –5 °C. Then, 1.20 equiv. of aluminium chloride (20.9 g, 156.75 mmol) was added in one portion and the mixture was stirred at –5 °C for 15 min. After that, 1.10 equiv. of **187** (16.0 mL/19.6 g, 143.56 mmol) was added dropwise (for 30 min) to

the reaction mixture, which was then spontaneously heated to RT and stirred for 48 h. The reaction mixture was then poured into distilled water with crushed ice (400 mL), acidified by the addition of 2M HCl (30 mL) and stirred for 30 min. After that, the reaction mixture was extracted with toluene (6×150 mL), the collected organic phases were washed with saturated NaHCO$_3$ solution (3×250 mL), followed by distilled water (2×250 mL), finally with brine (300 mL), then dried over anhydrous Na$_2$SO$_4$ and filtered through filter aid (Celite). After removal of the solvent under vacuum, the obtained crude mixture was purified by silica gel chromatography eluting with $n$-heptane/ethyl acetate 5:2 (v/v) to get pure product **67b** ($R_F$ = 0.45, eluent: $n$-heptane/ethyl acetate 5:2).
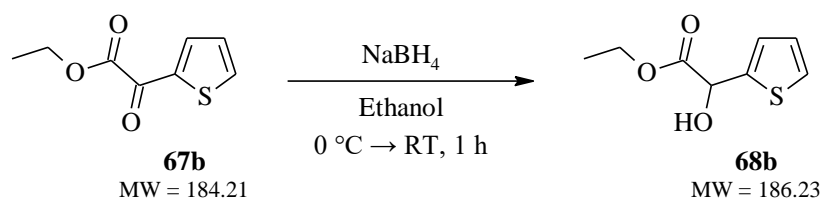
**67b**: Pale yellow oily material (8.91 g, yield 37%).

Refractive index: $n20/D$ = 1.551 (lit. 1.5505)[182].

Density: $\rho_{25}$ = 1.25 g cm$^{-3}$ (lit. 1.25 g cm$^{-3}$)[182].

$^1$H NMR (300 MHz, CDCl$_3$, ppm): $\delta$ = 8.13 (d, $J$ = 4.7 Hz, 1H), 7.82 (d, $J$ = 4.8 Hz, 1H), 7.25–7.20 (m, 1H), 4.39 (q, $J$ = 7.1 Hz, 2H), 1.40 (t, $J$ = 7.2 Hz, 3H).

### Preparation of ethyl hydroxy(thiophen-2-yl)acetate (68b)



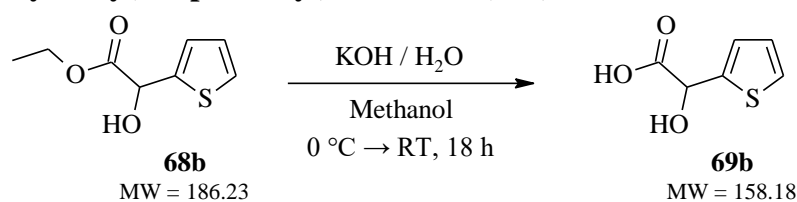**Scheme 96**: *Preparation of ethyl hydroxy(thiophen-2-yl)acetate (68b)*

**67b** (8.50 g, 46.14 mmol) was stirred in ethanol (90 mL) under argon atmosphere, and the reaction mixture was cooled to 0 °C. Then, 0.50 equiv. of NaBH$_4$ (0.87 g, 23.00 mmol) was added portion-wise to the reaction mixture, it was stirred at 0 °C for an additional 15 min, and then the mixture was spontaneously warmed to RT and stirred for 45 min. Ethanol was then removed from the reaction mixture by a rotary evaporator to obtain a solid material, which was dissolved in diethyl ether (150 mL) and washed with distilled water (3×250 mL), finally with brine (300 mL), then dried over anhydrous Na$_2$SO$_4$ and filtered through filter aid (Celite). After removal of the solvent under vacuum, the obtained crude mixture was purified by silica gel chromatography eluting with DCM to get pure product **68b** ($R_F$ = 0.25, eluent: DCM).

**68b**: Yellow oily material (6.10 g, yield 71%).

$^1$H NMR (300 MHz, CDCl$_3$, ppm): $\delta$ = 7.28 (dd, $J$ = 5.0; 1.3 Hz, 1H), 7.10 (dt, $J$ = 3.6; 1.4 Hz, 1H), 7.00 (dd, $J$ = 5.1; 4.2 Hz, 1H), 5.40 (s, 1H), 4.34–4.24 (m, 2H), 3.30 (d, $J$ = 5.9 Hz, 1H), 1.29 (t, $J$ = 7.3 Hz, 3H).

## Preparation of hydroxy(thiophen-2-yl)acetic acid (69b)



*Scheme 97: Preparation of hydroxy(thiophen-2-yl)acetic acid (**69b**)*

**68b** (6.0 g, 32.22 mmol) was stirred in methanol (90 mL) at 0 °C and ~5 equiv. of potassium hydroxide (9.04 g, 161.12 mmol) dissolved in distilled water (10 mL) was added dropwise. The reaction mixture was then spontaneously warmed to RT and stirred for 18 h. The solvent was distilled off from the reaction mixture and the solid material as a distillation residue was suspended in distilled water (90 mL). This mixture was acidified by the addition of 35% HCl (until pH ~2) and then washed with ethyl acetate (4×60 mL). The collected organic phases were washed with saturated NaHCO$_3$ solution (3×250 mL), followed by distilled water (2×300 mL), finally with brine (300 mL), then dried over anhydrous Na$_2$SO$_4$ and filtered through filter aid (Celite). After removal of the solvent under vacuum, product **69b** was obtained and used to the next reaction step without further purification.

**69b**: Yellow-beige oily material (3.06 g, yield 60%).

$^1$H NMR (300 MHz, CDCl$_3$, ppm): $\delta$ = 7.33 (m, 1H), 7.18 (m, 1H), 7.02 (m, 1H), 5.51 (s, 1H).

## Preparation of 3,7-di(2-thienyl)benzo[1,2-*b*:4,5-*b'*]difuran-2,6-dione (10b)
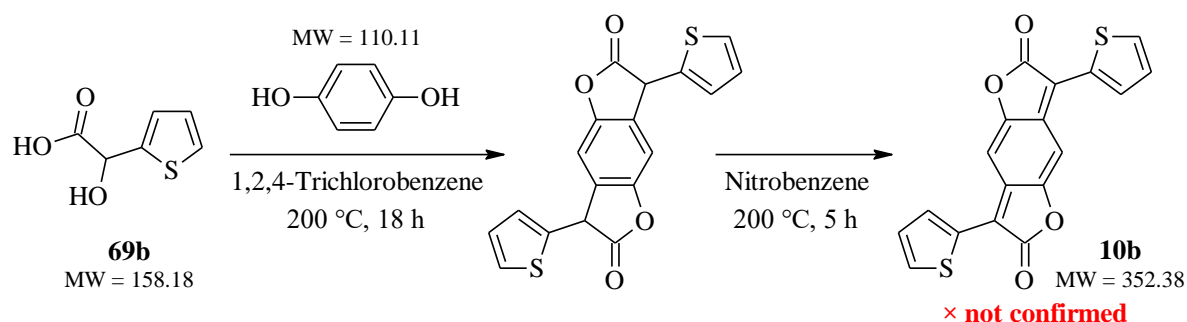


*Scheme 98: Preparation of 3,7-di(2-thienyl)benzo[1,2-b:4,5-b']difuran-2,6-dione (**10b**)*

The same procedure as for the **10a** (*Chapter 5.5.1.1* – **approach A**) was used to prepare the **10b**, starting with **69b** (1 equiv., 0.55 g, 3.48 mmol) and hydroquinone (0.5 equiv., 0.19 g, 1.73 mmol). The reaction time of stirring at 200 °C was extended by 2 h to a total of 18 h, and in particular, the oxidation in nitrobenzene (1.3 equiv., 0.46 mL/0.55 g, 4.47 mmol) was extended by 4 h to a total of 5 h. Work-up of the reaction mixture was identical to the above experiment. However, the obtained solid was almost insoluble in common solvents, so that it was washed with methanol (4×20 mL) and acetone (3×20 mL) on a filter cake. After that, the solid from the filter cake was suspended in toluene (10 mL), stirred at reflux for 1 h and then filtered off, washed with toluene (10 mL) and dried under vacuum at 60 °C for 18 h. Further purification was no longer possible.

**10b**: Dark blue-black solid (0.18 g, yield 29%). Melting point >320 °C.

^{1}H NMR (500 MHz, DMSO-d6 – while hot, ppm): *Not confirmed.*

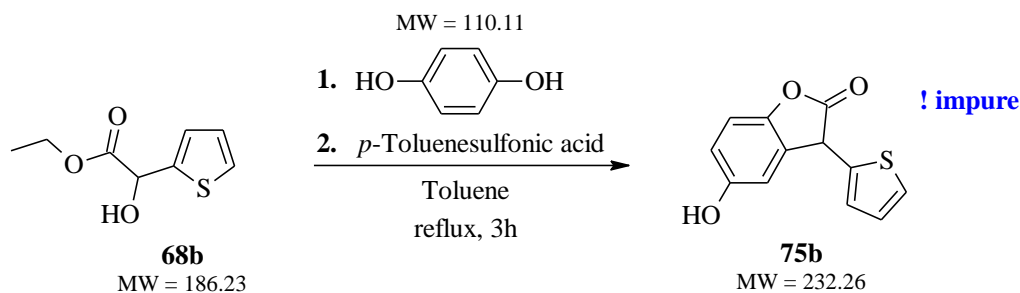## Preparation of 5-hydroxy-3-(2-thienyl)-1-benzofuran-2(3*H*)-one (75b) – approach A
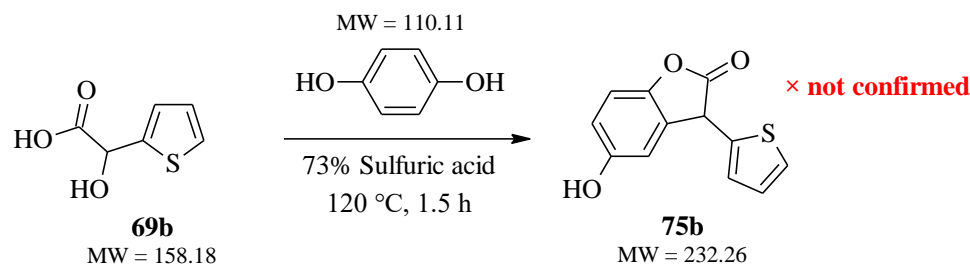


*Scheme 99: Preparation of 5-hydroxy-3-(2-thienyl)-1-benzofuran-2(3H)-one (75b) – approach A*

The same procedure as for the **75a** (*Chapter 5.5.1.1*) was used to prepare the **75b**, starting with **69b** (1 equiv., 0.10 g, 0.63 mmol) and hydroquinone (2.5 equiv., 0.17 g, 1.55 mmol). The reaction time of stirring at 120 °C was extended by 30 min to a total of 1.5 h. Work-up of the reaction mixture was identical to the above experiment. However, the obtained solid was almost insoluble in common solvents, so that further purification and analysis were no longer possible.

**75b**: Dark violet-black solid (0.03 g, yield 21%).

^{1}H NMR (500 MHz, DMSO-d6 – while hot, ppm): *Not confirmed.*

## Preparation of 5-hydroxy-3-(2-thienyl)-1-benzofuran-2(3*H*)-one (75b) – approach B



*Scheme 100: Preparation of 5-hydroxy-3-(2-thienyl)-1-benzofuran-2(3H)-one (75b) – approach B*

**68b** (0.100 g, 0.537 mmol) and hydroquinone (3.0 equiv., 0.177 g, 1.607 mmol) were stirred in toluene (4 mL) at reflux for 40 min in an apparatus equipped with a Dean-Stark trap. After that, *p*-toluenesulfonic acid monohydrate (0.1 equiv., 0.010 g, 0.054 mmol) was added in one portion, and the mixture was stirred at reflux for an additional 3 h. The reaction mixture was then cooled to RT, poured into petroleum ether (25 mL) and the formed precipitate was filtered off, washed with petroleum ether (10 mL) and dried in air. The obtained solid was then purified by silica gel chromatography eluting with chloroform/ethyl acetate 9:1 (v/v) to get product **V/20** ($R_F$ = 0.65, eluent: chloroform/ethyl acetate 9:1).

**75b**: Dark green solid (0.023 g, yield 18%). Melting point 125–130 °C.

$^1$H NMR (500 MHz, CDCl₃, ppm): δ = 7.30 (dd, $J$ = 5.0; 1.3 Hz, 1H), 7.05–7.03 (m, 2H), 7.03–7.01 (m, 2H), 6.87 (dd, $J$ = 2.9; 1.2 Hz, 1H), 6.85 (dd, $J$ = 2.6; 1.0 Hz, 0.5H), 6.83 (dd, $J$ = 2.5; 1.0 Hz, 0.5H), 4.92 (d, $J$ = 0.9 Hz, 1H).

### 5.5.1.3  Bis(5-bromo-4-dodecyl-2-thienyl)-BDF derivative (78c)

**Preparation of ethyl (5-bromo-4-dodecyl-2-thienyl)(oxo)acetate (67c)**
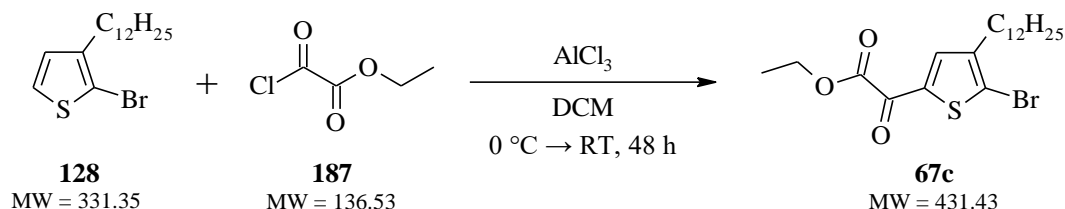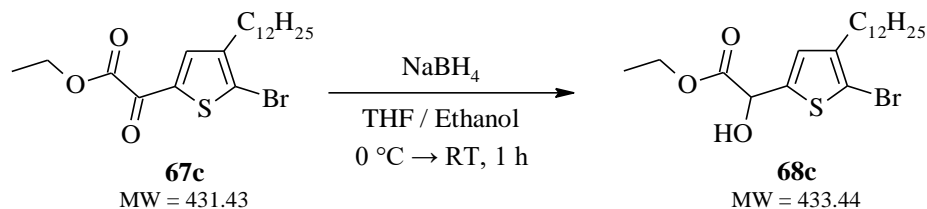


*Scheme 101: Preparation of ethyl (5-bromo-4-dodecyl-2-thienyl)(oxo)acetate (**67c**)*

The same procedure as for the **67b** (*Chapter 5.5.1.2*) was used to prepare the **67c**, starting with **128** (1 equiv., 20.0 g, 60.36 mmol) and using DCM as the solvent instead of *n*-heptane. Work-up of the reaction mixture was identical to the above experiment. The obtained crude mixture was purified by silica gel chromatography eluting with *n*-heptane/toluene 1:1 (v/v) to get pure product **67c** ($R_F$ = 0.63, eluent: *n*-heptane/toluene 1:1).

**67c**: Pale orange solid (9.11 g, yield 35%).

$^1$H NMR (300 MHz, CDCl₃, ppm): δ = 7.82 (s, 1H), 4.43 (q, $J$ = 7.1 Hz, 2H), 2.59 (t, $J$ = 7.4 Hz, 2H), 1.44 (t, $J$ = 7.1 Hz, 3H), 1.37–1.23 (m, 20H), 0.89 (t, $J$ = 6.2 Hz, 3H).

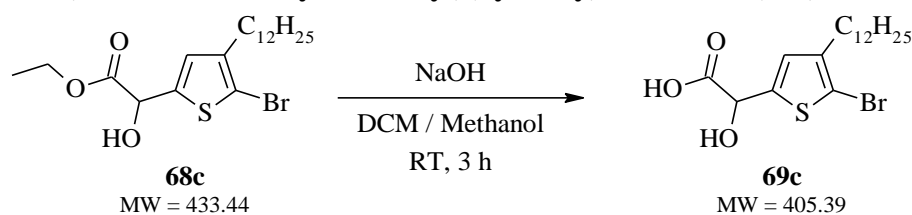**Preparation of ethyl (5-bromo-4-methyl-2-thienyl)(hydroxy)acetate (68c)**



*Scheme 102: Preparation of ethyl (5-bromo-4-methyl-2-thienyl)(hydroxy)acetate (**68c**)*

The same procedure as for the **68b** (*Chapter 5.5.1.2*) was used to prepare the **68c**, starting with **67c** (1 equiv., 2.00 g, 4.64 mmol) and using a mixture of THF and ethanol (35/25 mL) as the solvent instead of pure ethanol. Work-up of the reaction mixture was identical to the above experiment. The obtained crude mixture was purified by silica gel chromatography eluting with DCM to get pure product **68c** ($R_F$ = 0.65, eluent: DCM).

**68c**: Pale yellow oily material (1.47 g, yield 73%).

$^1$H NMR (500 MHz, CDCl₃, ppm): δ = 6.80 (s, 1H), 5.25 (d, $J$ = 6.2 Hz, 1H), 4.30 (qd, $J$ = 7.1, 5.6 Hz, 2H), 3.42 (d, $J$ = 6.3 Hz, 1H), 2.53–2.47 (m, 2H), 1.35–1.24 (m, 23H), 0.88 (t, $J$ = 6.9 Hz, 3H).

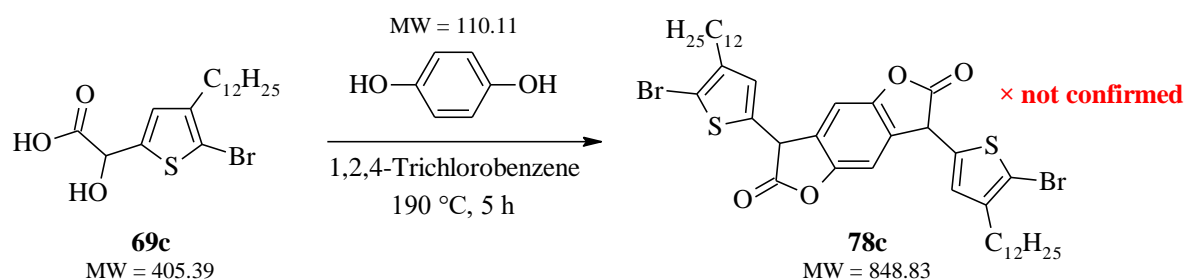**Preparation of (5-bromo-4-methyl-2-thienyl)(hydroxy)acetic acid (69c)**



*Scheme 103: Preparation of (5-bromo-4-methyl-2-thienyl)(hydroxy)acetic acid (69c)*

**68c** (1.40 g, 3.23 mmol) was stirred in a mixture of DCM (45 mL) and methanol (5 mL) at RT and ~1.5 equiv. of sodium hydroxide (0.20 g, 5.00 mmol) dissolved in methanol (2.5 mL) was added dropwise. The reaction mixture was stirred at RT for 3 h. The solvent was distilled off from the reaction mixture and the solid material as a distillation residue was dissolved in diethyl ether (100 mL). Water (400 mL) acidified by the addition of 35% HCl (until pH ~2) was added to this mixture, and it was stirred at RT for 10 min. The layers were then separated, the aqueous phase was washed with diethyl ether (3×40 mL), and the collected organic phases were washed with saturated NaHCO₃ solution (300 mL), followed by distilled water (2×300 mL), finally with brine (300 mL), then dried over anhydrous Na₂SO₄ and filtered through filter aid (Celite). After removal of the solvent under vacuum, product **69c** was obtained and used to the next reaction step without further purification.

**69c**: Pale yellowish oily material (1.17 g, yield 89%).

$^1$H NMR (500 MHz, CDCl₃, ppm): $\delta$ = 6.86 (s, 1H), 5.36 (s, 1H), 4.12 (q, $J$ = 7.1 Hz, 2H), 2.50 (t, $J$ = 4.0 Hz, 2H), 1.57–1.52 (m, 3H), 1.37–1.22 (m, 22H), 0.88 (t, $J$ = 6.9 Hz, 3H).


**Preparation of 3,7-bis(5-bromo-4-dodecyl-2-thienyl)-3,7-dihydro-BDF (78c)**



*Scheme 104: Preparation of 3,7-bis(5-bromo-4-dodecyl-2-thienyl)-3,7-dihydro-BDF (78c)*

**69c** (0.44 g, 1.085 mmol) and hydroquinone (0.5 equiv., 0.06 g, 0.545 mmol) were dissolved in 1,2,4-trichlorobenzene (1.5 mL) and stirred at 190 °C for 5 h in an apparatus equipped with a Dean-Stark trap. After that, the reaction mixture was cooled to RT and poured into methanol (80 mL). The formed precipitate was filtered off, washed with methanol (30 mL) and obtained solid on the filter cake was suspended in methanol (30 mL), refluxed for 20 min and then filtered off while hot and dried in air. The obtained crude material was finally purified by crystallisation in toluene (2 mL) with the addition of methanol (2 mL) to get product **78c**.
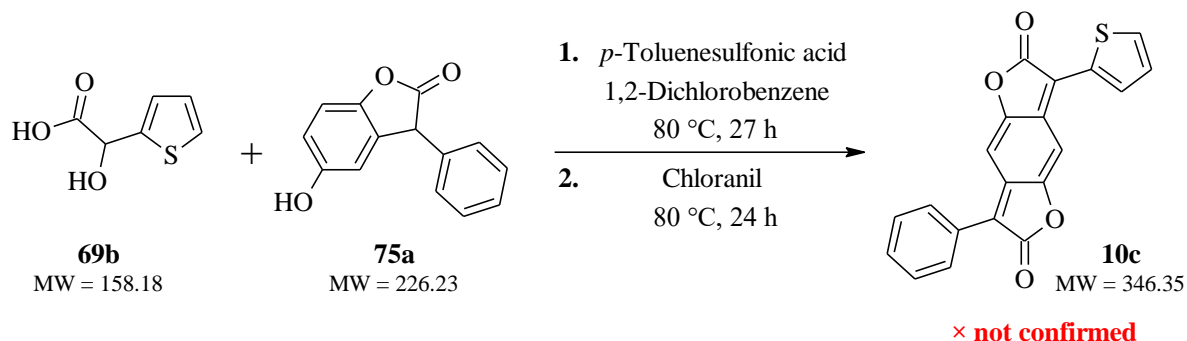
**78c**: Dark blue-black solid (0.13 g, yield 28%). Melting point >320 °C.

$^1$H NMR (500 MHz, CDCl₃, ppm): *Not confirmed*.

### 5.5.2  Synthesis of asymmetrical BDF derivatives

#### 5.5.2.1  *Phenyl-thienyl-BDF derivative (10c)*

**Preparation of 3-phenyl-7-(2-thienyl)benzo[1,2-*b*:4,5-*b′*]difuran-2,6-dione (10c)**



*Scheme 105: Preparation of 3-phenyl-7-(2-thienyl)benzo[1,2-b:4,5-b']difuran-2,6-dione (10c)*

**69b** (0.35 g, 2.21 mmol), half-condensed intermediate **75a** (1.0 equiv., 0.50 g, 2.21 mmol) and *p*-toluenesulfonic acid monohydrate (1.1 equiv., 0.46 g, 2.42 mmol) were stirred in 1,2-dichlorobenzene (6 mL) at 80 °C for 27 h. The reaction mixture was then cooled to 40 °C, chloranil (1.3 equiv., 0.70 g, 2.85 mmol) was added, and the mixture was heated to 80 °C and stirred for additional 24 h. After that, the solvent was distilled off from the reaction mixture by vacuum distillation; the solid material was dissolved in a small amount of hot chloroform (5 mL) and slowly added to vigorously stirred methanol (50 mL). The formed precipitate was filtered off and washed with methanol (20 mL). The obtained solid on the filter cake was suspended in methanol (80 mL), refluxed for 30 min and then filtered off while hot and dried in air. The obtained crude material was finally suspended in toluene (10 mL), stirred at reflux for 2 h, and after cooling to RT, it was filtered off and washed with toluene (2×10 mL) to get product **10c**.

**10c**: Dark violet-black solid (0.11 g, yield 14%). Melting point >320 °C.

^{1}H NMR (500 MHz, CDCl3, ppm): *Not confirmed*.

#### 5.5.2.2  *Phenyl-(5-bromo-4-dodecyl-2-thienyl)-BDF derivative (10d)*

**Preparation of 3-phenyl-7-(5-bromo-4-dodecyl-2-thienyl)benzo[1,2-*b*:4,5-*b′*]difuran-2,6-dione (10d)**
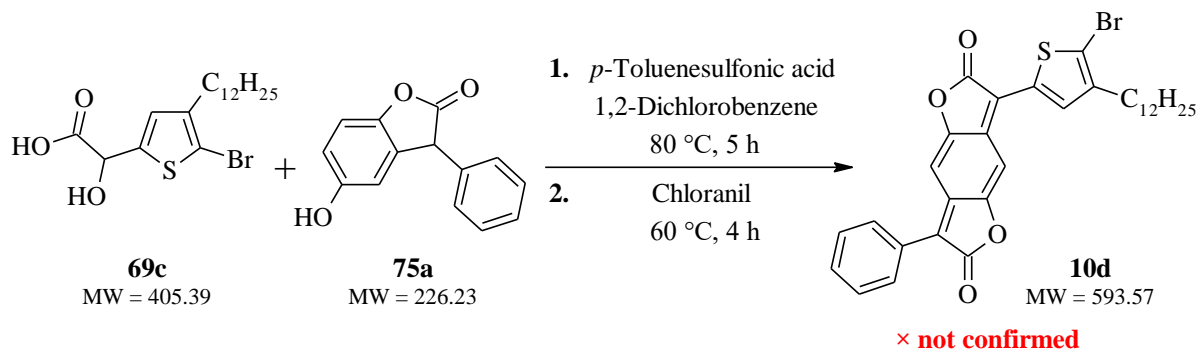


*Scheme 106: Preparation of 3-phenyl-7-(5-bromo-4-dodecyl-2-thienyl)benzo[1,2-b:4,5-b']difuran-2,6-dione (10d)*

The same procedure as for the **10c** (*Chapter 5.5.2.1*) was used to prepare the **10d**, starting with **69c** (1 equiv., 0.09 g, 0.22 mmol). The reaction time of stirring at 80 °C was reduced to 5 h, and the oxidation with chloranil was carried out at a lower temperature (60 °C) and in a shortened time (4 h). Work-up of the reaction mixture was identical to the above experiment. The crude material was suspended in methanol (50 mL), refluxed for 20 min and then filtered off while hot. This process was repeated once again. After drying in vacuum at RT, product **10d** was obtained.
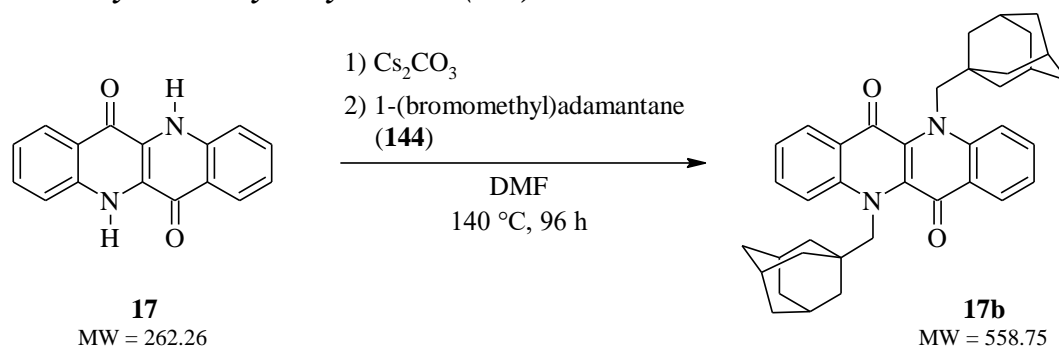
**10d**: Dark violet-black solid (0.045 g, yield 34%).

$^1$H NMR (500 MHz, CDCl$_3$, ppm): *Not confirmed*.


## 5.6　EP derivatives

### 5.6.1　Synthesis of *N*-alkylated EPs

#### 5.6.1.1　*Methyladamantyl-alkylated EP (17b)*



*Scheme 107: Preparation of N,N'-methyladamantyl-epindolidione (17b)*

**17** (0.485 g, 1.85 mmol) and caesium carbonate (6 equiv., 3.615 g, 11.10 mmol) were stirred at 140 °C for 40 min in anhydrous DMF (15 mL) and under argon atmosphere. Then, 4 equiv. of **144** (1.695 g, 7.40 mmol) was added in one portion, and the reaction mixture was stirred at 140 °C for 96 h. After that, DMF was distilled off by vacuum distillation and the solid material as a distillation residue was suspended in distilled water (30 mL), filtered off and washed with methanol (2×15 mL). The solid from the filter cake was then dissolved in chloroform (400 mL) and washed with distilled water (2×500 mL) and brine (500 mL), dried over anhydrous Na$_2$SO$_4$ and filtered through filter aid (Celite). After removal of the solvent under vacuum, the obtained crude mixture was purified by silica gel chromatography eluting with DCM/petroleum ether 3:1 (v/v) → DCM followed by precipitation in refluxing isopropyl alcohol (8 mL) to get pure product **17b** ($R_F$ = 0.45, eluent: DCM/petroleum ether 3:1).

**17b**: Intense yellow crystals (25.4 mg, yield 2.5%). Melting point >340 °C.

$^1$H NMR (500 MHz, CDCl$_3$, ppm): $\delta$ = 8.32 (d, *J* = 7.7 Hz, 2H), 7.84 (d, *J* = 8.8 Hz, 2H), 7.65 (ddd, *J* = 8.7; 6.9; 1.7 Hz, 2H), 7.32–7.27 (m, 2H), 5.78 (d, *J* = 15.4 Hz, 2H), 4.27 (d, *J* = 15.4 Hz, 2H), 1.66 (s, 4H), 1.57–1.50 (m, 2H), 1.45 (d, *J* = 12.2 Hz, 6H), 1.33 (d, *J* = 12.2 Hz, 6H), 1.17 (d, *J* = 12.3 Hz, 6H), 1.06 (d, *J* = 12.3 Hz, 6H).

Anal. calcd. for C$_{38}$H$_{42}$N$_2$O$_2$: C 81.68%, H 7.58%, N 5.01%; Found: C 81.92%, H 7.63%, N 4.88%.

## 5.6.1.2  Ethyladamantyl-alkylated EP (17a)
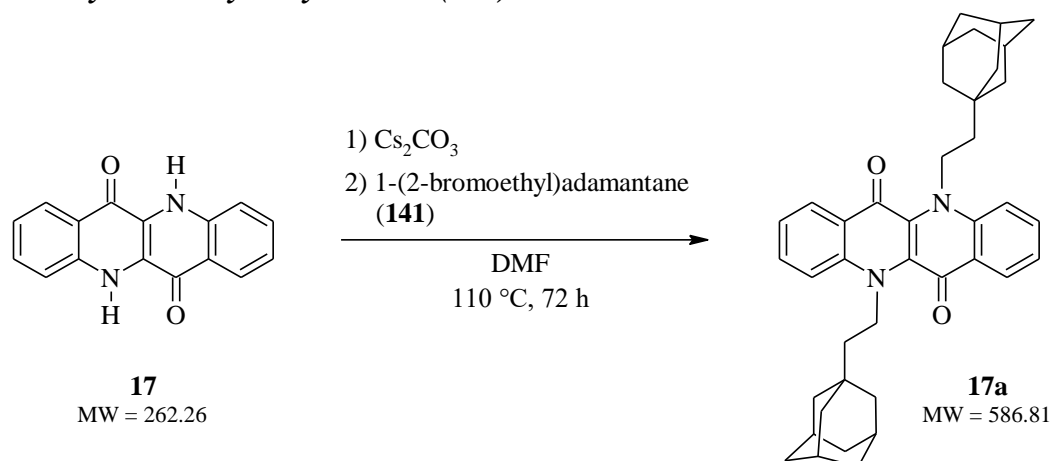


**Scheme 108**: *Preparation of N,N'-ethyladamantyl-epindolidione (17a)*

The same procedure as for the **17b** (*Chapter 5.6.1.1*) was used to prepare the **17a**, starting with **17** (1 equiv., 0.50 g, 1.91 mmol). The reaction was carried out at a lower temperature (110 °C) and in a shortened time (72 h) compared to the above experiment. Work-up of the reaction mixture was identical to the above experiment. The obtained crude mixture was purified by silica gel chromatography eluting with petroleum ether/DCM 3:2 (v/v) → DCM followed by precipitation in refluxing ethanol (8 mL) to get pure product **17a** ($R_F$ = 0.42, eluent: petroleum ether/DCM 3:2).

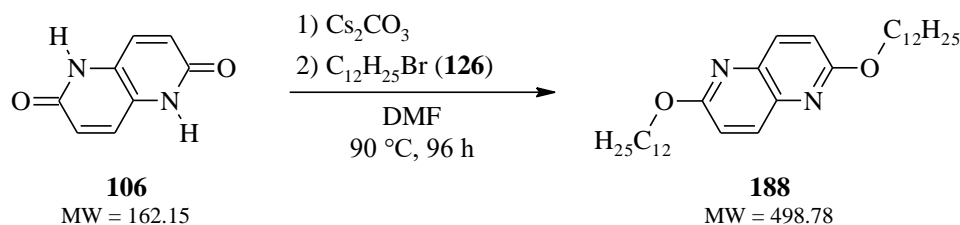**17a**: Bright yellow crystals (40.2 mg, yield 3.6%). Melting point 341 °C.

$^1$H NMR (500 MHz, CDCl$_3$, ppm): $\delta$ = 8.44 (d, *J* = 8.1 Hz, 2H), 7.72 (d, *J* = 2.9 Hz, 4H), 7.30 (dt, *J* = 7.9; 3.9 Hz, 2H), 5.02–4.95 (m, 4H), 2.02–1.97 (m, 6H), 1.76–1.62 (m, 24H), 1.57–1.50 (m, 4H).

Anal. calcd. for C$_{40}$H$_{46}$N$_2$O$_2$: C 81.87%, H 7.90%, N 4.77%; Found: C 81.98%, H 7.84%, N 4.59%.


## 5.7  NTD derivatives

### 5.7.1  Synthesis of *N*- and *O*-alkylated NTDs

#### 5.7.1.1  Synthesis of O,O'-dodecyl-NTD (188)



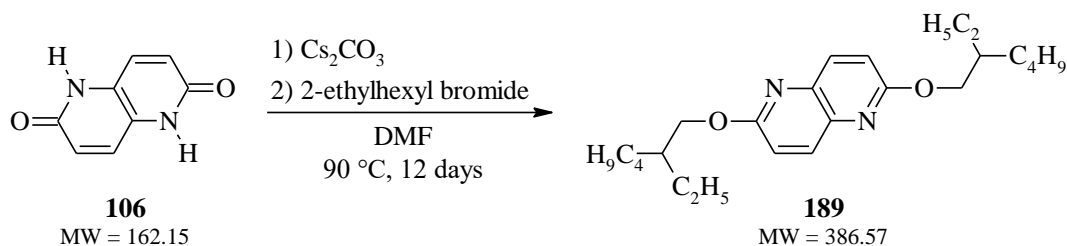**Scheme 109**: *Preparation of O,O'-dodecyl-NTD (188)*

**106** (0.054 g, 0.333 mmol) and caesium carbonate (2.50 equiv., 0.271 g, 0.833 mmol) were stirred at 80 °C for 3 h in anhydrous DMF (35 mL) and under argon atmosphere. Then, 5.75 equiv. of 1-bromododecane (**126**, 0.46 mL/0.477 g, 1.915 mmol) dissolved in anhydrous

DMF (10 mL) was added dropwise to the reaction mixture and it was stirred at 90 °C for 96 h. After that, the reaction mixture was poured into saturated $NH_4Cl$ solution (25 mL), and the formed precipitate was filtered off and washed with distilled water (3×20 mL) to remove unreacted caesium carbonate and residual DMF. The filter cake was then washed with ethyl acetate (3×50 mL) to dissolve the product. The organic filtrate was washed with distilled water (2×500 mL) and brine (500 mL), dried over anhydrous $Na_2SO_4$ and filtered through filter aid (Celite). After removal of the solvent under vacuum, the obtained crude mixture was purified by silica gel chromatography eluting with *n*-heptane/ethyl acetate 5:1 (v/v) followed by precipitation in a mixture of isopropyl alcohol/petroleum ether (4/1 mL) to get pure product **188** ($R_F$ = 0.88, eluent: *n*-heptane/ethyl acetate 5:1).

**188**: White solid (0.043 g, yield 26%). Melting point 75 °C (lit. 76–78 °C)[164].

$^1$H NMR (500 MHz, CDCl$_3$, ppm): $\delta$ = 7.95 (d, $J$ = 8.9 Hz, 2H), 7.00 (d, $J$ = 8.9 Hz, 2H), 4.40 (t, $J$ = 6.7 Hz, 4H), 1.81 (p, $J$ = 6.9 Hz, 4H), 1.53–1.43 (m, 4H), 1.42–1.25 (m, 32H), 0.88 (t, $J$ = 6.9 Hz, 6H).

### 5.7.1.2 Synthesis of O,O'-(2-ethylhexyl)-NTD (189)



**106**
MW = 162.15

1) $Cs_2CO_3$
2) 2-ethylhexyl bromide
DMF
90 °C, 12 days

**189**
MW = 386.57

*Scheme 110: Preparation of O,O'-(2-ethylhexyl)-NTD (189)*

The same procedure as for the **188** (*Chapter 5.7.1.1*) was used to prepare the **189**, starting with **106** (1 equiv., 0.055 g, 0.339 mmol). The reaction time of stirring at 90 °C was extended by 8 days to a total of 12 days. Work-up of the reaction mixture and subsequent purification of the crude product were performed as in the above experiment to get pure product **189** ($R_F$ = 0.40, eluent: *n*-heptane/ethyl acetate 5:1).

**189**: White solid (0.006 g, yield 4.6%). Melting point 58 °C.

$^1$H NMR (500 MHz, CDCl$_3$, ppm): $\delta$ = 7.94 (d, $J$ = 8.8 Hz, 2H), 7.00 (d, $J$ = 8.7 Hz, 2H), 4.36 (t, $J$ = 6.8 Hz, 4H), 1.89–1.86 (m, 2H), 1.56–1.32 (m, 16H), 0.94–0.84 (m, 12H).

### 5.7.1.3 Synthesis of O,O'-ethyladamantyl-NTD (190)
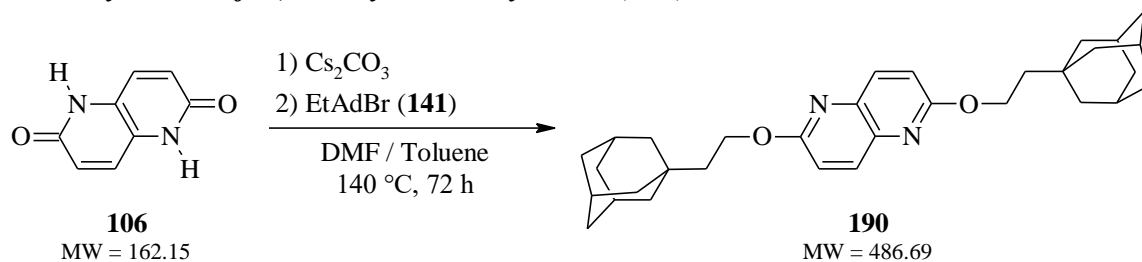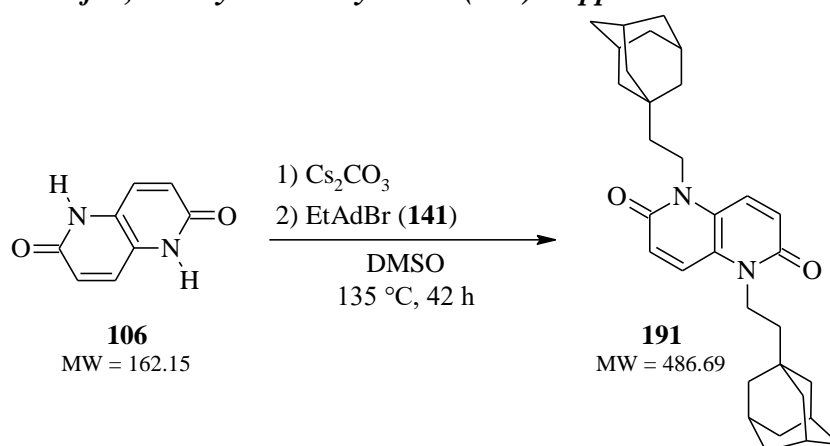


Scheme 111: Preparation of O,O'-ethyladamantyl-NTD (190)

106 (0.507 g, 2.97 mmol) and caesium carbonate (6 equiv., 5.807 g, 17.82 mmol) were stirred at 140 °C for 1 h in a mixture of anhydrous DMF (170 mL) and dried toluene (20 mL) under argon atmosphere. Then, 4 equiv. of 141 (2.890 g, 11.88 mmol) was added in one portion to the reaction mixture, and it was stirred at 140 °C for 72 h. After that, the solvents were distilled off from the reaction mixture by vacuum distillation and the solid material as a distillation residue was suspended in distilled water (100 mL), filtered off and washed with methanol (2×15 mL). The solid from the filter cake was then suspended in methanol (150 mL) and filtered off. The obtained crude mixture was purified by crystallisation in isopropyl alcohol (10 mL) to get pure product 190 ($R_F$ = 0.20, eluent: $n$-heptane/ethyl acetate 1:1).

190: White crystals (1.04 g, yield 72%). Melting point 216–218 °C.

$^1$H NMR (500 MHz, CDCl$_3$, ppm): $\delta$ = 7.96 (d, $J$ = 8.9 Hz, 2H), 6.99 (d, $J$ = 8.9 Hz, 2H), 4.47 (t, $J$ = 7.4 Hz, 4H), 1.98 (p, $J$ = 3.0 Hz, 6H), 1.73 (dt, $J$ = 12.5; 3.0 Hz, 6H), 1.68 (t, $J$ = 2.2 Hz, 4H), 1.65–1.59 (m, 16H), 1.52 (d, $J$ = 15.3 Hz, 2H).

Anal. calcd. for C$_{32}$H$_{42}$N$_2$O$_2$: C 78.97%, H 8.70%, N 5.76%; Found: C 78.63%, H 8.64%, N 5.71%.

### 5.7.1.4 Synthesis of N,N'-ethyladamantyl-NTD (191) – approach A



Scheme 112: Preparation of N,N'-ethyladamantyl-NTD (191) – approach A

106 (0.205 g, 1.26 mmol) and caesium carbonate (5.0 equiv., 2.060 g, 6.32 mmol) were stirred at RT for 4 h in anhydrous DMSO (140 mL) and under argon atmosphere. Then, 4.0 equiv. of 141 (1.23 g, 5.06 mmol) was added in one portion to the reaction mixture and it was stirred at 135 °C for 42 h. After that, the reaction mixture was poured into distilled water

(250 mL), and the formed precipitate was filtered off and washed with distilled water (4×150 mL) to remove unreacted caesium carbonate and residual DMF. The filter cake was then washed with toluene (3×150 mL) to dissolve the product. The organic filtrate was washed with distilled water (2×500 mL) and brine (500 mL), dried over anhydrous $Na_2SO_4$ and filtered through filter aid (Celite). After removal of the solvent under vacuum, the obtained crude mixture was purified by silica gel chromatography eluting with *n*-heptane/ethyl acetate 1:1 (v/v) followed by crystallisation in isopropyl alcohol (15 mL) to get pure product **190** ($R_F$ = 0.20, eluent: *n*-heptane/ethyl acetate 1:1) as the solid on the filter cake and pure product **191** ($R_F$ = 0.20, eluent: *n*-heptane/ethyl acetate 1:1) as the oily material after removal of the solvent from the filtrate by rotary evaporator.

**191**: Yellow oily material (0.021 g, yield 3.4%).

$^1$H NMR (500 MHz, CDCl$_3$, ppm): $\delta$ = 7.52 (d, $J$ = 8.8 Hz, 2H), 6.84 (d, $J$ = 8.9 Hz, 2H), 4.27 (t, $J$ = 7.2 Hz, 4H), 2.02 (s, 6H), 1.78–1.67 (m, 16H), 1.54 (s, 4H), 1.44 (t, $J$ = 8.9 Hz, 6H), 1.26–1.20 (m, 2H).

**190**: White crystals (0.412 g, yield 67%). Melting point 215–216 °C.

$^1$H NMR (500 MHz, CDCl$_3$, ppm): $\delta$ = 7.96 (d, $J$ = 8.8 Hz, 2H), 6.99 (d, $J$ = 8.9 Hz, 2H), 4.47 (t, $J$ = 7.4 Hz, 4H), 2.00–1.95 (m, 6H), 1.76–1.66 (m, 10H), 1.62 (dd, $J$ = 9.1; 5.1 Hz, 16H), 1.55 (s, 2H).

### 5.7.1.5  Synthesis of N,N'-ethyladamantyl-NTD (191) – approach B
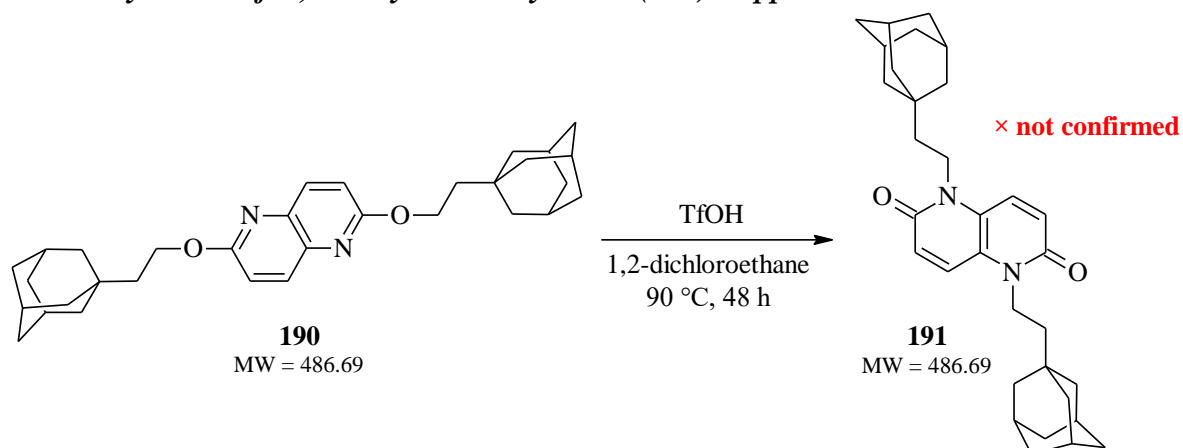


**Scheme 113**: Preparation of N,N'-ethyladamantyl-NTD (**191**) – approach B

**190** (0.114 g, 0.234 mmol) and triflic acid (**TfOH**, 0.2 equiv., 0.007 g, 0.047 mmol) were stirred at 90 °C for 48 h in anhydrous 1,2-dichloroethane (0.3 mL). After that, the solvent was distilled off from the reaction mixture by vacuum distillation and the solid material as a distillation residue was purified by silica gel chromatography eluting with *n*-heptane/ethyl acetate 1:1 (v/v) get product **191** ($R_F$ = 0.20, eluent: *n*-heptane/ethyl acetate 1:1).
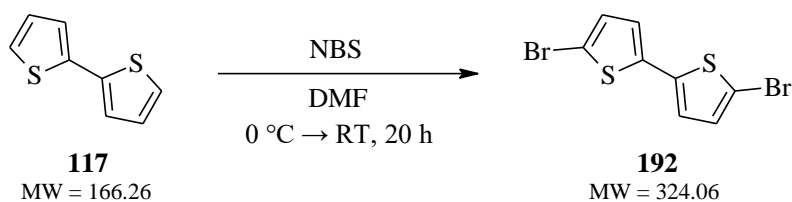
**191**: Slightly yellowish-white solid (0.104 g, yield 91%).

$^1$H NMR (500 MHz, CDCl$_3$, ppm): $\delta$ = 8.57 (d, $J$ = 8.6 Hz, 2H), 7.30 (d, $J$ = 9.3 Hz, 2H), 4.62 (s, 2H), 1.99 (p, $J$ = 3.2 Hz, 7H), 1.77–1.63 (m, 19H). *Not confirmed.*

## 5.8 Preparation of PT derivative

### 5.8.1 β,β'-didodecyl-α-sexithiophene-tetrafluorophenyl polymer (201)

#### 5.8.1.1 Synthesis of 5,5'-dibromo-2,2'-bithiophene (192)



**117**
MW = 166.26

**192**
MW = 324.06

*Scheme 114: Preparation of 5,5'-dibromo-2,2'-bithiophene (192)*

**117** (3.00 g, 18.04 mmol) was dissolved in anhydrous DMF (45 mL) under argon atmosphere; then the mixture was cooled to 0 °C and protected from light by aluminium foil. 2.1 equiv. of NBS (6.72 g, 37.76 mmol) was added piece by piece to the mixture and the temperature was spontaneously heated to RT and stirred for 20 h. The reaction mixture was then poured into distilled water with crushed ice (150 mL) and stirred for 30 min. After that, extraction was performed – the reaction mixture was washed with toluene (3×60 mL). The collected organic phases were washed with distilled water (3×150 mL), finally with brine (150 mL) and then dried over anhydrous Na₂SO₄ and filtered through filter aid (Celite). After removal of the solvent under vacuum, the obtained crude mixture was purified by crystallisation in *n*-heptane (50 mL) with the addition of chloroform (3 mL) to afford pure product **192** ($R_F$ = 0.67, eluent: *n*-heptane).

**192**: Pale yellow crystals (4.20 g, yield 72%). Melting point 143 °C (lit. 146.5 °C)[183].

¹H NMR (300 MHz, CDCl₃, ppm): $\delta$ = 6.96 (d, $J$ = 3.8 Hz, 2H), 6.85 (d, $J$ = 3.8 Hz, 2H).

GC-MS (method: *JJ_vseobecna met*): RT = 8.64 min; m/z = 323.89 (purity 95%).

#### 5.8.1.2 Synthesis of 2,2':5',2'':5'',2'''-quaterthiophene (194)



**192**
MW = 324.06

**156**
MW = 163.04

**193**
MW = 187.34

**194**
MW = 330.51
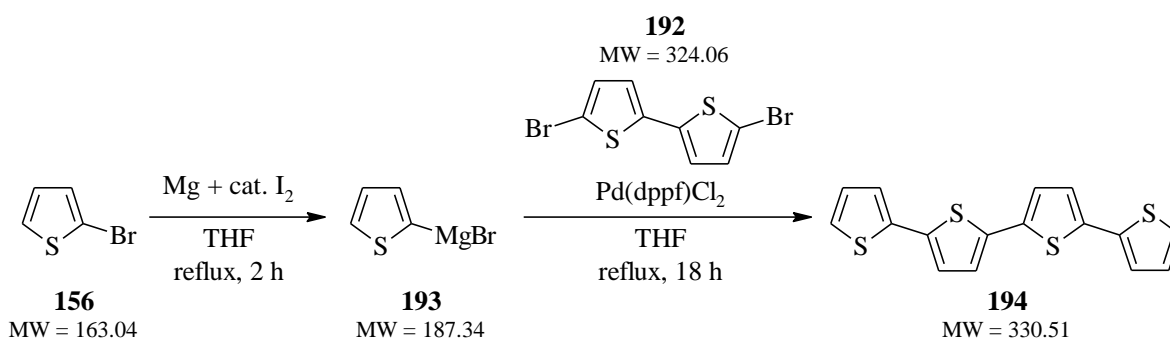
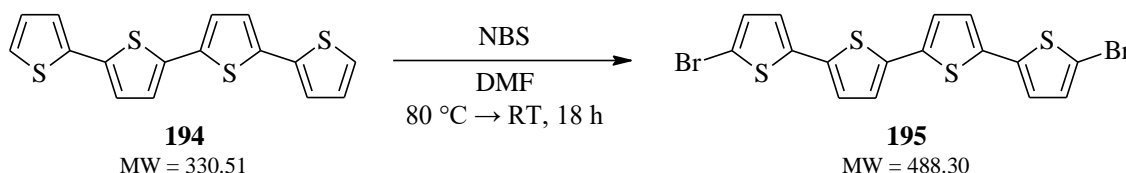*Scheme 115: Preparation of 2,2':5',2'':5'',2'''-quaterthiophene (194)*

Magnesium (1.2 equiv., 0.766 g, 31.53 mmol) was stirred in anhydrous THF (15 mL) with a catalytic amount of iodine under argon atmosphere. Then, **156** (1 equiv., 2.54 mL/4.284 g, 26.28 mmol) diluted in anhydrous THF (7 mL) was added dropwise to this mixture, and spontaneous foamy reflux and formation of the milky grey solution were observed. After 2 h of vigorous stirring at reflux, Grignard reagent **193** was prepared. The reaction mixture was

126

then cooled to RT and Pd(dppf)Cl$_2$ (36 mg, 0.049 mmol) was added as a catalyst. After that, 0.25 equiv. of **192** (2.129 g, 6.57 mmol) dissolved in anhydrous THF (20 mL) was added dropwise to the previous mixture and it was gradually heated to reflux and stirred for 18 h. The reaction mixture was then cooled to RT, poured into ethanol (180 mL) and the formed precipitate was filtered off. The solid from the filter cake was suspended in ethanol (200 mL) and filtered off again. After that, the solid was suspended in distilled water (250 mL) acidified by the addition of 35% HCl (2 mL) and stirred for 30 min. The orange precipitate was then filtered off, washed with distilled water (2×150 mL), finally with ethanol (150 mL) and dried under vacuum for 18 h to get product **194** ($R_F$ = 0.45, eluent: petroleum ether).

**194**: Orange-beige solid (1.90 g, yield 88%). Melting point 210–212 °C (lit. 212 °C)[184].

$^1$H NMR (300 MHz, CDCl$_3$, ppm): $\delta$ = 7.23 (dd, $J$ = 5.1; 1.4 Hz, 2H), 7.18 (dd, $J$ = 5.2; 1.6 Hz, 2H), 7.07 (d, $J$ = 5.4 Hz, 4H), 7.03–6.99 (m, 2H).

### 5.8.1.3  Synthesis of 5,5'''-dibromo-quaterthiophene (195)



Scheme 116: Preparation of 5,5'''-dibromo-quaterthiophene (195)

The same procedure as for the **192** (*Chapter 5.8.1.1*) was used to prepare the **195**, starting with **194** (1.0 equiv., 1.583 g, 4.79 mmol) and NBS (2.1 equiv., 1.755 g, 9.86 mmol). The reaction temperature was increased to 80 °C, and after 3 h of stirring at that temperature, the reaction mixture was stirred at RT for another 15 h. After that, the mixture was poured into distilled water with crushed ice (400 mL), and the formed precipitate was filtered off, washed with distilled water (2×150 mL), finally with ethanol (2×100 mL) and dried under vacuum for 18 h to get product **195** ($R_F$ = 0.40, eluent: *n*-heptane).

**195**: Orange solid (2.21 g, yield 94%). Melting point 261–267 °C (lit. 264 °C)[184].

$^1$H NMR (300 MHz, CDCl$_3$, ppm): $\delta$ = 7.09 (d, $J$ = 3.6 Hz, 2H), 7.02 (d, $J$ = 3.6 Hz, 2H), 7.01 (d, $J$ = 3.8 Hz, 2H), 6.92 (d, $J$ = 3.7 Hz, 2H).

### 5.8.1.4  Synthesis of trimethyl(3-dodecyl-2-thienyl)-stannane (196)
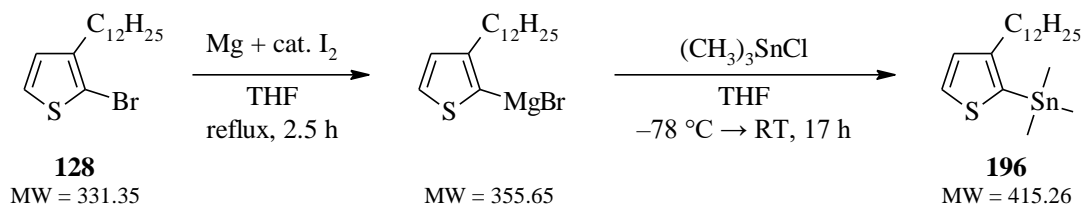


Scheme 117: Preparation of trimethyl(3-dodecyl-2-thienyl)-stannane (196)

The same procedure as for Grignard reagent **193** (*Chapter 5.8.1.2*) was used here to prepare the GR, starting with magnesium (1.15 equiv., 0.50 g, 20.57 mmol) and **128** (1.0 equiv.,

5.95 g, 17.96 mmol). After 2.5 h of vigorous stirring at reflux, the GR was prepared. Following that, the mixture was cooled to RT and slowly added dropwise (for 30 min) to the solution of trimethyltin chloride (1.1 equiv., 3.88 g, 19.47 mmol) in anhydrous THF (20 mL) cooled to –78 °C. The reaction mixture was stirred at –78 °C for 30 min, and then it was continuously warmed to RT and stirred for an additional 17 h. After that, the reaction mixture was poured into distilled water (150 mL) and extracted with $n$-heptane (4×50 mL). The collected organic phases were then washed with distilled water (3×150 mL), finally with brine (150 mL), dried over anhydrous $Na_2SO_4$ and filtered through filter aid (Celite). After removal of the solvent under vacuum, dried toluene (10 mL) was added to the concentrated product. It was carefully evaporated under vacuum (2 mbar) for 2 h (to minimalize water content) to get product **196** ($R_F$ = 0.80, eluent: $n$-heptane), which was used to the next reaction step without further purification and analysis.

**196**: Slightly brown-yellow liquid (6.42 g, yield 86%, purity ~55%).

### 5.8.1.5 Synthesis of β,β'-didodecylsexithiophene (197)
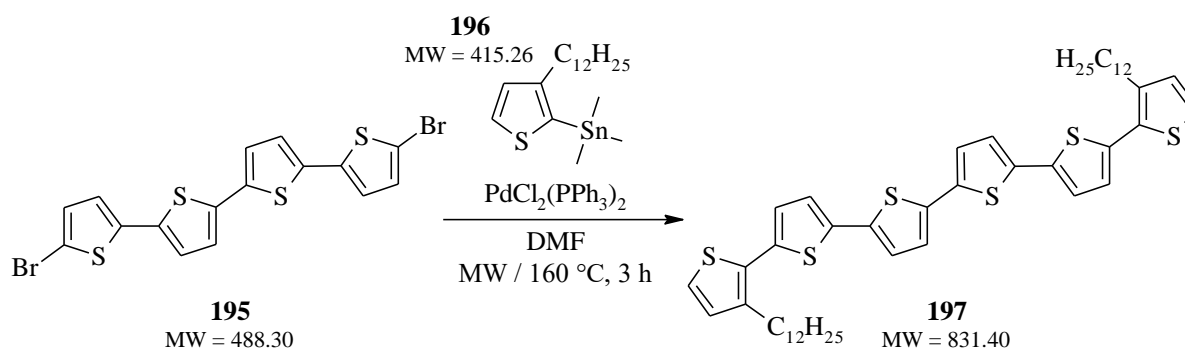


*Scheme 118: Preparation of β,β'-didodecylsexithiophene (**197**)*

**195**, ~4 equiv. of Stille intermediate **196** and a palladium$^{(II)}$ catalyst were stirred in anhydrous DMF under argon atmosphere in a microwave reactor. The reaction mixture was purged with argon for 15 min in an ultrasonic bath, and then it was transferred to a microwave oven, and the experiment was set to "**pulzy**" method. The reaction mixture was then poured into distilled water and extracted with DCM. The collected organic phases were then washed with distilled water, finally with brine, dried over anhydrous $Na_2SO_4$ and filtered through filter aid (Celite). After removal of the solvent under vacuum, the obtained crude mixture was purified by silica gel chromatography eluting with $n$-heptane → DCM to get pure product **197** ($R_F$ = 0.15, eluent: $n$-heptane). A summary of performed experiments is given in the following **Table 6**.

*Table 6*: *Summary of performed experiments for the preparation of derivative **197***

| Experiment | #1 | #2 | #3 |
|---|---|---|---|
| **195** (~95%) [g/mmol] | 0.075 / 0.146 | 0.075 / 0.146 | 0.282 / 0.549 |
| **196** (~55%) [g/mmol] | (4.14 equiv.) 0.251 / 0.604 | (4.08 equiv.) 0.247 / 0.595 | (3.99 equiv.) 0.909 / 2.189 |
| **Catalyst** [mg/mmol] | **PdCl₂(PPh₃)₂** (0.09 equiv.) 9.3 / 0.013 | **Pd(OAc)₂** (0.06 equiv.) 2.0 / 0.009 <br> **CuI** (0.23 equiv.) 6.4 / 0.034 <br> **PPh₃** (0.22 equiv.) 8.5 / 0.032 | **PdCl₂(PPh₃)₂** (0.09 equiv.) 36.2 / 0.052 |
| **Solvent used** [mL] | DMF 4.0 | DMF 4.0 | DMF 16.0 |
| **Temperature** [°C] | 90 → 110 → 90 (4x) / 90 → 160 → RT | 90 → 110 → 90 (4x) / 90 → 160 → RT | 90 → 110 → 90 (4x) / 90 → 160 → RT |
| **Overall time** [h] | 3 | 3 | 3 |
| **Yield [mg/%]** | **89.6 / 74.1** | – | **365.8 / 80.2** |

**197**: Intense orange solid (best #3: 0.366 g, yield 80.2%). Melting point 128–130 °C.

$^1$H NMR (500 MHz, CDCl₃, ppm): $\delta$ = 7.18 (d, *J* = 5.2 Hz, 2H), 7.12 (d, *J* = 3.7 Hz, 2H), 7.09 (s, 4H), 7.03 (d, *J* = 3.8 Hz, 2H), 6.94 (d, *J* = 5.3 Hz, 2H), 2.78 (t, *J* = 7.8 Hz, 4H), 1.65 (q, *J* = 7.7 Hz, 4H), 1.40–1.20 (m, 36H), 0.88 (t, *J* = 6.9 Hz, 6H).

$^{13}$C NMR (125 MHz, CDCl₃, ppm): $\delta$ = 139.97, 136.65, 136.14, 135.91, 135.55, 130.26, 130.10, 126.57, 124.34, 124.26, 123.96, 123.92, 31.93, 30.65, 29.70, 29.67, 29.60, 29.51, 29.45, 29.36, 29.27, 22.69, 14.10, 1.01.

### 5.8.1.6 Synthesis of α,α'-dibromo-β,β'-didodecylsexithiophene (198)
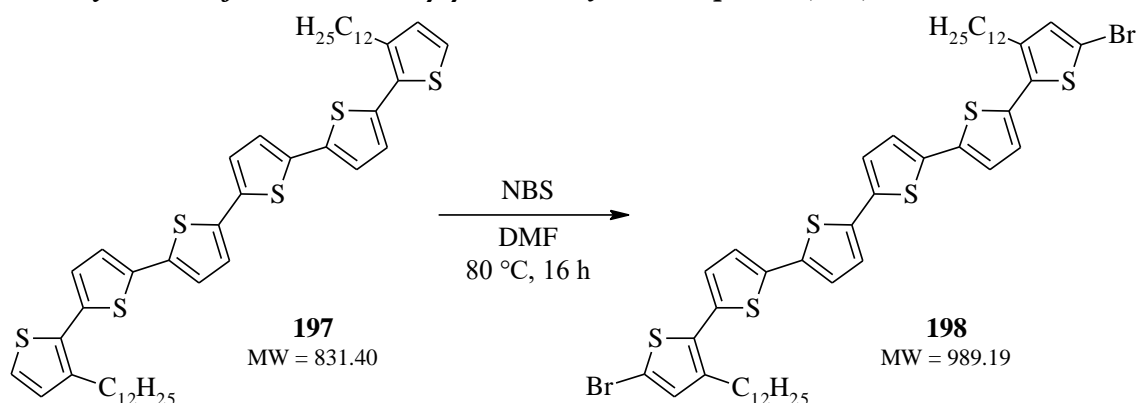


**Scheme 119**: *Preparation of α,α'-dibromo-β,β'-didodecylsexithiophene (198)*

The same procedure as for the **192** (*Chapter 5.8.1.1*) was used to prepare the **198**, starting with **197** (1.0 equiv., 0.206 g, 0.247 mmol) and NBS (2.7 equiv., 0.117 g, 0.657 mmol). The reaction mixture was stirred at 80 °C for 16 h. After that, the mixture was cooled to approx. 0 °C and the formed precipitate was rapidly filtered off, washed with distilled water (3×150 mL), finally with ethanol (2×100 mL) and dried under vacuum for 16 h to get product **198** ($R_F$ = 0.20, eluent: *n*-heptane).

**198**: Intense orange solid (0.149 g, yield 61%). Melting point 135–140 °C.

$^1$H NMR (500 MHz, CDCl$_3$, ppm): $\delta$ = 7.12–7.08 (m, 6H), 6.97 (d, $J$ = 3.9 Hz, 2H), 6.90 (s, 2H), 2.71 (t, $J$ = 7.8 Hz, 4H), 1.61 (q, $J$ = 7.5 Hz, 4H), 1.40–1.20 (m, 36H), 0.88 (t, $J$ = 6.7 Hz, 6H).

### 5.8.1.7 Synthesis of Stille intermediate (200)
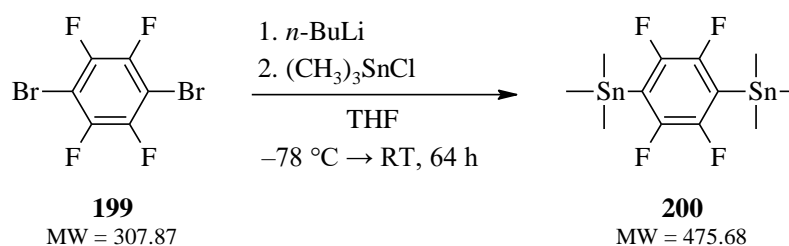


**Scheme 120**: *Preparation of 1,1'-(2,3,5,6-Tetrafluoro-1,4-phenylene)bis[1,1,1-trimethylstannane] (200)*

The same procedure as for the **157** (*Chapter 5.4.4.6*) was used to prepare the **200**, starting with **199** (1.0 equiv., 2.00 g, 6.50 mmol), *n*-BuLi (2.1 equiv. 1.6M, 8.53 mL, 13.65 mmol) and using trimethyltin chloride (2.2 equiv., 2.85 g, 14.30 mmol) as the reagent. The reaction time of stirring at RT was a total of 64 h. The reaction mixture was then poured into distilled water (80 mL) and extracted with diethyl ether (3×50 mL). The collected organic phases were then washed with distilled water (2×300 mL), finally with brine (300 mL), dried over anhydrous Na$_2$SO$_4$ and filtered through filter aid (Celite). After removal of the solvent under vacuum, the obtained crude mixture was purified by crystallisation in *n*-heptane (10 mL) to get product **200**.

**200**: Bright white crystals (2.09 g, yield 67%). Melting point 112.5–113.5 °C.

$^1$H NMR (300 MHz, CDCl$_3$, ppm): $\delta$ = 0.48 (s, 18H).

$^{19}$F NMR (471 MHz, CDCl$_3$, ppm): $\delta$ = –122.89.

### 5.8.1.8  Synthesis of the target polymer (201)
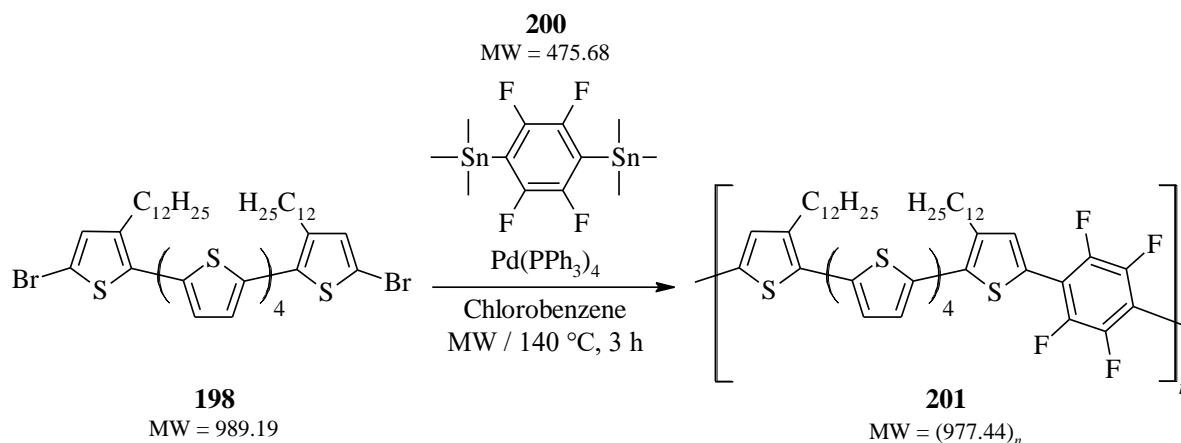


**Scheme 121**: *Preparation of β,β'-didodecyl-α-sexithiophene-tetrafluorophenyl polymer (**201**)*

**198** (0.122 g, 0.123 mmol), Stille intermediate **200** (0.058 g, 0.122 mmol) and Pd(PPh$_3$)$_4$ (8.3 mg, 0.007 mmol) as a catalyst were stirred in anhydrous chlorobenzene (18 mL) under argon atmosphere in a microwave reactor. The reaction mixture was purged with argon for 10 min in an ultrasonic bath, and then it was transferred to a microwave oven, and the experiment was set to "**pulzy**" method. The temperatures used were set for heating and cooling between 90 °C and 60 °C as fast as possible, and the final step was maintained at 140 °C for 3h. The solvent was then distilled off from the reaction mixture by rotary evaporator, the solid material was dissolved in a small amount of chloroform (5 mL) and slowly added dropwise to vigorously stirred acetone (220 mL). The formed precipitate was filtered off and washed with acetone (50 mL) and methanol (20 mL). The same precipitation process was repeated three times. The obtained material was finally purified by Soxhlet extraction with acetone for 65 h (approx. 7 cycles/h ≈ a total of 450 cycles) to afford polymer **201** ($R_F$ = 0, eluent: toluene).

**201**: Dark red rubberish solid with a fine metallic lustre (0.047 g, yield 39%).

$^1$H NMR (300 MHz, CDCl$_3$, ppm): $\delta$ = 7.15–7.07 (m, 6H), 7.02–6.89 (m, 4H), 2.74 (dt, $J$ = 28.2; 7.9 Hz, 4H), 1.70 (q, $J$ = 7.7 Hz, 2H), 1.53 (s, 2H), 1.34–1.21 (m, 36H), 0.88 (t, $J$ = 6.8 Hz, 6H)

$^{19}$F NMR (471 MHz, CDCl$_3$, ppm): $\delta$ = –140.53.

# 6 RESULTS AND DISCUSSION

## 6.1 DPP derivatives

### 6.1.1 Synthesis of basic DPPs and with extended π-conjugation

A well-known and studied *succinic method* was used to prepare the target DPP derivatives. As depicted in **Scheme 122**, this method uses base-promoted condensation of arylnitrile-derivative with succinic acid ester in an equimolar ratio of 2 to 1.



**Scheme 122**: *General synthetic approach ("succinic method") to preparation the DPP molecule*
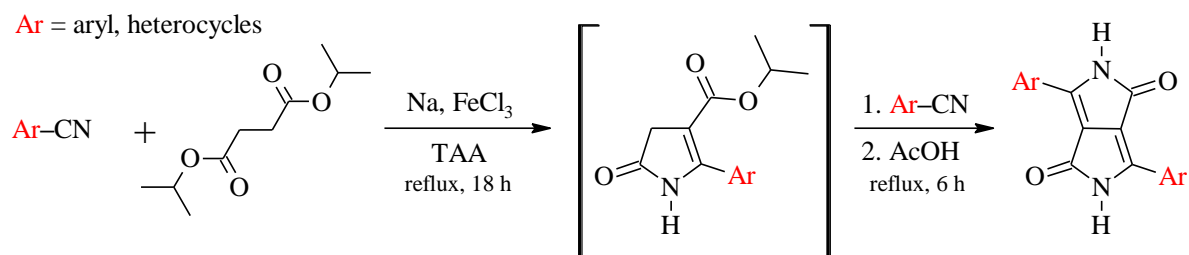
Diisopropyl succinate was specifically used as a starting material as an ester of succinic acid with branched alcohols, which are generally much less prone to the dimerization reaction by the *Claisen condensation* mechanism, leading to the formation of cyclic diester (**Scheme 123**). This undesirable side reaction is favoured by increasing concentration and decreasing steric hindrance of the succinic acid ester used[87].
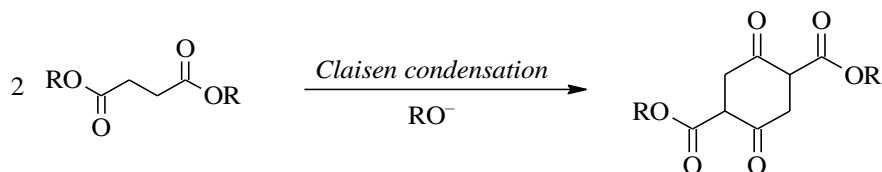


**Scheme 123**: *Base-promoted self-condensation of the succinic acid ester to the cyclic diester*

Sodium *tert*-amyl alkoxide was used as the base due to its sufficient basicity to deprotonate succinic acid esters and, conversely, due to its relatively low nucleophilicity to the undesired nucleophilic addition to the cyano group of arylnitriles. An in-depth, long-term study and optimization of this reaction has shown that performing in the presence of tertiary alkoxides as bases has a positive effect on the yield of the reaction[45,87,105].

Although the generation of anions from succinic acid esters takes place at low temperature, all reactions leading to the formation of the DPP molecules were performed at reflux due to the relatively low electrophilicity of arylnitriles, preventing key nucleophilic addition of these anions to the cyano group[45]. However, at such elevated temperatures, it was necessary to keep the succinic acid ester concentration at a low level, which was accomplished by slowly adding it dropwise in a dilute state to the reaction mixture.

Furthermore, it is well known that the character of an aromatic nitrile-derivative plays a crucial role in the formation of the DPP molecule. In general, electron-poor and sterically unhindered aromatic nitriles provide the highest yields, while on the other hand electron-rich and bulky nitriles exhibit much lower reactivity leading to significantly worse yields of the resulting DPPs[45].

**31a**
MW = 300.36

**31b**
MW = 288.30

**35**
MW = 464.60

**125**
MW = 412.53
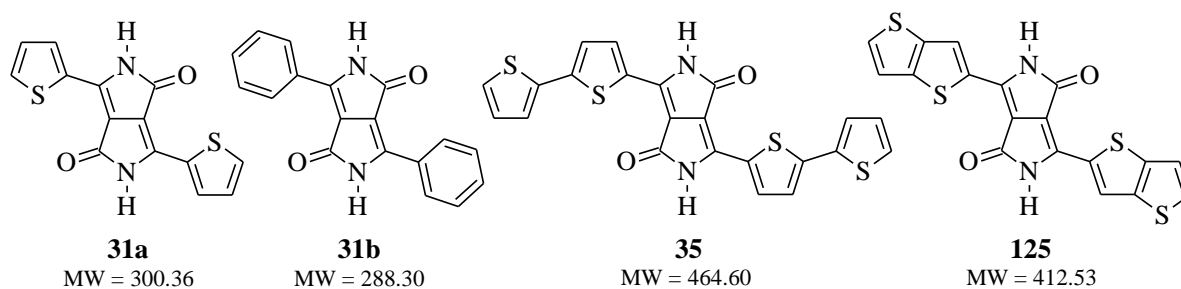
***Figure 32****: All four prepared basic N,N'-unsubstituted DPP derivatives*

In this work, a total of four basic *N*,*N'*-unsubstituted DPP derivatives were prepared (***Figure 32***), and the obtained yields are in good agreement with the above regularities. While thiophene-2-carbonitrile as a small five-membered ring gave the DPP molecule in the highest yield obtained (**31a**, yield 59 %), the bulkier and relatively electron-rich 2,2'-bithiophene-5-carbonitrile resulted in the DPP molecule in the lowest yield obtained (**35**, yield 35 %) when carrying out the reactions under the same conditions.

***Table 7****: Summary of yields of preparation of basic DPP derivatives*

| **DPP** | **31a** | **31b** | **35** | **125** |
|---|---|---|---|---|
| **Yield [%]** | 59 | 52 | 35 | 41 |

In summary, all of the above-mentioned basic DPPs were prepared in moderate yields (***Table 7***) and then successfully used for further synthetic steps. The above synthetic procedure is very advantageous, both for laboratory and industrial scale[38,89]. Its main benefits are simplicity, easy availability and low cost of starting materials, together with a relatively wide range of usable aromatic nitrile-derivatives. Purification of the obtained DPPs, which were suspended in refluxing methanol and filtered off while hot, was also very easily feasible, thus obtaining the materials in sufficient purity for further synthesis.

### 6.1.1.1 Synthesis of appropriate aromatic nitriles

While the basic arylnitriles thiophene-2-carbonitrile and benzonitrile used for the preparation of DPPs **31a** and **31b** were purchased from *Sigma-Aldrich*, *Inc*.; the other two required arylnitriles were prepared from more available starting materials, mainly for financial reasons.

2,2'-bithiophene-5-carbonitrile (**36**) was prepared by a total of two-step synthesis (***Scheme 124***), where in the first step commercially-obtained 2,2'-bithiophene (**117**) was subjected to *Vilsmeier-Haack* reaction to afford formyl derivative (**118**), which was then transformed to the resulting nitrile (**36**) using hydroxylamine hydrochloride. In both cases, these are well described synthetic approaches[185,186] that provided the desired products in yields corresponding with the literature.
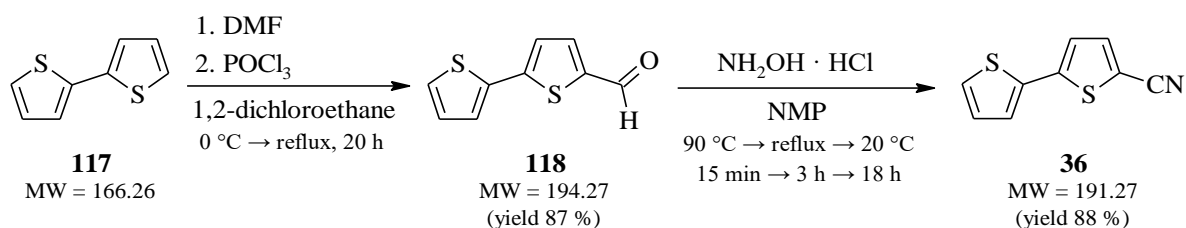
Scheme 124: Synthetic approach used to prepare 2,2'-bithiophene-5-carbonitrile (36)

The synthesis of thieno[3,2-*b*]thiophene-2-carbonitrile (124) consists of five synthetic steps (Scheme 125). It starts with the commercially available 3-bromothiophene (119), its lithiation by LDA and subsequent formylation using 1-formylpiperidin. The formyl derivative (120) then reacted with ethyl thioglycolate in the presence of potassium carbonate to provide the cyclization product of ethyl thieno[3,2-*b*]thiophene-2-carboxylate (121). Intermediate 121 was subsequently converted by base catalysed hydrolysis to its carboxylic acid (122). Free carboxylic acid 122 was transformed first to the more reactive acid chloride, followed by amide (123). In the last step, the already prepared amide (123) was effectively converted to the desired thieno[3,2-*b*]thiophene-2-carbonitrile (124) using phosphoryl trichloride. Above-mentioned synthetic approach is also well described[187], and the resulting nitrile (124) was obtained in a total yield of 25.8 %.
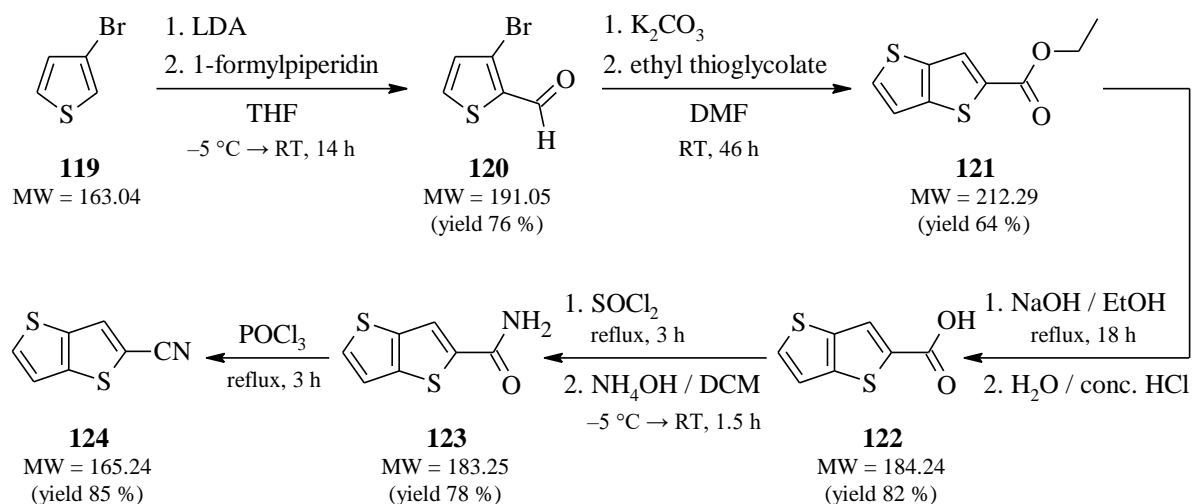


Scheme 125: Synthetic approach used to prepare thieno[3,2-b]thiophene-2-carbonitrile (124)

## 6.1.2 Synthesis of basic DPPs with alkylated side 3,6-aryl units

As already mentioned in *Chapter 3.2.1.1*, the basic *N,N'*-unsubstituted DPP derivatives form intermolecular hydrogen bonds (–NH–O=, *Figure 33*), which together with π-π molecular stacking are responsible for exceptional thermal stability, high crystal lattice energies and excellent photostability of these DPPs. In addition, Głowacki et al.[188] described that even these *N,N'*-free DPPs could function as organic semiconductors when, based on the calculated charge transfer integrals, the H-bonded contacts between adjacent molecules can also contribute to charge transport in the crystal.
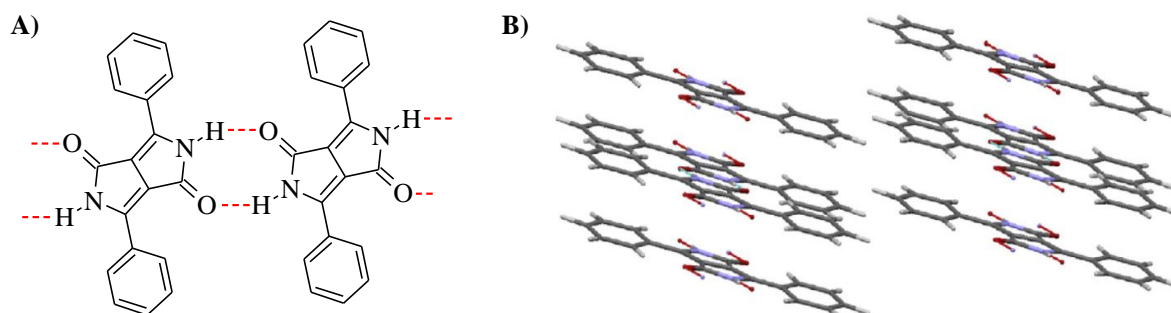
**Figure 33**: *Molecular structure of the DPP with formed hydrogen bonds between adjacent molecules (A) and crystal structure of the DPP (B)*[188]*, where the red lines indicate H-bonds.*

On the contrary, the intermolecular H-bonds discussed above result in a very limited solubility of the resulting DPPs in most common organic solvents, which disables their solution processability and generally makes it very difficult to apply these derivatives in organic electronics. One of the solutions to increase their applicability is *N,N'*-alkylation, which, however, causes the interruption of hydrogen bonds and thus the resulting possible advantages mentioned above. Therefore, the aim was to prepare novel, as yet undescribed DPP derivatives, which will be *N,N'*-unsubstituted and, in addition, will contain alkyl chains on the 3,6-aromatic side units, which could ensure a higher solubility of the resulting DPPs in common organic solvents and thus also their potential applicability. The structures of the three target such modified DPP derivatives are shown in the following **Figure 34**.
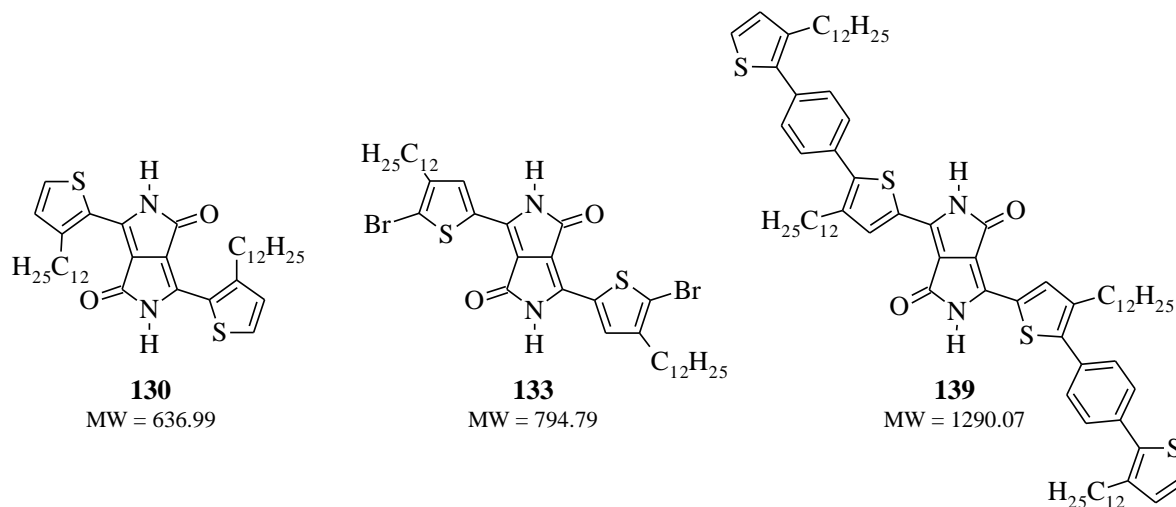


**Figure 34**: *Three target basic DPP derivatives with alkylated side 3,6-aryl units*

The *succinic method*, discussed in the previous chapter (*6.1.1*), was used to prepare the resulting three derivatives under the same conditions. Nevertheless, two of the three target derivatives were not successfully prepared, as shown in the following **Table 8**. In the case of the first-mentioned derivative **130**, the main reason for the failure of the reaction may be the steric hindrance of the starting aromatic nitrile caused by the dodecyl chains adjacent to the cyano groups. This their position and potential orientation into the DPP core could prevent the double-cyclization to the resulting DPP **130**, as this reaction is exceptionally susceptible to steric hindrance.

**Table 8**: *Summary of yields of preparation of basic DPP derivatives with alkylated side 3,6-aryl units*

| DPP | 130 | 133 | 139 |
|-----|-----|-----|-----|
| Yield [%] | × / **not prepared** | 9.4 | × / **not prepared** |

This assumption was confirmed by the successful preparation of DPP derivative **133**, where the starting nitrile contained dodecyl chains in position 4, which considerably reduced steric repulsions compared to the previous nitrile. Moreover, the orientation of the alkyl groups after successful cyclization to the DPP molecule was "out" from the DPP core, which could also facilitate the reaction progress. With respect that the resulting derivative **133** contained bromine atoms in its structure at the 5-positions of the thiophene side rings, it dramatically expands its potential synthetic utilization to a diverse range of *cross-coupling* reactions.

The third and last target derivative **139** was not successfully prepared, as well as **130**. Due to the very low solubility of the "trimer-carbonitrile" in tertiary alcohol as the required solvent and thus the heterogeneous reaction features, the preparation of the derivative **139** by the *succinic method* was prevented.

### 6.1.2.1 *Synthesis of appropriate aromatic nitriles*

All three relevant aromatic nitriles for the preparation of the DPP derivatives discussed above were prepared from well available starting materials.

The preparation of 3-dodecylthiophene-2-carbonitrile (**129**) consisted of four synthetic steps (*Scheme 126*), starting with the reaction of commercial 1-bromododecane (**126**) with magnesium and a catalytic amount of iodine in freshly distilled diethyl ether by *Grignard* reaction to the organomagnesium intermediate.
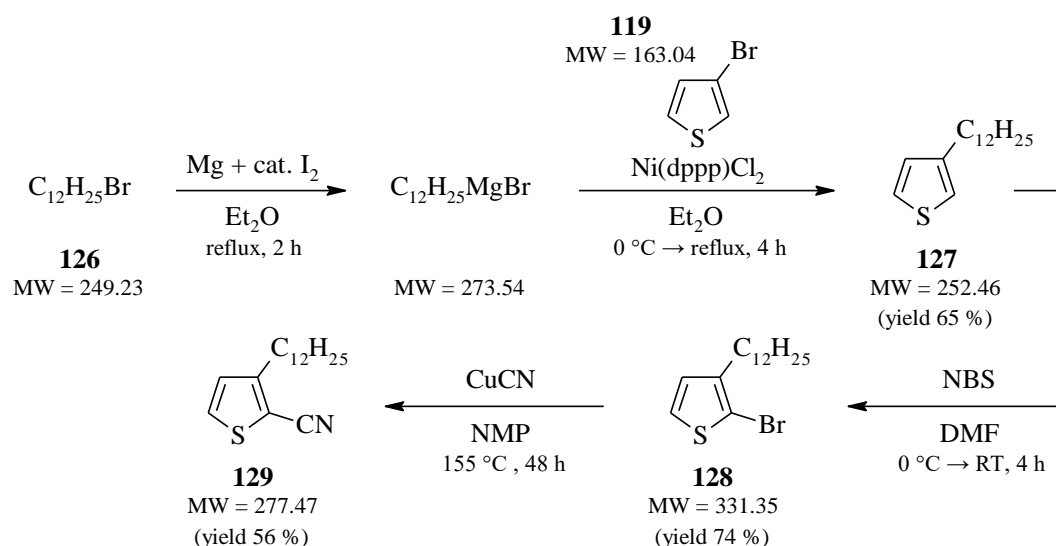


**Scheme 126**: *Synthetic approach used to prepare 3-dodecylthiophene-2-carbonitrile (129)*

The resulting dodecylmagnesium bromide directly reacted under *Kumada cross-coupling* reaction[189] with 3-bromothiophene (**119**) catalysed by Ni(dppp)Cl$_2$ to give 3-dodecyl-

thiophene (**127**, yield 65 %). **127** was then selectively brominated into 2-position using 1.1 molar equivalent of NBS in DMF[190,191] to obtain **128**, which was subsequently subjected to nucleophilic substitution using an excess of copper cyanide[192] to give the desired cyano derivative (**129**) in a yield of 56 %. All products were obtained and confirmed in good agreement with the literature.

Intermediate **128** from the previous synthetic pathway was used to synthesize the target 5-bromo-4-dodecylthiophene-2-carbonitrile (**132**) using a two-step synthesis (*Scheme 127*). **128** was subjected to *Vilsmeier-Haack* reaction to afford formyl derivative (**131**), which was subsequently transformed to the resulting nitrile (**132**) using hydroxylamine hydrochloride. This synthetic approach is analogous to that for the preparation of 2,2'-bithiophene-5-carbonitrile (**36**) discussed in the previous chapter (*6.1.1.1*, *Scheme 124*). Herein, the target nitrile **132** was prepared in a yield of 51 % relative to the starting derivative **128**.
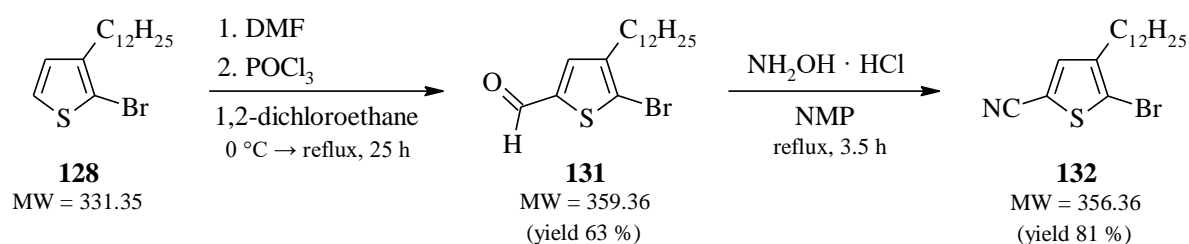


**Scheme 127**: *Synthetic approach used to prepare 5-bromo-4-dodecylthiophene-2-carbonitrile (**132**)*

The synthesis of the last target nitrile **138** started from basic dodecyl trimer **27**. The derivative **128** was again used as starting material, which was converted to Grignard reagent **134** using isopropylmagnesium chloride. **134** reagent was then subjected to the *Kumada cross-coupling* reaction with 1,4-dibromobenzene (**135**) catalysed by Ni(dppp)Cl$_2$ to afford the resulting trimer **27** in a yield of 19 % (*Scheme 128*, **A**). The great advantage of this synthetic path is the work in an easily feasible range of reaction temperatures ($0 \rightarrow 80\,°C$) and the use of relatively cheap, available and non-toxic chemicals. However, due to the too low yield of the desired product **27**, an alternative synthetic path had to be chosen.

The *Stille cross-coupling* reaction was used as an alternative synthetic path of the target derivative **27** (*Scheme 128*, **B**). This synthesis again started with the derivative **128**, which was converted to Stille intermediate **136** through the lithium-halogen exchange using *n*-butyllithium and subsequent reaction with tributyltin chloride. The prepared intermediate **136** was then subjected to the *Stille* reaction with 1,4-dibromobenzene (**135**) catalysed by Pd(PPh$_3$)$_4$ to give the desired trimer **27**[84]. *Stille* reaction resulted in the target trimer **27** in the yield almost doubled compared to the previous *Kumada* reaction (36 % vs 19 %).

However, both synthetic pathways provided a sufficient amount of **27** for further synthesis, so the reactions were not optimized anymore, and the possible cause of yield deviations from the literature data[84,193] was thus not identified.
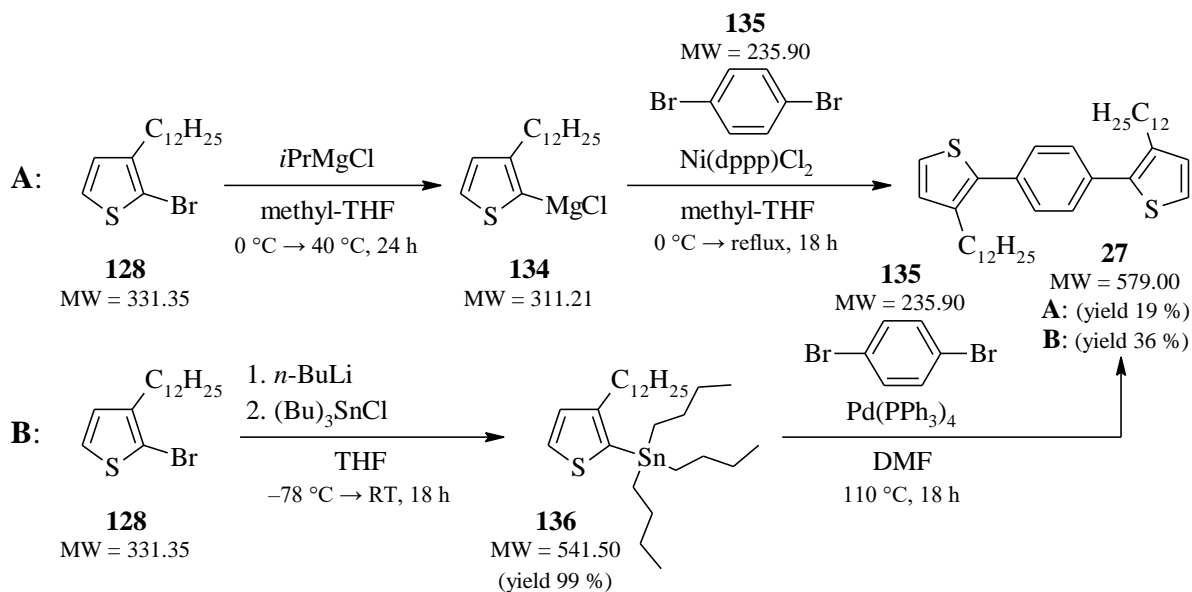
**Scheme 128**: *Synthetic approaches **A/B** used to prepare "dodecyl-(Th-Ph-Th)-trimer" (**27**)*

The target trimer-nitrile **138** was prepared in a two-step synthesis (**Scheme 129**) analogous to the preparation of the previous two discussed nitrile-derivatives **36** (**Scheme 124**) and **132** (**Scheme 127**). The total yield of the target nitrile-derivative **138** was 34 %.
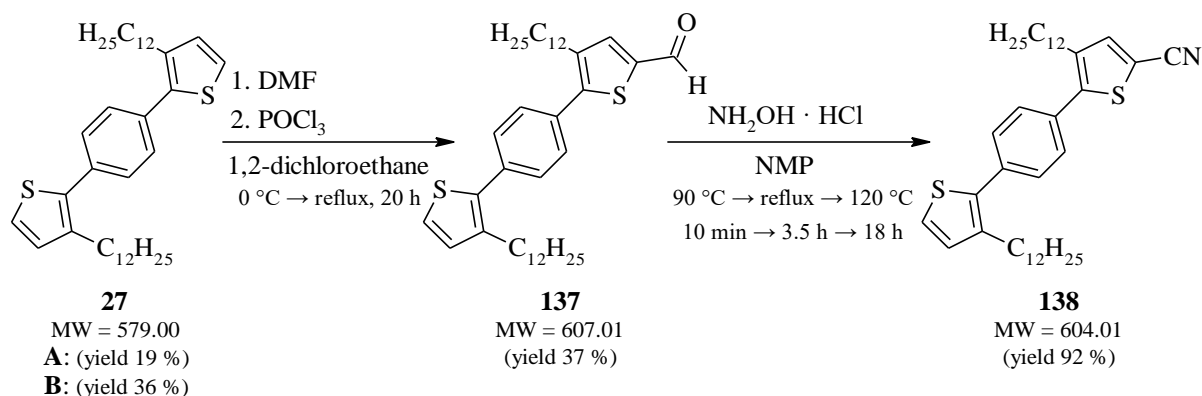


**Scheme 129**: *Synthetic approach used to prepare dodecyl-(Th-Ph-Th)-trimer-5-carbonitrile (**138**)*

### 6.1.3 Synthesis of alkylating reagents

As already described in the review section of this work (*Chapter 3.2.1.1*, **Figure 9**), the incorporation of bulky adamantane chains into the DPP structure by our team has brought a unique, as yet undescribed effect on the resulting derivative properties caused by the adamantane-induced highly organized arrangement of the DPP molecules into triads[50]. This modification was achieved by one simple synthetic step, namely *N,N'*-alkylation using appropriate alkyl bromide as starting reagent. As a result, the following three alkylating reagents containing bulky adamantane chains (**Figure 35**) were selected and prepared.

| **141** | **142** | **144** |
| MW = 243.18 | MW = 290.18 | MW = 229.16 |
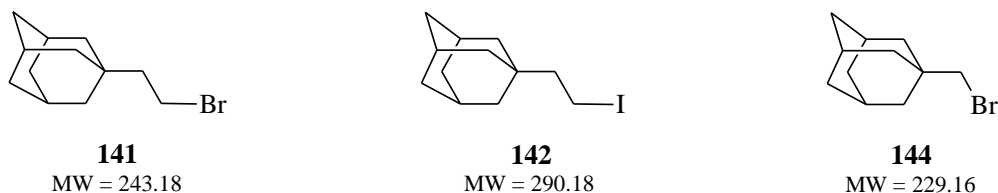
***Figure 35****: Structures of four target alkylating reagents*

***Table 9****: Summary of yields of preparation of alkylating reagents*

| **Alkylating reagent** | **141** | **142** | **144** |
|---|---|---|---|
| **Yield [%]** | 80 | 98 | 48 |

Derivatives **141** and **144** were prepared according to a known synthetic approach[194] starting from the corresponding alcohols by reaction (nucleophilic substitution) with 48% hydrobromic acid (***Scheme 130***).

$$R\!-\!OH \xrightarrow[\text{reflux, ~20 h}]{\text{aq. HBr}} R\!-\!Br$$
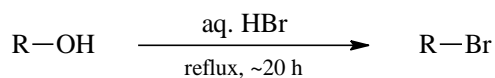
***Scheme 130****: Conversion of alcohol to alkyl bromide using 48% hydrobromic acid*

In the case of derivative **141**, the reaction proceeded without difficulty in a yield of 80 %, which is in accordance with the literature[194]. Derivative **144** was obtained in a significantly lower yield of only 48 %; however, this may be caused by the neopentyl character of the starting alcohol, which significantly hampered the substitution ($S_N1$) of the bromine atom.

In general, alkyl bromide exhibits lower reactivity and thus lower conversion in nucleophilic substitution reactions compared to alkyl iodides, which is in good agreement with the article describing DPP derivatives[195]. Therefore, alkyl iodide **142** was prepared by the classical *Finkelstein* reaction[196] from alkyl bromide (**141**), which was reacted with potassium iodide in acetone, and the target product was obtained in almost quantitative yield.

The addition of KI directly into the reaction mixture consisting of a DPP derivative, a base and an alkyl bromide for *in situ* halogen exchange has also been reported with a positive effect on improving the yield of alkylated products[195]. However, this approach has not been tried in this work.

### 6.1.4   Synthesis of *N*- and *O*-alkylated DPPs

#### *6.1.4.1   Synthesis of N,N'-alkylated DPP derivatives – approach A*

*N,N'*-alkylation is one of the most significant and widely used modifications of DPPs, as already described in *Chapter 4.1.1*. The reason for this modification, in addition to the well-known increase in solubility, was the incorporation of adamantyl substituents into the basic DPP derivatives discussed in *Chapter 6.1.1*. The new approach presented herein has been used for many other commercially obtained basic DPPs, which have been identified as high potential based on data from the literature, where they have shown interesting properties even with common alkyl substituents, such as 2-ethylhexyl. The contribution of these adamantyl

substituents will then be studied on the resulting derivatives and compared with the already published exceptional results of ethyl-adamantyl thiophene DPP[50].

The reaction was performed by a well-described alkylation approach, where the basic DPP was first mixed with the appropriate base in a polar aprotic solvent (DMF) to form a DPP anion, followed by nucleophilic substitution with an alkylating agent to form an alkylated DPP product (**Scheme 131**)[45,90]. DPP anion has an ambiguous character, which leads to competitive substitution on the nitrogen and oxygen atoms and thus also to a marked decrease in the formation of the *N,N'*-substituted product[90]. The following **Table 10** provides an overview of all prepared *N,N'*-alkylated DPPs.
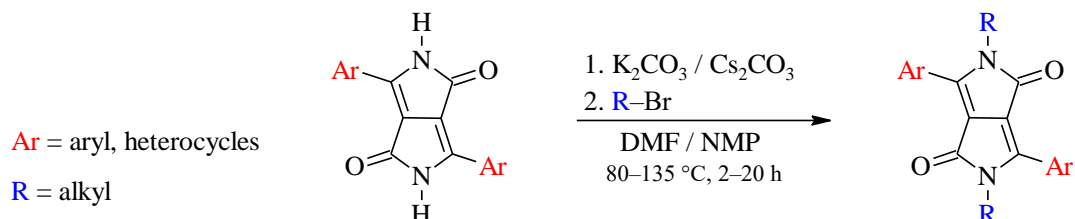


*Scheme 131: General synthetic approach used for alkylation of DPPs*

In most of the experiments performed, potassium carbonate was used as the base, DMF as the solvent, the reaction temperature was about 105 °C and the reaction time was several hours, as it has already been proved that these parameters do not have a very significant effect on the alkylation regioselectivity[92]. The variability in these factors was used only in problematic cases ([b] marked in **Table 10**), where it was complicated to obtain a weighable amount of sufficiently pure desired products.

In the case of the preparation of derivative **153** under standard conditions (base: $K_2CO_3$, solvent: DMF, temperature: 105 °C, time: 18 h) no *N,N'*-alkylated product was isolated. Based on TLC analysis, the desired product was present in a small amount in the reaction mixture, whereas a large number of likely decomposition products were observed. Replacement of $K_2CO_3$ base by $Cs_2CO_3$ did not bring any positive effect. An increase in the reaction temperature (up to 140 °C) as well as an extension of the reaction time (up to 96 h) led to the disappearance of the desired product **153** and, conversely, to the formation of a larger proportion of decomposition fragments. The highest yield of almost 16 % was obtained with the standard use of base (6 equiv. of $K_2CO_3$) and reaction time (20 h) but at a lower reaction temperature of 80 °C.

A similar trend was observed in the preparation of derivative **155a**, where the highest yield of almost 14 % was obtained when performing the reaction with a maximum of 80 °C and a reaction time of 20 h.

Increasing the reaction temperature (up to 135 °C) and the reaction time (112 h in total) in the preparation of derivative **169** also led to a complete loss of the desired product and the formation of many decomposition fragments. Conversely, by lowering the temperature to 115 °C and the reaction time to 17 h, the product **169** was obtained in a yield of 5 % (*Chapter 5.4.4.10*, **Table 5**). This acquired trend is entirely in accordance with previous derivatives.

**Table 10**: *Summary of all prepared N,N'-alkylated DPPs by the alkylation approach*

| DPP | Ar | R | Yield [%] |
|---|---|---|---|
| | **N,N′-alkylated DPP derivative** | | **Yield [%]** |
| **145a** | 2-thienyl | dodecyl | 75 |
| **146a** | 2-thienyl | 2-ethylhexyl | 41 |
| **6a** | 2-thienyl | ethyladamantyl | 36 |
| **147** | 2-thienyl | methyladamantyl | 7 |
| **150** | benzofuranyl-2-thienyl | dodecyl | 6 |
| **151** | benzofuranyl-2-thienyl | ethyladamantyl | 3[a] |
| **152** | 2-thieno[3,2-*b*]thienyl | ethyladamantyl | 7[a] |
| **153** | 2-bithienyl | 2-ethylhexyl | 16[b] |
| **154** | 2-bithienyl | methyladamantyl | – |
| **155a** | 2-bithienyl | ethyladamantyl | 14[b] |
| **164** | phenyl | dodecyl | 63 |
| **165a** | phenyl | 2-ethylhexyl | 12 |
| **166a** | phenyl | ethyladamantyl | 14 |
| **168** | *p*-cyanophenyl | ethyl 2-(*N,N′*-DPP)acetate | 13 |
| **169** | 2-naphthyl | ethyladamantyl | 5[b] |

[a] based on NMR analysis, the obtained material was contaminated with *N,O′*-alkylated product

[b] the highest yield obtained from the experiments reported herein (leading to the optimization)

In order to increase the regioselectivity and yields of the desired *N,N′*-alkylated products, many parameters were tested, such as temperature, the base used, reaction time. Nevertheless, based on the number of experiments performed, it cannot be stated with certainty that any of these altered factors directly contributed to the better course of the reaction.

The finding that the character of alkyl chains has the most considerable influence on the course of alkylation of the DPP molecule is entirely in accordance with the literature data[94]. The relative reactivity of the used alkyl halides is shown in the following ***Figure 36***. *N,N′*-alkylated products were most efficiently formed with linear dodecyl bromides, with a significant decrease in yields being observed for branched 2-ethylhexyl bromides. A similar or slightly worse *N,N′*-alkylation progress was observed with bulky 1-(2-bromoethyl) adamantane (**141**). As expected, the very worst course of the reaction was obtained using 1-(bromomethyl)adamantane (**144**) having a neopentyl character, which has already been discussed (*Chapter 6.1.3*) as an undesirable structure for nucleophilic substitution.

*Figure 36: Relative reactivity of alkyl halides used for alkylation of DPPs*

In addition, it also turned out that the side 3,6-aromatic substituents in the DPP molecule had a significant effect on the course of *N,N'*-alkylation. From the obtained experimental data (*Table 10*), the range of these substituents was assembled according to the decreasing yield of *N,N'*-alkylation and is shown in the following *Figure 37*. It is obvious that with the increasing bulkiness of these substituents, the yield of the reaction decreases substantially. Thus, for example, when comparing the incorporation of ethyladamantyl substituents, by far the highest yield of *N,N'*-alkylated product was obtained with the simplest thienyl-DPP (36 %), while a large decrease in yield (14 %) was observed for bithienyl-DPP. In the case of the most complex and bulky benzofuranyl-thienyl-DPP, it was difficult to isolate the *N,N'*-alkylated product in sufficient purity at all (<3%).
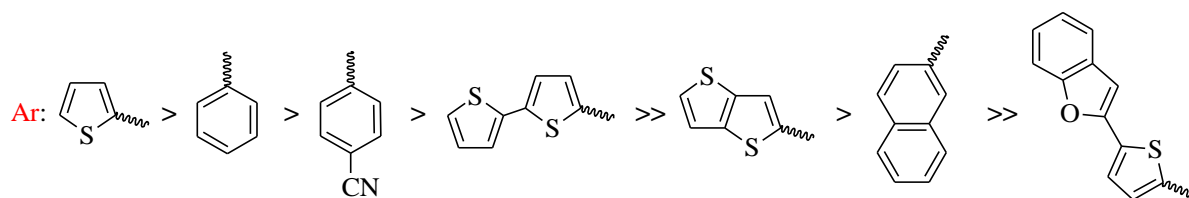


*Figure 37: Relative reactivity of DPPs used depending on their 3,6-aromatic substituents*

When comparing the reactivity of thienyl > phenyl and their fused analogues thieno[3,2-b]thienyl > naphthyl, the size of the substituents, where the thiophene nucleus is smaller than the benzene, also plays a key role[45]. However, another important factor is the presence of sulphur heteroatoms that form intramolecular hydrogen bonds contributing to the coplanar orientation and limiting the free rotation of these substituents[45]. Based on the study of the crystal structure of alkylated DPP derivatives, it was found that significant steric repulsions occur between the side 3,6-aromatic substituents and the *N,N'*-linked alkyl chains, causing the aromatic units to deviate. These repulsions and thus also the deviations are more extensive the larger the aromatic substituent, as confirmed by the geometry of the asymmetric derivative in *Figure 38*, where the steric repulsions between the methyl group and the phenyl ring caused its deviation by 31.1° (while for *N,N'*-unsubstituted DPP the dihedral angle between phenyl and DPP core is only 7.1°). For the much smaller furan substituent, its deviation due to the methyl group was only 0.9°. These steric repulsions also increase significantly with increasing alkyl chain bulkiness[45,100]. An example confirming this assumption may be the preparation of derivative **154**, containing bulky bithiophene units in 3,6-positions and alkyl chains of a neopentyl character. This product has not been isolated in a weighable amount and an adequate purity so that its structure can be confirmed.
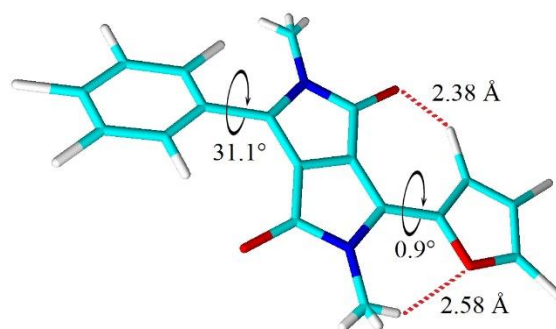
**Figure 38**: *Geometry of an asymmetric DPP derivative in a crystal structure with dark red marked hydrogen bonds (analogous to thiophene) and values of dihedral angles*

Based on the findings obtained from the performed experiments, it can be concluded that the temperature and time of the reaction have an important effect on the yield of *N,N'*-alkylation, but in a relatively small range. Rather, the suitable setting of these parameters can prevent especially the undesired course of the reaction leading to decomposition products. On the other hand, the nature of the substituents (both the side 3,6-aromatics and alkyl chains used for the reaction), especially in terms of their bulkiness, have a crucial influence on the reaction yield.

### 6.1.4.2 Synthesis of N,N'-alkylated DPP derivatives – approach B

Another synthetic goal was to prepare six DPP derivatives **146a**, **6a**, **153**, **155a**, **162** and **163** (*Figure 39*) in sufficient quantities (>50 mg) and purity for a comprehensive study of optical and electrical properties. It was focused on the effect of the alkyl chains character (branched vs bulky) together with the prolongation of the π-conjugation on these properties.
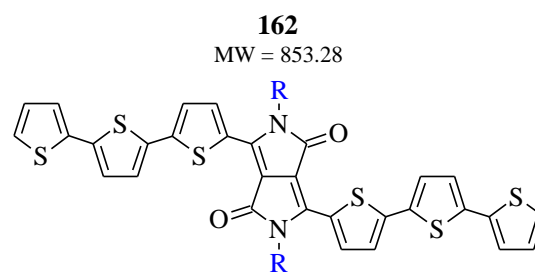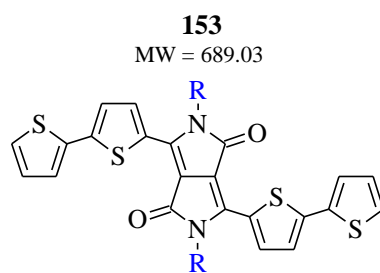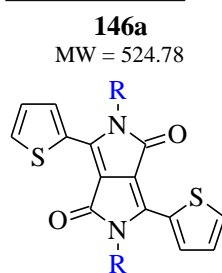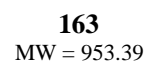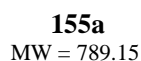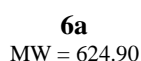


**Figure 39**: *Six target DPP derivatives with different alkyl chains and prolonged π-conjugation*

Derivatives **146a** and **6a** were easily prepared by the above-discussed alkylation method. In contrast, derivatives **153** and **155a** were relatively complicated to obtain by *N,N'*-alkylation in the required amount, and especially derivatives **162** and **163** could not be prepared at all by this method due to the failure of the basic *N,N'*-unsubstituted terthiophene-DPP preparation, as already mentioned. Thus, an alternative synthetic path based on the *Stille cross-coupling* reaction was used for the last four derivatives. (*Scheme 132*)[108].

R = 2-ethylhexyl:
**158**
MW = 682.57

R = ethyladamantyl:
**159**
MW = 782.69

Ar = H: **153**, MW = 689.03 (yield 58 %)
Ar = 2-thienyl: **162**, MW = 853.28 (yield 66 %)

Ar = H: **155a**, MW = 789.15 (yield 28 %)
Ar = 2-thienyl: **163**, MW = 953.39 (yield 80 %)

Pd(PPh$_3$)$_4$
DMF
MW / 130 °C, 3 h
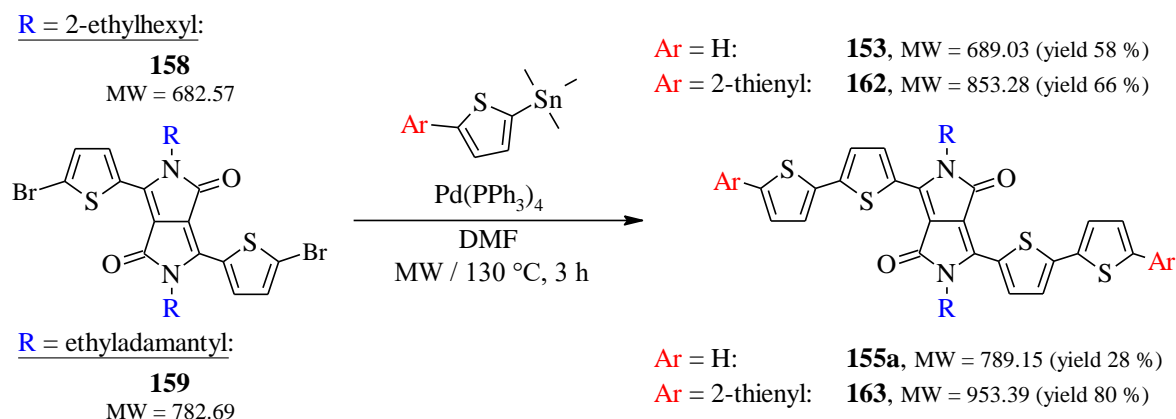
*Scheme 132*: *General synthetic approach using Stille cross-coupling reaction for the preparation of N,N'-alkylated DPPs with prolonged π-conjugation*

*Table 11*: *Summary of four prepared N,N'-alkylated DPPs by the Stille cross-coupling approach*

| DPP | 153 | 155a | 162 | 163 |
|---|---|---|---|---|
| **Yield [%]** | 57.6[a] | 28.3 | 65.8 | 79.5[a] |

[a] the highest yield obtained from the experiments reported herein (leading to the optimization)

The synthesis of the four mentioned derivatives was carried out under microwave-assisted synthesis, in which the reaction mixture was fast heated to 90 °C in a microwave reactor and after 10 min, the mixture was cooled rapidly to 60 °C (repeated 4×). The mixture was then heated to 115 °C (130 °C, respectively) and maintained at this temperature for 2.5 h (2 h, respectively). Subsequently, the reaction was quenched and worked up to isolate the desired products. Appropriate experiments are described in detail in *Chapters 5.4.4.6* and *5.4.4.7*.

In all cases, Pd(PPh3)4 was used as a catalyst for the *Stille cross-coupling* reaction in DMF. Bithienyl-DPP derivatives **153** and **155a** were initially prepared only in yields ranging from 28–29 % using a maximum temperature of 115 °C for 2.5 h. Increasing the temperature to 130 °C and shortening the reaction time to 2 h provided more than double the yield (57.6 %) in the case of derivative **153**. The same trend was observed in the preparation of derivative **163** when a much higher yield was achieved from the previous 63.5 % to almost 80 %. The synthetic procedures of derivatives **155a** and **162** were not optimized, as they were already obtained in the moderate yields.

The preparation of the four discussed derivatives was preceded by the synthesis of key starting materials for the *Stille* reaction: a brominated DPP derivative and an organotin coupling partner[108]. Bromination of *N,N'*-alkylated-thienyl-DPP derivatives (**146a** and **6a**) was performed by a conventional synthetic approach using the brominating agent NBS in a mixture of chloroform/acetic acid (10/1)[197]. After stirring for about 40 h at elevated temperature (50 °C), the desired products **158** and **159** were obtained in decent yields of 41 % and 46 %, respectively.

The key organotin compounds **157** and **161** were prepared by a well-described two-step synthetic approach[198] (*Scheme 133*) from commercial thiophene (**21**) and 2,2'-bithiophene

(**117**). First, mono-brominated derivatives were prepared, which were then subjected to lithiation followed by reaction with trimethyltin chloride to give the desired *Stille intermediates* in high yields. An alternative to lithiation can be the *Grignard* reaction using magnesium powder[84] or *i*-PrMgCl solution[199], which does not require cryogenic temperatures of the reaction mixture compared to lithiation using *n*-BuLi[198].
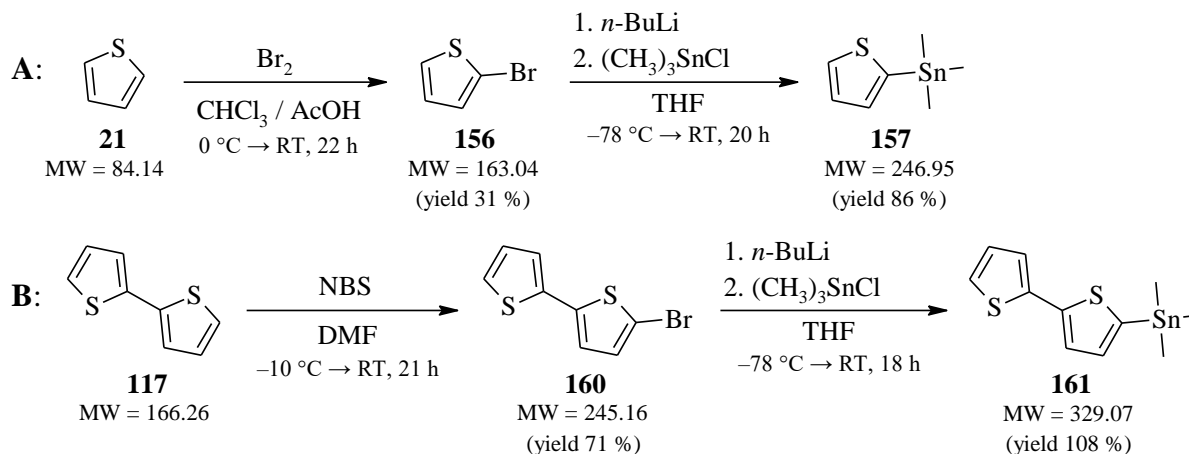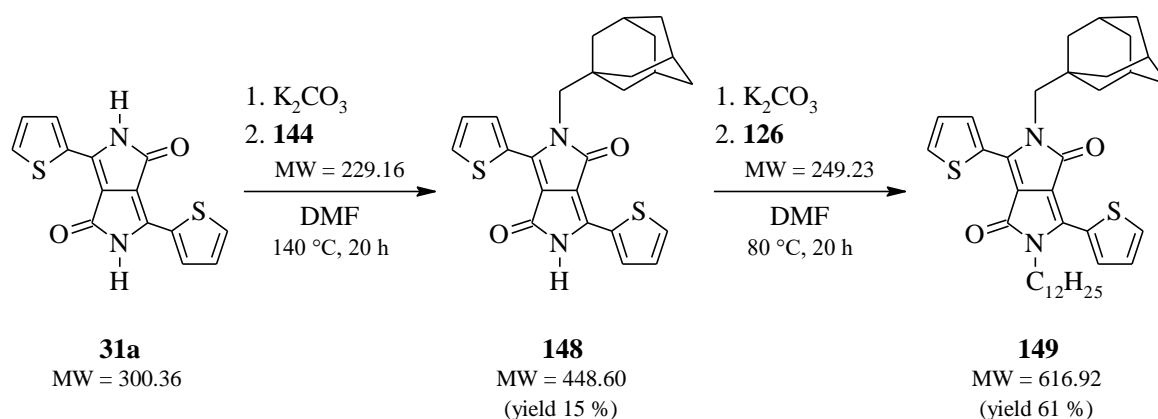


**Scheme 133**: *Two-step synthetic approach used to prepare Stille intermediates **157** and **161***

### 6.1.4.3  Synthesis of asymmetrically N,N'-alkylated DPP derivative

The synthesis was divided into two parts. The very limited reactivity of the above-discussed neopentyl alkyl bromide 1-(bromomethyl) adamantane (**144**) was used to synthesize the unique asymmetrically *N,N'*-alkylated DPP (***Scheme 134***). For sterically less hindered and thus more reactive alkylation reagents, the amount of forming mono-*N*-alkylated product is usually very negligible.

In the first synthetic step, the basic thienyl-DPP (**31a**) in the presence of 3 equiv. of the base (K$_2$CO$_3$) was reacted with 1.5 molar equiv. of alkylating reagent **144** and the reaction progress was monitored by TLC analysis. After stirring at 140 °C for 20 h, a significant occurrence of the mono-*N*-alkylated product was observed, followed by the quenching of the reaction. The product was then isolated and purified by silica gel chromatography with a yield of 15 %. The structure of the new product (**148**) was confirmed by $^1$H NMR and CHNS analysis.

**148** was subjected to further alkylation under milder conditions (80 °C) using a sterically readily accessible dodecyl chain. The resulting product **149** was thus prepared in a decent yield of 61 %. However, the overall yield of product **149** relative to the starting derivative **31a** was only 9.2 %. The obtained derivative **149** will be subjected to a detailed study of physical properties.

**Scheme 134**: *Synthetic approach used to prepare asymmetrically N,N'-alkylated DPP (**149**)*

### 6.1.5 A comprehensive study of the selected series of DPPs[200]

Two series of thienyl-DPP derivatives alkylated with 2-ethylhexyl and ethyladamantyl chains were selected (***Figure 40***). The main goal was to isolate all forming *N,N'-*; *N,O'-* and *O,O'-* substituted products and subsequently subject them to an in-depth study of thermal and optical properties, both in solution and in thin layers. This comprehensive study was focused mainly on the study of the effect of the alkyl chains' character and their binding position in the DPP molecule on physicochemical properties of the resulting derivatives.
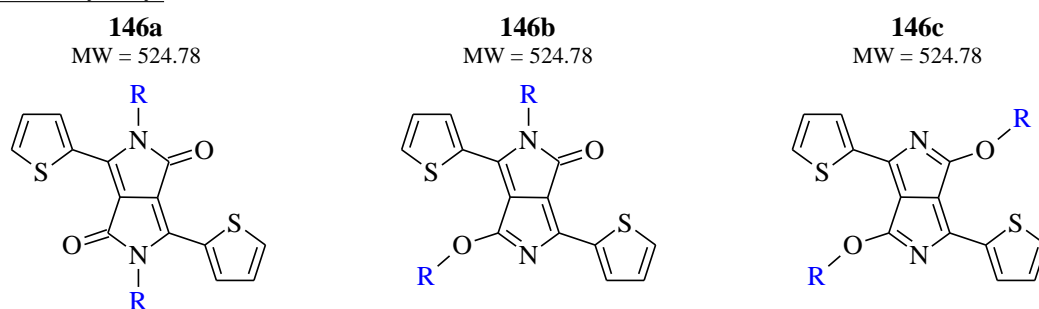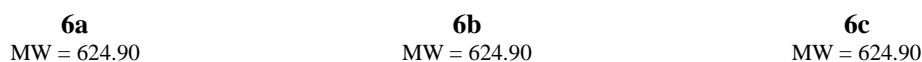


**Figure 40**: *Summary of the prepared and isolated two series of alkylated DPP derivatives*

### 6.1.5.1 Synthesis: N- vs. O-alkylation

All six isolated alkylated DPPs were prepared by the standard method using base-promoted nucleophilic substitution of alkyl halides[45,90], discussed in detail in *Chapter 6.1.4.1*. A milder temperature (105 °C) and a significantly shorter reaction time (only 2 h) were used, as many experiments have shown that undesired decomposition products of alkylated DPPs are formed with increasing temperature and extending the reaction time. In addition, by reducing the reaction time to just 2 h, it was possible to isolate a weighable amount of the rare *O,O'-* substituted products, which was an important objective in this synthesis.

*Table 12: Summary of yields from preparation of N,N'-; N,O'- and O,O'-alkylated DPPs*

| DPP | *N,N'-* | *N,O'-* | *O,O'-* |
|---|---|---|---|
| **2-Ethylhexyl** | **146a** | **146b** | **146c** |
| **Yield [g/%]** | 41 | 18 | 3 |
| **Ethyladamantyl** | **6a** | **6b** | **6c** |
| **Yield [g/%]** | 36 | 20 | 6 |

As can be seen from ***Table 12*** summarizing the yields for the preparation of the target DPP derivatives, the reactivity of both alkylating reagents was similar, as already discussed (***Figure 36***). Due to the bulkiness of the adamantyl chains and thus the increase in possible steric repulsions, a slight decrease in yield was observed for the resulting *N,N'*-substituted derivative, while the yield of *O*-substitution slightly increased. In particular, the yield of the symmetrical *O,O'*-product was doubled compared to the branched 2-ethylhexyl substituent.

### 6.1.5.2 Thermal properties

TG and DSC analyses were performed for an in-depth study of the thermal properties of all obtained DPP derivatives. A summary of the selected determined parameters is listed in the following ***Table 13***.

*Table 13: Summarized thermal properties (TG and DSC) of the DPP derivatives under investigation*

| DPP | DSC | Melting I [°C] | Melting II [°C] | Cold crystal. [°C] | Crystal. [°C] | $T_{DEG}$ [°C] |
|---|---|---|---|---|---|---|
| **146a** | first heating | 55 | 118 | | | |
| | after fast cooling | 55 | 118 | | | 289 |
| | after slow cooling | 53 | 118 | | | |
| **146b** | first heating | 30[a] | | | | |
| | after fast cooling | 20 | | | | 270 |
| | after slow cooling | 22 | | | | |
| **6a** | first heating | 321 | 330 | 133 | 6 | |
| | after fast cooling | 320 | | 163 | 36 | 368 |
| | after slow cooling | 274 | 300 | 186 | 30 | |
| **6b** | first heating | 210 | | | | |
| | after fast cooling | 207 | | 157 | 1 | 264 |
| | after slow cooling | | | | | |
| **6c** | first heating | | | | | |
| | after fast cooling | 221 | | | | n.d. |
| | after slow cooling | | | | | |

[a] started simultaneously with experiment

147

The degradation of material **146a** was determined at 289 °C based on the TG record. Subsequent DSC analysis revealed two distinct crystalline structures of this material, which are probably formed from 2-ethylhexyl chains, as longer aliphatic chains tend to form packed structures. However, their substitution can cause the formation of several stable forms that are energetically close to each other[201,202]. Asymmetrically substituted 2-ethylhexyl derivative **146b** showed a slight decrease in the degradation temperature to 270 °C and in particular, compared to the symmetrical analogue **146a**, it showed only one type of crystals. Thus, it can be concluded that the crystallites are predominantly formed from 2-ethylhexyl chains attached to an *N*-atom, while the *O*-substitution does not promote crystal formation. Based on this, larger crystals of 2-ethylhexyls probably composed of chains from adjacent molecules could lead to a higher melting point of material **146a**.

The degradation temperature of the *N,N'*-ethyladamantyl substituted derivative (**6a**) was determined at 368 °C, which is a significantly higher value compared to the 2-ethylhexyl *N,N'*-analogue **146a**. The asymmetrically *N,O'*-ethyladamantyl substituted **6b** showed degradation at 264 °C, i.e. more than 100 °C less than in the case of the *N,N'*-derivative **6a**. Based on the DSC record and a comparison of **6a** and **6b**, it follows that the asymmetric substitution in the case of material **6b** prevents the formation of crystals and the resulting structure of the derivative thus tends to remain amorphous rather than crystalline. For the symmetrical *O,O'*-substituted derivative **6c**, it was not possible to determine the exact degradation temperature, as in the TG record a 20% mass loss was observed in the temperature range of 100 to 250 °C, followed by a sharp decrease after exceeding this temperature. Even so, the *O,O'*-substitution led to the formation of a much less stable material than in the case of *N,N'*-alkylated **6a**.

When comparing the influence of the substituents' character, it can be concluded that the ethyladamantyl chains contributed very significantly to the formation of crystalline forms of the resulting derivatives, with a substantial increase in the melting points of all three studied regioisomers.


### 6.1.5.3 Optical properties

First, the optical properties of all six isolated products in chloroform solutions were studied. The determined optical parameters are summarized in the following ***Table 14***.

***Table 14***: *Optical data of solutions determined from fluorescence and absorption measurements*

| DPP | $\lambda_{ABS\ max}$ [nm] | $\lambda_{ABS\ edge}$ [nm] | $\lambda_{PL}$ [nm] | PLQY [%] | $\tau$ [ns] | $E_{g\ opt}$ [eV] |
|---|---|---|---|---|---|---|
| **146a** | 547 | 569 | 563 | 63 ± 6 | 6.05 ± 0.01 | 2.23 |
| **146b** | 533 | 602 | 602 | 0.8 ± 0.5 | 0.63 ± 0.02 | 2.16 |
| **146c** | 505 | 598 | – | – | 0 | n.d. |
| **6a** | 549 | 572 | 562 | 65 ± 5 | 6.07 ± 0.01 | 2.23 |
| **6b** | 533 | 602 | 598 | 0.7 ± 0.5 | 0.65 ± 0.02 | 2.16 |
| **6c** | 505 | 598 | 731 | – | 0.32 ± 0.05 | 2.05 |

From the data obtained, it is obvious that while the type of alkyl chain had almost no influence on the optical spectra in solution, the position of substitution played a crucial role. The absorption maxima of the derivatives are shifted to shorter wavelengths with a trend from *N,N'*- (approx. 548 nm) followed by *N,O'*- (533 nm) to *O,O'*-substituted (505 nm).

The binding position of alkyl chains had a fundamental influence also on the fluorescence emission spectra, where a shift to higher wavelengths of the emission maxima was obtained in the order from *N,N'*- (563 nm) followed by *N,O'*- (approx. 600 nm) to *O,O'*-substituted derivative (731 nm for **6c**; unfortunately for 2-ethylhexyl **146c** it was not possible to measure a clear emission spectrum). Interestingly, the emission spectra of *N,O'*-substituted derivatives had a resolved vibronic structure in contrast to the absorption/excitation spectra, which may be due to the higher planarity of the molecule in the excited state than in the ground state. All obtained absorption and fluorescence emission spectra measured in solution are summarized in *Figure 41*.

Moreover, the substitution of the alkyl chains on the *O*-atom further led to a significant decrease in the photoluminescence quantum yields (PLQY) of the resulting products, from an average of 64 % for *N,N'*-derivatives to only 1 % for *N,O'*-derivatives. The PLQY of *O,O'*-products was determined to be too low for quantitative evaluation. The PLQY related to the fluorescence lifetime, which also decreased dramatically due to *O*-substitution (*Table 14*).
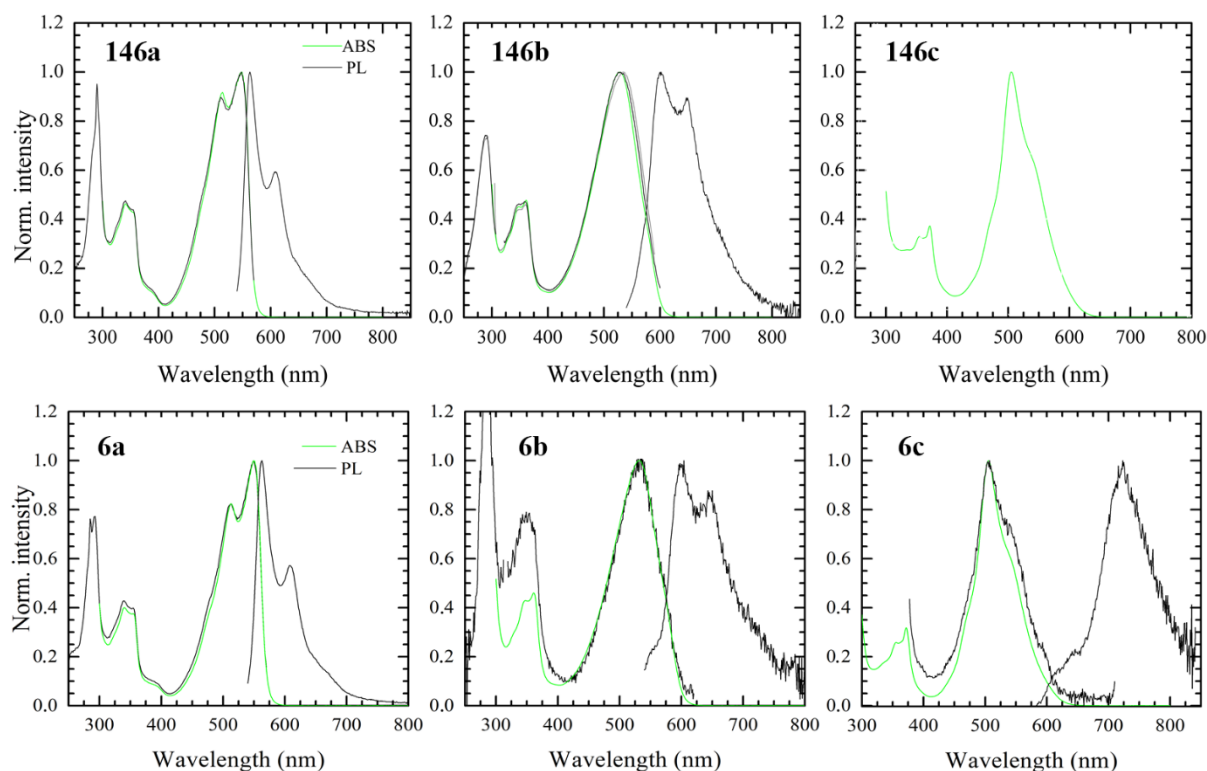


***Figure 41***: *Absorption and fluorescence spectra of studied DPPs dissolved in chloroform*

Subsequently, thin layers were prepared from the studied derivatives by the spin-coating method, and these were annealed at six different temperatures from the range of 50–300 °C with a step of 50 °C. The determined optical parameters of the appropriate layers, both as cast

and annealed, are summarized in **Table 15**; and all the absorption and fluorescence spectra obtained are plotted in **Figure 42**.

**Table 15**: *Optical parameters of thin films of the DPP derivatives under investigation*

| DPP | as cast film | | | annealed film | | |
|---|---|---|---|---|---|---|
| | $\lambda_{\text{ABS max}}$ [nm] | $\lambda_{\text{ABS edge}}$ [nm] | $\lambda_{\text{PL}}$ [nm] | $\lambda_{\text{ABS max}}$ [nm] | $\lambda_{\text{ABS edge}}$ [nm] | $\lambda_{\text{PL}}$ [nm] |
| **146a** | 508 | 613 | 696 | 510 | 613 | 695 |
| **146b** | 518 | 671 | 732 | 562 | 672 | – |
| **146c** | 508 | 622 | – | 509 | 621 | – |
| **6a** | 566 | 600 | 691 | 593 | 608 | 588 |
| **6b** | 541 | 623 | 740 | 547 | 633 | – |
| **6c** | 506 | 730 | – | 627 | ~750 | – |

In thin layers' study, the character of alkyl substituents had a significant effect on the absorption and emission spectra of the resulting DPPs in addition to their binding position, which is a big difference compared to the study of these derivatives in solutions.

The fundamental difference between the layers based on ethyladamantyl and 2-ethylhexyl DPPs was their thermal stability. While the films prepared from 2-ethylhexyl DPP derivatives lost their integrity upon annealing at lower temperatures and they vanished from the substrate after exceeding 150 °C, the layers based on ethyladamantyl DPPs showed stability even above 200 °C. However, this behaviour is entirely consistent with the data obtained from the DSC study of materials' thermal properties. In optical spectra, the loss of layer integrity was related to the decrease of signal intensity (**Figure 42**).
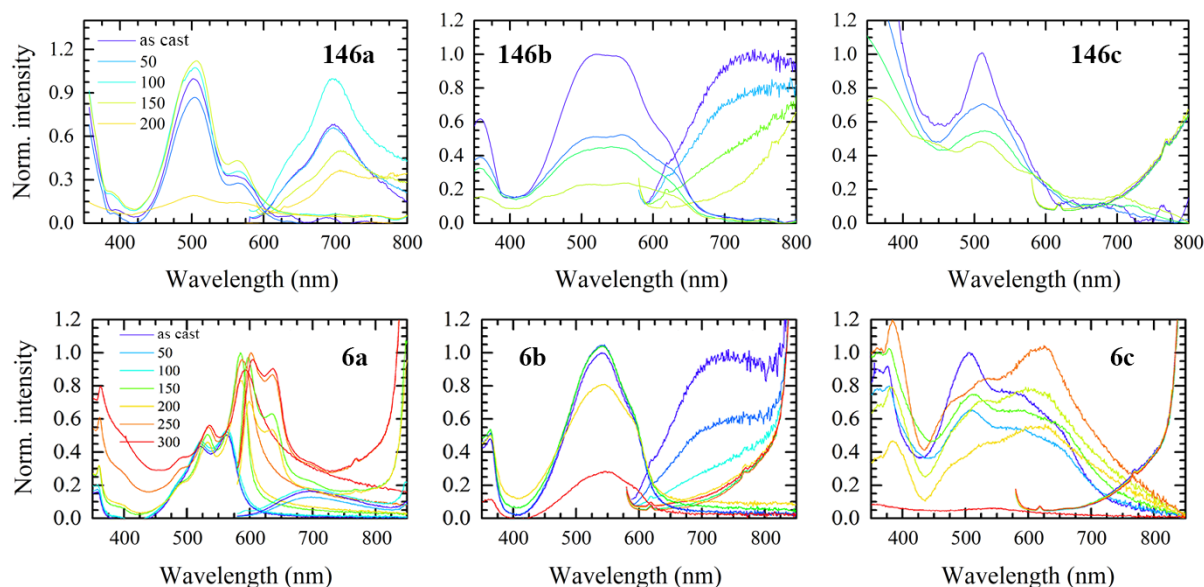


**Figure 42**: *Optical spectra of thin films from the studied DPPs annealed at different temperatures*

A common feature of both alkyl substituents was that their *O,O'*-products exhibited no fluorescence (**Figure 42** – only the background signal of the fluorimeter was observed), which was expected following the determined fluorescence data in the solutions (**Table 14**).

150

Furthermore, for both *N,O′*-substituted derivatives, a decrease in fluorescence intensity was observed after annealing at higher temperatures, indicating a loss of thin films' integrity. However, the same trend was also observed for the *N,N′*-2-ethylhexyl derivative (**146a**), while for the layers based on the *N,N′*-ethyladamantyl DPP (**6a**) the fluorescence intensity increased substantially after annealing. Thus, the quantum yield of fluorescence increased as well, which may be evidence of longer excitons lifetime due to higher molecular order.

A key difference between the two studied *N,N′*-products was also observed in the absorption spectra. As cast layers based on **146a** derivative showed a hypsochromic shift of the absorption maximum compared to the solution and the subsequent annealing of the layers up to 150 °C had only a slight effect on the shape of the spectrum. When annealing at 200 °C and above, no absorption was observed due to the vanishing of the material from the substrate, as already mentioned. In contrast, as cast layers from **6a** exhibited absorption similar to the solution, however, the annealing of the layers caused dramatic changes resulting in a significant bathochromic shift (by 27 nm, *Table 15*) indicating strong intermolecular interactions induced by the ethyladamantyl chains attached to *N*-atoms. Incidentally, these interactions are one of the key contributions to the high charge carrier mobilities of derivative **6a**, described in our previous work[50].
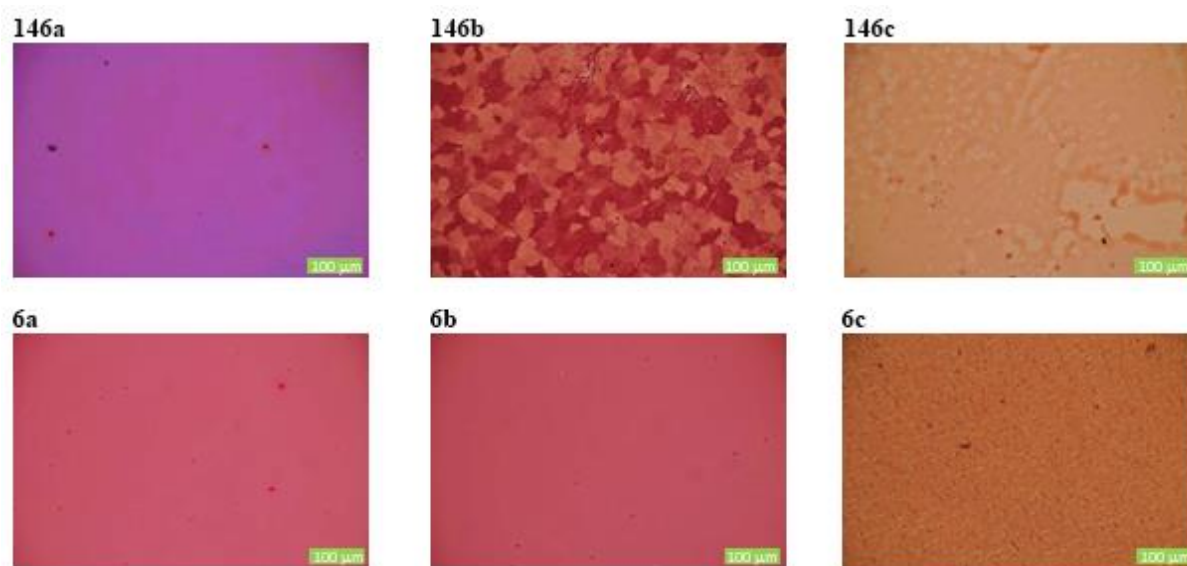


***Figure 43**: As-cast thin films prepared by spin-coating from the DPP derivatives under investigation*

As cast layers of both *N,O′*-products, **146b** and **6b**, had the absorption maxima similar to the solutions, which implies a rather individual character of the molecules in thin films, without strong interactions. However, a fundamental difference was observed in the absorption edge of both derivatives, when the layer of derivative **146b** had it at 671 nm, while the derivative of **6b** at only 623 nm. Interestingly, in solution, both derivatives had the same absorption edge at 602 nm. The extension of the absorption band of the layers to longer wavelengths indicates intermolecular interactions, which are thus more obvious in the case of as cast layer of the *N,O′*-2-ethylhexyl derivative **146b** due to its much larger shift. This finding can also be confirmed by optical microscopy photos (***Figure 43***), where the as cast layer of **146b** has a crystalline structure, while the **6b** based appears rather amorphous. The

present intermolecular interactions of both derivatives in films also confirm the significant bathochromic shifts of the emission maxima in comparison with the solutions.

The absorption maxima similar to the solutions also exhibited as cast thin layers prepared from both *O,O′*-derivatives, **146c** and **6c**. However, in the case of **146c** layer, the only weak bathochromic shift of absorption edge was observed in contrast to the layer based on **6c**, where the absorption edge was shifted by 120 nm to longer wavelengths compared to the solution. This indicated the presence of intermolecular π–π interactions in layers of **6c**, resulting in an at least partially ordered character of this derivative. On the other hand, 2-ethylhexyl derivative **146c** showed a waxy character, appearing as a liquid rather than a solid. These findings are again evident from optical microscopy photos (*Figure 43*). It should be noted that all isolated pure products showed a crystalline character with the exception of *N,O′*- and *O,O′*-2-ethylhexyl derivatives (**146b** and **146c**), which were rather waxy, as can be seen from *Figure 44*.
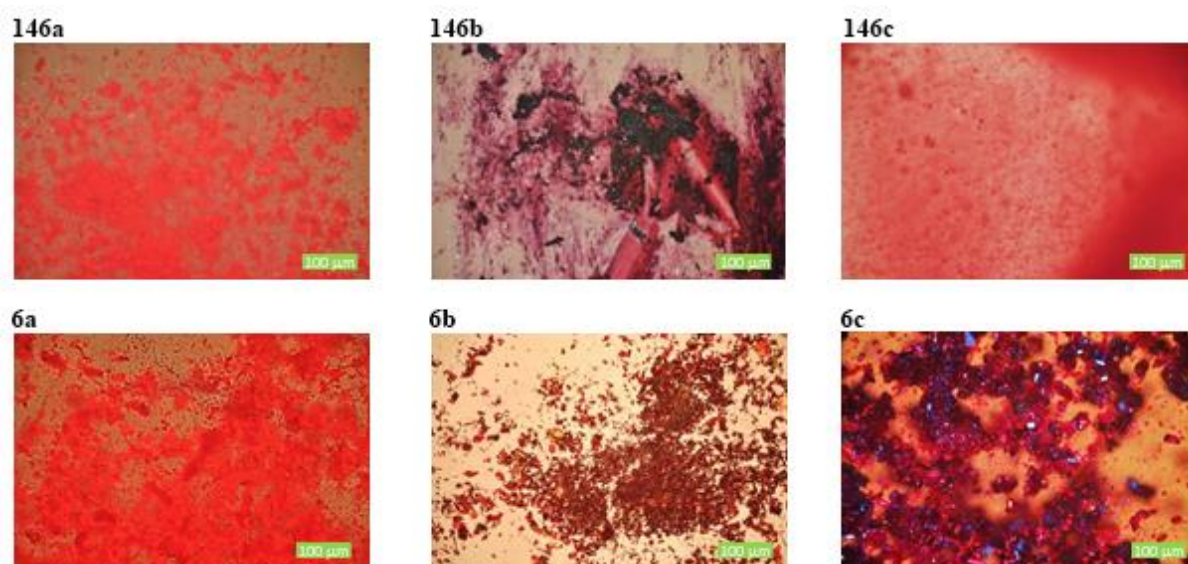


*Figure 44: Pictures of the studied DPP derivatives from optical microscopy*

In summary, it has been found that *O*-substitution generally leads to a significantly worse thermal stability of the resulting materials and a reduction in the formation of crystalline structures compared to *N*-alkylation. However, the 2-ethylhexyl side chains promote the formation of thin layer crystal structures based on the asymmetrically *N,O′*-substituted derivative, while the ethyladamantyl chains show a better molecular arrangement in the case of symmetrical *O,O′*-derivative according to the obtained optical and thermal data. Moreover, the ethyladamantyl substituent contributes to a significant increase in the melting points of all studied regioisomers and also improves their thermal stability compared to 2-ethylhexyl. In general, both the type of alkyl chain used and the position of its attachment in the DPP molecule have a major effect on the properties of the thin films. All these findings were successfully published in an impacted journal[200].

### 6.1.6 Synthesis of DPP-based polymers

#### 6.1.6.1 Polymerization by cross-coupling reactions

It is well known that *Stille cross-coupling* reactions are a very powerful tool for the preparation of a wide range of conjugated polymers[70,71,203,204] including DPP derivatives[109]. Herein is described the synthesis of a novel block copolymer based on a unique ethyladamantyl DPP derivative (**6a**) alternating with a thiophene unit. The thiophene organotin intermediate was prepared by a standard synthetic approach including lithiation of 2,5-dibrominated thiophene followed by reaction with tributyltin chloride[198]. The already prepared dibrominated derivative of ethyladamantyl DPP (**159**) was used as the second starting monomer for the polymerization (*Scheme 135*).
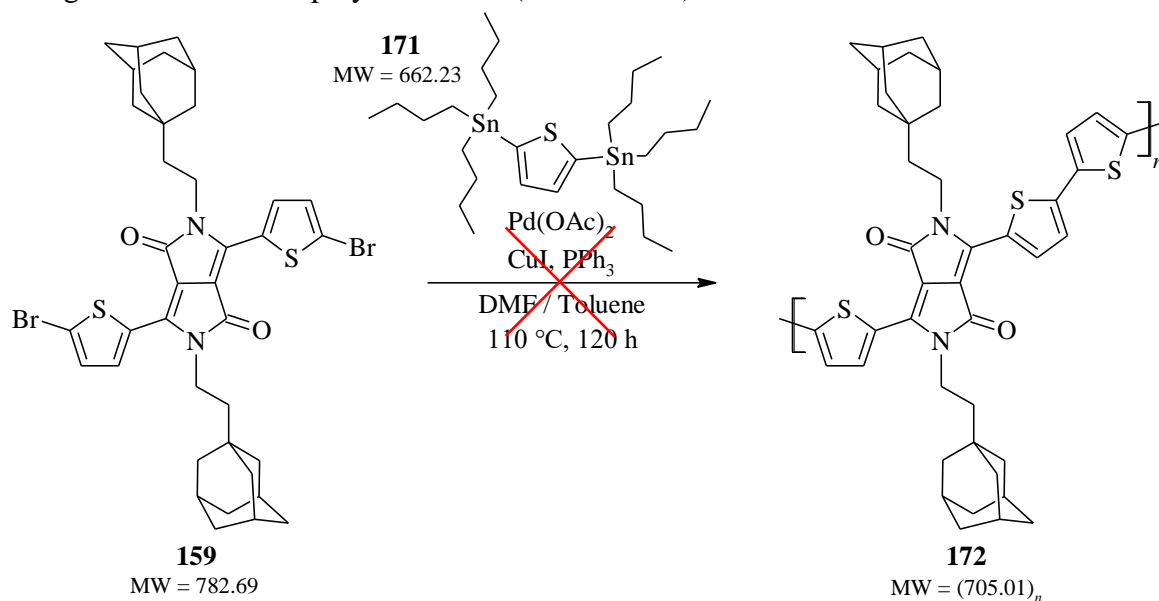


**Scheme 135**: *Preparation of ethyladamantyl-DPP based polymer by Stille cross-coupling reaction*

Based on information from the literature[204], the following mixture of catalyst, ligand and additive was used for the most efficient *Stille cross-coupling polymerization*. Palladium[II] acetate [Pd(OAc)$_2$] was chosen as the palladium catalyst. Next, triphenylphosphine (PPh$_3$) ligand was added to the reaction mixture as a reducing reagent leading to the immediate formation of a complex [Pd(OAc)$_2$(PPh$_3$)$_2$], which forms a Pd$^{(0)}$ complex by slow intramolecular reduction. The reason is the fact that *Stille* reaction is a Pd$^{(0)}$-catalysed cross-coupling reaction, where only Pd$^{(0)}$ complexes are active species in the catalytic cycle. Thus, when using Pd$^{(II)}$ sources, their reduction to Pd$^{(0)}$ is necessary, which can be mediated either by organostannane intermediates before entering the catalytic cycle itself or by the use of phosphine ligands. In addition, an additive in the form of an inorganic salt – copper iodide (CuI) – was used for the reaction. It is described that Cu$^{(I)}$ salts can enhance the *Stille* reaction by the so-called *copper effect*[204]. Liebeskind et al.[205] found that CuI acts as a free ligand scavenger, especially for strong ligands such as the PPh$_3$ used, which are known to inhibit transmetalation process. They further determined the optimized stoichiometric ratio of Pd$^{(II)}$ : ligand : Cu$^{(I)}$ = 1 : 4 : 2 to best increase both reaction rate and yield. An excessive amount of CuI is not desirable for the reaction because it then removes the ligand from the active

catalytic species, thereby reducing the stability of the catalyst and thus decreasing the yield of the reaction.

In this experiment, the used stoichiometric ratio of the three components discussed [Pd(OAc)$_2$:PPh$_3$:CuI] was approximately 1:3.5:3.3 and a 3:2 mixture of freshly distilled toluene and DMF was used as solvents. The solvent used is also a crucial parameter influencing the course of the reaction, especially the polymerization. It is important to sufficiently dissolve the starting monomers, to stabilize the catalyst and further maintain its functionality, as well as to be able to dissolve the growing conjugated polymer chain to form a high molecular weight polymer with narrow dispersity. It is therefore very convenient to use a mixture of solvents, typically, e.g. toluene/DMF (4:1), where the advantages of each of the solvents are exploited, while eliminating possible disadvantages. A suitable combination can then lead to a substantial improvement in the yield of the high molecular weight polymer formation[204,206].

Nevertheless, the performed experiment did not lead to the successful formation of the desired polymer **172**, despite an extreme extension of the reaction time (up to 120 h) and several partial additions of a new catalyst/ligand/copper salt mixture. Based on TLC analysis, starting material **159** was still observed as the majority. However, it is almost impossible to determine the cause of the failure in carrying out only one experiment, since almost unlimited variability is offered in the catalysts or ligands and additives used, as well as in the solvents, the temperature and the reaction time. The character of the starting monomers also has a significant effect on the course of the *Stille polymerization*. Unfortunately, especially for time reasons, priority was given to another synthetic branch, and polymerization using *cross-coupling* reactions was not addressed further in this work.

### 6.1.7 Incorporation of electron-accepting groups into DPPs

As previously described, the most important and widely used electron-accepting groups for the derivatization of DPPs include dicyanovinyl groups[46,51] and rhodanine derivatives[128–130]. Based on the information discussed in the review part (*Chapter 3.2.1.1*), the incorporation of dicyanovinyl groups into the DPP skeleton brought in many cases (**2**[46], **7**[51], **9**[51] molecules) very interesting electrical properties of the resulting derivatives. Therefore, the aim here was to modify the exceptional ethyladamantyl-thienyl-DPP derivative (**6a**) with these functional groups. The synthesis of *N,N′*-2-ethylhexyl-thienyl-DPP derivative was performed to verify the synthetic path[46].

#### 6.1.7.1 *N,N′-(2-EtHex)-bis(5-dicyanovinyl-2-thienyl)-DPP*

The target derivative *N,N′*-(2-ethylhexyl)-bis(5-dicyanovinyl-2-thienyl)-DPP (**2**) was synthesized according to the described two-step synthetic approach (*Scheme 136*)[46] starting with the basic *N,N′*-alkylated DPP (**146a**). By lithiation using LDA at cryogenic temperature, the DPP-dianion was prepared, which was subsequently reacted with the formylation reagent DMF to give the diformyl derivative **49a** in a yield of 15 % (literature yield 27.8 %)[46]. The reaction was performed without prior optimization, which could be the reason for the lower

yield. In the second step, a *Knoevenagel condensation* of the formyl derivative was performed with 3 equivalents of malononitrile and in the presence of an excess of aluminium oxide (7 equiv.) as the base. The desired product **2** was successfully prepared with a decent yield of 41 %.
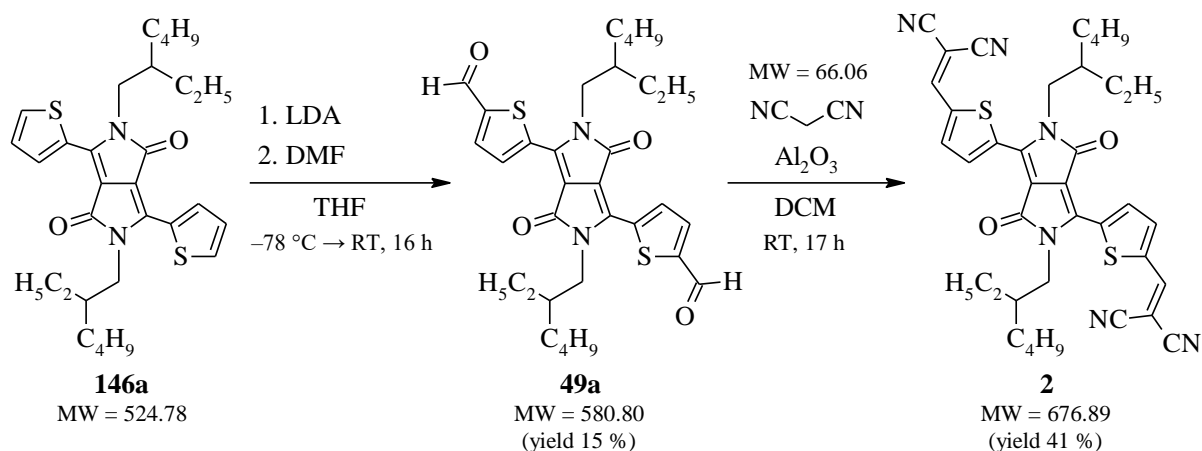


**Scheme 136**: *Two-step synthetic approach used to prepare the target DPP derivative 2*

### 6.1.7.2  N,N'-EtAd-bis(5-dicyanovinyl-2-thienyl)-DPP

As already described in the review section (*Chapter 4.1.3.2*), due to the extremely limited solubility of the starting *N,N'*-ethyladamantyl DPP derivative (**6a**), it was not possible to prepare its diformyl derivative by lithiation and subsequent formylation using DMF/*N*-formylpiperidine unlike the 2-ethylhexyl analogue (**49a**). Therefore, an alternative synthetic path was chosen (also outlined in *Chapter 4.1.3.2 – Scheme 10*) involving the incorporation of formyl functional groups already into the DPP skeleton in the form of acetal-protected groups. This synthetic approach was first tested on the preparation of the phenyl-DPP derivative requiring only two simple synthetic steps (**Scheme 137**).
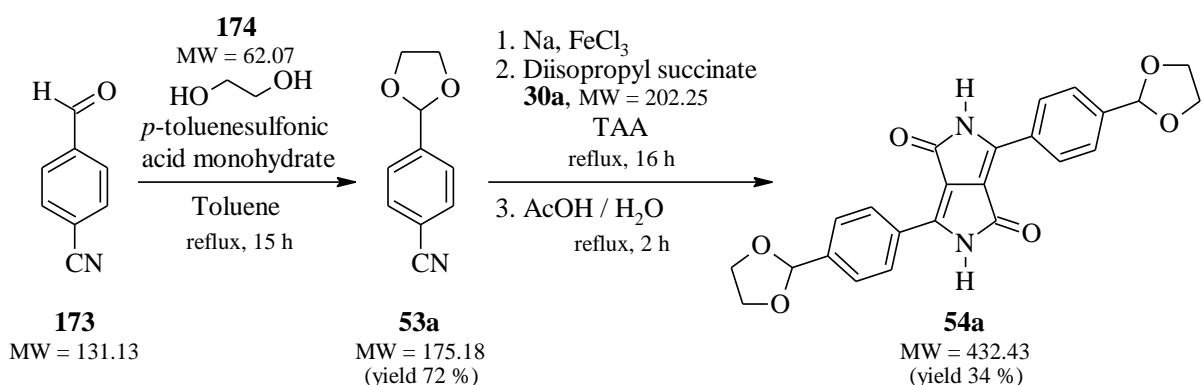


**Scheme 137**: *Test synthetic approach for the preparation of DPP derivative 54a*

It started with the readily commercially available 4-formylbenzonitrile (**173**) and the protection of its formyl functional group with 1,3-dioxolane by a well-known procedure[207]. The obtained formyl-protected arylnitrile **53a** in a decent yield of 72 % was subsequently

used for the synthesis of the DPP skeleton (**54a**) by a conventional *succinic method*[87]. Derivative **54a** was successfully prepared in a yield of 34 %.

Thiophene-carbonitrile **53b** was synthesized *via* a two-step synthesis started with thiophene, which was subjected to a classical *Vilsmeier-Haack* reaction to form product **50b** in a yield of 76 %, followed by protection of the formyl group to give derivative **175**. Intermediate **175** was subsequently brominated to afford **52b** (**approach A**, *Scheme 138*). However, bromination of derivative **175** exhibited poor regioselectivity according to GC-MS analysis, and therefore pure product **52b** was not isolated, and an alternative synthetic approach had to be applied (**approach B**, *Scheme 138*).

In the second synthetic path, derivative **50b** was first selectively brominated to give pure product **51b** with a purity of 98 % (GC-MS) in a yield of 42 %. The obtained derivative **51b** was then subjected to formyl group protection to successfully afford the product **52b** in an excellent yield of 74 %. In the last step, the nucleophilic substitution of the bromine atom for a cyano group was performed according to a known procedure[192]; thus obtaining the desired arylnitrile **53b** in a yield of 27 %.
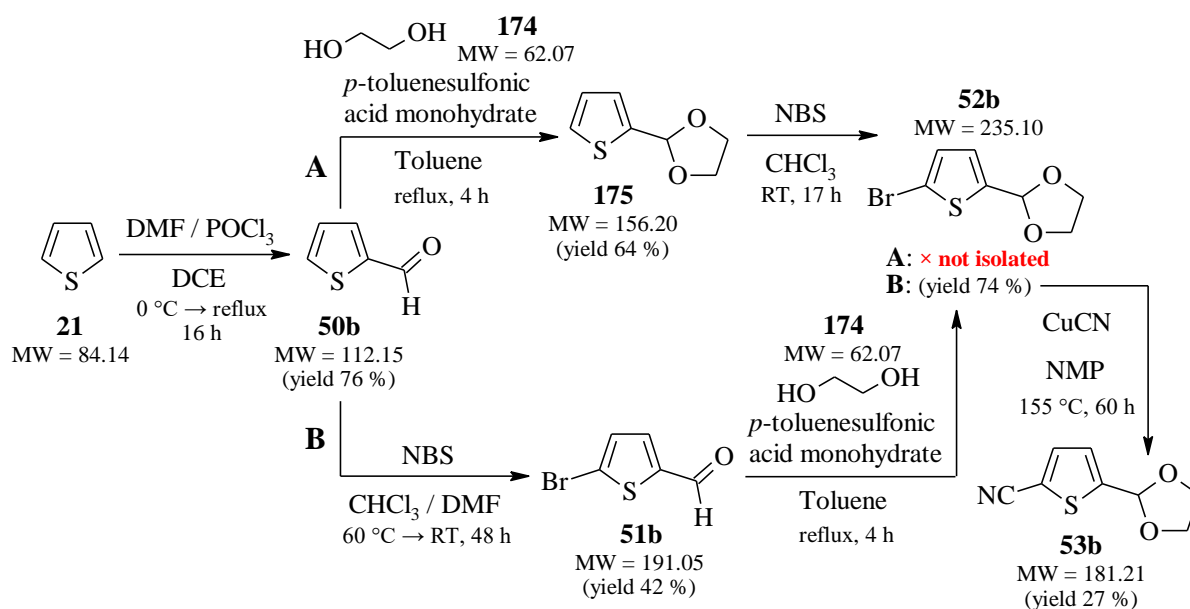


*Scheme 138: Synthetic approaches A/B used to prepare targeted aromatic nitrile 53b*

The following **Scheme 139** outlines the ongoing synthetic procedure to obtain the desired diformyl derivative from *N,N′*-ethyladamantyl-thienyl-DPP (**6a**). The preparation of the basic DPP (**54b**) will be realized by the classical *succinic method*[87], as in the test case (**Scheme 137**). Subsequently, a conventional base catalysed alkylation[45,90] will be performed focusing on the isolation of the *N,N′*-alkylated product (**202**). In the last step, the acid-catalysed deprotection of derivative **202** using dilute hydrochloric acid solution[132] will be carried out to give the final diformyl derivative **49b** as starting material for the already verified *Knoevenagel condensation* with malononitrile (**Scheme 136**).

This synthetic path (**Scheme 139**) has not yet been realized due to time constraints. In principle, however, there should be nothing to prevent the successful preparation of the targeted derivative.
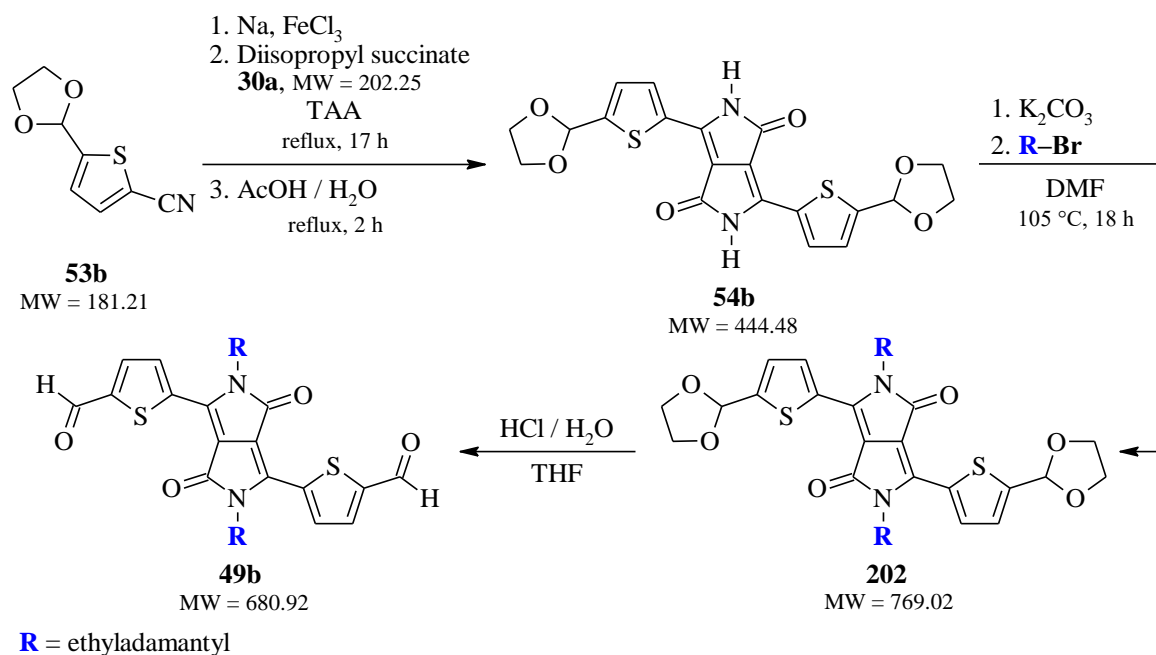
**Scheme 139**: *The proposed synthetic approach for the preparation of diformyl-DPP derivative **49b***

### 6.1.8 Synthesis of thioketo analogues of DPPs (DTPPs)

#### 6.1.8.1 Synthesis of basic DTPPs and with extended π-conjugation

The transformation of basic DPP derivatives into their thioketo analogues was performed *via* the well-described thionation[140,141] using Lawesson's reagent in chlorobenzene (**Scheme 140**). The reaction mixtures were stirred for 20 h at reflux, and the desired products were isolated in yields from 52 % to 96 % (**Table 16**), which is in accordance with the literature[140,141,143].
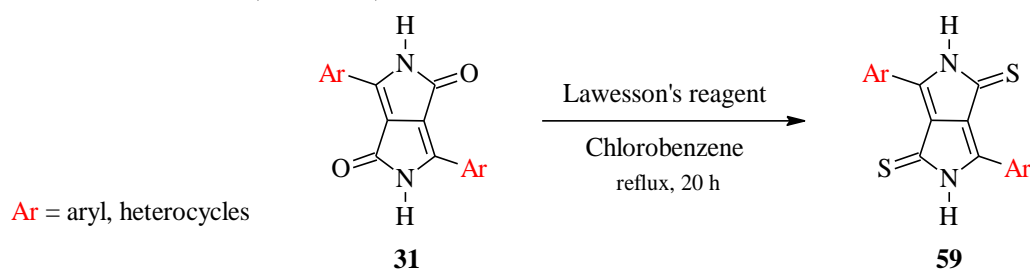


**Scheme 140**: *General synthetic approach used for thionation of DPPs using Lawesson's reagent*

**Table 16**: *Summary of all prepared dithioketopyrrolopyrroles (DTPPs)*

| DPP | 59a | 176 | 59b | 177 | 178 |
|---|---|---|---|---|---|
| Ar | 2-thienyl | 2-bithienyl | phenyl | 2-naphthyl | 4-pyridinyl |
| Yield [%] | 87 | 96 | 82 | 87 | 52 |

The prepared derivatives were used both for next synthetic steps (discussed further) and for an in-depth study of their physicochemical properties, which are currently the subject of intensive research.

157

### 6.1.8.2 Synthesis of N- and S-alkylated DTPPs

Furthermore, the series of *N*- and *S*-alkylated DTPP derivatives were prepared. In terms of reactivity and reaction mechanism, it is necessary to use different synthetic approaches for the preparation of these two series of alkylated products (*Scheme 141*).
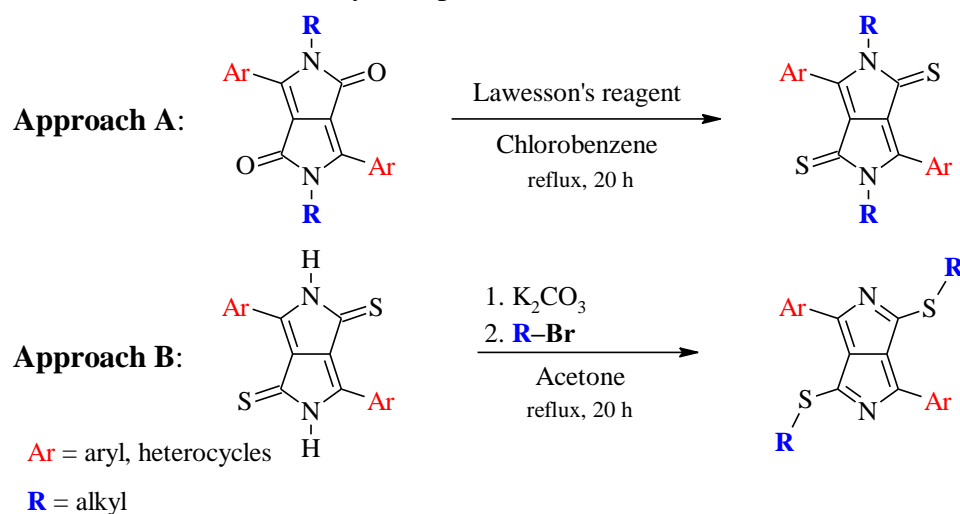


Scheme 141: Two synthetic approaches used to prepare N- (**A**) and S-alkylated (**B**) DTPPs

For the selective preparation of *N,N'*-alkylated DTPPs, it is necessary to start with already *N,N'*-alkylated DPP derivatives and subject them to thionation using Lawesson's reagent (**Approach A**, *Scheme 141*). The reason is the relative reactivity of DPP- vs DTPP-anion to nucleophilic substitution (discussed in *Chapter 4.1.5*), where the sulphur-anion is a better nucleophile than the nitrogen-anion. Therefore, alkylation occurs primarily at *S*-positions in the case of the DTPP molecule, which thereby largely gives the second desired product: *S,S'*-alkylated DTPPs (**Approach B**, *Scheme 141*). Based on the experiments performed, it is impossible to isolate any proportion of *N,N'*-alkylated DTPPs using synthetic **approach B**.

Table 17: Summary of all prepared N- and S-alkylated DTPP derivatives

| DPP | Approach | Ar | R | Yield [%] |
|-----|----------|-----|---|-----------|
| 179 | A | 2-thienyl | ethyladamantyl | 79 |
| 180 | A | phenyl | ethyladamantyl | 61 |
| 181 | B | 2-thienyl | dodecyl | 47 |
| 182 | B | 2-thienyl | ethyladamantyl | 63 |
| 183 | B | 2-thienyl | methyladamantyl | –[a] |
| 184 | B | 2-bithienyl | ethyladamantyl | 20 |
| 185 | B | phenyl | dodecyl | –[a] |
| 186 | B | phenyl | ethyladamantyl | 30 |

[a] product was most likely completely decomposed

Two derivatives substituted with ethyladamantyl chains (**179** and **180**) were successfully prepared by synthetic **approach A** in yields exceeding 60 % (***Table 17***). An analogous synthesis has been described in the literature for the *N,N'*-dioctyl derivative, but the authors emphasize the need to perform the reaction in the dark to prevent early decomposition of the product. They also described that even with all handling in the dark, the product decomposed within 30 minutes of being in solution[145]. However, nothing similar was observed with the derivatives **179** and **180** prepared in this work, and they appeared relatively well stable in the light. The reason could be the presence of adamantyl side chains and their contribution to increasing the stability of the resulting derivatives, as observed for the recently published series of *N,N'*-; *N,O'*- and *O,O'*-alkylated DPPs (*Chapter 6.1.5*)[200]. However, an in-depth stability study of the prepared derivatives has not yet been performed, and therefore the exact cause is not yet known.

A total of four derivatives were successfully prepared by synthetic **approach B**. The reactions proceeded analogously to the alkylation of the basic DPP derivatives described above, i.e. the base-promoted nucleophilic substitution of alkyl bromides (*Chapter 6.1.4.1*). In all cases, poor product stability was observed; however, the effect of degradation due to light exposure is known from the literature[145] for alkylated DTPP analogues. Nevertheless, all manipulation were performed under ambient conditions with access to light, which probably led to the complete decomposition of derivatives **183** and **185**. The properties of isolated products are further the subject of an in-depth study of physicochemical properties.

## 6.2 BDF derivatives

### 6.2.1 Symmetrical BDF derivatives

The mechanism of the BDF skeleton formation was described in detail in the review section (*Chapter 4.2*). The key starting materials are α-hydroxy acids (AHAs), which react with hydroquinone in acidic conditions, and the resulting BDF molecule is formed after double cyclization followed by oxidation of the di-condensate formed (***Scheme 15–17***)[146,149,150].

#### 6.2.1.1 Synthesis of diphenyl-BDF derivative (10a)

In the beginning, the main interest was focused on the verification of the synthetic possibilities for the preparation of the basic diphenyl-BDF derivative, already described in the literature[54,55] (***Scheme 142***).

Two synthetic approaches were used: **Approach A** uses the reaction of mandelic acid (**69a**) with 0.5 equimolar amount of hydroquinone (**42**) leading directly to double cyclization. After oxidation with nitrobenzene, the desired BDF derivative was prepared in a yield of 38 % (lit. 35 %[54]). **Approach B** first involves the reaction of mandelic acid (**69a**) with an excess (2.5 equiv.) of hydroquinone (**42**) to prepare the mono-condensate **75a**[150], which was isolated in 58% yield, followed by reaction with mandelic acid (**69a**) in a stoichiometric ratio of 1 : 1 to give the di-condensate. After its oxidation, the resulting BDF derivative was prepared in a yield of 35 %.
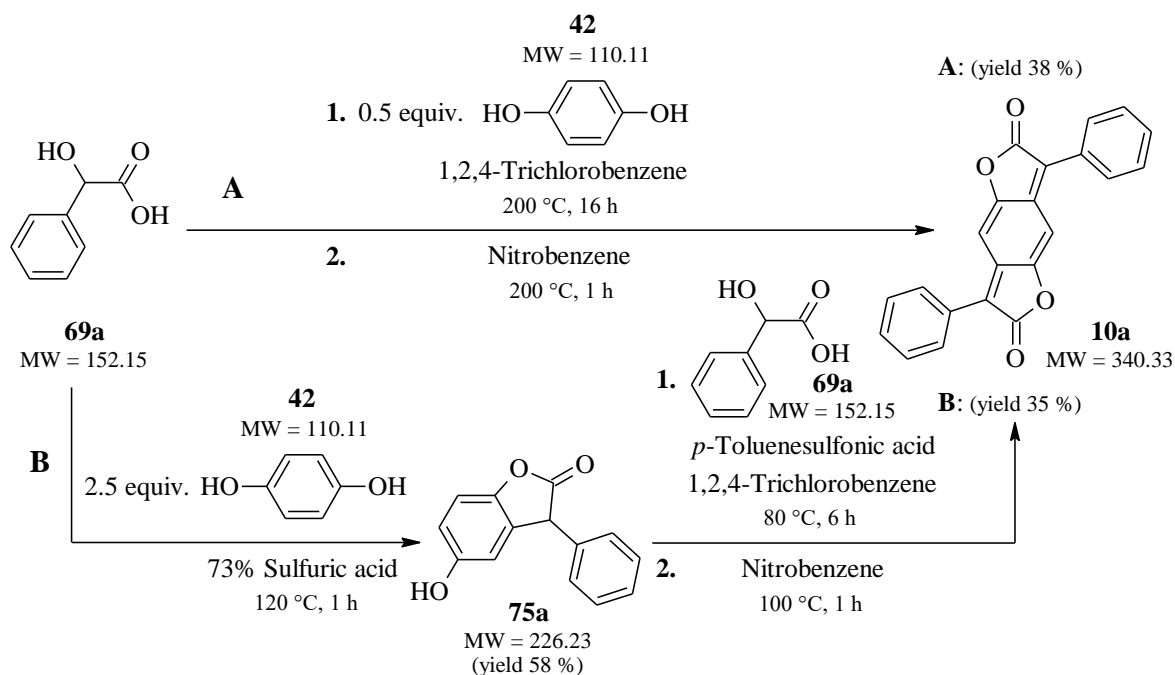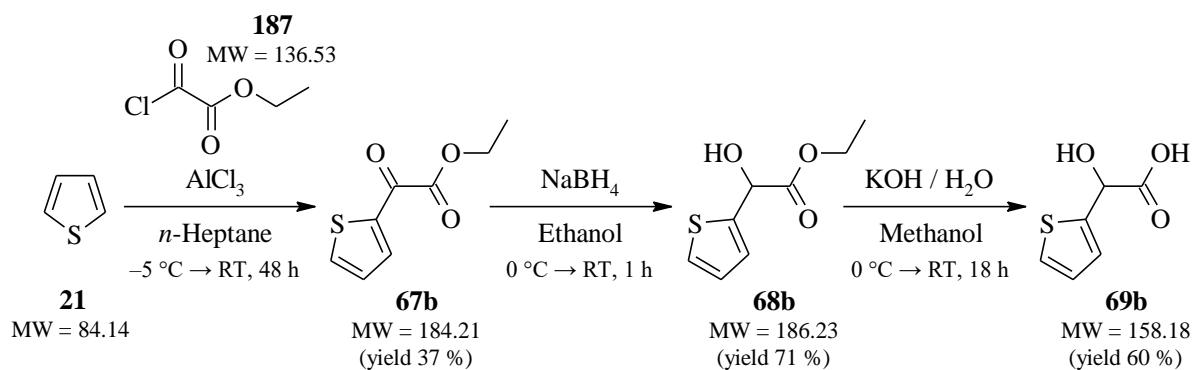
**Scheme 142**: Two synthetic approaches (**A/B**) used to prepare the diphenyl-BDF derivative **10a**

According to the experimental results, both of the above-mentioned synthetic paths are applicable. **Approach A** provided higher overall yields; on the other hand, **approach B** opens the possibility of preparing asymmetric BDF derivatives, which will be discussed further.
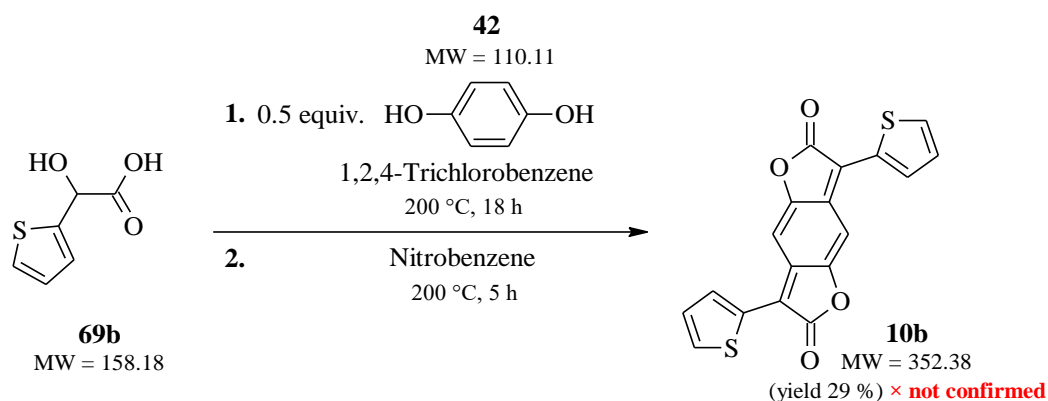
### 6.2.1.2 Synthesis of dithienyl-BDF derivative (10b)

Hydroxy(thiophen-2-yl)acetic acid (**69b**) was prepared according to the synthetic approach discussed in the review section (*Chapter 4.2.1*)[148]. First, a classical *Friedel-Crafts acylation* of thiophene was performed using ethyl chlorooxoacetate (**187**) and aluminium chloride to give the derivative **67b** in a yield of 37 %. Subsequently, the α-keto ester was reduced with sodium borohydride to the α-hydroxy ester **68b** in 71% yield. The final step was base catalysed hydrolysis of the ester to afford the desired thienyl-AHA **69b** in 60% yield (**Scheme 143**).



**Scheme 143**: Three-step synthetic approach used to prepare the target thienyl-AHA (**69b**)

The prepared derivative **69b** was subsequently used for an analogous synthesis of the BDF derivative, as in the case of **approach A** in the previous chapter (*6.2.1.1*, **Scheme 142**). The reaction time of the condensation and the following oxidation were extended, and probably the desired product **10b** was obtained in a yield of 29 % as a dark black-blue solid (***Scheme 144***).



**Scheme 144**: *Preparation of a novel dithienyl-BDF derivative **10b***

Nevertheless, the structure of the obtained material could not be confirmed, probably due to its extremely limited solubility in most organic solvents. This significantly hampered the possibilities of both its analysis and purification only for stirring in refluxing toluene followed by the filtration while hot. Structural analysis was performed using $^1$H NMR spectroscopy measured in hot DMSO-$d_6$; however, the spectra obtained were very indeterminate, and it was not possible to confirm the structure of product **10b**.

Therefore, an alternative synthetic path was chosen, where the formation of the final BDF core is preceded by the preparation and isolation of the mono-condensate, as described in the previous chapter as **approach B** (*Chapter 6.2.1.1*, **Scheme 142**). Thienyl based mono-condensate (**75b**) was expected to have better solubility in organic solvents and thus a higher probability for better purification and its structural analysis. Two approaches were used to prepare mono-condensate **75b**, the first starting from the thienyl-AHA (**69b**), which was reacted with hydroquinone in the presence of sulphuric acid (**approach A**, **Scheme 145**)[150]. The second method started with the α-hydroxy ester **68b**, which also reacted with hydroquinone, but in the presence of *p*-toluenesulfonic acid (**approach B**, **Scheme 145**)[208].
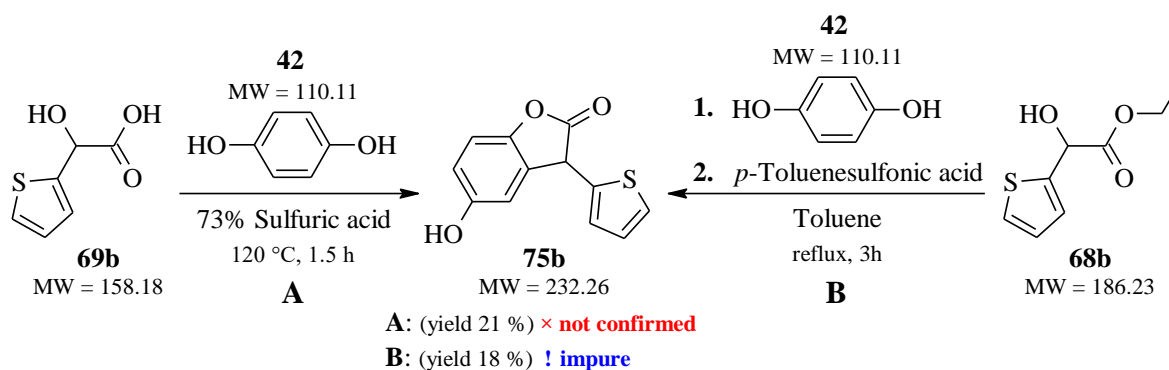


**Scheme 145**: *Two synthetic approaches (**A/B**) used to prepare the thienyl mono-condensate **75b***

In both cases, materials were obtained in approximately the same yield (**A**: 21 % vs **B**: 18 %); however, the substances were of a different character (**A**: dark violet-black solid vs **B**: dark green solid). In the case of **approach A**, contrary to expectations, the obtained product exhibited extremely limited solubility in most organic solvents, which led to a failure of both its purification and identification, as in the previous derivative **10b**. In contrast, the product obtained in **approach B** showed a relatively good solubility, which allowed its purification by column chromatography in a mixture of chloroform/ethyl acetate 9 : 1. Nevertheless, even the purification of the obtained material did not lead to a sufficiently pure product **75b**, the structure of which would be definitively confirmed by $^1$H NMR analysis (spectrum listing is given in the experimental part, *Chapter 5.5.1.2*).

However, efforts to obtain and confirm the structure of both derivatives, **75b** and especially dithienyl-BDF **10b**, will continue in the future, as they are still completely novel and highly promising molecules.

### 6.2.1.3 Synthesis of bis(4-alkyl-2-thienyl)-BDF derivative (78c)

Since in the previous cases the characterization of the thienyl-BDF derivative (**10b**) and his intermediate (**75b**) always failed due to their extremely poor solubility in organic solvents, its BDF-analogue containing side solubilising alkyl groups was prepared (**78c**). The presence of dodecyl chains should improve the solubility of the resulting BDF derivative. In addition, bromine atoms were present in the α-positions of the thiophene, giving the product very extensive synthetic possibilities for *cross-coupling* reactions and thus its further advanced structural modifications.

The key intermediate (5-bromo-4-methyl-2-thienyl)(hydroxy)acetic acid (**69c**) was prepared using a three-step synthetic approach (***Scheme 146***), identical to the previous synthesis of thienyl-AHA **69b** (*Chapter 6.2.1.2*, ***Scheme 143***). The final product **69c** was isolated in an overall yield of 23 % relative to the starting 2-bromo-3-dodecylthiophene (**128**).
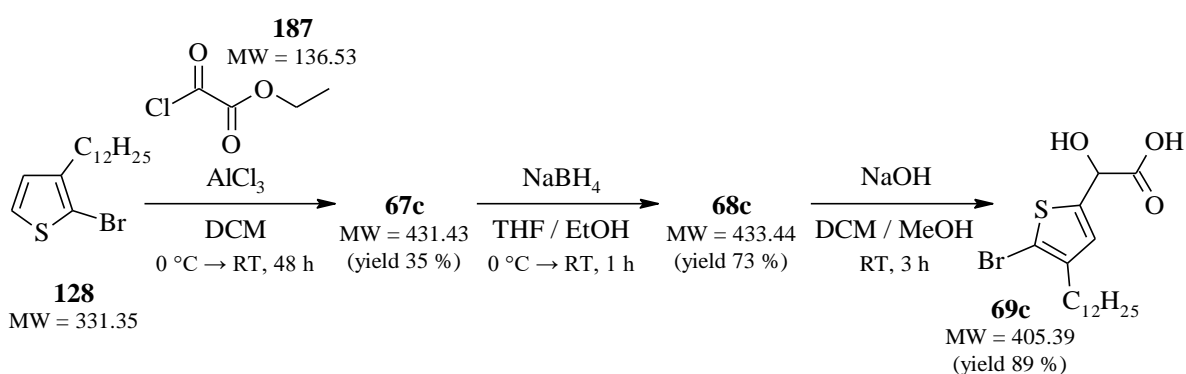


*Scheme 146*: Three-step synthetic approach used to prepare the target thienyl-AHA (*69c*)

The obtained derivative **69c** was used for the direct synthesis of the di-condensate by its reaction with 0.5 equimolar amount of hydroquinone (**42**), using the same synthetic method mentioned above (***Scheme 147***). However, the oxidation was not performed immediately, but the product **78c** was isolated in 28% yield as a dark blue-black solid and purified by crystallisation from 1 : 1 toluene/methanol. $^1$H NMR analysis again did not confirm the

structure of the desired product **78c**, and therefore its successful preparation could not be verified.
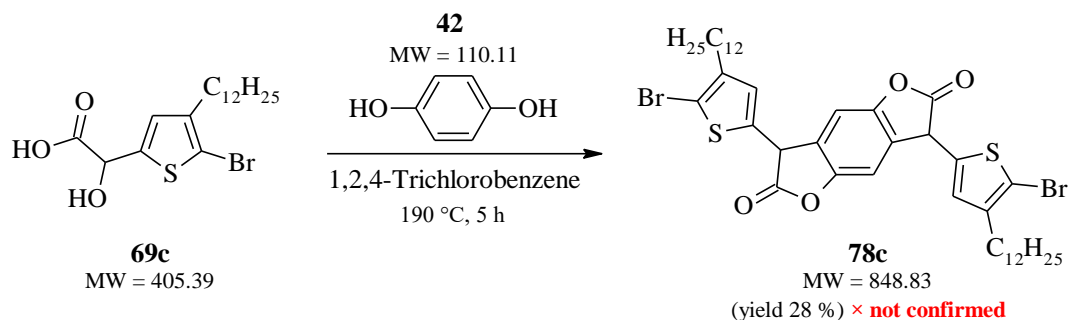


**Scheme 147**: *Preparation of 3,7-bis(5-bromo-4-dodecyl-2-thienyl)-3,7-dihydro-BDF (**78c**)*

### 6.2.2 Asymmetrical BDF derivatives

The obtained and structurally confirmed intermediates from the previous synthetic paths were used for preparation two asymmetric derivatives BDF, **10c** and **10d** (*Scheme 148*). Both reactions started with phenyl mono-condensate **75a** as starting material, and the reaction conditions were set according to the verified synthetic **approach B** in the synthesis of symmetric phenyl-BDF **10a** (*Chapter 6.2.1.1*, *Scheme 142*), only the oxidising agent chloranil was used instead of nitrobenzene.
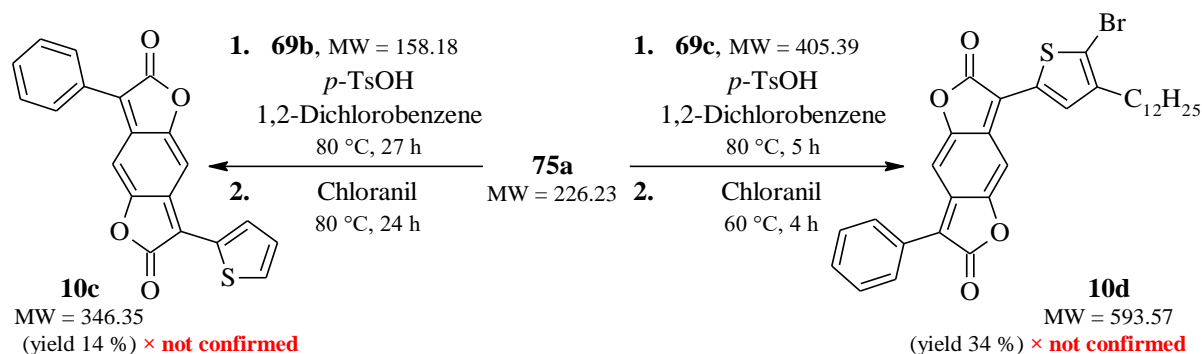


**Scheme 148**: *Preparation of asymmetrical BDF derivatives **10c** and **10d***

Thienyl-AHA **69b** was reacted with 1.0 equiv. of mono-condensate **75a** in the presence of *p*-toluenesulfonic acid and after subsequent oxidation with chloranil, probably product **10c** was obtained in a yield of 14 %. Under the same conditions, but with a shortened reaction time, **75a** reacted with β-alkylated-thienyl-based AHA **69c**, followed by oxidation with chloranil to give the potential product **10d** in a decent yield of 34 %. Both materials obtained, **10c** and **10d**, had the character of dark violet-black high-melting solids ($T_{MP}$ of **10c** was above 320 °C), exhibiting typical pigment properties, as expected. However, none of these derivatives could be obtained in sufficiently high purity to confirm their structure.

So even here, the result from previous experiments in the preparation of BDF derivatives containing thiophene units was repeated. In all cases, the materials having organic pigment properties were isolated; however, their structure could not be confirmed by conventional characterization techniques as, e.g. NMR spectroscopy. Considerable efforts will undoubtedly be further made to prepare and validate the target thienyl-BDFs mentioned herein.

## 6.3 EP derivatives

### 6.3.1 Synthesis of *N,N'*-alkylated EPs
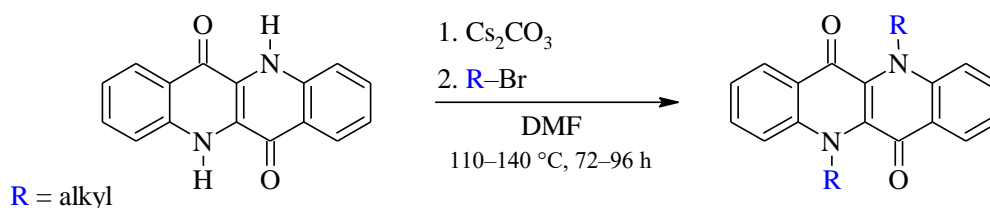


**Scheme 149**: *General synthetic approach used for alkylation of EP molecule*

The base catalysed nucleophilic substitution of alkyl bromides was used to prepare the two target *N,N'*-alkylated EP derivatives (**Scheme 149**), the same synthetic approach as for the DPP derivatives discussed above (*Chapter 6.1.4.1*)[45,90]. The alkylating reagents used were 1-(bromomethyl)adamantane (**144**) and 1-(2-bromoethyl)adamantane (**141**).
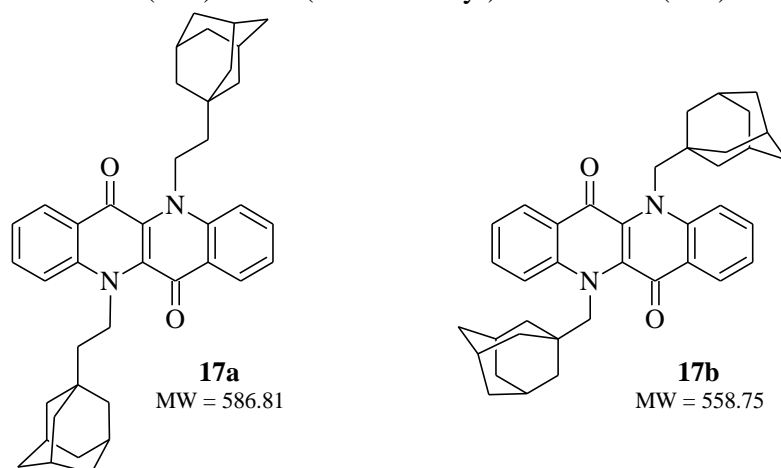


**Figure 45**: *Structures of two prepared derivatives of EP – 17a and 17b*

**Table 18**: *Summary of the preparation of two EP derivatives – 17a and 17b*

| EP | Temperature [°C] | Reaction time [h] | Yield [%] |
|-----|-----|-----|-----|
| 17a | 110 | 72 | 3.6 |
| 17b | 140 | 96 | 2.5 |

Both reactions required a high temperature above 100 °C and long reaction time in the order of several tens of hours. The yield in both syntheses was only percent units (**Table 18**), which was probably due to the bulkiness of the adamantyl substituents. As expected, the yield was worse in the case of substitution with methyladamantyl chains (**17b**) due to the more difficult steric accessibility of the neopentyl chain compared to ethyladamantyl, as already discussed for DPPs. The regioselectivity of the reactions was very poor according to TLC analysis and a number of by-products, most likely *O*- and mono-substituted, were observed. These by-products were not isolated and identified in this work; however, they significantly devalued the yields of the desired molecules **17a** and **17b**.

Further characterizations of thermal, optical and electrical properties will be provided and, in addition, the contribution of adamantyl substituents to the resulting properties of EP derivatives in comparison with DPPs will be investigated.

## 6.4 NTD derivatives

### 6.4.1 Synthesis of *N*- and *O*-alkylated NTDs

#### 6.4.1.1 Synthesis of O,O'-alkylated NTD derivatives

Alkylation of the NTD molecule *via* nucleophilic substitution is one of the most significant and widely used modifications of these derivatives. Although the NTD molecule containing dilactam groups is structurally similar to DPP, the alkylation process is significantly different here caused by the position of the nitrogen heteroatoms in the molecule together with steric factors. Therefore, the asymmetric *N,O'*-derivative is always formed as a majority, while *N,N'*-alkylated is the least formed[70,164], which is the exact opposite of DPP alkylation[45,90]. Since asymmetric *N,O'*-products were not evaluated as potentially interesting materials in terms of structural properties and ability to self-assembly in thin layers; the aim was to prepare and isolate symmetrical *O,O'*-alkylated products. The alkylation chains were used analogously to the modification of DPP derivatives: dodecyl as linear, 2-ethylhexyl as branched and ethyladamantyl as bulky.

The reaction was performed by the above-mentioned synthetic approach using a base (Cs2CO3) and an alkyl bromide (**Scheme 150**). Various solvents were tested to improve the regioselectivity of the alkylation (**Table 19**) but without significant effect. The most important parameter appeared to be a longer reaction time of the order of several days. Ethyladamantyl bromide exhibited the best regioselectivity of the alkylation leading to the formation of the *O,O'*-substituted NTD derivative (**190**), which was prepared in the highest yield of about 70 % compared to other derivatives.
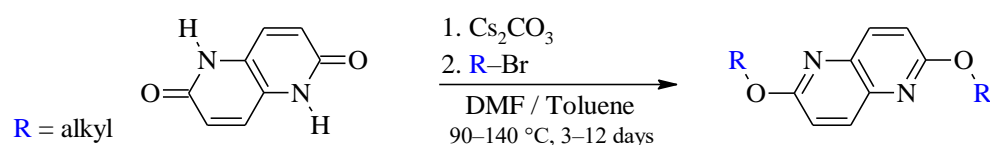


*Scheme 150*: *General synthetic approach used for alkylation of NTD molecule*

*Table 19*: *Summary of the preparation of O,O'-alkylated NTD derivatives*

| NTD | 188 | 189 | 190 | 190[a] |
|---|---|---|---|---|
| R | dodecyl | 2-ethylhexyl | ethyladamantyl | ethyladamantyl |
| Solvent | DMF | DMF | DMF / Toluene | DMSO |
| Temperature [°C] | 90 | 90 | 140 | 135 |
| Reaction time [h] | 96 (4 days) | 288 (12 days) | 72 (3 days) | 42 h |
| Yield [%] | 26 | 4.6 | 72 | 67 |

[a] there has been an effort to obtain as much *N,N'*-product (**191**) as possible – described below

All three prepared *O,O'*-alkylated NTD derivatives will be studied from the point of view of optical and thermal properties. In particular, the contribution of adamantyl side chains and their effect on the resulting properties of the product will be studied and compared to other related compounds.

### 6.4.1.2 Synthesis of N,N'-alkylated NTD (191)

To prepare the *N,N'*-ethyladamantyl-NTD derivative (**191**), the alkylation synthetic approach (discussed in the previous *Chapter 6.4.1.1*, *Scheme 150*) was first used, referred to herein as **approach A**. DMSO was used as a solvent for the reaction, and the mixture was stirred at 135 °C for almost 2 days. However, as can be seen from *Table 19*, the *O,O'*-product (**190**, yield 67 %) was again isolated as the majority, while the *N,N'*-alkylated derivative (**191**) was obtained only in a yield of 3.4 % (*Table 20*) as yellow low-melting substance. The structures of both isolated products and the positions of the alkyl chains' attachment were confirmed by NMR analysis. Therefore, it is a very inefficient synthetic method, which can never be used for the targeted preparation of *N,N'*-substituted product in larger quantities.

*Table 20: Summary of obtained yields of N,N'-derivative (191) by two different approaches*

| NTD 191 | Approach A [a] | Approach B |
|---|---|---|
| Yield [%] | 3.4 | – |

[a] detail of the experiment in *Table 19*; *O,O'*-product (**190**) was obtained as the majority

Thus, an alternative synthetic approach using an alkyl-migration rearrangement, referred to herein as **approach B** (*Scheme 151*), has been tried. *O,O'*-alkylated NTD (**190**) was used as the starting material, which was reacted with triflic acid (TfOH) in DCE solvent.
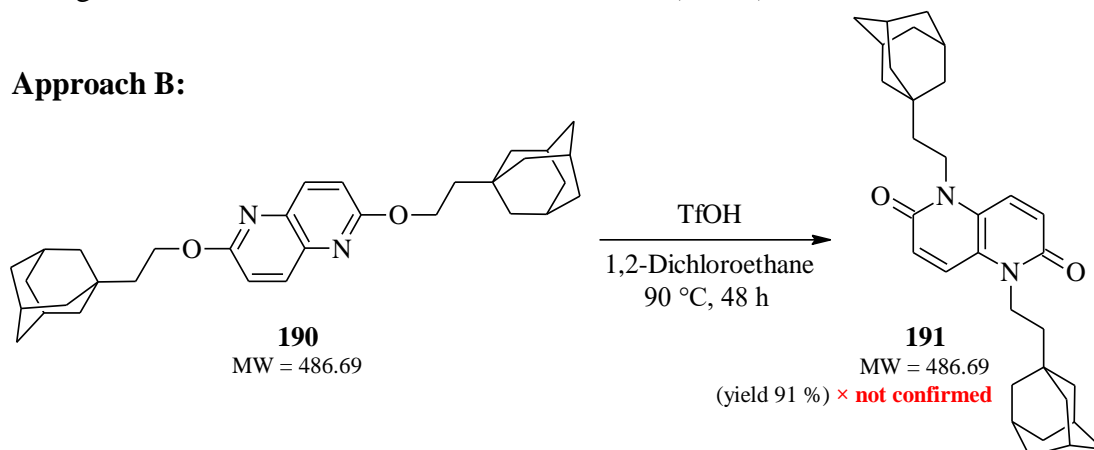


*Scheme 151: Preparation of N,N'-ethyladamantyl-NTD (191) – approach B*

The inspiration for the chosen synthetic **approach B** was the work published in 2018 by Mishra et al.[209], where they described a very efficient metal-free transition of alkyl chains from *O*- to *N*-atoms in the preparation of *N*-alkylated pyridones and benzothiazolones. Authors optimized the reaction parameters on the transformation of 2-methoxypyridine to *N*-methylpyridone (*Scheme 152*). The optimum temperature was determined at 90 °C, and the reaction time was required at least 24 h. The resulting *N*-alkylated product (**204**) was obtained

in an excellent yield of 83 % using 1.0 mmol of the starting *O*-alkyl derivative (**203**), 20 mol% of catalyst TfOH and only 0.3 mL of DCE solvent. By reducing the proportion of catalyst TfOH (to 10 mol%) and solvent DCE (to 0.15 mL), the desired product **204** was obtained in a yield of even 98 %. However, due to the handling of the reaction components, the transformation of the alkyl chains in the NTD molecule was carried out under the afore-mentioned conditions, which should also sufficiently provide the *N,N'*-product (**191**). The assumed mechanism of *O*- to *N*-alkyl migratory rearrangement catalysed by TfOH in DCE is described in detail in **Scheme 152**, which Mishra et al.[209] substantiated by DFT calculations.
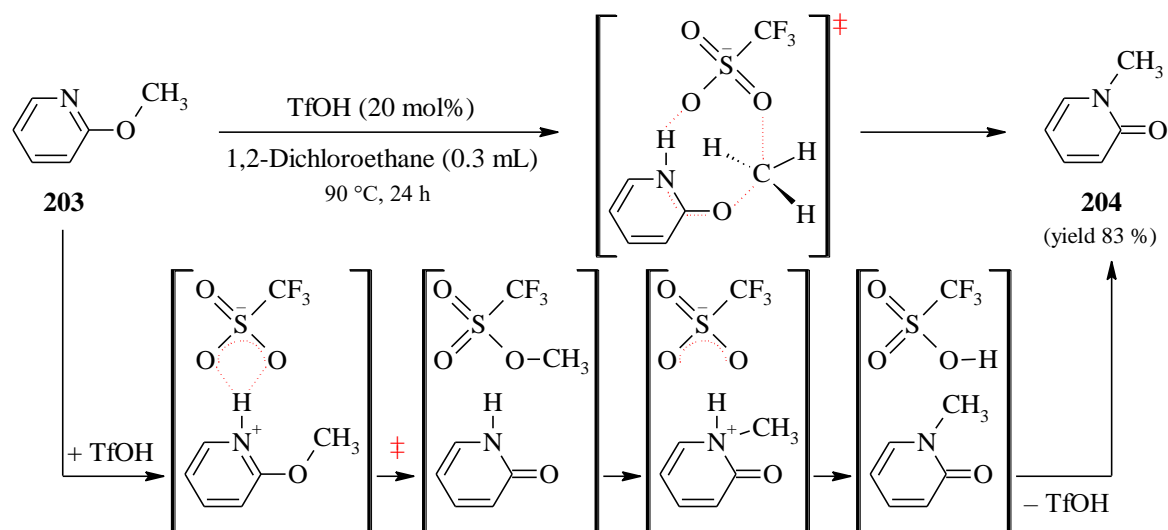


***Scheme 152***: *Published reaction of 2-methoxypyridine (**203**) to N-methylpyridone (**204**) with possible mechanism of O- to N-alkyl migratory rearrangement*[209]

Therefore, the above-mentioned synthetic procedure was performed on the *O,O'*-ethyladamantyl NTD (**190**) and a slightly yellowish solid product was isolated in a yield of 91 %. However, $^1$H NMR analysis did not confirm the structure of the expected *N,N'*-product (**191**). Nevertheless, this promising synthetic approach has been performed without optimization, and there is still a wide variety of catalysts/solvents and their ratios that can be used to achieve the expected results.

## 6.5 Preparation of PT derivative

### 6.5.1 Synthetic route to the key monomer based on sexithiophene

#### 6.5.1.1 Preparation of key Stille intermediates

In this synthetic route, a total of two *Stille intermediates* were prepared and subsequently used for *cross-coupling* reactions. The first of these, referred to herein as **196** (***Figure 46***), was prepared from 2-bromo-3-dodecylthiophene, which was first converted by reaction with magnesium in the presence of iodine as the catalyst to *Grignard reagent*, then reacted at cryogenic temperature with trimethyltin chloride to give the final product **196** in a yield of 86 %. This is the already described synthetic approach, which was carried out in full accordance with the literature and with the expected result[84]. However, the purity of the obtained material **196** was determined by GC-MS to only 55 %, which was unexpected and

therefore, this had to be considered in further reactions. The stoichiometric ratio of the *Stille intermediate* **196** was thus doubled from that required to compensate for its low purity. A negative effect on the course of the reaction due to this excess was not expected, as the majority of impurities were 3-dodecylthiophene, which should not react under the conditions of the following *Stille cross-coupling* reaction.



**196**
MW = 415.26
(yield 86 %)

**200**
MW = 475.68
(yield 67 %)
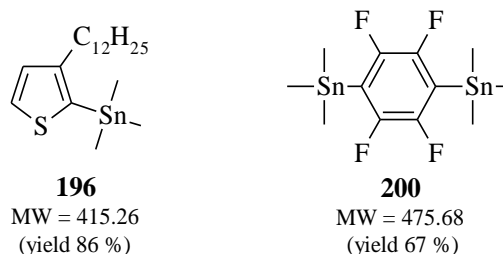
*Figure 46*: *Structures of two prepared Stille intermediates – 196 and 200*

The latter Stille intermediate **200** was prepared from 1,4-dibromobenzene by its lithiation with *n*-BuLi at –78 °C followed by reaction with trimethyltin chloride. After purification by crystallization in *n*-heptane, the product **200** was prepared in a yield of 67 % and subsequently used for the final *polymerization* step.

### 6.5.1.2 *Preparation of the key monomer based on sexithiophene*

Since the final polymerization step was performed using *Stille cross-coupling* reaction, the key monomer for the preparation of the resulting polymer based on β,β'-dialkylated sexithiophene was its dibrominated derivative (**198**). Five steps of the synthetic route led to the preparation of **198** (*Scheme 153*), starting with 2-bromothiophene (**156**) and its conversion to the *Grignard reagent* **193** in a conventional way. **193** was subsequently used for the reaction with 5,5'-dibromo-2,2'-bithiophene (**192**) in the presence of a palladium[II] catalyst by *Kumada cross-coupling* reaction to give quaterthiophene (**194**) in a great yield of 88 %. In the next step, **194** was brominated with NBS to give the dibromo derivative **195** in a yield of 94 %. **195** was used for the subsequent reaction with the already prepared *Stille intermediate* **196** to obtain β,β'-dialkylated sexithiophene (**197**) by *Stille cross-coupling* reaction and using pulsed microwave heating in a high yield of 80 %. The previously discussed catalyst/ligand/additive mixture [Pd(OAc)$_2$/PPh$_3$/CuI] was also tested in this synthesis but did not lead to any product. The commonly used PdCl$_2$(PPh$_3$)$_2$ catalyst proved to be excellent. In the final step, bromination of **197** was performed with NBS to give the final target monomer **198** in a yield of 61 %. Both brominations in this synthetic approach required elevated temperature (~80 °C) and relatively high dilution due to the limited solubility of the starting polythiophene derivatives.
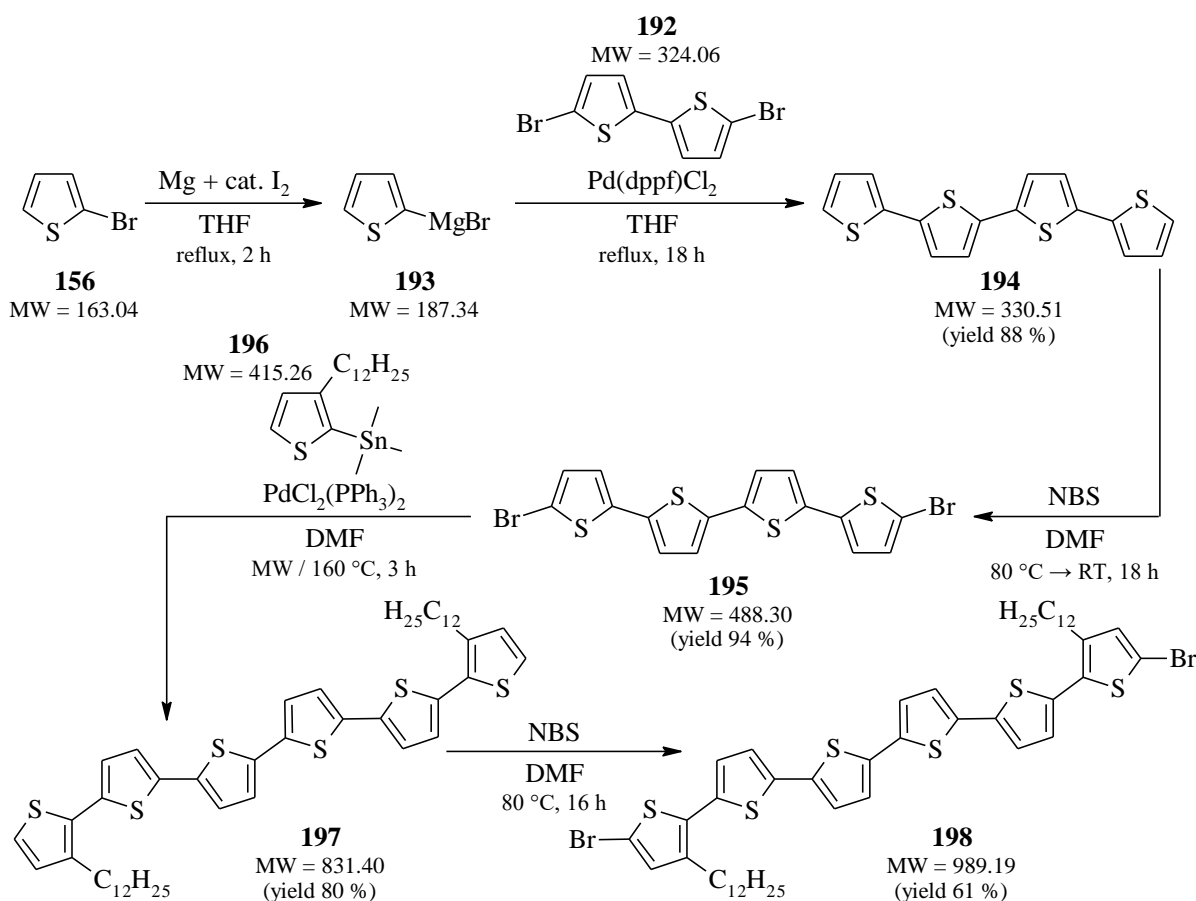
**Scheme 153**: *Five-step synthetic route to the key monomer based on sexithiophene (**198**)*

In summary, the resulting monomer **198** was prepared in an overall yield of 40 %, which is an excellent value since none of the steps was optimized. In addition, **198** is a novel derivative, not yet described in the literature.

### 6.5.2 Final polymerization to the targeted polymer (201)

As already mentioned, the final polymerization was performed by reacting the dibromo-derivative **198** with the *Stille intermediate* **200** by *Stille cross-coupling* reaction (**Scheme 154**). Numerous experiments have been performed in which various solvents (chlorobenzene, DMF, toluene) and catalysts [Pd(PPh$_3$)$_4$, PdCl$_2$(PPh$_3$)$_2$, a mixture of Pd(OAc)$_2$/PPh$_3$/CuI] have been tested. In all cases, microwave heating of the reaction mixture with a pulse technique was used, the maximum temperatures being chosen according to the nature of the solvent.

The best polymerization results were obtained using a chlorobenzene solvent with a dilution of approx. 7 mg/mL and 5–6 mol% of Pd(PPh$_3$)$_4$ catalyst. The maximum heating temperature was set at 140 °C and the reaction time of one MW cycle was 3 h. It proved to be beneficial to repeat the MW cycle 1–2 times after the addition of another 5 mol% of catalyst. At best, polymer **201** was prepared with a narrow distribution of about 4 500 g mol$^{-1}$ in a yield of 39 %.

**200**
MW = 475.68

Pd(PPh₃)₄

Chlorobenzene
MW / 140 °C, 3 h

**198**
MW = 989.19

**201**
MW = (977.44)ₙ
(yield 39 %)
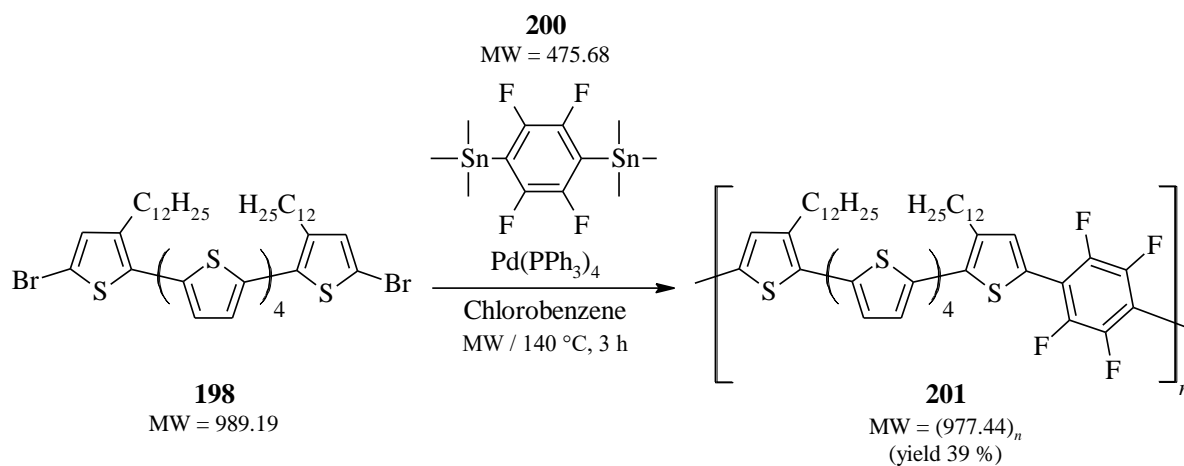
*Scheme 154: Preparation of β,β′-didodecyl-α-sexithiophene-tetrafluorophenyl polymer (**201**)*

The experiment was repeated many times, and the target polymer **201** was prepared in moderate yields from 39 % to 65 % and with a sufficient degree of polymerization (MW ≈ 4 100 g mol$^{-1}$ according to GPC) for the purposes of the following study of the optical, electrical as well as photovoltaic characteristics planned for this material.

# 7 CONCLUSIONS

The doctoral thesis deals with organic high-performance pigments applicable in the fields of organic electronics. The first part of the theoretical section of the thesis introduced the issue of organic electronics and photonics and the basic parameters that materials applicable in these areas must meet. Furthermore, a group of substances called organic high-performance pigments was characterized, and gradually selected groups of these substances (DPPs, BDFs, ID/IID/EPs, NTDs, PTs) were introduced. From each group, the most important derivatives showing exceptional properties in the fields of organic electronics were described, especially in terms of the transport characteristics in OFET devices, but also PCE in BHJ-SC devices. Moreover, the influence between the structure of derivatives and the resulting properties was briefly discussed. Therefore, the structures of individual derivatives subsequently served as inspiration for the own design of completely novel derivatives, potentially useful in similar applications. In the second part of the theoretical section, the synthetic possibilities of appropriate groups of derivatives and their most common structural modifications were described. Emphasis was focused primarily on the description of the latest and most effective synthetic possibilities leading to the desired final derivatives.

In the experimental part of the thesis, all performed experiments were described in detail. A total of 103 molecules were successfully prepared in this doctoral thesis, of which 54 were intermediates, and 49 were target products. Of the target products, 27 were completely novel, not yet described in the literature (their overview is listed in *Chapter 10*). On the other hand, the 14 experiments performed were unsuccessful and did not lead to the desired products.

In the following results and discussion section, the individual synthetic approaches were gradually evaluated. One of the main motives of the experimental part of the thesis was the incorporation of bulky adamantyl derivatives into the molecules of organic high-performance pigments and the study of their influence on the resulting properties. In particular, an in-depth study was performed on the series of *N,N'*-; *N,O'*- and *O,O'*-alkylated thiophene DPP derivatives by ethyladamantyl chains and for comparison 2-ethylhexyl's as the most commonly used alkylated DPPs in the literature. No comprehensive study describing their physicochemical properties has been published so far for these relatively overlooked derivatives. On the other hand, these are by-products, the formation of which must be considered in every alkylation of lactam groups by branched or bulky alkyl chains. Herein, 2 series with a total of 6 derivatives were prepared, on which the selectivity of alkylation, thermal properties and optical properties in both solutions and thin films were studied.

It has been found that the nature of the alkyl chains have a crucial influence on the formation of *N,N'*-alkylated products and with the increasing bulkiness of these substituents the ratio of *O*-alkylated products formed increases. Furthermore, it has been shown that *O*-substitution leads to a significant deterioration in the thermal stability of the resulting derivatives compared to *N*-substitution. On the contrary, the contribution of adamantyl chains proved to be distinctive, as it significantly increased the melting points and thermal stability of all 3 regioisomers in comparison with 2-ethylhexyl derivatives. The obtained results were published in an impacted journal[200].

In the same trend, adamantane chains have been incorporated into a diverse range of other DPPs and also into the molecule of another representative of organic pigments, epindolidone. For the vast majority of these derivatives, the expected result of increased thermal stability and melting points due to the presence of adamantyl substituents was observed. Other physicochemical properties and especially the application potentials of these novel derivatives are further studied in detail, and the results will be published in the future.

Furthermore, a series of thioketo analogues of DPP derivatives (DTPPs) were prepared, both basic non-alkylated and substituted by alkyl chains on sulphur and nitrogen atoms. Detailed studies of the properties of all these derivatives are further in progress. Efforts have also been focused on the synthesis of a DPP derivative containing both adamantyl chains and strong electron-accepting dicyanovinyl groups in its structure, which should bring a significant improvement in the transport characteristics of the derivative based on published results discussed in the review section. However, this is a relatively demanding, multi-step synthetic route, which, unfortunately, was not completed for this doctoral thesis.

A series of *O,O'*-alkylated NTD derivatives containing bicyclic lactam groups analogous to DPP derivatives was also prepared using dodecyl, 2-ethylhexyl and ethyladamantyl chains. Studies of physicochemical properties and the study of their application potentials are also being carried out on isolated derivatives. The formation of *N,N'*-alkylated NTDs is minor compared to DPPs and in the case of *N,N'*-ethyladamantyl NTD, it was not possible to obtain a yield higher than 3.4 %. Unfortunately, the possibility of preparing this derivative by metal-free *O*- to *N*-alkyl migratory rearrangement using TfOH and DCE as solvent[209] has also failed.

Moreover, as part of this doctoral thesis, a completely novel, as yet undescribed polymer containing alternating units of β,β'-didodecyl-sexithiophene and tetrafluorobenzene was prepared. The study of physicochemical properties, especially in terms of the effect of π-conjugation prolongation of the monomer, is also in progress and the polymer application potential in photovoltaic devices is further investigated. The results should be published soon.

Unfortunately, the synthetic branch leading to thiophene analogues of BDF has so far proved unsuccessful. The reference synthesis of the already described phenyl-BDF was successful by both known approaches – through the direct double condensation and through the isolation of mono-condensate with subsequent cyclisation by AHA molecule. In the case of thiophene analogues of BDFs, both symmetrical unsubstituted or substituted by solubilising dodecyl chains, and asymmetrical, the structures of the resulting derivatives were not confirmed in any of the cases. Nevertheless, the isolated substances usually showed the character of an organic pigment, but the used structural analyses did not confirm the existence of the desired skeleton. It is very difficult to determine the exact cause of this failure; however, the obstacle was most likely in the structural analysis and not in the synthesis itself. This issue will be further intensively solved.

# 8 REFERENCES

1   U.S. ENERGY INFORMATION ADMINISTRATION: *International energy outlook 2019* [online]. U.S. Department of Energy, Washington DC, 20585 (09-24-**2019**) [cited 2020-02-20]. Available from: https://www.eia.gov/outlooks/ieo/pdf/ieo2019.pdf

2   BAGHER, A. M. Comparison of Organic Solar Cells and Inorganic Solar Cells. *Int. J. Renew. Sustain. Energy*. 2014, **3**(3), 53–58. DOI: 10.11648/j.ijrse.20140303.12

3   HOPPE, H. and N. S. SARICIFTCI. Organic solar cells: An overview. *J. Mater. Res*. 2004, **19**(7), 1924–1945. DOI: 10.1557/JMR.2004.0252

4   SNAITH, H. J. Perovskites: The Emergence of a New Era for Low-Cost, High-Efficiency Solar Cells. *J. Phys. Chem. Lett*. 2013, **4**(21), 3623–3630. DOI: 10.1021/jz4020162

5   LOGOTHETIDIS, S. Flexible organic electronic devices: Materials, process and applications. *Mater. Sci. Eng., B*. 2008, **152**(1–3), 96–104. DOI: 10.1016/j.mseb.2008.06.009

6   PONOMARENKO, S. A., Y. N. LUPONOSOV, J. MIN, et al. Design of donor-acceptor star-shaped oligomers for efficient solution-processible organic photovoltaics. *RSC: Faraday Discuss.* 2014, **174**, 313–339. DOI: 10.1039/C4FD00142G

7   LIU, X., Y. SUN, B. B. Y. HSU, A. LORBACH, L. QI, A. J. HEEGER and G. C. BAZAN. Design and Properties of Intermediate-Sized Narrow Band-Gap Conjugated Molecules Relevant to Solution-Processed Organic Solar Cells. *J. Am. Chem. Soc*. 2014, **136**(15), 5697–5708. DOI: 10.1021/ja413144u

8   SIRRINGHAUS, H. 25th Anniversary Article: Organic Field-Effect Transistors. *Adv. Mater.* 2014, **26**(9), 1319–1335. DOI: 10.1002/adma.201304346

9   IDTechEx: *Printed, Organic and Flexible Electronics 2020-2030: Forecasts, Technologies, Markets* [online]. 12-**2019**. [cited 2020-02-20]. Available from: https://www.idtechex.com/en/research-report/printed-organic-and-flexible-electronics-2020-2030-forecasts-technologies-markets/687

10  XU, R-P., Y-Q. LI and J-X. TANG. Recent advances in flexible organic light-emitting diodes. *J. Mater. Chem. C*. 2016, **4**(39), 9116–9142. DOI: 10.1039/C6TC03230C

11  RIM, Y. S., S-H. BAE, H. CHEN, N. DE MARCO and Y. YANG. Recent Progress in Materials and Devices toward Printable and Flexible Sensors. *Adv. Mater*. 2016, **28**(22), 4415–4440. DOI: 10.1002/adma.201505118

12  VAN HEERDEN, D., H. YOON, Y. DU, J. SALAMI and Z. YANG. Ultrafine nanoparticle-based conductive inks for printed electronics and solar applications. *Adv. Microelectron*. 2010, **37**(6), 8–10. DOI: 10.4071/amim-37-6

13  QUINN, J. T. E., J. ZHU, X. LI, J. WANG and Y. LI. Recent progress in the development of n-type organic semiconductors for organic field effect transistors. *J. Mater. Chem. C*. 2017, **5**(34), 8654–8681. DOI: 10.1039/C7TC01680H

14  LI, X., W. ZHANG, K. USMAN and J. FANG. Small Molecule Interlayers in Organic Solar Cells. *Adv. Energy Mater.* 2018, **8**(28), 1702730. DOI: 10.1002/aenm.201702730

15  SOKOLOV, A. N., M. E. ROBERTS and Z. BAO. Fabrication of low-cost electronic biosensors. *Mater. Today*. 2009, **12**(9), 12–20. DOI: 10.1016/S1369-7021(09)70247-0

16 SHI, L., Y. GUO, W. HU and Y. LIU. Design and effective synthesis methods for high-performance polymer semiconductors in organic field-effect transistors. *Mater. Chem. Front.* 2017, **1**(12), 2423–2456. DOI: 10.1039/C7QM00169J

17 LIN, Y., Y. LI and X. ZHAN. Small molecule semiconductors for high-efficiency organic photovoltaics. *Chem. Soc. Rev.* 2012, **41**(11), 4245–4272. DOI: 10.1039/c2cs15313k

18 SHIRAKAWA, H., E. J. LOUIS, A. G. MACDIARMID, Ch. K. CHIANG and A. J. HEEGER. Synthesis of electrically conducting organic polymers: halogen derivatives of polyacetylene, $(CH)_x$. *J. Chem. Soc., Chem. Commun.* 1977, (16), 578–580. DOI: 10.1039/c39770000578

19 The Nobel Prize in Chemistry 2000. *Nobelprize.org: The Official Web Site of the Nobel Prize* [online]. Nobel Media AB 2014. [cited 2020-02-21]. Available from: http://www.nobelprize.org/nobel_prizes/chemistry/laureates/2000/

20 GLOBAL ORGANIC ELECTRONICS MARKET PROFESSIONAL SURVEY 2019 BY MANUFACTURERS, REGIONS, TYPES AND APPLICATIONS, FORECAST TO 2024. *360 ResearchReports* [online]. Powered by Absolute Reports, Pune 411045, Maharashtra, India, 146. (04-09-**2019**) [cited 2020-02-21]. SKU ID: HJR-14664291. Available from: https://www.360researchreports.com/global-organic-electronics-market-14664291

21 GUPTA, M. C. and J. BALLATO. *The handbook of photonics*. 2nd ed. Boca Raton: CRC/Taylor & Francis, 2007. ISBN 978-0-8493-3095-7

22 SAYAGO, J., F. ROSEI and C. SANTATO. Organic photonics: Blending organic building blocks. *Nat. Photonics*. 2012, **6**(10), 639–640. DOI: 10.1038/nphoton.2012.235

23 CIMINELLI, C., F. DELL'OLIO and M. N. ARMENISE. *Photonics in Space: Advanced photonic devices and systems*. New Jersey: WORLD SCIENTIFIC, 2016. ISBN 978-981-4725-10-1

24 CLARK, J. and G. LANZANI. Organic photonics for communications. *Nat. Photonics*. 2010, **4**(7), 438–446. DOI: 10.1038/nphoton.2010.160

25 KAFAFI, Z. H., R. J. MARTÍN-PALMA, A. F. NOGUEIRA, et al. The role of photonics in energy. *J. Photonics Energy*. 2015, **5**(1), 1–44. DOI: 10.1117/1.JPE.5.050997

26 SANDANAYAKA, A. S. D., T. MATSUSHIMA, F. BENCHEIKH, et al. Indication of current-injection lasing from an organic semiconductor. *Appl. Phys. Express*. 2019, **12**(6), 1–6. DOI: 10.7567/1882-0786/ab1b90

27 STEUDEL, R. *Chemistry of the non-metals: with an introduction to atomic structure and chemical bonding*. English ed. New York: W. de Gruyter, 1977. ISBN 9783110048827. Available from: https://app.knovel.com/hotlink/toc/id:kpCNM00011/chemistry-non-metals/chemistry-non-metals

28 KLIKORKA, J., B. HÁJEK and J. VOTINSKÝ. Obecná a anorganická chemie. 2. vyd. Praha: STNL, 1989.

29 MCMURRY, J. *Organic chemistry*. 6th ed. Belmont: Thomson-Brooks/Cole, 2004. ISBN 0-534-42005-2

30 CHIANG, C. K., S. C. GAU, C. R. FINCHER, Y. W. PARK, A. G. MACDIARMID and A. J. HEEGER. Polyacetylene, $(CH)_x$: *n*-type and *p*-type doping and compensation. *Appl. Phys. Lett*. 1978, **33**(1), 18–20. DOI: 10.1063/1.90166

31 COROPCEANU, V., J. CORNIL, D. A. DA SILVA FILHO, Y. OLIVIER, R. SILBEY and J.-L. BRÉDAS. Charge Transport in Organic Semiconductors. *Chem. Rev.* 2007, **107**(4), 926–952. DOI: 10.1021/cr050140x

32 THE EDITORS OF ENCYCLOPAEDIA BRITANNICA: *Band theory* [online]. Encyclopædia Britannica, inc. Chicago, Illinois, USA (01-17-**2014**) [cited 2020-02-23]. Available from: https://www.britannica.com/science/band-theory

33 SOLYMAR, L. and D. WALSH. *Electrical properties of materials*. 8th ed. New York: Oxford University Press, 2010. ISBN 978-0-19-956592-4. Available from: https://app.knovel.com/hotlink/toc/id:kpEPME0008/electrical-properties/electrical-properties

34 THE EDITORS OF ENCYCLOPAEDIA BRITANNICA: *Semiconductor* [online]. Encyclopædia Britannica, inc. Chicago, Illinois, USA (01-25-**2019**) [cited 2020-02-23]. Available from: https://www.britannica.com/science/semiconductor

35 COSTA, J.C.S., R.J.S. TAVEIRA, C.F.R.A.C. LIMA, A. MENDES and L.M.N.B.F. SANTOS. Optical band gaps of organic semiconductor materials. *Opt. Mater.* 2016, **58**, 51–60. DOI: 10.1016/j.optmat.2016.03.041

36 MISHRA, A. and P. BÄUERLE. Small Molecule Organic Semiconductors on the Move: Promises for Future Solar Energy Technology. *Angew. Chem. Int. Ed.* 2012, **51**(9), 2020–2067. DOI: 10.1002/anie.201102326

37 FACCHETTI, A. π-Conjugated Polymers for Organic Electronics and Photovoltaic Cell Applications. *Chem. Mater.* 2011, **23**(3), 733–758. DOI: 10.1021/cm102419z

38 HAO, Z. and A. IQBAL. Some aspects of organic pigments. *Chem. Soc. Rev.* 1997, **26**(3), 203–213. DOI: 10.1039/cs9972600203

39 CHANDRAN, D. and K-S. LEE. Diketopyrrolopyrrole: A versatile building block for organic photovoltaic materials. *Macromol. Res.* 2013, **21**(3), 272–283. DOI: 10.1007/s13233-013-1141-3

40 FARNUM, D. G., G. MEHTA, G. G. I. MOORE and F. P. SIEGAL. Attempted reformatskii reaction of benzonitrile, 1,4-diketo-3,6-diphenylpyrrolo[3,4-C]pyrrole. A lactam analogue of pentalene. *Tetrahedron Lett.* 1974, **15**(29), 2549–2552. DOI: 10.1016/S0040-4039(01)93202-2

41 TAMAYO, A. B., B. WALKER and T-Q. NGUYEN. A Low Band Gap, Solution Processable Oligothiophene with a Diketopyrrolopyrrole Core for Use in Organic Solar Cells. *J. Phys. Chem. C.* 2008, **112**(30), 11545–11551. DOI: 10.1021/jp8031572

42 BÜRGI, L., M. TURBIEZ, R. PFEIFFER, F. BIENEWALD, H-J. KIRNER and C. WINNEWISSER. High-Mobility Ambipolar Near-Infrared Light-Emitting Polymer Field-Effect Transistors. *Adv. Mater.* 2008, **20**(11), 2217–2224. DOI: 10.1002/adma.200702775

43 LI, Y., P. SONAR, L. MURPHY and W. HONG. High mobility diketopyrrolopyrrole (DPP)-based organic semiconductor materials for organic thin film transistors and photovoltaics. *Energy Environ. Sci.* 2013, **6**(6), 1684–1710. DOI: 10.1039/c3ee00015j

44 LIU, Q., S. E. BOTTLE and P. SONAR. Developments of Diketopyrrolopyrrole-Dye-Based Organic Semiconductors for a Wide Range of Applications in Electronics. *Adv. Mater.* 2019, 1903882, 1–46. DOI: 10.1002/adma.201903882

45 GRZYBOWSKI, M. and D. T. GRYKO. Diketopyrrolopyrroles: Synthesis, Reactivity, and Optical Properties. *Adv. Opt. Mater.* 2015, **3**(3), 280–320. DOI: 10.1002/adom.201400559

46 YOON, W. S., S. K. PARK, I. CHO, J-A. OH, J. H. KIM and S. Y. PARK. High-Mobility n-Type Organic Transistors Based on a Crystallized Diketopyrrolopyrrole Derivative. *Adv. Funct. Mater.* 2013, **23**(28), 3519–3524. DOI: 10.1002/adfm.201203065

47 SURARU, S-L., U. ZSCHIESCHANG, H. KLAUK and F. WÜRTHNER. Diketopyrrolopyrrole as a p-channel organic semiconductor for high performance OTFTs. *Chem. Commun.* 2011, **47**(6), 1767–1769. DOI: 10.1039/c0cc04395h

48 STOLTE, M., S-L. SURARU, P. DIEMER, T. HE, Ch. BURSCHKA, U. ZSCHIESCHANG, H. KLAUK and F. WÜRTHNER. Diketopyrrolopyrrole Organic Thin-Film Transistors: Impact of Alkyl Substituents and Tolerance of Ethylhexyl Stereoisomers. *Adv. Funct. Mater.* 2016, **26**(41), 7415–7422. DOI: 10.1002/adfm.201602994

49 GHOSH, S., R. RAVEENDRAN, A. SAEKI, S. SEKI, M. NAMBOOTHIRY and A. AJAYAGHOSH. Charge Carrier Polarity Modulation in Diketopyrrolopyrrole-Based Low Band Gap Semiconductors by Terminal Functionalization. *ACS Appl. Mater. Interfaces.* 2019, **11**(1), 1088–1095. DOI: 10.1021/acsami.8b16714

50 KOVALENKO, A., C. YUMUSAK, P. HEINRICHOVA, et al. Adamantane substitutions: a path to high-performing, soluble, versatile and sustainable organic semiconducting materials. *J. Mater. Chem. C.* 2017, **5**(19), 4716–4723. DOI: 10.1039/C6TC05076J

51 LIN, G., Y. QIN, J. ZHANG, Y-S. GUAN, H. XU, W. XU and D. ZHU. Ambipolar organic field-effect transistors based on diketopyrrolopyrrole derivatives containing different π-conjugating spacers. *J. Mater. Chem. C.* 2016, **4**(20), 4470–4477. DOI: 10.1039/c6tc00687f

52 HE, T., P. LEOWANAWAT, Ch. BURSCHKA, V. STEPANENKO, M. STOLTE and F. WÜRTHNER. Impact of 2-Ethylhexyl Stereoisomers on the Electrical Performance of Single-Crystal Field-Effect Transistors. *Adv. Mater.* 2018, **30**(44), 1804032. DOI: 10.1002/adma.201804032

53 ANNEN, O., R. EGLI, R. HASLER, B. HENZI, H. JAKOB and P. MATZINGER. Replacement of disperse anthraquinone dyes. *Rev. Prog. Coloration.* 1987, **17**(1), 72–85. DOI: 10.1111/j.1478-4408.1987.tb03753.x

54 GREENHALGH, C. W., J. L. CAREY and D. F. NEWTON. The synthesis of quinodimethanes in the benzodifuranone and benzodipyrrolidone series. *Dyes Pigm.* 1980, **1**(2), 103–120. DOI: 10.1016/0143-7208(80)80010-6

55 GREENHALGH, C. W., J. L. CAREY, N. HALL and D. F. NEWTON. The benzodifuranone chromogen and its application to disperse dyes. *J. Soc. Dyers Colour.* 1994, **110**(5-6), 178–184. DOI: 10.1111/j.1478-4408.1994.tb01636.x

56 DENG, Z., K. YANG, L. LI, W. BAO, X. HAO, T. AI and K. KOU. Solution processed air-stable p-channel organic crystal field-effect transistors of Aminobenzodifuranone. *Dyes Pigm.* 2018, **151**, 173–178. DOI: 10.1016/j.dyepig.2017.12.052

57 SPLITSTOSER, J. C., T. D. DILLEHAY, J. WOUTERS and A. CLARO. Early pre-Hispanic use of indigo blue in Peru. *Sci. Adv.* 2016, **2**(9), 1501623. DOI: 10.1126/sciadv.1501623

58  GUPTA, D. Biotechnology applications in textile industry. *Indian J. Fibre Text. Res*. 2001, **26**(1–2), 206–213.

59  GSÄNGER, M., D. BIALAS, L. HUANG, M. STOLTE and F. WÜRTHNER. Organic Semiconductors based on Dyes and Color Pigments. *Adv. Mater.* 2016, **28**(19), 3615–3645. DOI: 10.1002/adma.201505440

60  IRIMIA-VLADU, M., E. D. GŁOWACKI, P. A. TROSHIN, et al. Indigo - A Natural Pigment for High Performance Ambipolar Organic Field Effect Transistors and Circuits. *Adv. Mater.* 2012, **24**(3), 375–380. DOI: 10.1002/adma.201102619

61  GŁOWACKI, E. D., D. H. APAYDIN, Z. BOZKURT, et al. Air-stable organic semiconductors based on 6,6′-dithienylindigo and polymers thereof. *J. Mater. Chem. C*, 2014, **2**(38), 8089–8097. DOI: 10.1039/c4tc00651h

62  PITAYATANAKUL, O., K. IIJIMA, T. KADOYA, M. ASHIZAWA, T. KAWAMOTO, H. MATSUMOTO and T. MORI. Ambipolar Organic Field-Effect Transistors Based on Indigo Derivatives. *Eng. J.* 2015, **19**(3), 61–74. DOI: 10.4186/ej.2015.19.3.61

63  GŁOWACKI, E. D., M. IRIMIA-VLADU, M. KALTENBRUNNER, et al. Hydrogen-Bonded Semiconducting Pigments for Air-Stable Field-Effect Transistors. *Adv. Mater.* 2013, **25**(11), 1563–1569. DOI: 10.1002/adma.201204039

64  MEI, J., K. R. GRAHAM, R. STALDER and J. R. REYNOLDS. Synthesis of Isoindigo-Based Oligothiophenes for Molecular Bulk Heterojunction Solar Cells. *Org. Lett.* 2010, **12**(4), 660–663. DOI: 10.1021/ol902512x

65  SHIROTA, Y. Organic materials for electronic and optoelectronic devices. *J. Mater. Chem.* 2000, **10**(1), 1–25. DOI: 10.1039/a908130e

66  SHIROTA, Y. and H. KAGEYAMA. Charge Carrier Transporting Molecular Materials and Their Applications in Devices. *Chem. Rev*. 2007, **107**(4), 953–1010. DOI: 10.1021/cr050143+

67  ALLEN, C. F. H. The Naphthyridines. *Chem. Rev*. 1950, **47**(2), 275–305. DOI: 10.1021/cr60147a004

68  FRYDMAN, B., M. LOS and H. RAPOPORT. Synthesis of substituted 1,5- and 1,7-naphthyridines and related lactams. *J. Org. Chem*. 1971, **36**(3), 450–454. DOI: 10.1021/jo00802a018

69  NANSON, L., N. BLOUIN, W. MITCHELL, S. TIERNEY and T. CULL (MERCK PATENT GMBH). *Organic Semiconductors*. PCT Int. Appl. WO 2013/182262 A1. Dec 12, 2013.

70  YOON, W. S., D. W. KIM, J-M. PARK, et al. A Novel Bis-Lactam Acceptor with Outstanding Molar Extinction Coefficient and Structural Planarity for Donor–Acceptor Type Conjugated Polymer. *Macromolecules*. 2016, **49**(22), 8489–8497. DOI: 10.1021/acs.macromol.6b01680

71  YOON, W. S., D. W. KIM, M-W. CHOI, J-M. PARK and S. Y. PARK. Designing 1,5-Naphthyridine-2,6-dione-Based Conjugated Polymers for Higher Crystallinity and Enhanced Light Absorption to Achieve 9.63% Efficiency Polymer Solar Cells. *Adv. Energy Mater*. 2018, **8**(2), 1701467. DOI: 10.1002/aenm.201701467

[72] BARBARELLA, G., M. MELUCCI and G. SOTGIU. The Versatile Thiophene: An Overview of Recent Research on Thiophene-Based Materials. *Adv. Mater.* 2005, **17**(13), 1581–1593. DOI: 10.1002/adma.200402020

[73] DICKEY, J. B., E. B. TOWNE, M. S. BLOOM, W. H. MOORE, B. H. Smith JR. and D. G. HEDBERG. Azo Dyes from Substituted 2-Aminothiophens. *J. Soc. Dyers Colour.* 1958, **74**(3), 123–132. DOI: 10.1111/j.1478-4408.1958.tb02242.x

[74] WU, Ch., E. R. DECKER, N. BLOK, et al. Discovery, Modeling, and Human Pharmacokinetics of *N*-(2-Acetyl-4,6-dimethylphenyl)-3-(3,4-dimethylisoxazol-5-ylsulfamoyl)thiophene-2-carboxamide (TBC3711), a Second Generation, ET$_A$ Selective, and Orally Bioavailable Endothelin Antagonist. *J. Med. Chem.* 2004, **47**(8), 1969–1986. DOI: 10.1021/jm030528p

[75] HALIK, M., H. KLAUK, U. ZSCHIESCHANG, G. SCHMID, S. PONOMARENKO, S. KIRCHMEYER and W. WEBER. Relationship Between Molecular Structure and Electrical Performance of Oligothiophene Organic Thin Film Transistors. *Adv. Mater.* **15**(11), 917–922. DOI: 10.1002/adma.200304654

[76] ROST, C., S. KARG, W. RIESS, M. A. LOI, M. MURGIA and M. MUCCINI. Ambipolar light-emitting organic field-effect transistor. *Appl. Phys. Lett.* 2004, **85**(9), 1613–1615. DOI: 10.1063/1.1785290

[77] LARIK, F. A., M. FAISAL, A. SAEED, et al. Thiophene-based molecular and polymeric semiconductors for organic field effect transistors and organic thin film transistors. *J. Mater. Sci.: Mater. Electron.* 2018, **29**(21), 17975–18010. DOI: 10.1007/s10854-018-9936-9

[78] TSUMURA, A., H. KOEZUKA and T. ANDO. Macromolecular electronic device: Field-effect transistor with a polythiophene thin film. *Appl. Phys. Lett.* 1986, **49**(18), 1210–1212. DOI: 10.1063/1.97417

[79] DANG, M. T., L. HIRSCH and G. WANTZ. P3HT:PCBM, Best Seller in Polymer Photovoltaic Research. *Adv. Mater.* 2011, **23**(31), 3597–3602. DOI: 10.1002/adma.201100792

[80] ONG, B. S., Y. WU, P. LIU and S. GARDNER. High-Performance Semiconducting Polythiophenes for Organic Thin-Film Transistors. *J. Am. Chem. Soc.* 2004, **126**(11), 3378–3379. DOI: 10.1021/ja039772w

[81] SIRRINGHAUS, H., P. J. BROWN, R. H. FRIEND, et al. Two-dimensional charge transport in self-organized, high-mobility conjugated polymers. *Nature.* 1999, **401**(6754), 685–688. DOI: 10.1038/44359

[82] MCCULLOCH, I., M. HEENEY, C. BAILEY, et al. Liquid-crystalline semiconducting polymers with high charge-carrier mobility. *Nat. Mater.* 2006, **5**(4), 328–333. DOI: 10.1038/nmat1612

[83] RIEGER, R., D. BECKMANN, W. PISULA, W. STEFFEN, M. KASTLER and K. MÜLLEN. Rational Optimization of Benzo[2,1-*b*;3,4-*b'*]dithiophene-Containing Polymers for Organic Field-Effect Transistors. *Adv. Mater.* 2010, **22**(1), 83–86. DOI: 10.1002/adma.200901286

84  KRAJČOVIČ, J., A. KOVALENKO, P. HEINRICHOVÁ, M. VALA and M. WEITER. Solid-state deep blue and UV fluorescent dyes based on para-bis(2-thienyl)phenylene. *J. Lumin*. 2015, **167**, 222–226. DOI: 10.1016/j.jlumin.2015.06.043

85  KRAJČOVIČ, J., A. KOVALENKO, P. HEINRICHOVÁ, M. VALA and M. WEITER. Adamantyl side groups boosting the efficiency and thermal stability of organic solid-state fluorescent dyes. *J. Lumin*. 2016, **175**, 94–99. DOI: 10.1016/j.jlumin.2016.02.019

86  DEEPAK, V. D. and S. K. ASHA. Self-Organization-Induced Three-Dimensional Honeycomb Pattern in Structure-Controlled Bulky Methacrylate Polymers: Synthesis, Morphology, and Mechanism of Pore Formation. *J. Phys. Chem. B*. 2006, **110**(43), 21450–21459. DOI: 10.1021/jp063469a

87  IQBAL, A., M. JOST, R. KIRCHMAYR, J. PFENNINGER, A. ROCHAT and O. WALLQUIST. The synthesis and properties of 1,4-diketo-pyrrolo[3,4-*c*]pyrroles. *Bull. Soc. Chim. Belg*. 1988, **97**(8–9), 615–644. DOI: 10.1002/bscb.19880970804

88  FAULKNER, E. B. and R. J. SCHWARTZ: *High Performance Pigments*. Weinheim: WILEY-VCH Verlag GmbH & Co, **2009**. 538 s. ISBN 978-3-527-31405-8

89  TIEKE, B., A. R. RABINDRANATH, K. ZHANG and Y. ZHU. Conjugated polymers containing diketopyrrolopyrrole units in the main chain. *Beilstein J. Org. Chem.* 2010, **6**, 830–845. DOI: 10.3762/bjoc.6.92

90  FREBORT, Š., Z. ELIÁŠ, A. LYČKA, S. LUŇÁK, J. VYŇUCHAL, L. KUBÁČ, R.HRDINA and L. BURGERT. *O*- and *N*-alkylated diketopyrrolopyrrole derivatives. *Tetrahedron Lett*. 2011, **52**(44), 5769–5773. DOI: 10.1016/j.tetlet.2011.08.113

91  NAIK, M. A., N. VENKATRAMAIAH, C. KANIMOZHI and S. PATIL. Influence of Side-Chain on Structural Order and Photophysical Properties in Thiophene Based Diketopyrrolopyrroles: A Systematic Study. *J. Phys. Chem. C*. 2012, **116**(50), 26128–26137. DOI: 10.1021/jp306365q

92  STAS, S., S. SERGEYEV and Y. GEERTS. Synthesis of diketopyrrolopyrrole (DPP) derivatives comprising bithiophene moieties. *Tetrahedron*. 2010, **66**(10), 1837–1845. DOI: 10.1016/j.tet.2010.01.027

93  FANG, Y.-Q., M. M. BIO, K. B. HANSEN, M. S. POTTER and A. CLAUSEN. Magnesium Coordination-Directed N-Selective Stereospecific Alkylation of 2-Pyridones, Carbamates, and Amides Using α-Halocarboxylic Acids. *J. Am. Chem. Soc*. 2010, **132**(44), 15525–15527. DOI: 10.1021/ja107709w

94  ZHAO, B., K. SUN, F. XUE and J. OUYANG. Isomers of dialkyl diketo-pyrrolo-pyrrole: Electron-deficient units for organic semiconductors. *Org. Electron*. 2012, **13**(11), 2516–2524. DOI: 10.1016/j.orgel.2012.07.015

95  KIM, J., J. E. KWON, A. A. BOAMPONG, J-H. LEE, M-H. KIM, S. Y. PARK, T-D. KIM and J. H. KIM. Threshold voltage modulation of polymer transistors by photoinduced charge–transfer between donor–acceptor dyads. *Dyes Pigm*. 2017, **142**, 387–393. DOI: 10.1016/j.dyepig.2017.03.063

96  WANG, Z., Z. LIU, L. NING, et al. Charge Mobility Enhancement for Conjugated DPP-Selenophene Polymer by Simply Replacing One Bulky Branching Alkyl Chain with Linear One at Each DPP Unit. *Chem. Mater*. 2018, **30**(9), 3090–3100. DOI: 10.1021/acs.chemmater.8b01007

[97] RAYCHEV, D., G. SEIFERT, J-U. SOMMER and O. GUSKOVA. A comparative analysis of symmetric diketopyrrolopyrrole-cored small conjugated molecules with aromatic flanks: From geometry to charge transport. *J. Comput. Chem.* 2018, **39**(30), 2526–2538. DOI: 10.1002/jcc.25609

[98] DHAR, J., N. VENKATRAMAIAH, A. Anitha and S. PATIL. Photophysical, electrochemical and solid state properties of diketopyrrolopyrrole based molecular materials: importance of the donor group. *J. Mater. Chem. C*. 2014, **2**(17), 3457–3466. DOI: 10.1039/C3TC32251C

[99] HOLLIDAY, S., J. E. DONAGHEY and I. MCCULLOCH. Advances in Charge Carrier Mobilities of Semiconducting Polymers Used in Organic Transistors. *Chem. Mater.* 2013, **26**(1), 647–663. DOI: 10.1021/cm402421p

[100] MORTON, C.J.H, R. GILMOUR, D.M. SMITH, P. LIGHTFOOT, A.M.Z. SLAWIN and E.J. MACLEAN. Synthetic studies related to diketopyrrolopyrrole (DPP) pigments. Part 1: The search for alkenyl-DPPs. Unsaturated nitriles in standard DPP syntheses. *Tetrahedron*. 2002, **58**(27), 5547–5565. DOI: 10.1016/S0040-4020(02)00443-X

[101] HUO, L., J. HOU, H-Y. CHEN, S. ZHANG, Y. JIANG, T.L. CHEN and Y. YANG. Bandgap and Molecular Level Control of the Low-Bandgap Polymers Based on 3,6-Dithiophen-2-yl-2,5-dihydropyrrolo[3,4-*c*]pyrrole-1,4-dione toward Highly Efficient Polymer Solar Cells. *Macromolecules*. 2009, **42**(17), 6564–6571. DOI: 10.1021/ma9012972

[102] SHAHID, M., T. MCCARTHY-WARD, J. LABRAM, et al. Low band gap selenophene–diketopyrrolopyrrolepolymers exhibiting high and balanced ambipolar performance in bottom-gate transistors. *Chem. Sci.* 2012, **3**(1), 181–185. DOI: 10.1039/C1SC00477H

[103] LIU, Q., H. SUN, CH. BLAIKIE, et al. Naphthalene flanked diketopyrrolopyrrole based organic semiconductors for high performance organic field effect transistors. *New J. Chem.* 2018, **42**(15), 12374–12385. DOI: 10.1039/C8NJ01453A

[104] YAMAMOTO, H, N. DAN and O. WALLQUIST. Fluorescent diketopyrrolopyrroles and their use. PCT Int. Appl. WO 2003002672. Jan 9, 2003.

[105] ROCHAT, A. C., L. CASSAR and A. IQBAL (Ciba-Geigy AG). Preparation of pyrrolo[3,4-*c*] pyrroles. Eur. Pat. Appl. 94911. May 11, 1983.

[106] CIGÁNEK, M. The synthesis and study of new derivatives of diketopyrrolopyrroles for organic electronics (diploma thesis). *Brno University of Technology, Brno*. 2017, 103.

[107] TAMAYO, A. B., M. TANTIWIWAT, B. WALKER and T-Q. NGUYEN. Design, Synthesis, and Self-assembly of Oligothiophene Derivatives with a Diketopyrrolopyrrole Core. *J. Phys. Chem. C*. 2008, **112**(39), 15543–15552. DOI: 10.1021/jp804816c

[108] STILLE, J. K. The Palladium-Catalyzed Cross-Coupling Reactions of Organotin Reagents with Organic Electrophiles[New Synthetic Methods(58)]. *Angew. Chem., Int. Ed. Engl.* 1986, **25**(6), 508–524. DOI: 10.1002/anie.198605081

[109] CHAN, W. K., Y. CHEN, Z. PENG and L. YU. Rational designs of multifunctional polymers. *J. Am. Chem. Soc*. 1993, **115**(25), 11735–11743. DOI: 10.1021/ja00078a012

[110] MIYAURA, N., T. ISHIYAMA, H. SASAKI, M. ISHIKAWA, M. SATO and A. SUZUKI. Palladium-catalyzed inter- and intramolecular cross-coupling reactions of B-alkyl-9-borabicyclo[3.3.1]nonane derivatives with 1-halo-1-alkenes or haloarenes. Syntheses of functionalized alkenes, arenes, and cycloalkenes via a hydroboration-coupling sequence. *J. Am. Chem. Soc*. 1989, **111**(1), 314–321. DOI: 10.1021/ja00183a048

[111] BEYERLEIN, T. and B. TIEKE. New photoluminescent conjugated polymers with 1,4-dioxo-3,6-diphenylpyrrolo[3,4-*c*]pyrrole (DPP) and 1,4-phenylene units in the main chain. *Macromol. Rapid Commun*. 2000, **21**(4), 182–189. DOI: 10.1002/(SICI)1521-3927(200003)21:4<182::AID-MARC182>3.0.CO;2-O

[112] FTOUNI, H., F. BOLZE, H. DE ROCQUIGNY and J-F. NICOUD. Functionalized Two-Photon Absorbing Diketopyrrolopyrrole-Based Fluorophores for Living Cells Fluorescent Microscopy. *Bioconjugate Chem*. 2013, **24**(6), 942–950. DOI: 10.1021/bc300623q

[113] JIANG, Y., Y. WANG, J. HUA, S. QU, S. QIAN and H. TIAN. Synthesis and two-photon absorption properties of hyperbranched diketo-pyrrolo-pyrrole polymer with triphenylamine as the core. *J. Polym. Sci., Part A: Polym. Chem*. 2009, **47**(17), 4400–4408. DOI: 10.1002/pola.23493

[114] GRZYBOWSKI, M., V. HUGUES, M. BLANCHARD-DESCE and D.T. GRYKO. Two-Photon-Induced Fluorescence in New π-Expanded Diketopyrrolopyrroles. *Chem. Eur. J*. 2014, **20**(39), 12493–12501. DOI: 10.1002/chem.201402569

[115] MCGLACKEN, G. P. and L. M. BATEMAN. Recent advances in aryl–aryl bond formation by direct arylation. *Chem. Soc. Rev*. 2009, **38**(8), 2447–2464. DOI: 10.1039/b805701j

[116] LAFRANCE, M., CH. N. ROWLEY, T. K. WOO and K. FAGNOU. Catalytic Intermolecular Direct Arylation of Perfluorobenzenes. *J. Am. Chem. Soc*. 2006, **128**(27), 8754-8756. DOI: 10.1021/ja062509l

[117] ZHANG, J., D-Y. KANG, S. BARLOW and S. R. MARDER. Transition metal-catalyzed C–H activation as a route to structurally diverse di(arylthiophenyl)-diketopyrrolopyrroles. *J. Mater. Chem*. 2012, 22(40), 21392–21394. DOI: 10.1039/c2jm35398a

[118] LIU, S-Y., M-M. SHI, J-CH. HUANG, et al. C–H activation: making diketopyrrolopyrrole derivatives easily accessible. *J. Mater. Chem. A*. 2013, **1**(8), 2795–2805. DOI: 10.1039/c2ta01318e

[119] GORELSKY, S. I., D. LAPOINTE and K. FAGNOU. Analysis of the Palladium-Catalyzed (Aromatic)C–H Bond Metalation–Deprotonation Mechanism Spanning the Entire Spectrum of Arenes. *J. Org. Chem*. 2011, **77**(1), 658–668. DOI: 10.1021/jo202342q

[120] GAO, Y., J. BAI, Y. SUI, Y. HAN, Y. DENG, H. TIAN, Y. GENG and F. WANG. High Mobility Ambipolar Diketopyrrolopyrrole-Based Conjugated Polymers Synthesized via Direct Arylation Polycondensation: Influence of Thiophene Moieties and Side Chains. *Macromolecules*. 2018, **51**(21), 8752–8760. DOI: 10.1021/acs.macromol.8b01112

[121] SCHIPPER, D. J. and K. FAGNOU. Direct Arylation as a Synthetic Tool for the Synthesis of Thiophene-Based Organic Electronic Materials. *Chem. Mater*. 2011, **23**(6), 1594–1600. DOI: 10.1021/cm103483q

[122] BÜRCKSTÜMMER, H., A. WEISSENSTEIN, D. BIALAS and F. WÜRTHNER. Synthesis and Characterization of Optical and Redox Properties of Bithiophene-Functionalized Diketopyrrolopyrrole Chromophores. *J. Org. Chem.* 2011, **76**(8), 2426–2432. DOI: 10.1021/jo2003117

[123] YAMAGATA, T., J. KUWABARA and T. KANBARA. Synthesis and Characterization of Dioxopyrrolopyrrole Derivatives Having Electron-Withdrawing Groups. *Eur. J. Org. Chem.* 2012, **2012**(27), 5282–5290. DOI: 10.1002/ejoc.201200761

[124] LUŇÁK, S., J. VYŇUCHAL, M. VALA, L. HAVEL and R. HRDINA. The synthesis, absorption and fluorescence of polar diketo-pyrrolo-pyrroles. *Dyes Pigm.* 2009, **82**(2), 102–108. DOI: 10.1016/j.dyepig.2008.12.001

[125] ANTHOPOULOS, T. D., G. C. ANYFANTIS, G. C. PAPAVASSILIOU and D. M. DE LEEUW. Air-stable ambipolar organic transistors. *Appl. Phys. Lett.* 2007, **90**(12), 122105. DOI: 10.1063/1.2715028

[126] ROCHAT, A. C., O. WALLQUIST, A. IQBAL, J. MIZUGUCHI (Ciba-Geigy AG). Process for the preparation of aminated diketodi(het)aryl-pyrrolopyrroles and use of the same as photoconducting substances. Eur. Pat. Appl. 353184. Jan 31, 1990.

[127] WALLQUIST O., B. LAMATSCH, T. RUCH (Ciba-Geigy AG). Blue diketopyrrolopyrrole pigments. Eur. Pat. Appl. 755933. Jan 29, 1997.

[128] LIM, B., H. SUN, J. LEE and Y-Y. NOH. High Performance Solution Processed Organic Field Effect Transistors with Novel Diketopyrrolopyrrole-Containing Small Molecules. *Sci. Rep.* 2017, **7**(1). DOI: 10.1038/s41598-017-00277-7

[129] PRIVADO, M., V. CUESTA, P. DE LA CRUZ, M. L. KESHTOV, G. D. SHARMA and F. LANGA. Tuning the optoelectronic properties for high-efficiency (>7.5%) all small molecule and fullerene-free solar cells. *J. Mater. Chem. A.* 2017, **5**(27), 14259–14269. DOI: 10.1039/C7TA03815A

[130] WU, S-L., Y-F. HUANG, CH-T. HSIEH, et al. Roles of 3-Ethylrhodanine in Attaining Highly Ordered Crystal Arrays of Ambipolar Diketopyrrolopyrrole Oligomers. *ACS Appl. Mater. Interfaces.* 2017, **9**(17), 14967–14973. DOI: 10.1021/acsami.7b01702

[131] KARSTEN, B. P., J. C. BIJLEVELD and R. A. J. JANSSEN. Diketopyrrolopyrroles as Acceptor Materials in Organic Photovoltaics. *Macromol. Rapid Commun.* 2010, **31**(17), 1554–1559. DOI: 10.1002/marc.201000133

[132] WANG, L., X. CHEN and D. CAO. A nitroolefin functionalized DPP fluorescent probe for the selective detection of hydrogen sulfide. *New J. Chem.* 2017, **41**(9), 3367–3373. DOI: 10.1039/C6NJ03432B

[133] YILMAZ, M., M. ERKARTAL, M. OZDEMIR, U. SEN, H. USTA and G. DEMIREL. Three-Dimensional Au-Coated Electrosprayed Nanostructured BODIPY Films on Aluminum Foil as Surface-Enhanced Raman Scattering Platforms and Their Catalytic Applications. *ACS Appl. Mater. Interfaces.* 2017, **9**(21), 18199–18206. DOI: 10.1021/acsami.7b03042

[134] FOLKES, A., M. B. ROE, S. SOHAL, J. GOLEC, R. FAINT, T. BROOKS and P. CHARLTON. Synthesis and in vitro evaluation of a series of diketopiperazine inhibitors of plasminogen activator inhibitor-1. *Bioorg. Med. Chem. Lett.* 2001, **11**(19), 2589–2592. DOI: 10.1016/S0960-894X(01)00508-X

[135] GHAFFARZADEH, M., M. BOLOURTCHIAN and M. HOSSEINI. High yield synthesis of aryl cyanides under microwave irradiation. *J. Chem. Res*. 2003, **2003**(12), 814–815. DOI: 10.3184/030823403322840512

[136] UNO, M., K. SETO and S. TAKAHASHI. A new method of synthesis of arylmalononitriles catalysed by a palladium complex. *ChemComm*. 1984, (14). DOI: 10.1039/c39840000932

[137] QIAO, Y., Y. GUO, CH. YU, F. ZHANG, W. XU, Y. LIU and D. ZHU. Diketopyrrolopyrrole-Containing Quinoidal Small Molecules for High-Performance, Air-Stable, and Solution-Processable n-Channel Organic Field-Effect Transistors. *J. Am. Chem. Soc.* 2012, **134**(9), 4084–4087. DOI: 10.1021/ja3003183

[138] ZHONG, H., J. SMITH, S. ROSSBAUER, A. J. P. WHITE, T. D. ANTHOPOULOS and M. HEENEY. Air-Stable and High-Mobility n-Channel Organic Transistors Based on Small-Molecule/Polymer Semiconducting Blends. *Adv. Mater*. 2012, **24**(24), 3205-3211. DOI: 10.1002/adma.201200859

[139] LU, J., A. DADVAND, Ta-ya CHU, R. MOVILEANU, J-M. BARIBEAU, J. DING and Y. TAO. Inkjet-printed unipolar n-type transistors on polymer substrates based on dicyanomethylene-substituted diketopyrrolopyrrole quinoidal compounds. *Org. Electron*. 2018, **63**, 267–275. DOI: 10.1016/j.orgel.2018.09.035

[140] CLOSS, F and R. GOMPPER. 2,5-Diazapentalenes. *Angew. Chem. Int. Ed. Engl*. 1987, **26**(6), 552–554. DOI: 10.1002/anie.198705521

[141] MIZUGUCHI, J. and A. C. ROCHAT. *Ber. Bunsenges. Phys. Chem*. 1992, **96**(4), 607–619.

[142] QIAN, G., J. QI, J. A. DAVEY, J. S. WRIGHT and Z. Y. WANG. Family of Diazapentalene Chromophores and Narrow-Band-Gap Polymers: Synthesis, Halochromism, Halofluorism, and Visible–Near Infrared Photodetectivity. *Chem. Mater*. 2012, **24**(12), 2364–2372. DOI: 10.1021/cm300938s

[143] QIAN, G. and Z. Yuan WANG. Near-Infrared Thermochromic Diazapentalene Dyes. *Adv. Mater*. 2012, **24**(12), 1582–1588. DOI: 10.1002/adma.201104711

[144] RIPAUD, E., D. DEMETER, T. ROUSSEAU, E. BOUCARD-CÉTOL, M. ALLAIN, R. PO, P. LERICHE and J. RONCALI. Structure–properties relationships in conjugated molecules based on diketopyrrolopyrrole for organic photovoltaics. *Dyes Pigm*. 2012, **95**(1), 126–133. DOI: 10.1016/j.dyepig.2012.03.021

[145] LÉVESQUE, S., D. GENDRON, N. BÉRUBÉ, F. GRENIER, M. LECLERC and M. CÔTÉ. Thiocarbonyl Substitution in 1,4-Dithioketopyrrolopyrrole and Thienopyrroledithione Derivatives: An Experimental and Theoretical Study. *J. Phys. Chem. C*. 2014, **118**(8), 3953–3959. DOI: 10.1021/jp411300h

[146] CHEN, L., F. ZHOU, T-D. SHI and J. ZHOU. Metal-Free Tandem Friedel–Crafts/Lactonization Reaction to Benzofuranones Bearing a Quaternary Center at C3 Position. *J. Org. Chem*. 2012, **77**(9), 4354–4362. DOI: 10.1021/jo300395x

[147] CURINI, M., F. EPIFANO, S. GENOVESE, M. C. MARCOTULLIO and O. ROSATI. Ytterbium Triflate-Promoted Tandem One-Pot Oxidation−Cannizzaro Reaction of Aryl Methyl Ketones: New Acceptor for Donor–Acceptor Low Band Gap Polymers. *Org. Lett*. 2005, **7**(7), 1331–1333. DOI: 10.1021/ol050125e

[148] WANG X., Y. WANG, D. DA-MING and J. XU. Solvent-free, AlCl₃-promoted tandem Friedel–Crafts reaction of arenes and aldehydes. *J. Mol. Catal. Chem.* 2006, **255**, 31–35. DOI: 10.1016/j.molcata.2006.03.060

[149] SMITH, M. B. *March's Advanced Organic Chemistry: Reactions, Mechanisms, and Structure*. 5th Ed. New York: John Wiley and Sons, Inc., **2001**. ISBN 04-715-8589-0.

[150] HALLAS, G and CH. YOON. The synthesis and properties of red and blue benzodifuranones. *Dyes Pigm.* 2001, **48**(2), 107–119. DOI: 10.1016/S0143-7208(00)00092-9

[151] GUO, X., M. BAUMGARTEN and K. MÜLLEN. Designing π-conjugated polymers for organic electronics. *Prog. Polym. Sci.* 2013, **38**(12), 1832–1908. DOI: 10.1016/j.progpolymsci.2013.09.005

[152] HAYOZ, P. and M. DUEGGELI (BASF SE). Polymers based on benzodiones. Int. Appl. WO 2013/050401. Apr 11, 2013.

[153] STEINGRUBER, E. Indigo and Indigo Colorants. *Ullmann's Encyclopedia of Industrial Chemistry*. Weinheim, Germany: Wiley-VCH Verlag GmbH & Co., **2000**, 19. DOI: 10.1002/14356007.a14_149.pub2

[154] BAEYER A. and V. DREWSEN. "Darstellung von Indigblau aus Orthonitrobenzaldehyd". *Ber. Dtsch. Chem. Ges.* 1882, **15**(2), 2856–2864. DOI: 10.1002/cber.188201502274

[155] PULLAGURLA, M. R. and J. B. RANGISETTY. Novel process for the preparation of indigotindisulfonate sodium (indigo carmine). Int. Appl. WO 2018/116325 (A1). June 28, 2018.

[156] PHILLIPS, M. Alkali Fusions. Ill-Fusion of Phenylgylcine-o-CarboxylicAcid for the Production of Indigo. *J. Ind. Eng. Chem.* 1921, **13**(9), 759–762. DOI: 10.1021/ie50141a011

[157] VENKATARAMAN, K.: Chemistry of Synthetic Dyes. *Academic Press, New York*. 1952, **2**, 1003–1022.

[158] BOGDANOV, A. V., L. I. MUSIN and V. F. MIRONOV. Advances in the synthesis and application of isoindigo derivatives. *Arkivoc*. 2015, **2015**(6). DOI: 10.3998/ark.5550190.p009.090

[159] JAFFE, E. E. and H. MATRICK. Synthesis of epindolidione. *J. Org. Chem.* 1968, **33**(11), 4004–4010. DOI: 10.1021/jo01275a002

[160] HAUCKE, G. and G. GRANESS. Thermal Isomerization of Indigo. *Angew. Chem. Int. Ed. Engl.* 1995, **34**(1), 67–68.

[161] GŁOWACKI, E. D., G. ROMANAZZI, C. YUMUSAK, et al. Epindolidiones-Versatile and Stable Hydrogen-Bonded Pigments for Organic Field-Effect Transistors and Light-Emitting Diodes. *Adv. Funct. Mater.* 2015, **25**(5), 776–787. DOI: 10.1002/adfm.201402539

[162] RAPOPORT, H. and A. D. BATCHO. 1,5-Naphthyridine and Some of Its Alkyl Derivatives. *J. Org. Chem.* 1963, **28**(7), 1753–1759. DOI: 10.1021/jo01042a005

[163] HAMEED S. P., V. PATIL, S. SOLAPURE, et al. Novel N-Linked Aminopiperidine-Based Gyrase Inhibitors with Improved hERG and in Vivo Efficacy against Mycobacterium tuberculosis. *J. Med. Chem.* 2014, **57**(11), 4889–4905. DOI: 10.1021/jm500432n

[164] NANSON, L., N. BLOUIN, W. MITCHELL, J. CAMERON and P. SKABARA (MERCK PATENT GMBH). *[1,5]Naphthyridine Compounds And Polymers As Semiconductors*. PCT Int. Appl. WO 2017/133752 A1. Aug 10, 2017.

[165] DATA, P., A. KUROWSKA, S. PLUCZYK, et al. Exciplex Enhancement as a Tool to Increase OLED Device Efficiency. *J. Phys. Chem. C*. 2016, **120**(4), 2070–2078. DOI: 10.1021/acs.jpcc.5b11263

[166] RIGGS, R. L., C. J. H. MORTON, A. M. Z. SLAWIN, D. M. SMITH, N. J. WESTWOOD, W. S. D. AUSTEN and K. E. STUART. Synthetic studies related to diketopyrrolopyrrole (DPP) pigments. Part 3: Syntheses of tri- and tetra-aryl DPPs. *Tetrahedron*. 2005, **61**(47), 11230–11243. DOI: 10.1016/j.tet.2005.09.005

[167] RAIMUNDO, J.-M., P. BLANCHARD, N. GALLEGO-PLANAS, N. MERCIER, I. LEDOUX-RAK, R. HIERLE and J. RONCALI. Design and Synthesis of Push−Pull Chromophores for Second-Order Nonlinear Optics Derived from Rigidified Thiophene-Based π-Conjugating Spacers. *J. Org. Chem*. 2002, **67**(1), 205–218. DOI: 10.1021/jo010713f

[168] ISMAIL, M. A. An efficient synthesis of 5'-(4-cyanophenyl)-2,2'-bifuran-5-carbonitrile and analogues. *J. Chem. Res*. 2006, **2006**(11), 733–737. DOI: 10.3184/030823406779173334

[169] FULLER, L. S., B. IDDON and K. A. SMITH. Thienothiophenes. Part 2.1 Synthesis, metallation and bromine→lithium exchange reactions of thieno[3,2-*b*]thiophene and its polybromo derivatives. *J. Chem. Soc., Perkin Trans. 1*. 1997, –(22), 3465–3470. DOI: 10.1039/a701877k

[170] Chemicals catalogue: *Sigma-Aldrich*. 3-Dodecylthiophene (CAS: 104934-52-3). Available here: https://www.sigmaaldrich.com/catalog/product/aldrich/456365

[171] Chemicals catalogue: *Sigma-Aldrich*. 2-Bromo-3-dodecylthiophene (CAS: 139100-06-4). Available here: https://www.sigmaaldrich.com/catalog/product/aldrich/688312

[172] STETTER, H. and P. GOEBEL. Über Verbindungen mit Urotropin-Struktur, XXII. Zur Kenntnis des Adamantyl-(1)-acetylens. *Chem. Ber*. 1962, **95**(4), 1039–1042. DOI: 10.1002/cber.19620950435

[173] DUBOIS, J. E., K. LEBBAR, C. LION, J. Y. DUGAST. Synthesis of cage structures derived from adamantane and its analogs by alkylation of trimethylsilyl enol ethers. *Bull. Soc. Chim. Fr*. 1985, –(5), 905–910. ISSN: 0037-8968.

[174] Chemicals catalogue: *Sigma-Aldrich*. 2-Bromothiophene (CAS: 1003-09-4). Available here: https://www.sigmaaldrich.com/catalog/product/aldrich/124168

[175] CARPITA, A., R. ROSSI and C. A. VERACINI. Synthesis and $^{13}$C NMR characterization of some π-excessive heteropolyaromatic compounds. *Tetrahedron*. 1985, **41**(10),1919–1929. DOI: 10.1016/S0040-4020(01)96555-X

[176] LUŇÁK, S., M. VALA, J. VYŇUCHAL, I. OUZZANE, P. HORÁKOVÁ, P. MOŽÍŠKOVÁ, Z. ELIÁŠ and M. WEITER. Absorption and fluorescence of soluble polar diketo-pyrrolo-pyrroles. *Dyes Pigm*. 2011, **91**(3), 269–278. DOI: 10.1016/j.dyepig.2011.05.004

[177] Chemicals catalogue: *Sigma-Aldrich*. 2,5-Dibromothiophene (CAS: 3141-27-3). Available here: https://www.sigmaaldrich.com/catalog/product/aldrich/108472

[178] CRESTEY, F., C. LEBARGY, M-C. LASNE and C. PERRIO. A Simple and Efficient Synthesis of New Mono- and Bis([1,2,4]-oxadiazol)-benzaldehyde Building Blocks. *Synth.* 2007, **2007**(21), 3406–3410. DOI: 10.1055/s-2007-990834

[179] QIAO, Z., Y. XU, S. LIN, J. PENG and D. CAO. Synthesis and characterization of red-emitting diketopyrrolopyrrole-alt-phenylenevinylene polymers. *Synth. Met.* 2010, **160**(13–14), 1544–1550. DOI: 10.1016/j.synthmet.2010.05.019

[180] Chemicals catalogue: *Sigma-Aldrich*. 2-Thiophenecarboxaldehyde (CAS: 98-03-3). Available here: https://www.sigmaaldrich.com/catalog/product/aldrich/t32409

[181] Chemicals catalogue: *Sigma-Aldrich*. 5-Bromo-2-thiophenecarboxaldehyde (CAS: 4701-17-1). Available here: https://www.sigmaaldrich.com/catalog/product/aldrich/152625

[182] Chemicals catalogue: *FisherScientific: Alfa Aesar™ Chemicals*. Ethyl thiophene-2-glyoxylate, 97% (CAS: 4075-58-5). Available here: https://www.fishersci.ca/shop/products/ethyl-thiophene-2-glyoxylate-97/p-7027727

[183] WYNBERG, H. and A. BANTJES. Pyrolysis of Thiophene. *J. Org. Chem.* 1959, **24**(10), 1421–1423. DOI: 10.1021/jo01092a008

[184] LIGHTOWLER, S. and M. HIRD. Monodisperse Aromatic Oligomers of Defined Structure and Large Size through Selective and Sequential Suzuki Palladium-Catalyzed Cross-Coupling Reactions. *Chem. Mater.* 2005, **17**(22), 5538–5549. DOI: 10.1021/cm0512068

[185] CHU, H.-Ch., D. SAHU, Y.-Ch. HSU, et al. Structural planarity and conjugation effects of novel symmetrical acceptor–donor–acceptor organic sensitizers on dye-sensitized solar cells. *Dyes Pigm.* 2012, **93**(1–3), 1488–1497. DOI: 10.1016/j.dyepig.2011.09.012

[186] MAGNAN, F., I. KOROBKOV and J. BRUSSO. Influence of substitution pattern and enhanced π-conjugation on a family of thiophene functionalized 1,5-dithia-2,4,6,8-tetrazocines. *New J. Chem.* 2015, **39**(9), 7272–7280. DOI: 10.1039/C5NJ01345C

[187] YU, J., B. ZHAO, X. NIE, et al. Correlation of structure and photovoltaic performance of benzo[1,2-b: 4,5-b′]dithiophene copolymers alternating with different acceptors. *New J. Chem.* 2015, **39**(3), 2248–2255. DOI: 10.1039/C4NJ02192D

[188] GŁOWACKI, E. D., H. COSKUN, M. A. BLOOD-FORSYTHE, et al. Hydrogen-bonded diketopyrrolopyrrole (DPP) pigments as organic semiconductors. *Org. Electr.* 2014, **15**(12), 3521–3528. DOI: 10.1016/j.orgel.2014.09.038

[189] KUMADA, M. Nickel and palladium complex catalyzed cross-coupling reactions of organometallic reagents with organic halides. *Pure Appl. Chem.* 1980, **52**(3), 669–679. DOI: 10.1351/pac198052030669

[190] BÄUERLE, P., F. PFAU, H. SCHLUPP, F. WÜRTHNER, K.-U. GAUDL, M. B. CARO and P. FISCHER. Synthesis and structural characterization of alkyl oligothiophenes—the first isomerically pure dialkylsexithiophene. *J. Chem. Soc., Perkin Trans. 2.* 1993, (3), 489–494. DOI: 10.1039/P29930000489

[191] MITCHELL, R. H., Y.-H. LAI and R. V. WILLIAMS. *N*-Bromosuccinimide-dimethylformamide: a mild, selective nuclear monobromination reagent for reactive aromatic compounds. *J. Org. Chem.* 1979, **44**(25), 4733–4735. DOI: 10.1021/jo00393a066

[192] KIM, D. H., B.-L. LEE, H. MOON, et al. Liquid-Crystalline Semiconducting Copolymers with Intramolecular Donor−Acceptor Building Blocks for High-Stability Polymer Transistors. *J. Am. Chem. Soc*. 2009, **131**(17), 6124–6132. DOI: 10.1021/ja8095569

[193] NG, S. C., J. M. XU and H. S. O. CHAN. Electrically conductive and fluorescent poly[1,4-bis(3-alkyl-2- thienyl)phenylenes]: syntheses and preliminary characterization aspects. *Synth. Met*. 1998, **92**(1), 33–37. DOI: 10.1016/S0379-6779(98)80019-2

[194] GRAVEL, J. and A. R. SCHMITZER. Transmembrane anion transport mediated by adamantyl-functionalised imidazolium salts. *Supramol. Chem*. 2015, **27**(5–6), 364–371. DOI: 10.1080/10610278.2014.969265

[195] POP, F., J. HUMPHREYS, J. SCHWARZ, L. BROWN, A. VAN DEN BERG and D. B. AMABILINO. Towards more sustainable synthesis of diketopyrrolopyrroles. *New J. Chem*. 2019, **43**(15), 5783–5790. DOI: 10.1039/C9NJ01074B

[196] FINKELSTEIN, H. Darstellung organischer Jodide aus den entsprechenden Bromiden und Chloriden. *Ber. Dtsch. Chem. Ges*. 1910, **43**(2), 1528–1532. DOI: 10.1002/cber.19100430257

[197] PALAI, A. K., S. P. MISHRA, A. KUMAR, R. SRIVASTAVA, M. N. KAMALASANAN and M. PATRI. Synthesis and Characterization of Red-Emitting Poly(aryleneethynylene)s Based on 2,5-Bis(2-ethylhexyl)-3,6-di(thiophen-2-yl)pyrrolo[3,4-*c*]pyrrole-1,4(2H,5H)-dione (DPP). *Macromol. Chem. Phys*. 2010, **211**(9), 1043–1053. DOI: 10.1002/macp.200900706

[198] HA, J. S., K. H. KIM and D. H. CHOI. 2,5-Bis(2-octyldodecyl)pyrrolo[3,4-*c*]pyrrole-1,4-(2*H*,5*H*)-dione-Based Donor–Acceptor Alternating Copolymer Bearing 5,5′-Di(thiophen-2-yl)-2,2′-biselenophene Exhibiting 1.5 cm$^2$·V$^{-1}$·s$^{-1}$ Hole Mobility in Thin-Film Transistors. *J. Am. Chem. Soc*. 2011, **133**(27), 10364–10367. DOI: 10.1021/ja203189h

[199] GETMANENKO, Y. A. and R. J. TWIEG. Unprecedented Negishi Coupling at C–Br in the Presence of a Stannyl Group as a Convenient Approach to Pyridinylstannanes and Their Application in Liquid Crystal Synthesis. *J. Org. Chem*. 2008, **73**(3), 830–839. DOI: 10.1021/jo701812t

[200] CIGÁNEK, M., P. HEINRICHOVÁ, A. KOVALENKO, J. KUČERÍK, M. VALA, M. WEITER and J. KRAJČOVIČ. Improved crystallinity of the asymmetrical diketopyrrolopyrrole derivatives by the adamantane substitution. *Dyes Pigm*. 2020, **175**, 108141. DOI: 10.1016/j.dyepig.2019.108141

[201] DAVID, J., M. WEITER, M. VALA, J. VYŇUCHAL and J. KUČERÍK. Stability and structural aspects of diketopyrrolopyrrole pigment and its N-alkyl derivatives. *Dyes Pigm*. 2011, **89**(2), 137–143. DOI: 10.1016/j.dyepig.2010.10.001

[202] KUČERÍK, J., J. DAVID, M. WEITER, M. VALA, J. VYŇUCHAL, I. OUZZANE and O. SALYK. Stability and physical structure tests of piperidyl and morpholinyl derivatives of diphenyl-diketo-pyrrolopyrroles (DPP). *J. Therm. Anal. Calorim*. 2012, **108**(2), 467–473. DOI: 10.1007/s10973-011-1896-8

[203] IRAQI, A. and G. W. BARKER. Synthesis and characterisation of telechelic regioregular head-to-tail poly(3-alkylthiophenes). *J. Mater. Chem*. 1998 **8**(1), 25–29. DOI: 10.1039/a706583c

[204] LECLERC, M. and J.-F. MORIN, ed. *Synthetic Methods for Conjugated Polymers and Carbon Materials*. Weinheim, Germany: Wiley-VCH Verlag GmbH & Co., 2017. DOI: 10.1002/9783527695959. ISBN 9783527695959

[205] FARINA, V., S. KAPADIA, B. KRISHNAN, Ch. WANG and L. S. LIEBESKIND. On the Nature of the "Copper Effect" in the Stille Cross-Coupling. *J. Org. Chem.* 1994, **59**(20), 5905–5911. DOI: 10.1021/jo00099a018

[206] BAO, Z., W. K. CHAN and L. YU. Exploration of the Stille Coupling Reaction for the Synthesis of Functional Polymers. *J. Am. Chem. Soc*. 1995, **117**(50), 12426–12435. DOI: 10.1021/ja00155a007

[207] HERGERT, T., B. VARGA, A. THURNER, F. FAIGL and B. MÁTRAVÖLGYI. Copper-facilitated Suzuki-Miyaura coupling for the preparation of 1,3-dioxolane-protected 5-arylthiophene-2-carboxaldehydes. *Tetrahedron*. 2018, **74**(16), 2002–2008. DOI: 10.1016/j.tet.2018.03.001

[208] LI, S. and Y. DUAN. *Method for synthesizing benzodifuranone dye*. Faming Zhuanli Shenqing. CN 108410204 (A). Aug 17, 2018.

[209] MISHRA, A. K., N. H. MORGON, S. SANYAL, A. ROBINSON DE SOUZA and S. BISWAS. Catalytic *O-* to *N*-Alkyl Migratory Rearrangement: Transition Metal-Free Direct and Tandem Routes to *N*-Alkylated Pyridones and Benzothiazolones. *Adv. Synth. Catal*. 2018, **360**(20), 3930–3939. DOI: 10.1002/adsc.201800664

# 9 LIST OF USED ABBREVIATIONS AND SYMBOLS

## 9.1 Abbreviations

| abbreviation | meaning |
|---|---|
| $(Bu)_3SnCl$ | tributyltin chloride |
| $(CH_3)_3SnCl$ | trimethyltin chloride |
| 3D | three-dimensional |
| AcOH | acetic acid |
| AFM | atomic force microscopy |
| AHA | α-hydroxy acid |
| $Al_2O_3$ | aluminium oxide |
| $AlCl_3$ | aluminium chloride |
| BDF | benzodifuranone (furo[2,3-*f*][1]benzofuran-2,6-dione) |
| BHJ-SC | bulk heterojunction solar cell |
| $Br_2$ | bromine |
| Bu | butyl |
| $CDCl_3$ | deuterated chloroform |
| $CHCl_3$ | chloroform |
| $CH_2(CN)_2$ | malononitrile |
| CMD | concerted metalation-deprotonation |
| $CO_2$ | carbon dioxide |
| $Cs_2CO_3$ | caesium carbonate |
| CuCN | copper cyanide |
| CuI | copper(I) iodide |
| D–A | donor–acceptor |
| DCE | 1,2-dichloroethane |
| DCM | dichloromethane |
| DMF | *N,N*-dimethylformamide |
| DMSO | dimethyl sulfoxide |
| DMSO-$d_6$ | deuterated dimethyl sulfoxide |
| DPP | diketopyrrolopyrrole (2,5-dihydropyrrolo[4,3-*c*]pyrrole-1,4-dione) |
| DSC | differential scanning calorimetry |
| DTPP | dithioketopyrrolopyrrole (2,5-dihydropyrrolo[4,3-*c*]pyrrole-1,4-dithione) |
| EA | elemental analysis |
| EDG | electron-donating group |
| EIA | U.S. Energy Information Administration |
| EP | epindolidione (dibenzo[b,g][1,5]naftyridin-6,12(5*H*,11*H*)-dione) |

| | |
|---|---|
| equiv. | an equivalent, the amount of a substance relative to another substance in the chemical reaction |
| $Et_2O$ | diethyl ether |
| EtOH | ethanol |
| EWG | electron-withdrawing group |
| $FeCl_3$ | iron(III) chloride |
| FT-IR | Fourier transformation infrared spectroscopy |
| GC-MS | gas chromatography-mass spectrometry |
| GPC | gel permeation chromatography |
| GR | Grignard reagent |
| $H_2O$ | water |
| $H_2SO_4$ | sulphuric acid |
| HBr | hydrobromic acid |
| HCl | hydrochloric acid |
| HMPA | hexamethylphosphoramide |
| HOMO | highest occupied molecular orbital |
| HT | head-to-tail |
| $I_2$ | iodine |
| ID | indigo [(2*E*)-2-(3-oxo-1,3-dihydro-2*H*-indol-2-yliden)-1,2-dihydro-3*H*-indol-3-one] |
| IID | isoindigo [(3*E*)-3-(2-oxo-1,2-dihydro-3*H*-indol-3-yliden)-1,3-dihydro-2*H*-indol-2-one] |
| *i*PrMgCl | Isopropylmagnesium chloride |
| $K_2CO_3$ | potassium carbonate |
| KI | potassium iodide |
| KOH | potassium hydroxide |
| LDA | lithium diisopropylamide |
| LR | Lawesson's reagent |
| LUMO | lowest unoccupied molecular orbital |
| Mg | magnesium |
| MW | microwave |
| $N(CH_2CH_3)_3$ | triethylamine |
| Na | sodium |
| $Na_2S_2O_3$ | sodium thiosulfate |
| $Na_2SO_4$ | sodium sulfate |
| $NaBH_4$ | sodium tetrahydridoborate |
| NaH | sodium hydride |

| | |
|---|---|
| NaHCO$_3$ | sodium hydrogen carbonate |
| NaNH$_2$ | sodium amide |
| NaOH | sodium hydroxide |
| NBS | N-bromosuccinimide |
| *n*-BuLi | *n*-butyllithium |
| NH$_2$OH · HCl | hydroxylamine hydrochloride |
| NH$_4$Cl | ammonium chloride |
| NH$_4$OH | ammonium hydroxide |
| Ni(dppp)Cl$_2$ | [1,3-bis(diphenylphosphino)propane]dichloronickel(II) |
| NMP | *N*-methylpyrrolidone |
| NMR | nuclear magnetic resonance spectroscopy |
| NTD | naphthyridinedione (1,5-dihydro-1,5-naphthyridine-2,6-dione) |
| O$_2$ | oxygen |
| OECD | Organization of Economic Cooperation and Development |
| OFET | organic field-effect transistor |
| OLED | organic light-emitting diode |
| OPD | organic photodetectors |
| OPV | organic photovoltaics |
| OSC | organic solar cell |
| OTFT | organic thin-film transistor |
| P(*o*-MeOPh)$_3$ | tris(*o*-methoxyphenyl)phosphine |
| P(*o*-tol)$_3$ | tri(*o*-tolyl)phosphine |
| P(*t*-Bu)$_3$HBF$_4$ | tri-*tert*-butylphosphonium tetrafluoroborate |
| P3AT | poly-3-alkylthiophene |
| PCE | power conversion efficiency |
| Pd(dppf)Cl$_2$ | [1,1′-bis(diphenylphosphino)ferrocene]dichloropalladium(II) |
| Pd(OAc)$_2$ | palladium(II) acetate |
| Pd(PPh$_3$)$_4$ | tetrakis(triphenylphosphine)-palladium(0) |
| Pd$_2$(dba)$_3$ | tris(dibenzylideneacetone)dipalladium(0) |
| PdCl$_2$(PPh$_3$)$_2$ | bis(triphenylphosphine)palladium(II) dichloride |
| PET | polyethylene terephthalate |
| PivOH | pivalic acid |
| PLQY | photoluminescence quantum yields |
| POCl$_3$ | phosphoryl trichloride |
| PPA | polyphosphoric acid |
| PPh$_3$ | Triphenylphosphine |
| PT | polythiophene |

| | |
|---|---|
| $PtO_2$ | platinum oxide (Adams' catalyst) |
| QY | quantum yield |
| RT (analytic.) | retention time |
| RT (experim.) | room temperature (approx. 25 °C) |
| SC | single crystal |
| $S_EAr$ | electrophilic aromatic substitution |
| $SeO_2$ | selenium oxdie |
| $S_N1$ | unimolecular nucleophilic substitution |
| $S_NAr$ | nucleophilic aromatic substitution |
| $SOCl_2$ | thionyl chloride |
| TAA | *tert*-amyl alcohol |
| TEM | transmission electron microscopy |
| TF | thin film |
| TfOH | triflic acid (trifluoromethanesulfonic acid) |
| TGA | thermogravimetric analysis |
| THF | tetrahydrofuran |
| TLC | thin-layer chromatography |
| TMS | tetramethylsilane |
| UV-VIS | ultraviolet-visible spectroscopy |
| WAXS | wide-angle X-ray scattering |
| XRD | X-ray diffraction |
| $Yb(OTf)_3$ | ytterbium triflate |
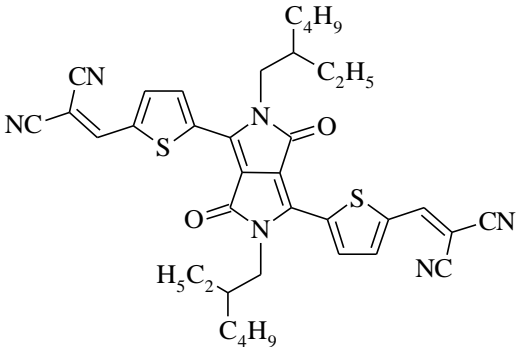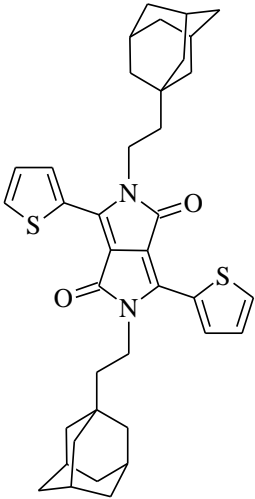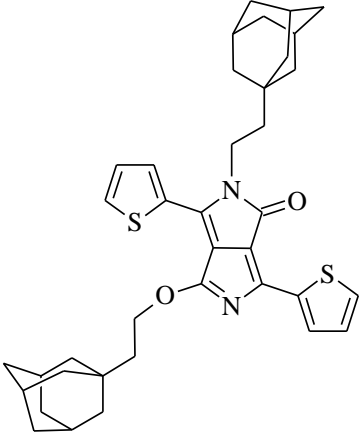
## 9.2 Symbols
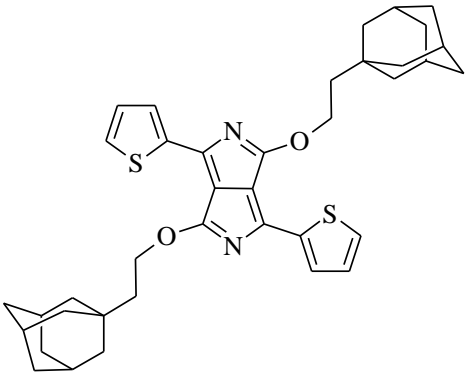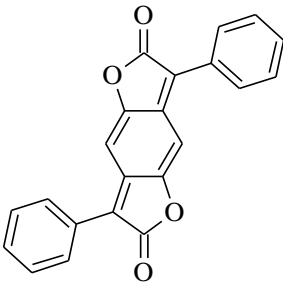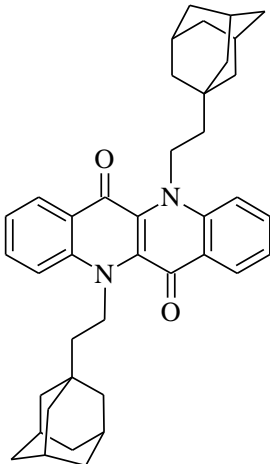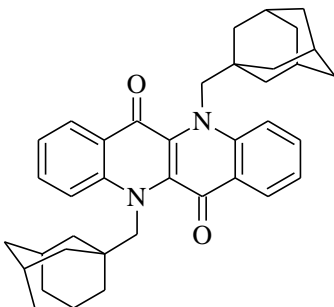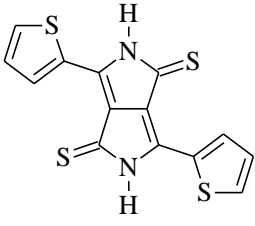
| *symbol* | *meaning* |
|---|---|
| $ | dollar |
| °C | the degree Celsius, unit of temperature |
| $\mu_{e/max}$ | electron mobility [$cm^2$ $V^{-1}$ $s^{-1}$] |
| $\mu_{h/max}$ | hole mobility [$cm^2$ $V^{-1}$ $s^{-1}$] |
| Å | Ångström, unit of length [$10^{-10}$ m] |
| bar | a metric unit of pressure [100 000 Pa] |
| d | doublet |
| dd | doublet of doublets |
| ddd | doublet of doublet of doublets |
| dt | doublet of triplets |
| $E_{GAP}$ | band gap energy |

| $E_{\text{g opt}}$ | optical energy gap [eV] |
|---|---|
| eV | electron volt, unit of energy |
| g | gram, unit of mass [$10^{-3}$ kg] |
| h | hour, unit of time |
| Hz | hertz, unit of frequency |
| $J$ | the coupling constant [Hz] |
| kWh | kilowatt-hour, unit of energy |
| m | multiplet |
| mbar | millibar, unit of pressure [100 Pa] |
| mg | milligram, unit of mass [$10^{-6}$ kg] |
| MHz | megahertz, unit of frequency [$10^6$ Hz] |
| min | minute, unit of time |
| mL | millilitre, unit of volume [1 cm$^3$] |
| mmol | millimole, unit of amount of substance |
| nm | nanometre, unit of length [$10^{-9}$ m] |
| ppm | parts per million |
| psi | pound-force per square inch, unit of pressure [6 894.757 Pa] |
| q | quartet |
| $R_{\text{F}}$ | retention factor [–] |
| s | singlet |
| t | triplet |
| td | triplet of doublets |
| $T_{\text{DEG}}$ | degradation temperature |
| $T_{\text{MP}}$ | melting point temperature [°C] |
| δ | chemical shift in NMR [ppm] |
| $\lambda_{\text{ABS edge}}$ | absorption edge [nm] |
| $\lambda_{\text{ABS max}}$ | absorption maxima [nm] |
| $\lambda_{\text{PL}}$ | emission maxima [nm] |
| μL | microlitre, unit of volume [$10^{-3}$ cm$^3$] |
| $\rho_{25}$ | density at 25 °C [g cm$^{-3}$] |
| τ | fluorescence lifetime [ns] |
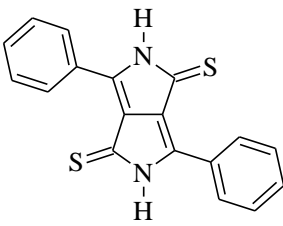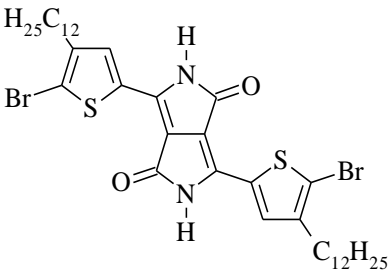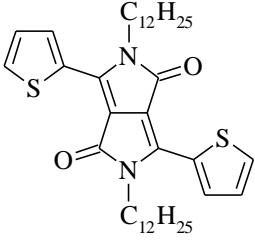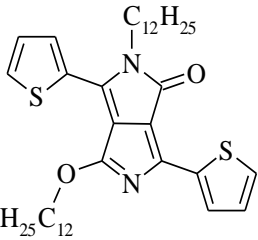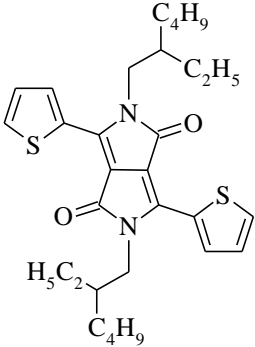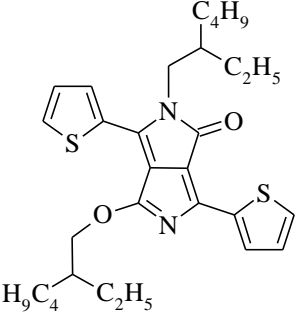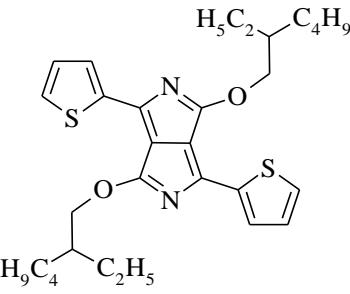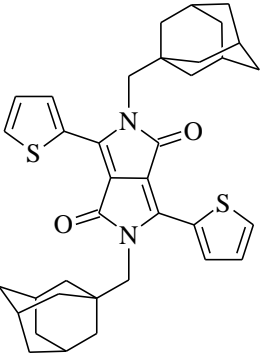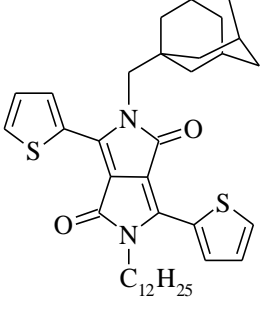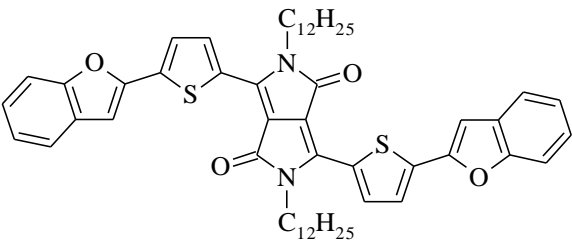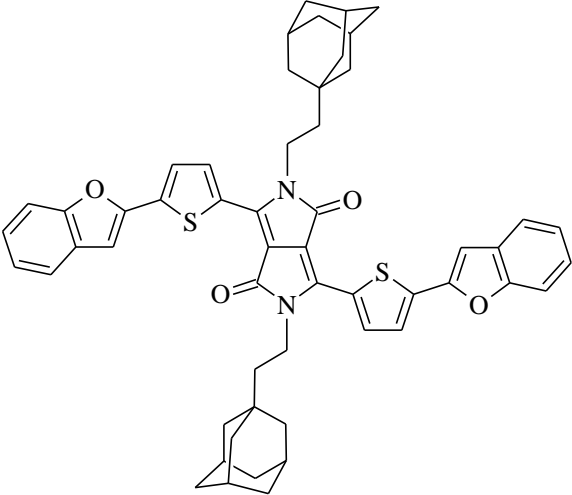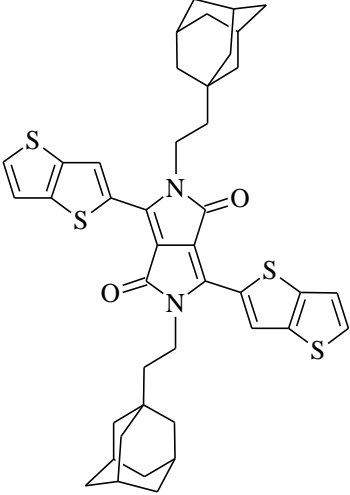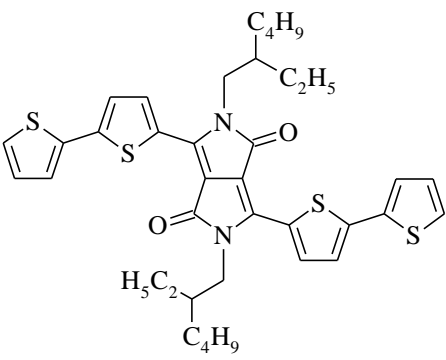
# 10  LIST OF PREPARED TARGET DERIVATIVES
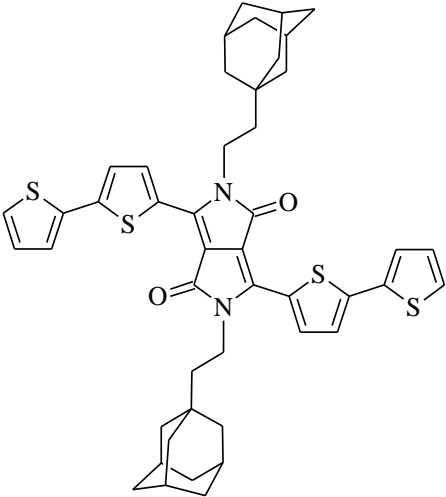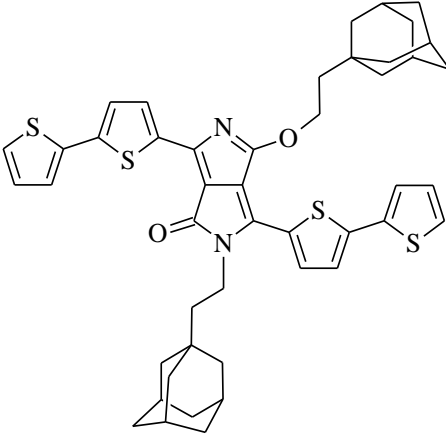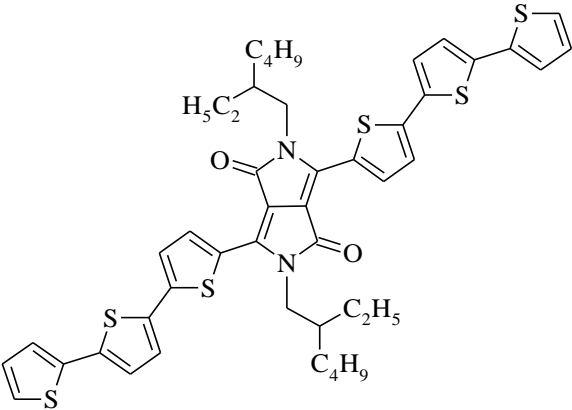
| Description | Structure |
|---|---|
| **1) Code: 2**<br><br>**CAS registry number:** 1450980-42-3<br><br>**Name:**  2,2'-[[2,5-bis(2-ethylhexyl)-2,3,5,6-tetrahydro-3,6-dioxopyrrolo[3,4-*c*]pyrrole-1,4-diyl]bis(5,2-thiophene-diylmethylidyne)]bis[propanedinitrile]<br><br>**Molecular formula** = $C_{38}H_{40}N_6O_2S_2$<br><br>**Molecular weight** = 676.89 g/mol |  |
| **2) Code: 6a**<br><br>**CAS registry number:** 2409052-13-5<br><br>**Name:**  2,5-dihydro-3,6-di-2-thienyl-2,5-bis(2-tricyclo[3.3.1.1$^{3,7}$]dec-1-ylethyl)pyrrolo[3,4-*c*]pyrrole-1,4-dione<br><br>**Molecular formula** = $C_{38}H_{44}N_2O_2S_2$<br><br>**Molecular weight** = 624.90 g/mol |  |
| **3) Code: 6b** (*novel derivative*)<br>**CAS registry number:** 2409052-14-6<br><br>**Name:**  3,6-di-2-thienyl-4-(2-tricyclo[3.3.1.1$^{3,7}$]dec-1-ylethoxy)-2-(2-tricyclo[3.3.1.1$^{3,7}$]dec-1-ylethyl)pyrrolo[3,4-*c*]pyrrol-1(2*H*)-one<br><br>**Molecular formula** = $C_{38}H_{44}N_2O_2S_2$<br><br>**Molecular weight** = 624.90 g/mol |  |
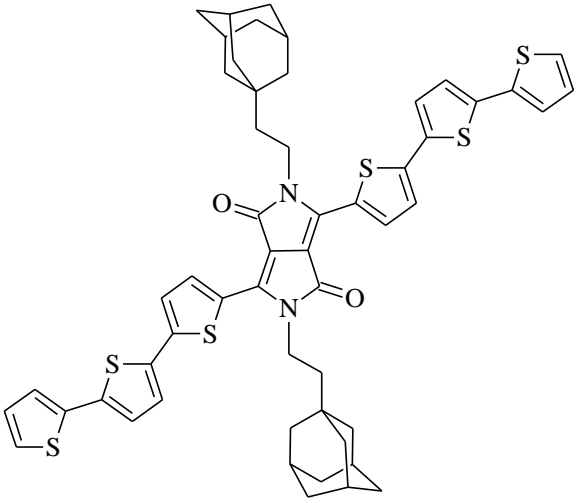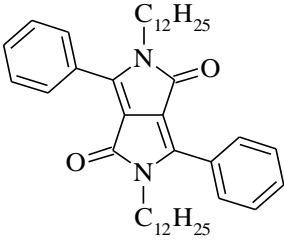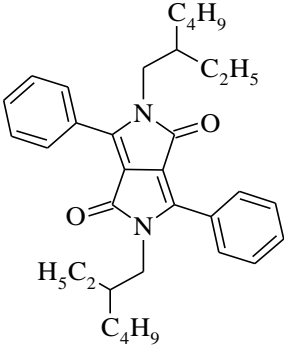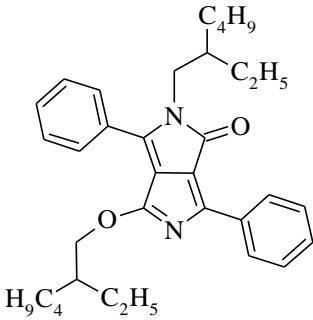
**4) Code: 6c** (*novel derivative*)

**CAS registry number:** 2409052-15-7

**Name:** 1,4-di-2-thienyl-3,6-bis(2-tricyclo[3.3.1.1$^{3,7}$]dec-1-ylethoxy) pyrrolo[3,4-c]pyrrole

**Molecular formula** = $C_{38}H_{44}N_2O_2S_2$

**Molecular weight** = 624.90 g/mol



---

**5) Code: 10a**

**CAS registry number:** 64501-49-1

**Name:** 3,7-diphenylbenzo[1,2-b:4,5-b'] difuran-2,6-dione

**Molecular formula** = $C_{22}H_{12}O_4$

**Molecular weight** = 340.33 g/mol



---

**6) Code: 17a** (*novel derivative*)

**CAS registry number:** –

**Name:** N,N'-ethyladamantyl-epindolidione

**Molecular formula** = $C_{40}H_{46}N_2O_2$

**Molecular weight** = 586.81 g/mol



---

**7) Code: 17b** (*novel derivative*)

**CAS registry number:** –

**Name:** N,N'-methyladamantyl-epindolidione

**Molecular formula** = $C_{38}H_{42}N_2O_2$

**Molecular weight** = 558.75 g/mol



---

**8) Code: 59a**

**CAS registry number:** 952146-92-8

**Name:** 2,5-dihydro-3,6-di-2-thienyl pyrrolo[3,4-c]pyrrole-1,4-dithione

**Molecular formula** = $C_{14}H_8N_2S_4$

**Molecular weight** = 332.49 g/mol

## 9) Code: 59b

**CAS registry number:** 104616-26-4

**Name:** 2,5-dihydro-3,6-diphenylpyrrolo[3,4-*c*]pyrrole-1,4-dithione

**Molecular formula** = $C_{18}H_{12}N_2S_2$

**Molecular weight** = 320.43 g/mol

## 10) Code: 133

**CAS registry number:** 2364478-30-6

**Name:** 3,6-bis(5-bromo-4-dodecyl-2-thienyl)-2,5-dihydropyrrolo[3,4-*c*]pyrrole-1,4-dione

**Molecular formula** = $C_{38}H_{54}Br_2N_2O_2S_2$

**Molecular weight** = 794.79 g/mol

## 11) Code: 145a

**CAS registry number:** 1057401-09-8

**Name:** 2,5-didodecyl-2,5-dihydro-3,6-di-2-thienylpyrrolo[3,4-*c*]pyrrole-1,4-dione

**Molecular formula** = $C_{38}H_{56}N_2O_2S_2$

**Molecular weight** = 636.99 g/mol

## 12) Code: 145b

**CAS registry number:** –

**Name:** 2-dodecyl-4-(dodecyloxy)-3,6-di-2-thienylpyrrolo[3,4-*c*]pyrrol-1(2*H*)-one

**Molecular formula** = $C_{38}H_{56}N_2O_2S_2$

**Molecular weight** = 636.99 g/mol

## 13) Code: 146a

**CAS registry number:** 1185885-86-2

**Name:** 2,5-bis(2-ethylhexyl)-2,5-dihydro-3,6-di-2-thienylpyrrolo[3,4-*c*]pyrrole-1,4-dione

**Molecular formula** = $C_{30}H_{40}N_2O_2S_2$

**Molecular weight** = 524.78 g/mol
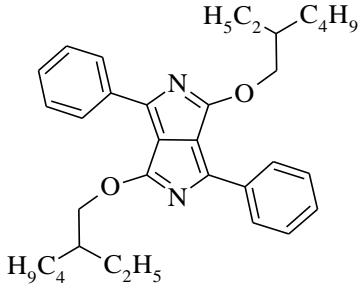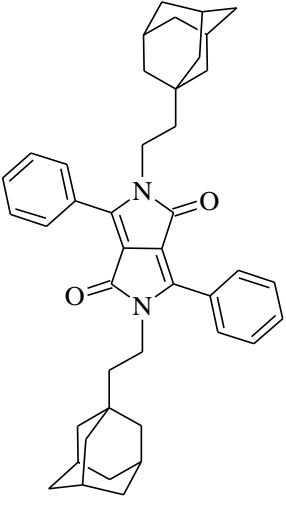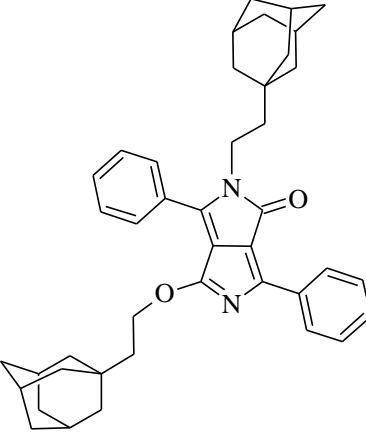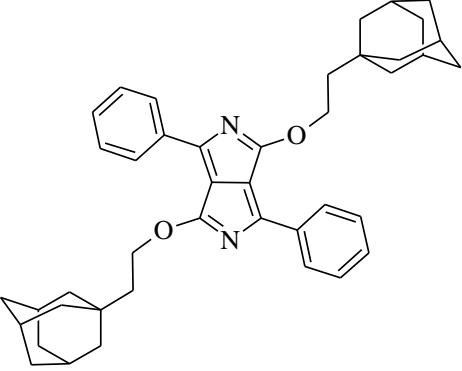
## 14) Code: 146b

**CAS registry number:** 1380497-22-2

**Name:**   2-(2-ethylhexyl)-4-[(2-ethylhexyl)oxy]-3,6-di-2-thienylpyrrolo[3,4-c]pyrrol-1(2H)-one

**Molecular formula** = $C_{30}H_{40}N_2O_2S_2$

**Molecular weight** = 524.78 g/mol

## 15) Code: 146c

**CAS registry number:** 1443743-29-0

**Name:**   1,4-bis[(2-ethylhexyl)oxy]-3,6-di-2-thienylpyrrolo[3,4-c]pyrrole

**Molecular formula** = $C_{30}H_{40}N_2O_2S_2$

**Molecular weight** = 524.78 g/mol

## 16) Code: 147 (*novel derivative*)

**CAS registry number:** –

**Name:**   2,5-dihydro-3,6-di-2-thienyl-2,5-bis(2-tricyclo[3.3.1.1^{3,7}]dec-1-ylmethyl)pyrrolo[3,4-c]pyrrole-1,4-dione

**Molecular formula** = $C_{36}H_{40}N_2O_2S_2$

**Molecular weight** = 596.85 g/mol

## 17) Code: 149 (*novel derivative*)

**CAS registry number:** –

**Name:**   2-dodecyl-2,5-dihydro-3,6-di-2-thienyl-5-(2-tricyclo[3.3.1.1^{3,7}]dec-1-ylmethyl)pyrrolo[3,4-c]pyrrole-1,4-dione

**Molecular formula** = $C_{37}H_{48}N_2O_2S_2$

**Molecular weight** = 616.92 g/mol

## 18) Code: 150

**CAS registry number:** 1639407-78-5

**Name:**   3,6-bis[5-(2-benzofuranyl)-2-thienyl]-2,5-didodecyl-2,5-dihydropyrrolo[3,4-c]pyrrole-1,4-dione

**Molecular formula** = $C_{54}H_{64}N_2O_4S_2$

**Molecular weight** = 869.23 g/mol
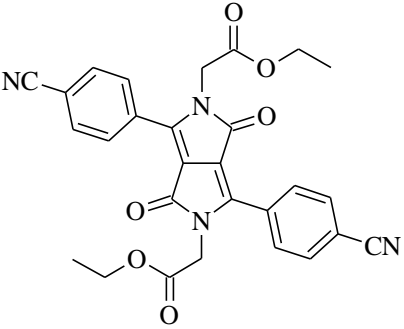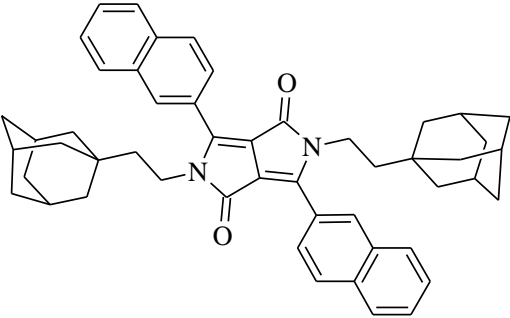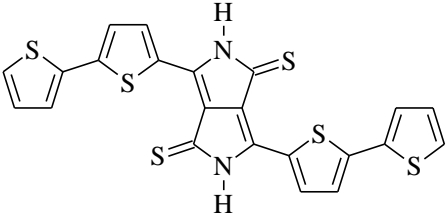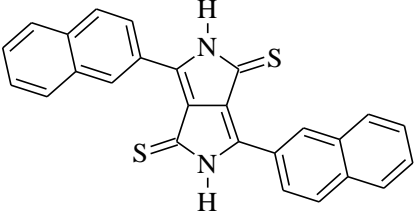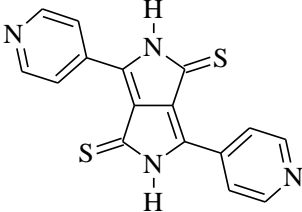
**19) Code: 151** (*novel derivative*)

**CAS registry number:** –

**Name:** 3,6-bis[5-(2-benzofuranyl)-2-thienyl]-2,5-dihydro-2,5-bis(2-tricyclo[3.3.1.1$^{3,7}$]dec-1-ylethyl)pyrrolo[3,4-*c*]pyrrole-1,4-dione

**Molecular formula** = $C_{54}H_{52}N_2O_4S_2$

**Molecular weight** = 857.13 g/mol

**20) Code: 152** (*novel derivative*)

**CAS registry number:** –

**Name:** 2,5-dihydro-3,6-dithieno[3,2-*b*]thien-2-yl-2,5-bis(2-tricyclo[3.3.1.1$^{3,7}$]dec-1-ylethyl)pyrrolo[3,4-*c*]pyrrole-1,4-dione

**Molecular formula** = $C_{42}H_{44}N_2O_2S_4$

**Molecular weight** = 737.07 g/mol

**21) Code: 153**

**CAS registry number:** 1269004-56-9

**Name:** 3,6-bis([2,2'-bithiophen]-5-yl)-2,5-bis(2-ethylhexyl)-2,5-dihydropyrrolo[3,4-*c*]pyrrole-1,4-dione

**Molecular formula** = $C_{38}H_{44}N_2O_2S_4$

**Molecular weight** = 689.03 g/mol
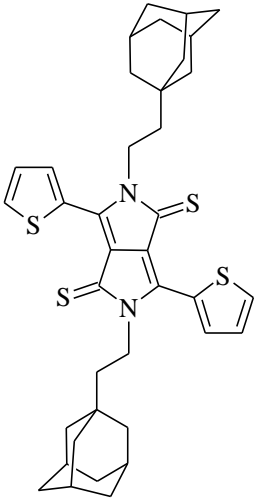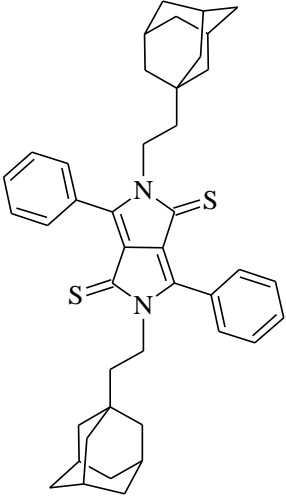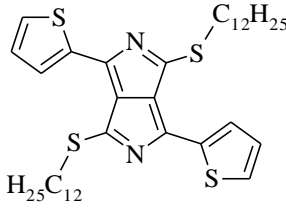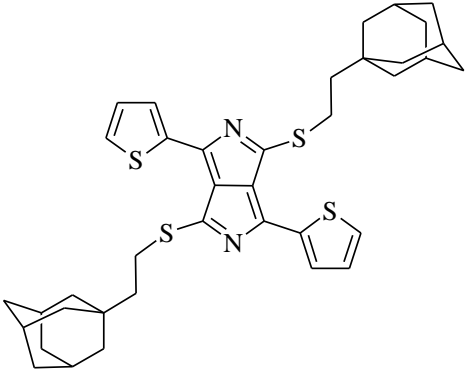
**22) Code: 155a** (*novel derivative*)

**CAS registry number:** –

**Name:** 3,6-bis([2,2'-bithiophen]-5-yl)-2,5-dihydro-2,5-bis(2-tricyclo[3.3.1.1$^{3,7}$]dec-1-ylethyl)pyrrolo[3,4-c]pyrrole-1,4-dione

**Molecular formula** = C$_{46}$H$_{48}$N$_2$O$_2$S$_4$

**Molecular weight** = 789.15 g/mol



**23) Code: 155b** (*novel derivative*)

**CAS registry number:** –

**Name:** 3,6-bis([2,2'-bithiophen]-5-yl)-4-(2-tricyclo[3.3.1.1$^{3,7}$]dec-1-ylethoxy)-2-(2-tricyclo[3.3.1.1$^{3,7}$]dec-1-ylethyl)pyrrolo[3,4-c]pyrrol-1(2H)-one

**Molecular formula** = C$_{46}$H$_{48}$N$_2$O$_2$S$_4$

**Molecular weight** = 789.15 g/mol



**24) Code: 162**

**CAS registry number:** 1143585-28-7

**Name:** 2,5-bis(2-ethylhexyl)-2,5-dihydro-3,6-bis([2,2':5',2''-terthiophen]-5-yl)pyrrolo[3,4-c]pyrrole-1,4-dione

**Molecular formula** = C$_{46}$H$_{48}$N$_2$O$_2$S$_6$

**Molecular weight** = 853.28 g/mol
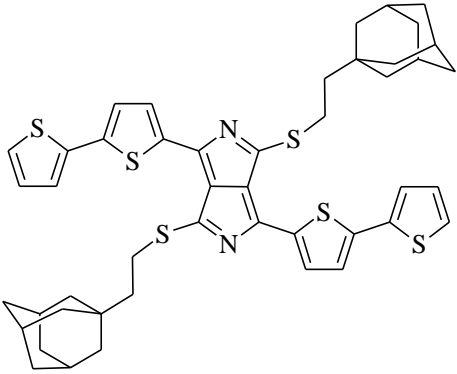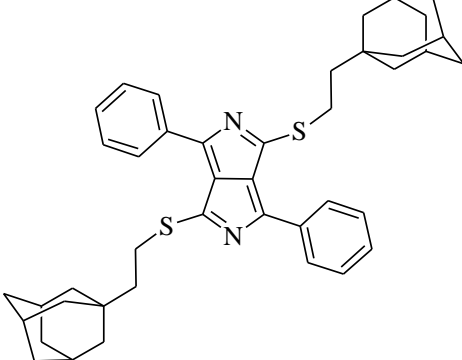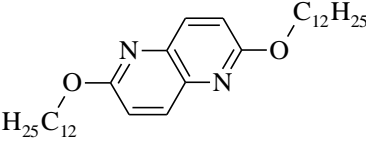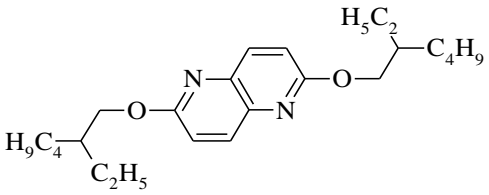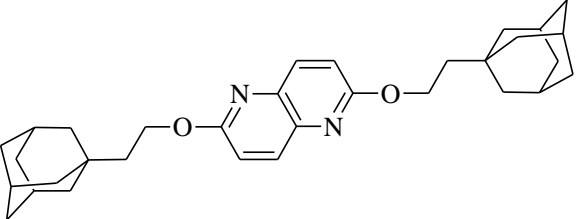
**25) Code: 163** (*novel derivative*)

**CAS registry number:** –

**Name:** 2,5-dihydro-3,6-bis([2,2':5',2"-terthiophen]-5-yl)-2,5-bis(2-tricyclo[3.3.1.1$^{3,7}$]dec-1-ylethyl)pyrrolo[3,4-c]pyrrole-1,4-dione

**Molecular formula** = C$_{54}$H$_{52}$N$_2$O$_2$S$_6$

**Molecular weight** = 953.39 g/mol

**26) Code: 164**

**CAS registry number:** 1224696-30-3

**Name:** 2,5-didodecyl-2,5-dihydro-3,6-diphenylpyrrolo[3,4-c]pyrrole-1,4-dione

**Molecular formula** = C$_{42}$H$_{60}$N$_2$O$_2$

**Molecular weight** = 624.94 g/mol

**27) Code: 165a**

**CAS registry number:** 132029-46-0

**Name:** 2,5-bis(2-ethylhexyl)-2,5-dihydro-3,6-diphenylpyrrolo[3,4-c]pyrrole-1,4-dione

**Molecular formula** = C$_{34}$H$_{44}$N$_2$O$_2$

**Molecular weight** = 512.73 g/mol

**28) Code: 165b** (*novel derivative*)

**CAS registry number:** –

**Name:** 2-(2-ethylhexyl)-4-[(2-ethylhexyl)oxy]-3,6-diphenylpyrrolo[3,4-c]pyrrol-1(2H)-one

**Molecular formula** = C$_{34}$H$_{44}$N$_2$O$_2$
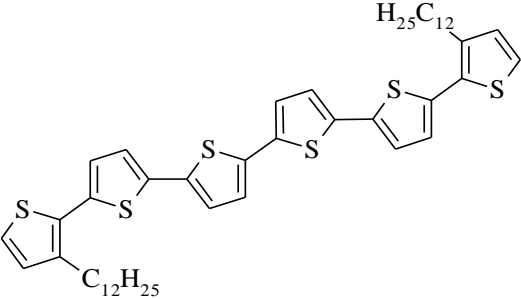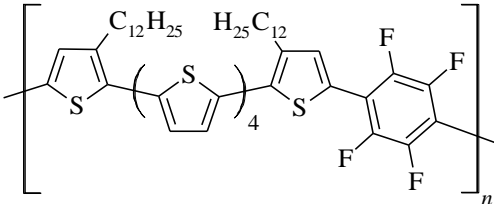
**Molecular weight** = 512.73 g/mol
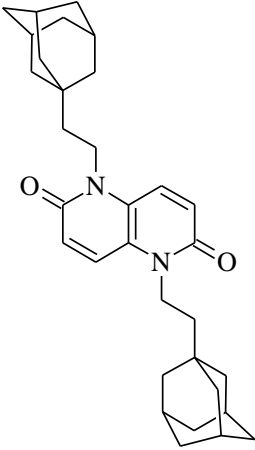
**29) Code: 165c** (*novel derivative*)

**CAS registry number:** –

**Name:** 1,4-bis[(2-ethylhexyl)oxy]-3,6-diphenylpyrrolo[3,4-*c*]pyrrole

**Molecular formula** = $C_{34}H_{44}N_2O_2$

**Molecular weight** = 512.73 g/mol



**30) Code: 166a** (*novel derivative*)

**CAS registry number:** –

**Name:** 2,5-dihydro-3,6-diphenyl-2,5-bis(2-tricyclo[3.3.1.1$^{3,7}$]dec-1-ylethyl)pyrrolo[3,4-*c*]pyrrole-1,4-dione

**Molecular formula** = $C_{42}H_{48}N_2O_2$

**Molecular weight** = 612.84 g/mol



**31) Code: 166b** (*novel derivative*)

**CAS registry number:** –

**Name:** 3,6-diphenyl-4-(2-tricyclo[3.3.1.1$^{3,7}$]dec-1-ylethoxy)-2-(2-tricyclo[3.3.1.1$^{3,7}$]dec-1-ylethyl)pyrrolo[3,4-*c*]pyrrol-1(2*H*)-one

**Molecular formula** = $C_{42}H_{48}N_2O_2$

**Molecular weight** = 612.84 g/mol



**32) Code: 166c** (*novel derivative*)

**CAS registry number:** –

**Name:** 1,4-diphenyl-3,6-bis(2-tricyclo[3.3.1.1$^{3,7}$]dec-1-ylethoxy)pyrrolo[3,4-*c*]pyrrole

**Molecular formula** = $C_{42}H_{48}N_2O_2$

**Molecular weight** = 612.84 g/mol

**33) Code: 168**

**CAS registry number:** 1315259-88-1

**Name:** diethyl 3,6-bis(4-cyanophenyl)-2,5-dihydro-1,4-dioxopyrrolo[3,4-*c*]pyrrole-2,5-diacetate

**Molecular formula** = $C_{28}H_{22}N_4O_6$

**Molecular weight** = 510.50 g/mol



**34) Code: 169** (*novel derivative*)

**CAS registry number:** –

**Name:** 2,5-dihydro-3,6-di(naphthalen-2-yl)-2,5-bis(2-tricyclo[3.3.1.1$^{3,7}$]dec-1-ylethyl)pyrrolo[3,4-*c*]pyrrole-1,4-dione

**Molecular formula** = $C_{50}H_{52}N_2O_2$

**Molecular weight** = 712.96 g/mol



**35) Code: 176**

**CAS registry number:** 952147-00-1

**Name:** 3,6-bis([2,2'-bithiophen]-5-yl)-2,5-dihydropyrrolo[3,4-*c*]pyrrole-1,4-dithione

**Molecular formula** = $C_{22}H_{12}N_2S_6$

**Molecular weight** = 496.73 g/mol



**36) Code: 177**

**CAS registry number:** 952146-98-4

**Name:** 2,5-dihydro-3,6-di-2-naphthalenyl pyrrolo[3,4-*c*]pyrrole-1,4-dithione

**Molecular formula** = $C_{26}H_{16}N_2S_2$

**Molecular weight** = 420.55 g/mol



**37) Code: 178**

**CAS registry number:** 104616-35-5

**Name:** 2,5-dihydro-3,6-di-4-pyridinyl pyrrolo[3,4-*c*]pyrrole-1,4-dithione

**Molecular formula** = $C_{16}H_{10}N_4S_2$

**Molecular weight** = 322.41 g/mol

**38) Code: 179** (*novel derivative*)

**CAS registry number:** –

**Name:** 2,5-dihydro-3,6-di-2-thienyl-2,5-bis(2-tricyclo[3.3.1.1$^{3,7}$]dec-1-ylethyl) pyrrolopyrrolo[3,4-*c*]pyrrole-1,4-dithione

**Molecular formula** = $C_{38}H_{44}N_2S_4$

**Molecular weight** = 657.03 g/mol



**39) Code: 180** (*novel derivative*)

**CAS registry number:** –

**Name:** 2,5-dihydro-3,6-diphenyl-2,5-bis(2-tricyclo[3.3.1.1$^{3,7}$]dec-1-ylethyl) pyrrolopyrrolo[3,4-*c*]pyrrole-1,4-dithione

**Molecular formula** = $C_{42}H_{48}N_2S_2$

**Molecular weight** = 644.97 g/mol



**40) Code: 181** (*novel derivative*)

**CAS registry number:** –

**Name:** 1,4-didodecylthio-3,6-di-2-thienyl pyrrolo[3,4-*c*]pyrrole

**Molecular formula** = $C_{38}H_{56}N_2S_4$

**Molecular weight** = 669.12 g/mol



**41) Code: 182** (*novel derivative*)

**CAS registry number:** –

**Name:** 1,4-bis[(2-tricyclo[3.3.1.1$^{3,7}$]dec-1-ylethyl)thio]-3,6-di-2-thienyl pyrrolo[3,4-*c*]pyrrole

**Molecular formula** = $C_{38}H_{44}N_2S_4$

**Molecular weight** = 657.03 g/mol

**42) Code: 184** (*novel derivative*)

**CAS registry number:** –

**Name:** 1,4-bis[(2-tricyclo[3.3.1.1$^{3,7}$]dec-1-ylethyl)thio]-3,6-bis([2,2'-bithiophen]-5-yl)pyrrolo[3,4-*c*]pyrrole

**Molecular formula** = $C_{46}H_{48}N_2S_6$

**Molecular weight** = 821.28 g/mol

---

**43) Code: 186** (*novel derivative*)

**CAS registry number:** –

**Name:** 1,4-bis[(2-tricyclo[3.3.1.1$^{3,7}$]dec-1-ylethyl)thio]-3,6-diphenylpyrrolo[3,4-*c*]pyrrole

**Molecular formula** = $C_{42}H_{48}N_2S_2$

**Molecular weight** = 644.97 g/mol

---

**44) Code: 188**

**CAS registry number:** 2122210-32-4

**Name:** 2,6-bis(dodecyloxy)-1,5-naphthyridine

**Molecular formula** = $C_{32}H_{54}N_2O_2$

**Molecular weight** = 498.78 g/mol

---

**45) Code: 189** (*novel derivative*)

**CAS registry number:** –

**Name:** 2,6-bis(2-ethylhexyloxy)-1,5-naphthyridine

**Molecular formula** = $C_{24}H_{38}N_2O_2$

**Molecular weight** = 386.57 g/mol

---

**46) Code: 190** (*novel derivative*)

**CAS registry number:** –

**Name:** 2,6-bis(2-tricyclo[3.3.1.1$^{3,7}$]dec-1-ylethyloxy)-1,5-naphthyridine

**Molecular formula** = $C_{32}H_{42}N_2O_2$

**Molecular weight** = 486.69 g/mol

**47) Code: 191** (*novel derivative*)

**CAS registry number:** –

**Name:** 1,5-dihydro-1,5-bis(2-tricyclo [3.3.1.1³,⁷]dec-1-ylethyl)-1,5-naphthyridine-2,6-dione

**Molecular formula** = $C_{32}H_{42}N_2O_2$

**Molecular weight** = 486.69 g/mol



**48) Code: 197**

**CAS registry number:** 2093007-40-8

**Name:** 3,3''''-didodecyl-2,2':5',2'':5'',2''':5''', 2'''':5'''',2'''''-sexithiophene

**Molecular formula** = $C_{48}H_{62}S_6$

**Molecular weight** = 831.40 g/mol



**49) Code: 201** (*novel derivative*)

**CAS registry number:** –

**Name:** poly[3,3''''-didodecyl-5-(2,3,5,6-tetrafluoro-4λ³-phenyl)-5''''''λ³-2,2':5', 2'':5'',2''':5''',2'''':5'''',2'''''-sexithiophene]

**Molecular formula** = $[C_{54}H_{60}F_4S_6]_n$

**Molecular weight** = $[977.44]_n$ g/mol